Ruthenium(II)-NHC Pincer Complexes: Tuning Ancillary Ligand Effects Towards Selective Catalysts

Ph.D. Thesis

by

DIBYA YADAV

DEPARTMENT OF CHEMISTRY

INDIAN INSTITUTE OF TECHNOLOGY INDORE

DECEMBER 2021

Ruthenium(II)-NHC Pincer Complexes: Tuning Ancillary Ligand Effects Towards Selective Catalysts

A THESIS

Submitted in partial fulfillment of the requirements for the award of the degree
of
DOCTOR OF PHILOSOPHY

by

DIBYA YADAV

DEPARTMENT OF CHEMISTRY
INDIAN INSTITUTE OF TECHNOLOGY INDORE
DECEMBER 2021

INDIAN INSTITUTE OF TECHNOLOGY INDORE

CANDIDATE'S DECLARATION

I hereby certify that the work which is being presented in the thesis entitled "**Ruthenium(II)-NHC Pincer Complexes: Tuning Ancillary Ligand Effects Towards Selective Catalysts"** in the partial fulfillment of the requirements for the award of the degree of **DOCTOR OF PHILOSOPHY** and submitted in the **DEPARTMENT OF CHEMISTRY, Indian Institute of Technology Indore**, is an authentic record of my own work carried out during the time period from December 2016 to December 2021 under the supervision of Dr. Amrendra K. Singh, Assistant Professor, Department of Chemistry, IIT Indore.

The matter presented in this thesis has not been submitted by me for the award of any other degree of this or any other institute.

Dibya Yadav
27/12/2021

Signature of the student with date
(DIBYA YADAV)

This is to certify that the above statement made by the candidate is correct to the best of my knowledge.

A.Singh.
27/12/2021

Signature of Thesis Supervisor with date
(Dr. AMRENDRA K. SINGH)

DIBYA YADAV has successfully given her Ph.D. Oral Examination held on **13-07-2022.**

A.Singh.
13/7/2022

Signature of Thesis Supervisor with date
(Dr. AMRENDRA K. SINGH)

Acknowledgments

It gives me great pleasure to thank all the people who helped me during my Ph.D. research work. Foremost, I would like to express my heartfelt gratitude to my Ph.D. thesis supervisor ***Dr. Amrendra K. Singh*** *for constant encouragement, enthusiasm, and support. I was able to attain the best results in all my ups and downs due to his faith and motivation which has encouraged me to strive for nothing less than perfection.*

I am also grateful to my ***PSPC members, Dr. Sanjay K. Singh,*** *and* ***Dr. Parimal Kar****, for their guidance and valuable suggestions during my research work. I am thankful to Convener,* ***DPGC*** *for their invaluable help. I would like to acknowledge* ***Dr. Biswarup Pathak (Head, Department of Chemistry)*** *for providing infrastructure and lab facilities.*

I would like to express my special gratitude and respect to ***Prof. Nilesh Jain, (Officiating Director, Indian Institute of Technology Indore)*** *for providing me endless support and for providing all supports and best research facilities available at the Indian Institute of Technology in Indore.*

I am grateful to ***Dr. Rajneesh Misra, Dr. Suman Mukhopadhyay, Dr. Apurba K. Das, Dr. Shaikh M.***

Mobin, Dr. Sampak Samanta, Dr. Anjan Chakraborty, Dr. C. Venkatesh, Dr. Tridib K. Sarma, Dr. Tushar K. Mukherjee, Dr. Satya S. Bulusu, Dr. Dipak Kumar Roy, Dr. Selvakumar Sermadurai, and Dr. Umesh A. Kshirsagar for their guidance and help during various activities in the Department of Chemistry, IIT Indore. I would like to express my special thanks to *Dr. Abhinav Raghuvanshi* for his valuable suggestions and encouragement throughout my P.hD.

I wish to thank the technical staff from *Sophisticated Instrumentation Center (SIC)*, IIT Indore, *Dr. Radhe Shyam Ji, Mr. Kinny Pandey, Mr. Ghanshyam Bhavsar, Mr. Manish Kushwaha, Mrs. Vinita Kothari, Mr. Parthiban P. K.* and *Mr. Rameshwar Dauhare* for their timely technical support without which it would never have been possible to complete my work. I would also like to thank all the technical, non-technical staff of IIT Indore for all their direct/ indirect help and support.

I want to express my heartfelt gratitude to my lab mates *Mr. Rahul Kumar Singh, Mr. Shambhunath Gupta, Mr. Navdeep Srivastava, Ms. Nida Shahid, Mr. Naveen Kumar, Ms. Achena Saha, Ms. Ekta Yadav, Mr. Ashu Singh* and *Mr. Vishal Jaiswal* for their generous support, and cooperation in making my work successful.

*I would like to convey my special thanks and gratitude to **Dr. Shilpi Misra** for her continuous support and encouragement throughout my Ph.D. at IIT Indore. I would also be grateful to my super seniors **Dr. Suryabhan Singh** and **Dr. Ramachandran** for their help and great co-operation during my Ph.D.*

*I am extremely thankful to **Mr. Abhishek Upadhyay** for his generous advice, motivation, and support in several ways throughout my Ph.D. I would like to extend my sincere thanks to all my friends who supported me directly or indirectly during my Ph.D.*

*I would want to convey my gratitude and respect to my beloved father, **Mr. Lalji Yadav,** and my adoring mother, **Mrs. Meera Devi**, for their unwavering love, constant encouragement, and patience throughout this time. Finally, I would want to express my gratitude to my younger brothers **Mr. Suryajit Yadav, Mr. Nitish Yadav,** and **Mr. Nikhil Yadav,** and my sister, **Ms. Anshika Yadav**, for their love, care, and support.*

Thank You!!!!!

DIBYA

Dedicated to

"My beloved Parents"

And

"My thesis supervisor

SYNOPSIS

The thesis, entitled "Ruthenium(II)-NHC Pincer Complexes: Tuning Ancillary Ligand Effects Towards Selective Catalysts" includes five chapters, which deal with the synthesis and development of Ru-complexes with smaller alkyl wingtips on NHCs and their application as catalysts for various organic transformations. The first chapter gives a general introduction to Ru-pincer complexes and their applications in catalysis. In the succeeding chapters, synthesis and characterization of new cationic ruthenium(II) pincer complexes, investigation of their catalytic activity, and possible steric and electronic effects of co-ligands have been described. Ruthenium(II) pincer complexes containing different co-ligands such as CO, COD, PPh_3, and DMSO gave us an opportunity to examine possible electronic effects for the development of selective catalysts. We have also studied the change in reactivity due to the steric effects of alkyl wingtips at NHCs. The synthesized complexes have been successfully implied for various organic conversions such as transfer hydrogenation of ketones, acceptorless dehydrogenation of alcohols, and dehydrogenative coupling of alcohols and amines. The catalytic reactions are also performed under microwave irradiation. Better catalytic activity was observed in microwave heating conditions than "oil-bath" heating, in less time and lower temperatures. In the last chapter, concluding remarks and a brief description of future directions have been described.

Chapter 1. Introduction and background: Ruthenium Pincer Complexes in Catalysis

Development and characterization of new homogeneous pincer catalysts based on transition metals have fascinated much more devotion in the field of organometallic chemistry.*[1–3]* One of the most important advantages of homogeneous catalysis is to allow the study of the mechanistic pathway of the reactions. To date, many transition metal-based catalysts have been explored for various catalytic transformations because of their higher

stability and high activity towards many conversions.*[4–8]* On comparing the other transition metals, ruthenium has an exceptional array of catalysis properties and has found several applications.

Ruthenium complexes have variable advantages viz, its rich coordination chemistry, variable oxidation states, tendency to accommodate a large number of ligands. In homogenous catalysis, ruthenium complexes have shown exciting chemistry. The complexes of ruthenium metal are also comparatively air stable. Ruthenium is less expensive than other late transition metal series like iridium, platinum, gold.

The ligand choice is also an important factor for designing a new catalyst.*[9]* Pincer ligands have many advantages in catalysis because of their rigidity and stability. As we know, phosphine containing transition metal complexes have high activity in catalysis, but it has some disadvantages. Complexes containing phosphines are not suitable for certain types of catalysis due to possible oxidation of the phosphine ligands. Carbenes are relatively more electron donor ligands than phosphine analogous. NHC carbenes are stronger sigma donors and weaker pi acceptors than alkyl phosphines. The steric properties of NHC ligands have further differentiated them from phosphine analogous. Their ability to tune the steric and electronic environment around the metal centre has resulted in many synthetic protocols. Pincer ligands containing NHC carbenes exhibit high thermal stability and a broad range of reactivity.*[10,11]* NHC based CNC ligands represent a potentially powerful combination for ligand design. In general, the final composition and structure of Ru-CNC complexes depend on the precursor Ru-complexes, the reagents used for the carbene generation, as well as the type of wingtip substituents on the *N*-heterocycle, which are used to influence the steric environment around the central metal atom. CNC ligands containing NHCs with bulky alkyl substituents have been explored widely,*[12–14]* but with smaller alkyl wingtips, it is less explored till now.

Objectives: The objectives of this study are as follows,

- To synthesize the Ru-CNC pincer complexes with smaller alkyl NHC wingtips.
- To study the reactivity and structure-property relationship.
- To study the effect of various co-ligands on the reactivity of these complexes.
- To utilize the acquired knowledge for tuning catalytic behaviour.

Ruthenium pincer complexes as catalysts are in high demand because they are readily available in different stable oxidation states and different coordination geometries, viz. square pyramidal, trigonal-bipyramidal and octahedral.*[1]* In synthetic organic chemistry, hydrogenation, dehydrogenation and dehydrogenative coupling reactions play a crucial role, and such reactions involving oxygenated and nitrogenous compounds are particularly useful for producing agrochemicals, pharmaceuticals, foods, and fuels.*[15–19]* Conventionally, these reactions have been carried out using high hydrogen pressure or hazardous reagents, various additives, and co-catalysts often produce numerous wastes. Alternatively, transfer hydrogenation, acceptorless dehydrogenation and dehydrogenative coupling reactions are some of the most atom-efficient ways to synthesize valuable intermediates and various organic transformations. Complexes with CNC-pincer ligands are less explored for these catalytic reactions. The present thesis describes the synthesis, characterization and catalytic activities of new cationic Ru(II)-NHC pincer complexes with smaller alkyl wingtips and a variety of co-ligands.

Chapter 2. Cationic Ru(II)-NHC Pincer Complexes: Synthesis and Characterization

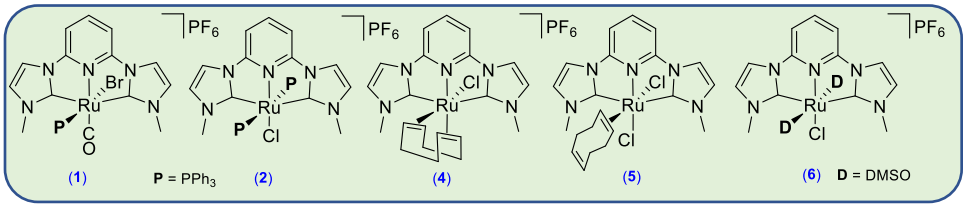

The ruthenium metal centre in all the complexes displays distorted octahedral geometry with the tridentate pincer ligand occupying the meridional coordination. The molecular structure of **4a** consists of CNC pincer ligand forming two almost planar five-membered metallacycles, a chloride ligand and a COD ligand coordinated to the Ru centre in η^2:η^2-mode. The C=C bond lengths of COD trans to pyridine are 1.381(8) Å (**4a**) and 1.384(7) Å (**4b**), whereas C-C bond lengths trans to halide are 1.392(8) Å (**4a**) and 1.399(7) Å (**5**) respectively. This data indicates that the Ru-C(COD) bond trans to pyridine is slightly weaker and more labile than the Ru-C(COD) bond trans to halide, which is also confirmed by the formation of compound **5** from **4a**. Complex **5** is a rare example of complexes in which COD is bound in a "non-bridging" η^2-mode. The second chloride ligand is coordinated trans to pyridine occupying the coordination site after dissociation of one of the alkene bonds of COD ligand. The solid-state structure of complex **5** shows an (E,Z) configuration for the η^2-COD ligand, instead of the expected (Z,Z) configuration, with the free alkene having an E-configuration. DFT study of isomeric forms of **5** with E,Z- and Z,Z-COD indicates that the complex with Z,Z-COD ligand is thermodynamically more stable and should be favoured in solution. In conclusion, four different types of co-ligands (CO, COD, PPh_3 & DMSO) are available for comparison during catalysis reactions.

Chapter 3. Catalytic Transfer Hydrogenation and Dehydrogenation of ketones and alcohols using Ru(II)-NHC Pincer Complexes

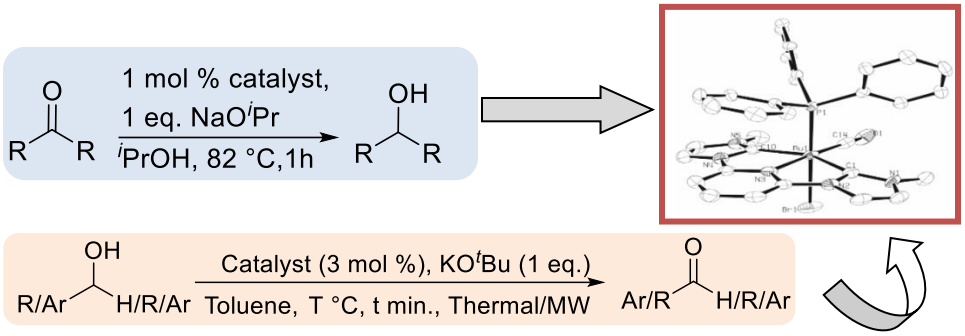

Catalytic activity: CO > COD > PPh_3 ≈ DMSO

This chapter describes catalytic hydrogenation and dehydrogenation reactions from newly synthesized ruthenium pincer complexes. The transfer hydrogenation of cyclohexanone in refluxing isopropanol was selected as a model reaction to evaluate the catalytic activity of complexes. Taking 2 mmol of ketone, 1 mol% of catalyst, and 1 equivalent of sodium iso-propoxide (NaO^{i}Pr) as a base, complex **1b** showed higher catalytic activity than other complexes viz: **2b**, **3b**, **4b** and **5b** resulting in >99 % conversion of cyclohexanone in 30 min. Additionally, the effect of various bases, e.g., NaOH, KOH and KO^{t}Bu with complex **1b** were also investigated, where NaO^{i}Pr was proved to be a better base among all the bases. The scope of catalyst **1b** was then examined using various ketone substrates. A variety of ketone derivatives with aliphatic and aromatic substituents, as well as electron-donating and withdrawing substituents were explored for transfer hydrogenation reaction.

With excellent conversions in transfer hydrogenation processes, all the catalysts were tested for acceptorless dehydrogenation of alcohols (AAD). Dehydrogenation of benzyl alcohol was examined first as a model reaction to investigate the reactivity of these complexes (**1b**, **2b**, **4b** and **6b**) for catalytic AAD reactions. Complex **1b** in toluene with KO^{t}Bu at 110 °C for 3h afforded >99% conversion to benzaldehyde while, complex **2b**, **4b** and **6b** gave 47, 89 and 60 % conversions, respectively. The catalytic

activity of complex **1b** with different bases was then studied under similar reaction conditions, and screening suggested that KO^{t}Bu is the best option for AAD of alcohols. Therefore, the complex **1b** (3 mol%) and KO^{t}Bu was then chosen as a suitable catalyst system for AAD of a range of primary and secondary alcohols under these optimized reaction conditions. In the case of COD complexes, no sign of dissociation or hydrogenation of the COD ligand during catalysis was observed. AAD catalysis under microwave was also examined, and it was observed that catalysis reactions under microwave took less time and low temperature than conventional heating. In microwave heating, the product selectivity is also better than conventional heating. Substrate scope for acceptorless dehydrogenation catalysis reaction was then explored with a variety of alcohols under thermal and microwave heating.

Chapter 4. Dehydrogenative coupling reactions under conventional and microwave heating using Ru(II)-NHC Pincer Complexes

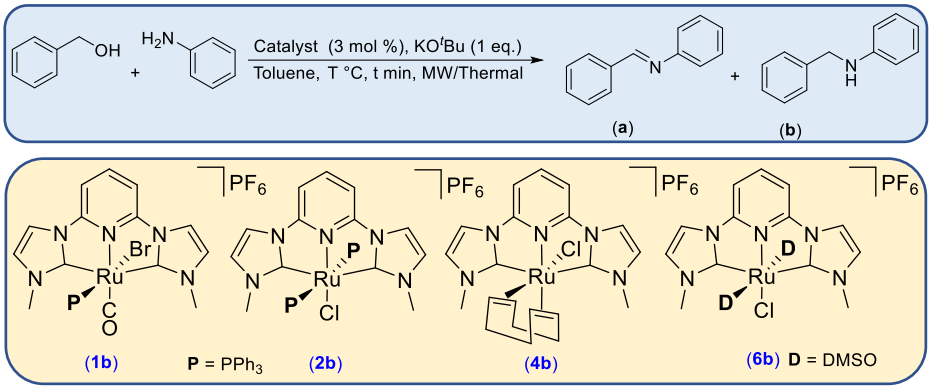

In this chapter, ruthenium pincer complexes are explored for dehydrogenative coupling catalytic reactions. The optimized conditions for the alcohol dehydrogenation reactions, viz., solvent, temperature, base, and catalyst amount, were used for dehydrogenative coupling reactions, as the first step in this case too is the alcohol dehydrogenation. The dehydrogenative coupling of aniline with benzyl alcohol was chosen as a model reaction for imine synthesis. In catalyst screening experiments, it was

observed that the Ru-catalyst **6b** performs better than catalyst **1b** for the ADC of alcohols and amines under both thermal and microwave conditions. This interesting reverse trend in catalytic activity indicates involvement of the Ru-metal centre in the dehydrogenative coupling step as, otherwise, the catalyst better at alcohol dehydrogenation should also have been better at the imine formation. The unexpected reversal in catalytic performance can be understood in terms of the trans effect of ligands in the aldehyde dissociation from an intermediate in the catalytic cycle. The relatively weaker trans effect of DMSO and PPh_3 ligand in case of **2b** and **6b** keeps the aldehyde intermediate attached to the metal and facilitates the nucleophilic attack of an amine for the dehydrogenative coupling step leading to the imine formation. The dehydrogenative coupling step involves a nucleophilic attack by the amine on metal-bound aldehyde formed after alcohol dehydrogenation. However, DMSO and PPh_3 ligands have a weaker trans effect than CO and COD which results in retaining the aldehyde on the complex. Therefore, complex **6b** with DMSO as a co-ligand gave better reactivity towards dehydrogenative coupling reactions, followed by complex **2b** with PPh_3 ligand. Dehydrogenative coupling was also examined under microwave to decrease the reaction time and temperature. We observed that catalysis reactions under conventional heating took higher time and higher temperature than microwave irradiation. Several substrates with electron-donating as well as electron-withdrawing groups were explored for dehydrogenative coupling reactions under conventional and microwave heating. Biologically active imine precursors were also efficiently synthesized using ruthenium pincer catalyst under microwave heating conditions.

Chapter 5. Role of Ancillary Ligands in Selectivity for Catalytic Applications

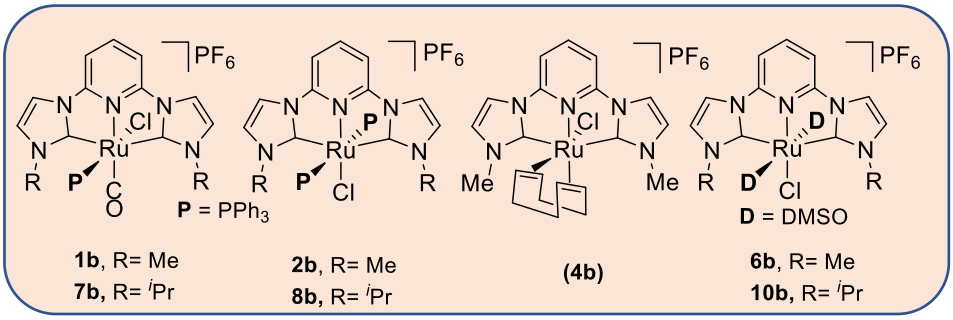

In this chapter, we have described the synthesis and characterization of new Ru(II)-NHC pincer complexes with isopropyl wingtip to study their steric and electronic effects and compare them with their *N*-methyl analogues. The lability of PPh_3 and DMSO ligands increased due to steric crowding around the ruthenium metal centre. Synthesis of COD containing complex has also been performed, which have some positive indications from mass spectrogram data; however, we were unable to fully characterize the COD complex due to COD dissociation, which was confirmed by mass analysis. The catalysis reported with COD complex was done by in situ generated catalyst.

The four new complexes with *N*-isopropyl wingtips have also been tested for various catalysis. In general, they show improved catalytic activity in comparison to complexes with methyl wingtips. The general trend of reactivity with respect to the trans effect of co-ligands is again observed for transfer hydrogenation and acceptorless dehydrogenation reactions. While in dehydrogenative coupling reactions, the *N*-isopropyl complexes show mixed reactivity, which is probably due to steric effects of the *N*-isopropyl and the trans effect of co-ligands.

Chapter 6. Summary and future scope

In summary, we have investigated the synthesis and characterization of Ru(II)-NHC pincer complexes containing "pyridine dicarbene" ligand with methyl and isopropyl wingtips. Furthermore, we have studied the catalytic activity of all the ruthenium complexes for AAD of alcohols and ADC of benzyl alcohol and amines. Compared to conventional "oil-bath" heating, microwave irradiation resulted in faster catalysis under milder conditions. An unexpected reversal in the catalytic activity of the complexes has been observed. Complex **1b** was found to be catalytically more active than its analogous complexes for AAD, while complex **6b** was found more active for direct synthesis of imines than complex **1b**. We observed that with *N*-isopropyl, steric effects were also affecting the general reactivity and catalysis along with electronic effects of various co-ligands. In the case of transfer hydrogenation and AAD reactions, the complexes with isopropyl groups follow the same trend of the trans effect of co-ligands (CO, COD, PPh_3 and DMSO) as like *N*-methyl complexes. In dehydrogenative coupling catalysis, comparatively, all the *N*-isopropyl complexes gave better reactivity than analogous *N*-methyl complexes.

References:

[1] Gunanathan C., Milstein D. (2014), Bond Activation and Catalysis in Pincer Complexes, *Chem. Rev.*, 114, 12024–12087 (https://doi.org/10.1021/cr5002782).

[2] Piccirilli L., Lobo Justo Pinheiro D., Nielsen M. (2020), Recent Progress with Pincer Transition Metal Catalysts for Sustainability, *Catalysts*, 10, 773 (https://doi.org/10.3390/catal10070773).

[3] Younus H. A., Ahmad N., Su W., Verpoort F. (2014), Ruthenium pincer complexes: Ligand design and complex synthesis, *Coord. Chem. Rev.*, 276, 112–152 (https://doi.org/10.1016/j.ccr.2014.06.016).

[4] Corma A., Navas J., Sabater M. J. (2012), Coupling of Two Multistep Catalytic Cycles for the One-Pot Synthesis of Propargylamines from Alcohols and Primary Amines on a Nanoparticulated Gold Catalyst, *Chem. Eur. J.*, 18, 14150–14156 (https://doi.org/10.1002/chem.201201837).

[5] Yang Y., Qin A., Zhao K., *et al.* (2016), Design and Synthesis of Alanine Triazole Ligands and Application in Promotion of Hydration, Allene Synthesis and Borrowing Hydrogen Reactions, *Adv. Synth. Catal.*, 358, 1433–1439 (https://doi.org/10.1002/adsc.201600141).

[6] Tang C.-H., He L., Liu Y.-M., *et al.* (2011), Direct One-Pot Reductive N-Alkylation of Nitroarenes by using Alcohols with Supported Gold Catalysts, *Chem. Eur. J.*, 17, 7172–7177 (https://doi.org/10.1002/chem.201100393).

[7] Yan T., Feringa B. L., Barta K. (2016), Benzylamines via Iron-Catalyzed Direct Amination of Benzyl Alcohols, *ACS Catal.*, 6, 381–388 (https://doi.org/10.1021/acscatal.5b02160).

[8] Mehta A., Thaker A., Londhe V., Nandan S. R. (2014), Reinvestigating Raney nickel mediated selective alkylation of amines with alcohols via hydrogen autotransfer methodology, *Appl. Catal. Gen.*, 478, 241–251 (https://doi.org/10.1016/j.apcata.2014.04.009).

[9] Peris E., Crabtree R. H. (2018), Key factors in pincer ligand design, *Chem. Soc. Rev.*, 47, 1959–1968 (https://doi.org/10.1039/C7CS00693D).

[10] Andrew R. E., González-Sebastián L., Chaplin A. B. (2016), NHC-based pincer ligands: carbenes with a bite, *Dalton Trans.*, 45, 1299–1305 (https://doi.org/10.1039/C5DT04429D).

[11] Wang Y., Zhang B., Guo S. (2021), Transition Metal Complexes Supported by *N*-Heterocyclic Carbene-Based Pincer Platforms: Synthesis, Reactivity and Applications. *Eur. J. Inorg. Chem.*, 2021, 188–204 (https://doi.org/10.1002/ejic.202000911).

[12] Peris E., Loch J. A., Mata J., Crabtree R. H. (2001), A Pd complex of a tridentate pincer CNC bis-carbene ligand as a robust homogenous Heck catalyst, *Chem. Commun.*, 201–202 (https://doi.org/10.1039/B008038L).

[13] Poyatos M., Mata J. A., Falomir E., *et al.* (2003), New Ruthenium(II) CNC-Pincer Bis(carbene) Complexes: Synthesis and Catalytic Activity, *Organometallics*, 22, 1110–1114 (https://doi.org/10.1021/om020817w).

[14] Danopoulos A. A., Winston S., Motherwell W. B. (2002), Stable *N*-functionalised 'pincer' bis carbene ligands and their ruthenium complexes; synthesis and catalytic studies, *Chem. Commun.*, 1376–1377 (https://doi.org/10.1039/B202814J).

[15] Jaiswal G., Landge V. G., Jagadeesan D., Balaraman E. (2017), Iron-based nanocatalyst for the acceptorless dehydrogenation reactions, *Nat. Commun.*, 8, 2147 (https://doi.org/10.1038/s41467-017-01603-3).

[16] Preuster P., Papp C., Wasserscheid P. (2017), Liquid Organic Hydrogen Carriers (LOHCs): Toward a Hydrogen-free Hydrogen Economy, *Acc. Chem. Res.*, 50, 74–85 (https://doi.org/10.1021/acs.accounts.6b00474).

[17] Rong Z.-Q., Zhang Y., Chua R. H. B., *et al.* (2015), Dynamic Kinetic Asymmetric Amination of Alcohols: From A Mixture of Four Isomers to Diastereo- and Enantiopure α-Branched Amines, *J. Am. Chem. Soc.*, 137, 4944–4947 (https://doi.org/10.1021/jacs.5b02212).

[18] Wiesner T., Leypold M., Steinmaurer A., *et al.* (2020), Synthesis of Stable Dianionic Cyclic Silenolates and Germenolates, *Organometallics*, (https://doi.org/10.1021/acs.organomet.0c00385).

[19] Yadav D., Misra S., Kumar D., *et al.* Cationic ruthenium(II)–NHC pincer complexes: Synthesis, characterisation and catalytic activity for transfer hydrogenation of ketones, *Appl. Organomet. Chem.*, 35, e6287 (https://doi.org/10.1002/aoc.6287).

LIST OF PUBLICATIONS

1. **D. Yadav**, S. Misra, D. Kumar, S. Singh and A. K. Singh*. Cationic Ruthenium(II)-NHC Pincer Complexes: Synthesis, Characterization and Catalytic Activity for Transfer Hydrogenation of Ketones. *Appl. Organomet. Chem.* 2021, *35*, e6287. Impact Factor: 4.105.
2. **D. Yadav**, R. K. Singh, S. Singh, P. Shirage and A. K. Singh*. Cationic Ruthenium(II)-NHC Pincer Complexes with Hemilabile COD: Solid-state Structural Characterisation and Theoretical Study of an η^2-(E,Z)-COD Ligand. *J. Organomet. Chem.* 2021, *953*, 122061. Impact Factor: 2.369.
3. **D. Yadav**, R. K. Singh, S. Misra and A. K. Singh*. Ancillary ligand effects and microwave-assisted enhancement on the catalytic performance of cationic ruthenium(II)-CNC pincer complexes for acceptorless alcohol dehydrogenation. *Appl. Organomet. Chem.* 2022, *36*, e6756. Impact Factor: 4.105.
4. **D. Yadav**, R. K. Singh, S. Misra and A. K. Singh*. Dehydrogenative Coupling of Alcohols and Amines Catalyzed by Cationic Ruthenium(II)-CNC Pincer Complexes. (*Manuscript under preparation*).
5. **D. Yadav**, N. Kumar, S. Misra and A. K. Singh*. Synthesis, Characterization, DFT and Fluorescent Studies of 1,4,5,8-Tetrafluroacridine (*Manuscript under preparation*).
6. R. K. Singh, **D. Yadav** and A. K. Singh*. Ruthenium Complexes with Multiple NHC Donor Ligands: Synthesis Characterization and Investigation of UV-Vis and Electrochemical Properties (*Manuscript under preparation*).

CONFERENCES AND WORKSHOPS

1. Poster presentation in ***Frontiers in Organometallics and Catalysis (FMOC-2021)*** at MNIT Jaipur, India (February 2021); **D. Yadav**, R. K. Singh, S. Singh, P. Shirage and A. K. Singh*, Cationic Ruthenium(II)-NHC Pincer Complexes with Hemilabile COD: Solid-state Structural Characterization and Theoretical Study of an η^2-(E,Z)-COD Ligand.

2. Poster presentation in ***Modern Trends in Inorganic Chemistry (MTIC-2019)*** at IIT Guwahati, India (December 2019); **D. Yadav**, S. Misra, D. Kumar, S. Singh and A. K. Singh*, Cationic Ruthenium(II)-NHC Pincer Complexes: Synthesis, Characterization and Catalytic Activity for Transfer Hydrogenation of Ketones.

3. Oral presentation in ***CHEM-2019*** at Indian Institute of Technology Indore on the occasion of 10th-year anniversary and National science Day, Indore, India (February 2019); Transition Metal Complexes with *N*-Heterocyclic Carbene and Pincer Ligands.

4. Poster presentation in ***Industrial Academia Conclave (IAC-2018)*** at Indian Institute of Technology Indore, India (November 2018); **D. Yadav** and A. K. Singh*, Synthesis, Crystal Structures and Some Interesting Catalytic Activity of Ruthenium-NHC Pincer Complexes.

5. Attended GIAN Course: "***Metal-Ligand Interplay in Advanced Coordination Chemistry***" (Course Instructor: **Prof. Pierre Braunstein**, CNRS-Université de Strasbourg, France) at IIT Indore, India (February 2018).

6. Poster presentation in ***Frontiers of Organometallic Chemistry (FOMC-2016)*** at The Leela Kovalam, Thiruvananthapuram, (December 2016); **D. Yadav** and A. K. Singh*, Synthesis and Characterization of Ruthenium-NHC Pincer Complexes.

TABLE OF CONTENTS

1.	**List of Figures**	XX
2.	**List of Schemes**	XX
3.	**List of Tables**	XX
4.	**Nomenclature**	XX
5.	**Acronyms**	XX
Chapter 1. Introduction and background: Ruthenium Pincer Complexes in Catalysis		**1-38**
1.1	**Introduction (Types of pincer ligands)**	1-5
1.2	**Advantages of *N*-heterocyclic carbenes as a ligand**	6-7
1.3	**Advantages of pincer ligands based on *N*-heterocyclic carbenes**	7
1.4	**Transition metal complexes based on NHCs containing CNC pincer ligands**	8-9
1.5	**Ruthenium complexes based on NHCs containing CNC pincer ligands**	9-10
1.6	**Application of transition metal complexes in transfer hydrogenation reactions**	10-13
1.7	**Application of transition metal complexes in the dehydrogenation of alcohols**	13-14
1.8	**Importance of microwave in catalytic reactions**	14-15
1.9	**Application of transition metal complexes in dehydrogenative coupling reactions**	15-16
1.10	**Mechanism of hydrogenation/dehydrogenation reactions**	17-20
1.11	**Objectives of the thesis**	21
1.12	**Organization of the Thesis**	22
1.13	**References**	23-38

Chapter 2. Cationic Ru(II)-NHC Pincer Complexes: Synthesis and Characterization **39-103**

2.1 **Introduction** 39-43

2.2 **Results and Discussion**

2.2.1 Synthesis and charaterization of Ru(II)-NHC Pincer Complexes 43-59

2.3 **Conclusions** 59

2.4 **Experimental section** 60-67

2.4.1 General considerations 60

2.4.2 Synthesis of Ru(II)-NHC Pincer Complexes 60-67

2.5 **Characterization data of metal complexes** 68-95

2.6 **References** 96-103

Chapter 3. Catalytic Transfer Hydrogenation and Dehydrogenation of ketones and alcohols using Ru(II)-NHC Pincer Complexes **103-130**

3.1 **Introduction** 104-106

3.2 **Results and Discussion** 107-117

3.2.1 Catalytic transfer hydrogenation of ketones using Ru(II) NHC-Pincer Complexes 107-112

3.2.4 Catalytic acceptorless dehydrogenation of alcohols ketones using Ru(II)-NHC Pincer Complexes 113-117

3.3 **Conclusions** 118

3.4 **Experimental section** 118-120

3.4.1 General considerations 118

3.4.2 General procedure for the catalytic transfer hydrogenation of ketones using Ru(II)-NHC Pincer Complex 118

3.4.3 General procedure for the catalytic acceptorless dehydrogenation of alcohols using Ru(II)-NHC Pincer Complexes under microwave heating 119-120
3.4.7 Spectral data for hydrogenated products of ketones 121-122
3.4.8 Spectral data for dehydrogenated products of alcohols 123-124
3.4.9 Mechanistic studies 125-126
3.5 References 127-132
***Chapter 4. Dehydrogenative coupling reactions under conventional and microwave heating using Ru(II)-NHC Pincer Complexes* 131-160**
4.1 Introduction 133-142
4.2 Results and discussion 135
4.2.1 Catalytic dehydrogenative coupling reactions using Ru(II)-NHC Pincer Complexes under thermal heating 137
4.2.2 Catalytic dehydrogenative coupling reactions using Ru(II)-NHC Pincer Complexes under microwave heating 138
4.2.5 Synthesis of some biologically active imine precursors under microwave heating 139
3.2.8 Mechanism for Catalytic dehydrogenative coupling reactions 140-142
4.3 Conclusions 142
4.4 Experimental section 143
4.4.1 General considerations 143
4.4.2 General procedure for the catalytic dehydrogenative coupling reactions using Ru(II)-

NHC Pincer Complexes under conventional heating microwave heating 144-145
4.4.4 Spectral data for dehydrogenative coupling reactions products 146-147
4.4.5 Mechanistic studies 148
4.5 References 149-162
Chapter 5. Role of Ancillary Ligands in Selectivity for Catalytic Applications
5.1 Introduction 163-165
5.2 Results and discussion 166-176
5.2.1 Synthesis and characterization of Ru(II)-NHC Pincer Complexes 166-171
5.2.2 Catalytic applications of Ru(II)-NHC Pincer Complexes for transfer hydrogenation 172-173
5.2.3 Catalytic applications of Ru(II)-NHC Pincer Complexes for acceptorless dehydrogenation reactions 174-175
5.2.4 Catalytic applications of Ru(II)-NHC Pincer Complexes for acceptorless dehydrogenative coupling 176
5.3 Conclusions 177
5.4 Experimental section 177-182
5.4.1 General considerations 177
5.4.2 Synthesis of Ru(II)-NHC Pincer Complexes 178-181
5.4.3 Procedures for catalytic reactions 181-182
5.4.4 Characterization data 183-196
5.5 References 197-204
Chapter 6. Conclusions and future scope **205-207**
6.1 Conclusions 205-206
6.2 Future scope 207

LIST OF FIGURES

Chapter 1. Introduction: Ruthenium Pincer Complexes in Catalysis

Figure 1.1 The basic aryl-based metalloid-pincer complex 1
Figure 1.2 ECE and ENE pincer ligands 2
Figure 1.3 PCP and PNP pincer ligands 3
Figure 1.4 SNS and SeNSe pincer ligands 3
Figure 1.5 NNN pincer ligands 4
Figure 1.6 PCN and CNN pincer ligands 4
Figure 1.7 NCN and CNC pincer ligands 5
Figure 1.8 Early examples of NHC–complexes and Arduengo's isolated free carbene 6
Figure 1.9 Grubbs first and second-generation metathesis catalysts 6
Figure 1.10 General structural features of NHCs 7
Figure 1.11 Common NHC-containing pincer complexes 7
Figure 1.12 Ru-CNC pincer complexes with bulky *N*-wingtips 10
Figure 1.13 Ru complexes for transfer hydrogenation reactions 12
Figure 1.14 Transition metal complexes for dehydrogenation reactions 14
Figure 1.15 Applications of microwave 15
Figure 1.16 Ru and Ir complexes for dehydrogenative coupling reactions 16
Figure 1.17 Homogeneous non-cooperation and cooperation hydrogenation/dehydrogenation catalysts 18
Figure 1.18 The schematic diagram of the non-cooperation mechanism 19
Figure 1.19 The schematic diagram of metal-ligand cooperation (MLC) mechanism 20

Chapter 2. Cationic Ru(II)-NHC Pincer Complexes: Synthesis and Characterization

Figure 2.1 Reported CNC pincer ruthenium complexes with different co-ligands 41
Figure 2.2 Iridium and rhodium complexes with COD-ligand 42
Figure 2.3 Molecular structure of **1a** 50

Figure 2.4 Molecular structure of **2a** 50
Figure 2.5 Molecular structure of **4a** 55
Figure 2.6 Molecular structure of **4b** 55
Figure 2.7 Molecular structure of **5** 56

Chapter 3. Catalytic Hydrogenation and Dehydrogenation of ketones and alcohols by using Ru(II)-NHC Pincer Complexes

Figure 3.1 Reported ruthenium pincer complexes for Transfer hydrogenation of ketones 104
Figure 3.2 Reported ruthenium pincer complexes for aceptorless dehydrogenation of alcohols 105
Figure 3.3 Cationic Ru(II)–CNC pincer complexes in this study 105

Chapter 4. Dehydrogenative coupling reactions under conventional and microwave heating using Ru(II)-NHC Pincer Complexes

Figure 4.1 Ruthenium and Iridium complexes for AAD and dehydrogenative coupling of alcohols and amines 132
Figure 4.2 Reported ruthenium NHC complexes for dehydrogenative coupling of alcohols and amines 133
Figure 4.3 Cationic Ru(II)–CNC pincer complexes in this study 134

Chapter 5. Role of Ancillary Ligands in Selectivity for Catalytic Applications

Figure 5.1 Cationic Ru(II)–CNC pincer complexes in this study 163
Figure 5.2 Molecular structure of **9a** 168
Figure 5.3 Molecular structure of **10a** 168

LIST OF SCHEMES

Chapter 1. Introduction: Ruthenium Pincer Complexes in Catalysis

Scheme 1.1 Various approach for the synthesis of NHC-based pincer complexes 8

Scheme 1.2 Hydrogen transfer in Meerwein-Ponndorf-Verley reduction 11

Chapter 2. Cationic Ru(II)-NHC Pincer Complexes: Synthesis and Characterization

Scheme 2.1 Synthesis of CNC pincer ruthenium complexes **1–6**. 45

Scheme 2.2 Isolation of [Ru(CNC)(η^2-COD)Cl_2], (**5**) during crystallization 48

Chapter 3. Catalytic Hydrogenation and Dehydrogenation of ketones and alcohols by using Ru(II)-NHC Pincer Complexes

Scheme 3.1 Plausible mechanism for transfer hydrogenation catalysis by **2b** 110

Scheme 3.2 Synthesis of CNC pincer ruthenium complexes **3a** and **3b** from **2a** 111

Scheme 3.3 Plausible mechanism for acceptorless dehydrogenation of alcohols catalysis by **2b** 117

Chapter 4. Dehydrogenative coupling reactions under conventional and microwave heating using Ru(II)-NHC Pincer Complexes

Scheme 4.1 Possible products from acceptorless alcohol dehydrogenation, amine double dehydrogenation or dehydrogenative coupling of alcohols and amines 132

Scheme 4.2 Plausible mechanism for aceptorless alcohol dehydrogenation and dehydrogenative coupling of amines by complexes **2** and **3** 140

Chapter 5. Role of Ancillary Ligands in Selectivity for Catalytic Applications

Scheme 5.1	Synthesis of CNC pincer ruthenium complexes **7a** to **10b**	164
Scheme 5.2	Synthesis of ruthenium pincer complex **9b** from **8b**	165
Scheme 5.3	Synthesis of CNC-COD pincer ruthenium complex	166

LIST OF TABLES

Chapter 2. Cationic Ru(II)-NHC Pincer Complexes: Synthesis and Characterization

Table 2.1 Crystal data and structural refinement parameters for **1a, 2a, 4a**, **4b** and **5** 51-52

Table 2.2 Selected bond lenths and bond angles of **1a, 2a, 4a, 4b** and **5** 53-54

Table 2.2 Selected bond lengths (Å) and angles (°) for **4a** and **5** obtained from single crystal X-ray diffraction and DFT studies 58

Chapter 3. Catalytic Hydrogenation and Dehydrogenation of ketones and alcohols by using Ru(II)-NHC Pincer Complexes

Table 3.1 Optimisation table of different catalysts for transfer hydrogenation reaction 106-107

Table 3.2 Transfer hydrogenation of various ketones with catalyst **1b** 108-109

Table 3.3 Optimisation table of different catalysts with different bases for acceptorless dehydrogenation reaction 112

Table 3.4 Screening of catalysts under microwave 113

Table 3.5 Acceptorless alcohol dehydrogenation of various alcohols with Ru catalyst **1b** under conventional heating 114-115

Table 3.6 Acceptorless alcohol dehydrogenation of various alcohols with Ru catalyst **1b** under microwave heating 115-116

Chapter 4. Dehydrogenative coupling reactions under conventional and microwave heating using Ru(II)-NHC Pincer Complexes

Table 4.1 Catalyst screening under thermal and microwave conditions 135

Table 4.2 Imine synthesis reaction from various amines and benzene methanol with catalyst **2b** under conventional heating 136

Table 4.3 Imine synthesis reaction from various amines and benzene methanol with catalyst **2b** under conventional heating 137

Table 4.4 Biologically active imine synthesis from various amines and alcohols with catalyst **2b** under microwave 138

Chapter 5. Role of Ancillary Ligands in Selectivity for Catalytic Applications

Table 5.1 Crystal data and structural refinement parameters for **9a** and **10a** 169

Table 5.2 Transfer hydrogenation reaction with different catalysts 170-171

Table 5.3 Acceptorless dehydrogenation of benzyl alcohol with different catalysts 172

Table 5.4 Dehydrogenative coupling of benzyl alcohol and aniline with different catalysts 173-174

NOMENCLATURE

A	Alpha
B	Beta
Λ	Gamma
Å	Angstrom
Λ	Wavelength
M	Micro
Σ	Sigma
Π	Pi
H	Eta
Δ	Delta
K	Kappa
J	Coupling constant
Hz	Hertz
MHz	Mega hertz
K	Kelvin
D	Density
V	Volume
mM	Milli Molar
Mm	Micro Molar
Cm	Centimeter
°	Degree
°C	Degree centigrade
mL	Milliliter
µL	Microliter
Min	Minute
mL	Milliliter
Mm	Millimeter

ACRONYMS

DFT	Density Functional Theory
NMR	Nuclear Magnetic Resonance
UV-vis	UV-visible Spectroscopy
ESI-MS	Electrospray Ionization- Mass Spectrometry
GC-MS	Gas Chromatography-Mass Spectrometry
TLC	Thin Layer Chromatography
SCXRD	Single crystal X-ray Diffraction
GOF	Goodness of fit
$CDCl_3$	Chloroform-*d*
DMSO-d_6	Dimethylsulphoxide-d_6
Ar	Argon
O_2	Oxygen
H_2	Dihydrogen
N_2	Nitrogen
O	*ortho*
M	*meta*
P	*para*
Ru	Ruthenium
Ir	Iridium
Os	Osmium
NHC	*N*-heterocyclic carbene
PPh_3	Triphenylphosphine
COD	1,4-cyclooctadiene
CO	Carbon Monoxide
DMSO	Dimethyl Sulphoxide
Mer	Meridional
Fac	Facial
TH	Transfer Hydrogenation

AAD	Acceptorless Dehydrogenation
ADC	Acceptorless Dehydrogenative Coupling
S	Singlet
D	Doublet
T	Triplet
Q	Quartet
m	Multiplet
Br	Broad
Ppm	Parts per million
r.t.	Room temperature
Temp	Temperature
TMS	Trimethylsilane
TON	Turnover number
TTN	Total turnover number
TOF	Turnover frequency
calc.	Calculated
cat.	Catalyst
cm^3	Cubic centimeter
Cy	Cyclohexane
Et	Ethyl
Me	Methyl
^{i}Pr	*iso*-propyl
^{t}Bu	*tert*-butyl
Ph	Phenyl
equiv.	Equivalents
gm	Gram
h	Hour
EtOH	Ethanol
MeOH	Methanol
DCM	Dichloromethane

CH_3CN	Acetonitrile
Et_2O	Diethyl ether
Atm	Atmospheres (pressure)

Chapter 1

Introduction and background: Ruthenium Pincer Complexes in Catalysis

Pincer complexes have evolved into preferred catalysts for a variety of difficult transformations in organic synthesis.*[1,2]* Pincer-based metal complexes are stable and have great reactivities towards homogenous catalytic systems, because of the rigid tri-dentate coordination with improved chemical and thermal stability. It can play a crucial role in the catalytic cycle by providing a suitable coordination site for the substrate, weakening selective bonds, or accepting/donating electrons and protons, for providing chemical stability.*[3]* Furthermore, the ligand can be tuned by modifying the central metal atom as well as the pincer ligand platform, depending on the steric/electronic environment and catalytic application.*[4–6]*

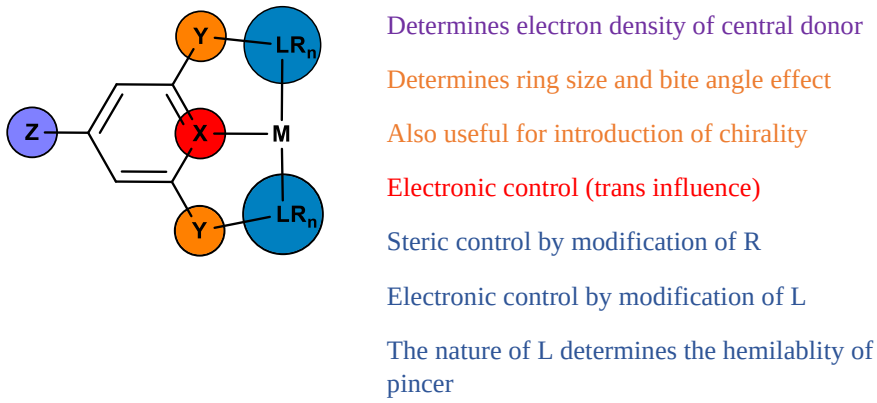

Typical groups, X = C, N; Y = $(CH_2)_n$, O, NH; L = P, N, O; Z = Halogen, R, RO

Figure 1.1 Basic aryl-based metalloid-pincer complex.

Pincer complexes exhibit a remarkably good balance between stability and reactivity, which can be controlled by systematic ligand modifications or variations of the metal center. Therefore, the reactivity, as well as the stability of Pyridine-based pincer transition metal complexes, can be enhanced.*[7–9]* Transition metal pincer complexes

have emerged as a highly promising set of catalysts for several processes over the last few years. They have been extensively used in energy production, dehydrogenative synthesis of high-value compounds, CO_2, N_2 hydrogenation, and carbon dioxide capture, as well as ammonia manufacturing processes. Therefore, this class of homogeneous catalysts improves the long-term viability of a wide range of chemical processes. The key advantages include strong catalytic activity under mild reaction conditions, low catalyst loading, high selectivity, and atom efficiency along with some drawbacks viz, catalyst deactivation and deterioration.*[10–13]*

1.1 Types of pincer ligands

1.1.1 ECE (E = N, P) and ENE (E = C, S, Se, P)-type pincer ligands

The monoanionic ECE pincer ligands have an aryl anionic carbon in the centre and ortho substituents with side-arm donor groups 'E,' where E is N or P. Consequently, ENE pincers feature a core nitrogen donor atom and a side-arm donor atom E, where E = C, S, Se, or P.

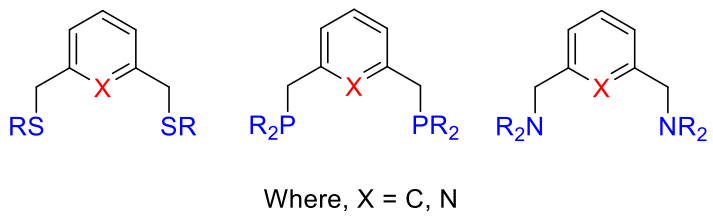

Figure 1.2 ECE and ENE-type pincer ligands.

These pincer systems are popular because of their aromatic backbone, due to which, synthesis of these complexes is easier as compared to other pincer ligands. The substituents around the coordination sites can induce chirality and impose steric requirements based on the ligand's coordination mode.*[14–19]*

1.1.2 PCP and PNP-type pincer ligands

Pincer ligands with phosphorous coordination sites, such as PCP and PNP, are found in a wide range of transition metal complexes and have been extensively used in catalysis. Phosphorus has been a popular donor

atom in organometallic chemistry, owing to its capacity to stabilize metal centres in both high and low oxidation states. Small modifications in the ligand backbone can have a huge impact on the reactivity of PCP and PNP pincer ligand metal complexes.

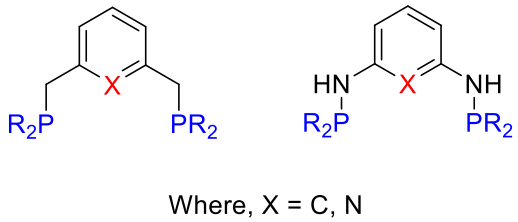

Figure 1.3 PCP and PNP-type pincer ligands.

A large number of metal complexes containing PCP and PNP pincers have been described in the literature. Generally, these complexes are synthesized by reacting the appropriate metal precursor with the pincer ligand in polar solvents such as CH_3CN under mild to moderate heating.*[10,20]*

1.1.3 SNS and SeNSe-type pincer ligands

Phosphorous has a strong nucleophilicity and reducing character at low oxidation states, however, requires bulky groups to ensure air stability. On the other hand, sulfur donor atoms have been utilized to modify the electronic features of several metal centres together with π-donor ligands owing to their capacity to accommodate both hard and soft auxiliary ligands and metal centres.

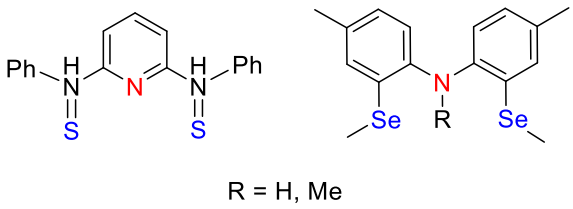

Figure 1.4 SNS and SeNSe-type pincer ligands.

SNS-pincer based complexes provide outstanding TONs under a variety of conditions in homogeneous catalytic transformations.*[21]*

1.1.4 NNN-type pincer ligands

NNN pincer ligands based on the bis(imino)pyridines, bis(pyridylimino)isoindoles, the 2,6-bis-amido-pyridine backbone, and 2,6-bis(5-tert-butyl-1H-pyrazol-3-yl) pyridine have been well studied.

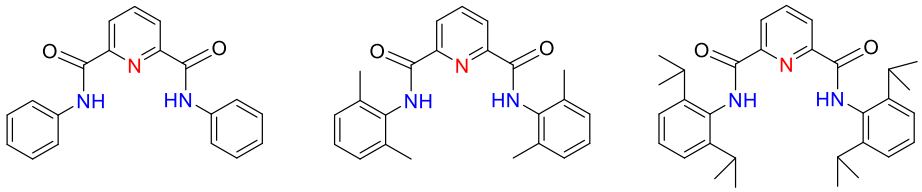

Figure 1.5 NNN-type pincer ligands.

Additionally, NNN pincer ligands are attractive scaffolds because of their ease of synthesis and modifications. Their metal complexes can easily synthesize from deprotonated ligands and have been used to stabilize first-row transition metals with high and low oxidation states.*[22]*

1.1.5 PCN and CNN-type pincer ligands

PCN and CNN-type ligands are two new categories of pincer ligands. PCN pincers ligands are mainly based on the pyrazolyl aminophosphine, aminophosphine–imidazoline, and (oxazolinyl)phenyl phosphinite templates. PCN and CNN ligand systems can provide a wide range of tunability for catalytic characteristics however, the intrinsic lack of symmetry of ligands requires a more difficult synthetic approach than the ECE and ENE type pincers. CNN-type pincer complexes are sensitive to air, as well as unstable to some extent, due to their *N*-arm hemilability. On the other hand, Pd complexes with PCN pincer ligand have excellent air and heat stability.

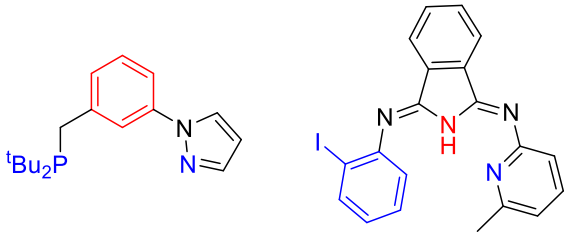

Figure 1.6 PCN and CNN-type pincer ligands.

Pd-PCN pincer systems have been reported as precatalysts for the Suzuki-Miyuara, Sonogashira, Hiyama, and vinyl-epoxide cross-coupling reactions. These complexes have also been used as enantioselective catalysts for the hydrophosphination of enones.*[22]*

1.1.6 NCN and CNC-type pincer ligands

In recent years, two major groups of pincer ligands have extensively emerged viz: NCN and CNC-type ligands. CNC pincer ligands bind in the terdentate mode with metal through two metal-carbon σ-bonds, whereas NCN ligand bind with one metal-carbon σ-bond. The metal-carbon σ-bond of these complexes offers increased stability, reducing metal leaching in homogeneous catalysis. The binding of NCN type pincers in terdentate meridional mode, exhibits fluxional behaviour in some situations, depending on the oxidation state of the metal centre. Fluxionality of these pincer ligands promotes variation in the binding modes, and this dynamic behaviour can be helpful in catalytic transformations, as the ligand adjusts to the steric and electronic demands of the reaction.

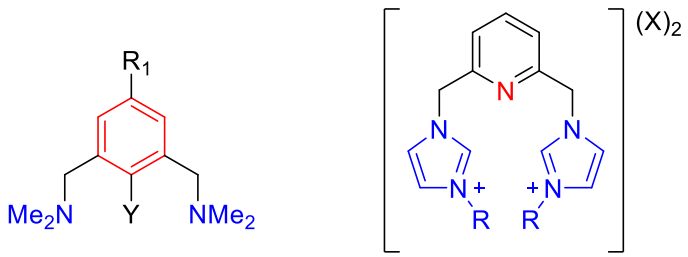

where, R_1 = H, NO_2, Ph
Y = H, Br

where, R = Me, IPr, n-butyl,
X = Cl, Br, BF_4

Figure 1.7 NCN and CNC-type pincer ligands.

Additionally, both mer-coordinated and the rare fac-coordinated CNC pincer complexes have been widely reported till now. The rare mode of facial coordination has been described in the literature in Ru(II) complexes with a lutidine-based NHC-backbone.*[3,8,9,12,23,24]*

1.3 Advantages of *N*-heterocyclic carbenes as a ligand

N-heterocyclic carbenes (NHCs) have been studied extensively since Arduengo's discovered 1,3-diadamantylimidazol-2- ylidene in 1991.

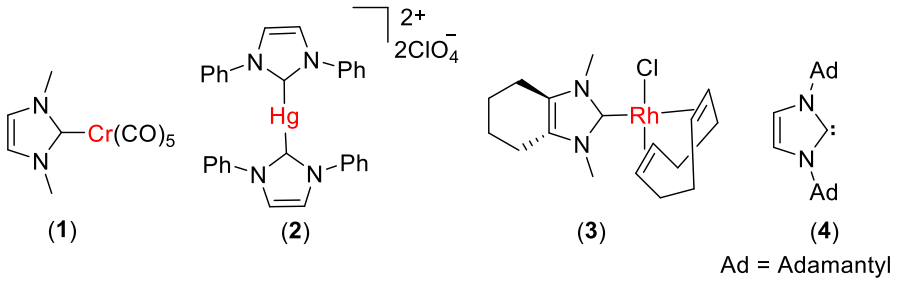

Figure 1.8 NHC–complexes and Arduengo's isolated free carbene.

The imidazolylidene framework carbene ligands dominate the other carbene ligands, by Grubbs second-generation metathesis catalyst which is serving as a golden example. Transition metal complexes with NHC carbene ligands have a specific role in catalysis than phosphines and imines ligand. NHCs were first used as ligands for transition metal complexes by Feile and Wanzlick. Nowadays, NHC carbenes are widely used as ligands on transition metals and give a wide range of transformations.*[25–28]*

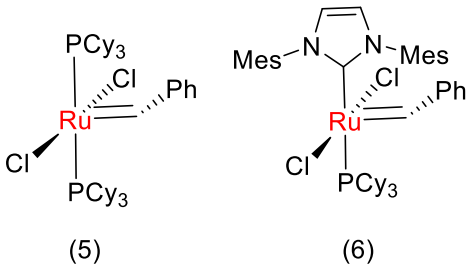

Figure 1.9 Grubbs first and second-generation metathesis catalysts.

Furthermore, recent research has shown the relevance of pi-back bonding from the metal to the NHC's empty p-orbitals, which is a crucial factor in the NHC's structure. NHC ligands are often considered as phosphine mimics, but they are usually more electron-rich and are more tightly bound to the metal center.

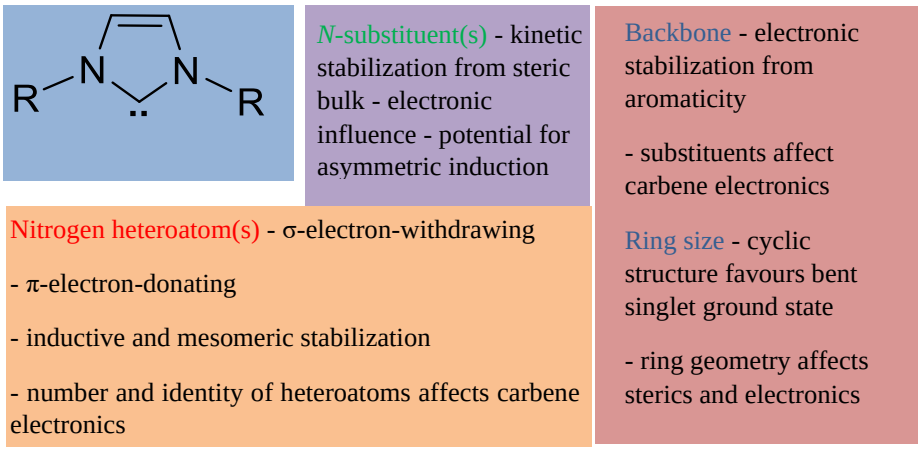

Figure 1.10 General structural features of NHCs.

Accordingly, organometallic complexes with NHC ligand have better reactivity, high stability and have a broader catalytic activity compared with phosphine ligands. Therefore, *N*-heterocyclic ligands have turned out to be more attractive in homogeneous catalysis.*[22,29–31]*

1.3 Advantages of pincer ligands based on *N*-heterocyclic carbenes

Pincer-type amine and phosphine complexes are well known however corresponding carbene analogs are less explored because of their ligand activation by a strong base.*[12,26,27,29,32]* It concludes there is a need for harsher conditions to generate the carbene pincer ligands in comparison to other pincer ligands. The incorporation of the NHC moiety into the pincer backbone has opened the opportunity for a variety of NHC-containing pincer-type ligands.

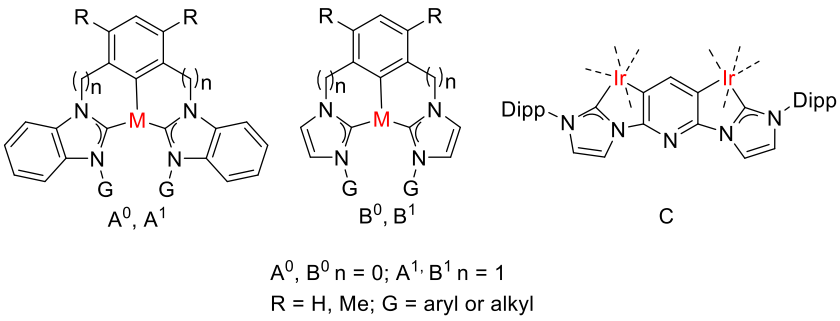

Figure 1.11 NHC-containing pincer complexes.

Pincer ligands with NHCs are the most demanding compounds owing to the high stability with a strong chelate effect which provides the most stable family of compounds with interesting catalytic behavior.*[33]*

1.4 Transition metal complexes based on NHCs containing CNC pincer ligands

Synthesis of the pincer ligand, as well as their metalation with different metals, is a challenging process. The easiest method is direct metalation which depends on the pincer ligand structure, metal source, reaction solvent, and other reaction conditions. The steric and electronic effects of ancillary ligands and substitution on the wingtips are also important aspects for the synthesis of the pincer complexes (Figure **1.12**).*[34,35]*

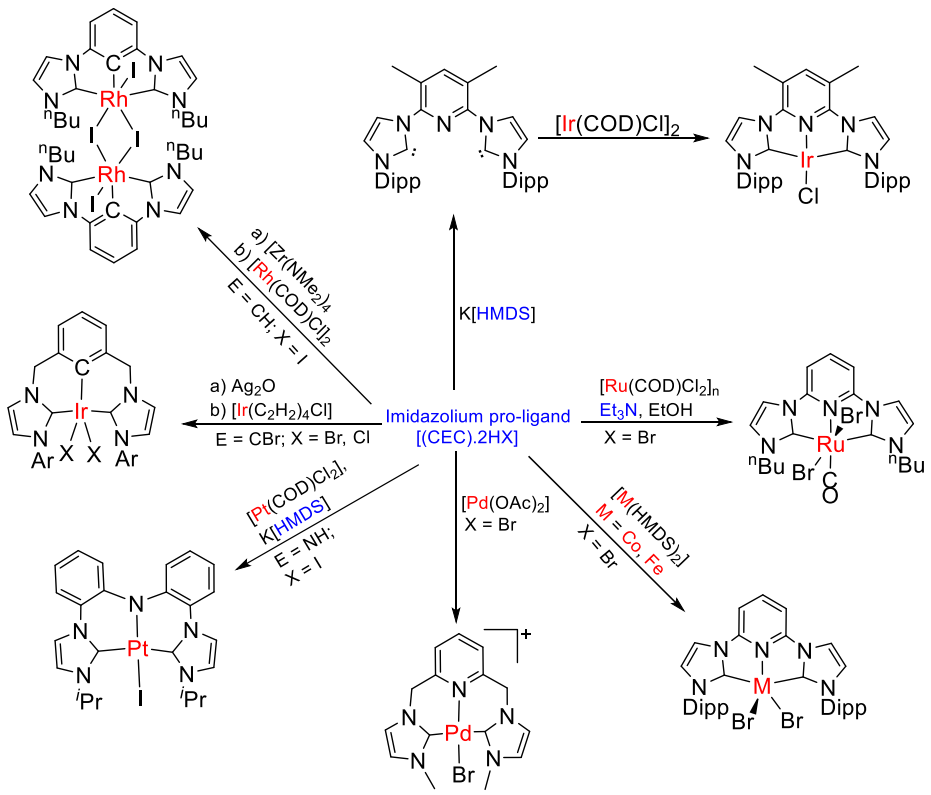

Scheme 1.1 Different approaches for the synthesis of NHC-based pincer complexes.

The robust pincer ligand platform provides high thermal stability to the transition metal complexes and has been applied to various catalytic reactions and small molecule activations, for example,

dinitrogen activation, labilization of the N-H bonds in ammonia, carbon dioxide reduction, and water splitting.*[36]*

Transition metal complexes with pincer-type ligands have been investigated widely and used in numerous catalytic transformations.*[36–38]* Among the variety of pincer ligands, pyridine–dicarbene pincer ligands with *N*-heterocyclic carbenes (CNC pincer ligands) have become highly popular ligands due to enhancement of the electron density at the coordinated metal and increased reactivity at the metal centre.*[39–41]*

1.5 Ruthenium complexes based on NHCs containing CNC pincer ligands

Ruthenium pincer complexes offer high efficiency and selectivity, as well as functional group tolerance, in comparison to standard ruthenium catalysts.*[42–45]* Ancillary ligands are important factors for the catalytic activity and stability of organometallic complexes.*[34,46–48]* Ru-CNC type pincer complexes are widely explored in the literature with a variety of co-ligands viz, halides, CO, phosphines, etc. The presence of different co-ligands at the ruthenium metal centre can influence the electronic and steric properties, also allow the interesting coordination chemistry. A variety of wing-tip substituents on the *N*-heterocycle are important structural features of CNC pincer-based complexes to influence the steric environment around the central metal atom. CNC pincer ligands with bulky aromatic substituents (Figure **1.12**) on the *N*-heterocycles are well-studied in literature *[8,9,24,41]* whereas examples with smaller, alkyl substituents are less explored till now.

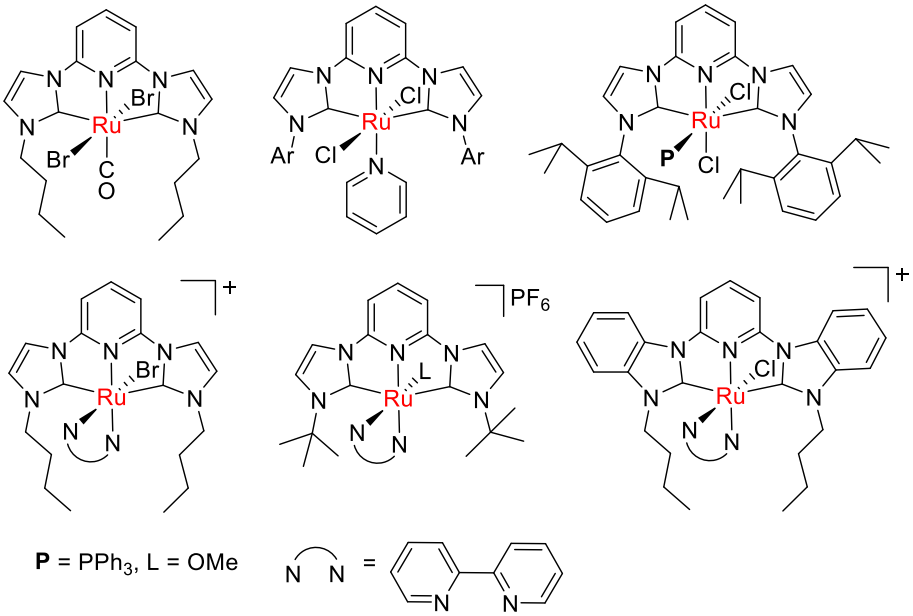

Figure 1.13 Ru-CNC pincer complexes with bulky *N*-wingtips.

A variety of wing-tip substituents on the *N*-heterocycle are important structural features of CNC pincer-based complexes to influence the steric environment around the central metal atom. CNC pincer ligands with bulky aromatic substituents (Figure **1.12**) on the *N*-heterocycles are well-studied in literature *[8,9,24,41]* whereas examples with smaller, alkyl substituents are less explored till now.

1.6 Application of transition metal complexes in transfer hydrogenation reactions

Catalytic hydrogenation and dehydrogenation reactions play an important role in both industrial processes and academic research. The reduction of carbonyl compounds to alcohols is an important process for the synthesis of fine chemicals, fragrances, agrochemicals, and medicines.*[49]* Traditionally, stoichiometric quantities of hydride reagents such as lithium aluminum hydride or sodium borohydride were used for hydrogenation reactions, although hydride reagents are extremely reactive and difficult to handle. Furthermore, metal hydride reduction produces hazardous waste as a by-product, proving the reduction process unsustainable for the environment. Catalytic

hydrogenation considerably increases the atom economy and sustainability of the reaction.*[50–53]*

Meerwein, Ponndorf, and Verley (MPV) have first reported the transfer hydrogenation (TH) of ketones catalyzed by aluminum alkoxides using isopropanol as a hydrogen source.*[54]* The reduction occurs via the coordination of the ketone and isopropanol simultaneously to the metal centre through a direct hydrogen transfer route and a cyclic six-membered transition state. (Scheme **1.2**).

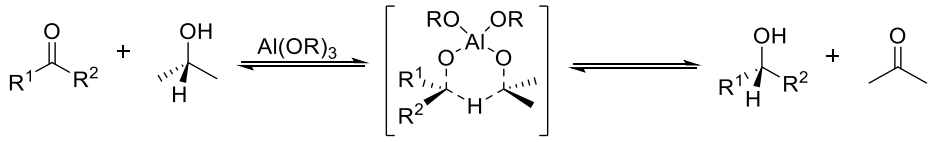

Scheme 1.2 Hydrogen transfer in Meerwein-Ponndorf-Verley reduction.

However, the MPV reduction has a few drawbacks, such as the use of a significant amount of aluminum reagent and unwanted side products. In the 1960s, Henbest, Mitchell, and colleagues reported the iridium-catalyzed reduction of cyclohexanones to alcohols in the presence of isopropanol.*[55,56]* A major breakthrough has happened after the discovery of transition metal complexes catalyzed the transfer hydrogenation of ketones.

The transfer hydrogenation of ketones through transition metal catalysts is usually accomplished by the hydridic method and involves a metal hydride intermediate. Transfer hydrogenation has emerged as a safe, eco-friendly, and versatile tool for the reduction of carbonyl compounds, compared to the commonly used reduction processes. TH has several advantages over other methods which involve high hydrogen pressure or hazardous reducing reagents. As a result, TH has become the focus of hydrogenation research in recent decades.*[49]*

It is well known that the electronic property of complex is an important factor to influence the catalytic activity of a catalyst, but the influence of electronic factors on the TH of ketones is not well-defined.

Therefore, it is very important to synthesize a family of complexes containing ligands with different electronic properties and elucidate the electronic effect on catalytic activity. Ruthenium catalysts are by far the most used catalyst for transfer hydrogenation processes. Ruthenium complexes have shown considerable potential in catalyzing transfer hydrogenation of ketone with isopropanol (^{i}PrOH) as the hydrogen donor and solvent.*[10,12,13,23]* TH are mainly useful for large-scale synthesis since these reactions avoid the need for high hydrogen pressure and potentially harmful reducing chemicals.

Selected examples of well-defined ruthenium complexes for transfer hydrogenation of ketones are listed in figure **1.13**. Ru-NHC pincer complexes were also utilized as a catalyst to speed up the TH processes significantly. Peris and Danopoulos have described pioneering work on TH employing Ru-NHC pincer complexes.*[23]* They have synthesized Ru "pincer" NHCs complexes with 2,6-bis(1-alkylimidazolium-3-yl)pyridine and Ru precursors. Later, Yu's group developed a novel Ru(II) compound with a "pincer"-type pyridyl-based (pyrazol-3-yl)-*N*-heterocyclic carbene ligand, showed good activity in the TH of ketones.

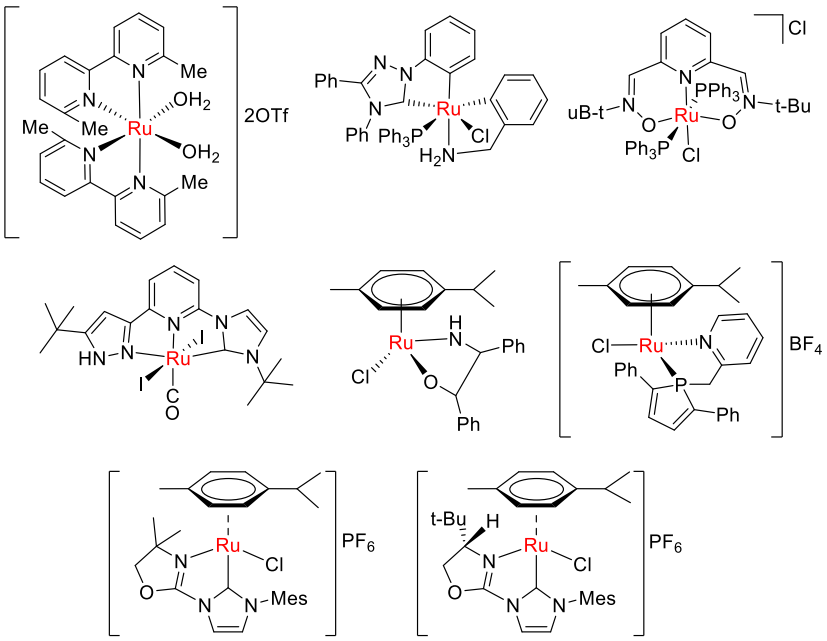

Figure 1.14 Ru complexes for transfer hydrogenation reactions.

Despite significant development in TH, numerous problems and hurdles remain unanswered in many reported works of literature. Transition metal catalysts are known in the literature for TH reactions as either limited in scope or lack the criteria for practical usage.

1.7 Application of transition metal complexes in the dehydrogenation of alcohols

The dehydrogenation of alcohols is a crucial step in the generation of a variety of compounds for both modest and large-scale industrial uses.*[20]* Traditional synthetic procedures for the dehydrogenation of alcohols have used stoichiometric amounts of oxidants such iodate, chlorite, and oxygen at high temperatures, resulting in copious waste. Transition metal-catalyzed dehydrogenation reactions have several advantages over traditional processes. The first homogeneous catalytic dehydrogenation of alcohols was illustrated by Charman and co-workers, using rhodium chloride as a catalyst.*[10]* Later, Robinson described the dehydrogenation of isopropanol, 1-butanol, ethanol, methanol, and glycerol with ruthenium complex $[Ru(OCOCF_3)_2(CO)(PPh_3)_2]$ in the presence of trifluoroacetic acid. Several advancements were executed over the subsequent years by combining different types of homogeneous catalysts and a variety of additives.

Homogeneous catalytic acceptorless alcohol dehydrogenation (AAD) is an effective and enduring approach for the synthesis of value-added chemicals and is far more atom and energy-efficient compared to traditional synthetic processes.*[57–61]*

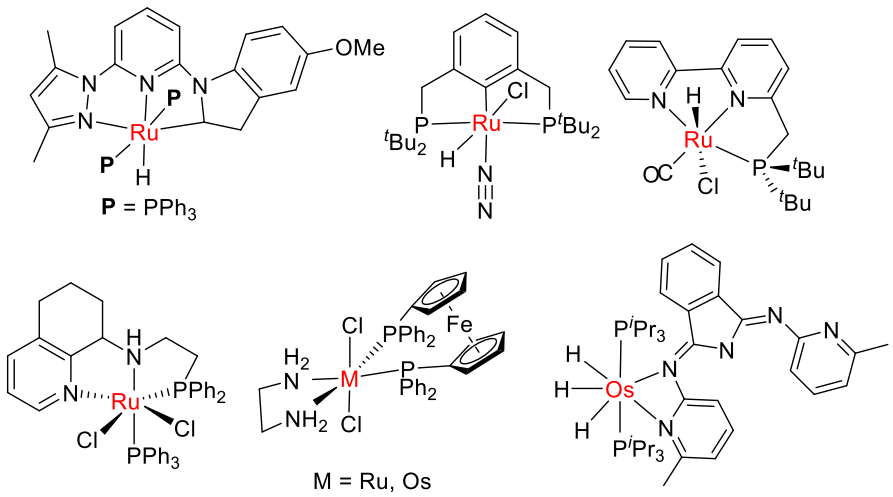

Figure 1.15 Ru and Os complexes for dehydrogenation reactions.

In terms of energy chemistry, the AAD reaction is particularly relevant which allows the synthesis of H_2 from renewable biomass-derived alcohols. AAD reaction is also an important step in the dehydrogenative coupling of primary and secondary alcohols, leading to alkylated ketones or alcohols.*[14,62–64]* In this regard, several research groups like Milstein, Barrata, Yu, Sun, Esteruelas, etc have been investigated AAD processes with a range of transition metal complexes, such as iridium, ruthenium, osmium, cobalt, nickel, and iron (Figure **1.15**).*[65–71]*

1.8 Importance of microwave in catalytic reactions

Microwaves have been used for the development of alternative economic, greener, and more sustainable approaches for organic reactions by modifying solvents, reagents, and catalysts. A substantial change in the number of significant and useful chemical transformations has been achieved using the microwave.*[72,73]*

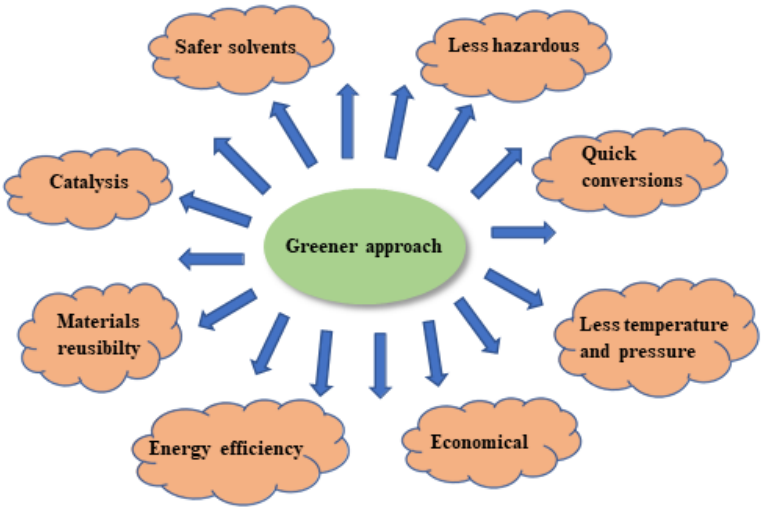

Figure 1.16 Green and sustainable approach towards MW-assisted reactions.

Microwave chemistry is gradually increasing interest in both industry and academia due to speeding up reactions, providing better yields and purity, and selectively with less energy.*[74]* Therefore, microwave-assisted synthesis rapidly becomes a promising approach in current chemical synthesis and drug discovery. Traditional organic synthesis methods often necessitate a longer heating time and a time-consuming apparatus system, resulting in excessive usage of solvents and reagents whereas, microwave irradiation can perform the reaction in minutes and reduce the reaction time.*[72]*

1.9 Application of transition metal complexes in dehydrogenative coupling reactions

Imine production is one of the most important reactions in organic and medicinal chemistry and has been employed in synthetic, biological, medicinal, and industrial applications as nitrogen sources.*[75–77]* Imines have been found to exhibit a variety of biological functions, including lipoxygenase inhibition, anti-inflammatory, anti-cancer, antibacterial, and antifungal properties.*[78,79]*

The reversible condensation of amines and aldehydes is one of organic chemistry's oldest and most common reactions, was first discovered by Hugo Schiff in 1864.*[80]* In the conventional approach,

desired imines were synthesized in the presence of an acid catalyst. Numerous extrinsic factors can affect the equilibrium between an imine and its precursors like solvent, concentration, pH, and temperature as well as steric and electronic aspects.

The reversible nature of the imine bond can be 'fixed' by reducing the C=N bond to convert a secondary amine.*[81]* Although the strategy of reductive amination is beneficial and widely used for the synthesis of substituted amines, however, lacks the reversibility factors that distinguish imines from nitrogenous compounds. Imines are used as electrophilic reagents in a variety of processes, including additions, condensations, asymmetric organocatalysis, cross-dehydrogenative couplings, and cycloadditions due to their high reactivity.*[82]*

Imines have been synthesized by self-condensation of primary amines, transition metal-assisted hydrogen transfer from secondary amines, direct nitroarenes and primary alcohols, oxidation of secondary amines, the aza-Wittig reaction, *N*-alkylation of ammonia with alcohols, and coupling of nitriles with amines.*[83]*

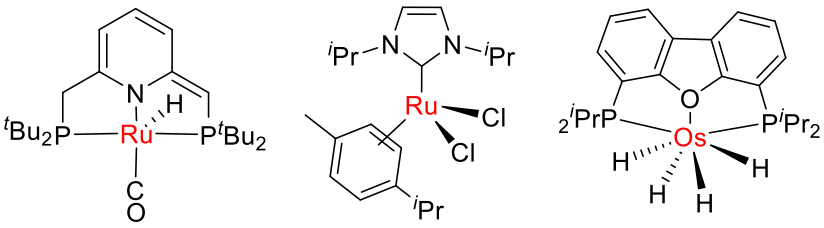

Figure 1.17 Ru and Os complexes for dehydrogenative coupling reactions.

Although numerous techniques have been developed in recent years, the synthesis of imines from alcohols and amines is highly demanding. Several research groups have made significant contributions to imine synthesis using a variety of transition metal complexes,*[75,78,84–90]* however, there are several drawbacks like high temperature and longer reaction time, etc. (Figure **1.17**).

1.10 Mechanism of hydrogenation/dehydrogenation reactions

Hydrogenations/dehydrogenations are the thoroughly investigated area in homogeneous catalysis for organic transformations.*[20,53,91]* Several strategies and mechanisms have been developed for homogeneously catalyzed hydrogenations/dehydrogenations reactions.*[92,93]* In recent days, hydrogenation/dehydrogenation catalysts have evolved from non-cooperative systems to metal-ligand cooperativity (MLC) systems. Cooperatively catalyzed hydrogenations/dehydrogenations proceed via Lewis base-transition metal (LB-TM) catalysts, Lewis acid-transition metal (LA-TM) catalysts, the ambiphilic cooperation mechanism, and the transition metal-transition metal (TM-TM) cooperation mechanisms (Figure **1.18**).*[91,94]* The involvement of the ligand, electronic properties of the metal centre, and the effect of the proton shuttle are significant elements for controlling the mechanistic preference.

The activation of H_2 and insertion of hydride into unsaturated molecules are referred as hydrogenations. On the other hand, dehydrogenations entail the removal of hydride from saturated compounds, followed by the release of H_2. The activation/release of H_2 and the insertion/elimination of hydride are the two main processes in these catalytic cycles. The reaction mechanisms underlying homogeneously catalyzed hydrogenations/dehydrogenations can be categorized according to the H_2 activation/release phase for convenience of understanding. Transition metal catalysts with a single reactive site worked on two non-cooperation mechanisms, the conventional oxidative addition/reductive elimination and bond metathesis processes (Figure **1.18**).*[95]* Bifunctional catalysts have two reactive sites and usually follow a cooperation-type mechanism.*[94]*

Hydrogenation and dehydrogenation reactions can be carried out with a concerted outer-sphere mechanism or inner-sphere mechanism. The outer-sphere mechanism, in the cooperative systems proceeds via

fascinating redox reactions, could provide one of the M-H moieties with proton followed by the reduction of the metal centre.

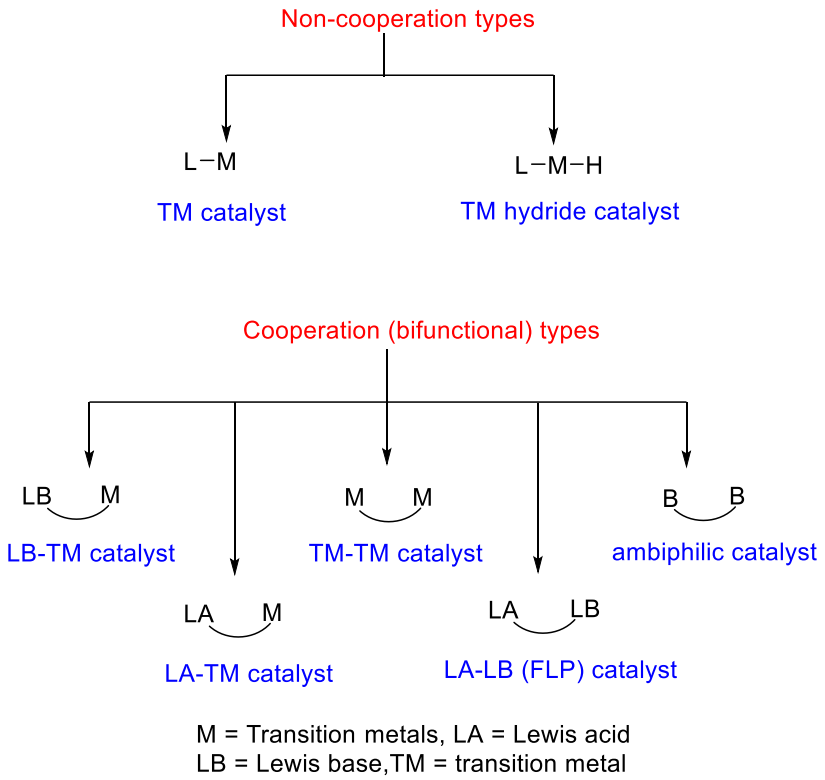

Figure 1.18 Homogeneous non-cooperation and cooperation hydrogenation/dehydrogenation catalysts.

As a result, the outer-sphere mechanism in cooperative systems is efficient for the transfer of a hydride and a proton. On the other hand, the hydrogenations/dehydrogenations in the inner-sphere mechanism occurred in a successive manner. The inner-sphere mechanisms are complicated and proceed via the following considerations: (1) the isomers of the hydride intermediates; (2) transition metal centre induced vacant site for the substrate; (3) terminal hydride or the bridging hydride prefers hydride insertion; and (4) the possibility of double activation of the substrate by two transition metal centres.*[95,96]* Ke and co-workers theoretically illustrated that the NNN ligand is unaffected during catalysis and does not function as a Lewis base due to the lack of tautomerization process. The Ru centre supports the inner-sphere hydride elimination process with the vacant site produced by the H_2 release.*[91]*

1.10.1 Non-cooperation mechanisms

The conventional oxidative addition/reductive elimination method and the bond metathesis (hydrogenolysis) process are two non-cooperation mechanisms for single-site transition metal catalysts. The classic oxidative addition/reductive elimination mechanism using Wilkinson's catalyst [$RhCl(PPh_3)_3$] is a well-known example of a single-site mechanism.*[97]*

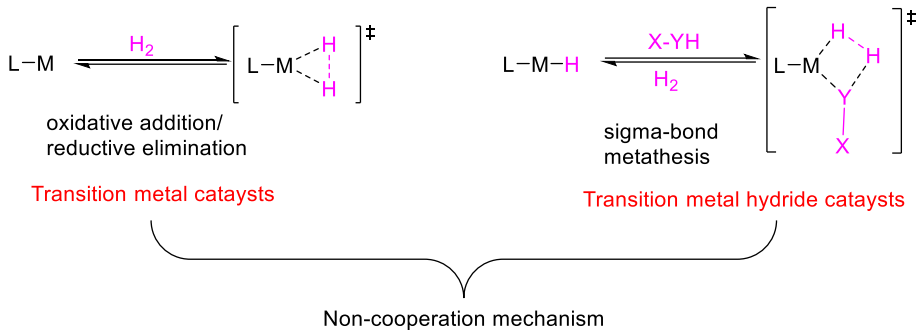

Figure 1.19 The schematic diagram of the non-cooperation mechanism.

The catalytic cycle begins with the coordination of H_2 to generate a dihydrogen complex, which is promptly oxidized to a dihydride intermediate. Further, the substrate moves to the metal centre for the hydride insertion, and finally, the reductive elimination yields the hydrogenated product with simultaneous catalyst renewal. The transition metal hydride (TM-H) catalysts are an alternative form of single-site transition metal catalyst, favour the bond metathesis mechanism to activate/release H_2.

1.10.2 Metal-ligand cooperation mechanisms

Pincer complexes have been exploited for effective metal-ligand cooperativity (MLC) in recent years, providing novel opportunities for homogenous catalysis. There are various MLC mechanisms described in the literature, and one of the categories is the aromatization–dearomatization process. The catalytic mechanism of transition metal complexes relies on the aromatization–dearomatization of the pyridine ring. Noyori's bifunctional transition metal catalysts efficiently catalyze the hydrogenation of diverse polar unsaturated substrates, by heterolytic

activation of H_2 via metal-amine-amide cooperativity.*[98–100]* The pyridine-based pincer complexes can be deprotonated at the pyridinyl-methylene carbon, resulting in the dearomatized pyridine ring. The dearomatized five-coordinate pincer complexes react stoichiometrically with various substrates (HX; X = H, C, OH, OR, NH_2, NR_2). Simultaneously, heterolytic activation of polar and nonpolar chemical bonds, where the proton is accepted by the dearomatized "methine carbon" and the X-fragments occupies the empty coordination site on the ruthenium.

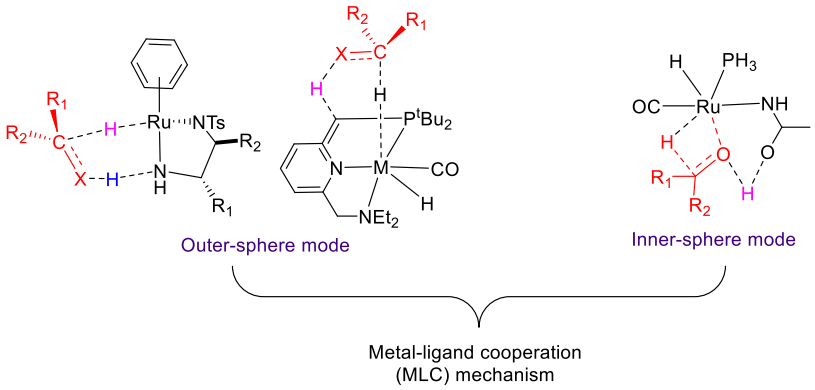

Figure 1.20 The schematic diagram of metal-ligand cooperation (MLC) mechanism.

The electronic properties and specific geometry of the metal complexes have a considerable effect on the catalyst's mechanistic pathways. The driving force of the pincer ligand originated by tautomerization from aromatization/dearomatization mechanism is an essential aspect of the MLC process.

Alternatively, transfer hydrogenation, acceptorless dehydrogenation, and dehydrogenative coupling reactions are the most atom-efficient methods for the conversion of various functional groups. However, complexes with CNC-pincer ligands are less studied for hydrogenation/dehydrogenation catalytic reactions. The present thesis describes the synthesis, characterization, and catalytic activities of new cationic Ru(II)-NHC pincer complexes with smaller alkyl wingtips and a variety of co-ligands.

1.11 Objectives of thesis

To date, many transition metal-based catalysts have been explored for hydrogenation and dehydrogenation reactions because of their higher stability and high activity towards many conversions.*[101–105]* On comparing the other transition metals, ruthenium has an exceptional array of catalysis properties and has found several applications, however ruthenium complexes with CNC-pincer ligands are less explored for TH, AAD, and ADC catalytic reactions. A few metal complexes with CNC pincer ligands have been explored mainly with bulkier aromatic substituents on the nitrogen atom, which prohibits to observe the electronic effects of other ancillary ligands present in the coordination sphere. In the present work we have tried to fill this gap of synthetic chemistry of CNC pincer complexes and their utilization. The basic objective of the current thesis are:

- To synthesize the Ru-CNC pincer complexes with smaller alkyl NHC wingtips.
- To study the reactivity and structure-property relationship.
- To study the effect of various co-ligands on the reactivity of these complexes.
- To utilize the acquired knowledge for tuning catalytic behaviour.

1.12 Organization of the Thesis

The present thesis describes the synthesis, characterization, and catalytic activities of new cationic Ru(II)-NHC pincer complexes with smaller alkyl wingtips and a variety of co-ligands.

In **chapter 1** Literature survey on ruthenium, pincer complexes have been described.

In **chapter 2** Synthesis and characterization of Ru(II)-NHC Pincer Complexes has been extensively studied.

In **chapter 3** Catalytic Hydrogenation and Dehydrogenation of ketones and alcohols by using Ru(II)-NHC Pincer Complexes has been described.

In **chapter 4** Dehydrogenative coupling reactions under conventional and microwave heating using Ru(II)-NHC Pincer Complexes have been studied.

In **chapter 5** Role of Ancillary Ligands in Selectivity for Catalytic Applications has been explored.

In **chapter 6** summary of this thesis has been described with various future scopes.

1.13 References

[1] Peris E., Crabtree R.H. (2018), Key factors in pincer ligand design, *Chem. Soc. Rev.*, 47, 1959–1968 (https://doi.org/10.1039/C7CS00693D).

[2] Piccirilli L., Lobo Justo Pinheiro D., Nielsen M. (2020), Recent Progress with Pincer Transition Metal Catalysts for Sustainability, *Catalysts*, 10, 773 (https://doi.org/10.3390/catal10070773).

[3] Valdés H., García-Eleno M. A., Canseco-Gonzalez D., Morales-Morales D. (2018), Recent Advances in Catalysis with Transition-Metal Pincer Compounds, *ChemCatChem*, 10, 3136–3172 (https://doi.org/10.1002/cctc.201702019).

[4] van Koten G. (1989), Tuning the reactivity of metals held in a rigid ligand environment, *Pure Appl. Chem.*, 61, 1681–1694 (https://doi.org/10.1351/pac198961101681).

[5] Danopoulos A. A., Pugh D., Smith H., Saßmannshausen J. (2009), Structural and Reactivity Studies of “Pincer” Pyridine Dicarbene Complexes of Fe0: Experimental and Computational Comparison of the Phosphine and NHC Donors, *Chem. Eur. J.*, 15, 5491–5502 (https://doi.org/10.1002/chem.200900027).

[6] Lawrence M. A. W., Green K.-A., Nelson P. N., Lorraine S. C. (2018), Review: Pincer ligands—Tunable, versatile, and applicable, *Polyhedron*, 143, 11–27 (https://doi.org/10.1016/j.poly.2017.08.017).

[7] Serra D., Cao P., Cabrera J., *et al.* (2011), Development of Platinum(II) and -(IV) CNC Pincer Complexes and Their Application in a Hydrovinylation Reaction, *Organometallics*, 30, 1885–1895 (https://doi.org/10.1021/om101128f).

[8] Peris E., Loch J. A., Mata J., Crabtree R. H. (2001), A Pd complex of a tridentate pincer CNC bis-carbene ligand as a robust homogenous Heck catalyst, *Chem. Commun.*, 201–202 (https://doi.org/10.1039/B008038L).

[9] Danopoulos A. A., Braunstein P., Saßmannshausen J., *et al.* (2020), "Pincer" Pyridine–Dicarbene–Iridium and -Ruthenium Complexes and Derivatives Thereof, *Eur. J. Inorg. Chem.*, 2020, 3359–3369 (https://doi.org/10.1002/ejic.202000429).

[10] Gunanathan C., Milstein D. (2014), Bond Activation and Catalysis by Ruthenium Pincer Complexes, *Chem. Rev.*, 114, 12024–12087 (https://doi.org/10.1021/cr5002782).

[11] Balaraman E., Srimani D., Diskin-Posner Y., Milstein D. (2015), Direct Synthesis of Secondary Amines From Alcohols and Ammonia Catalyzed by a Ruthenium Pincer Complex, *Catal. Lett.*, 145, 139–144 (https://doi.org/10.1007/s10562-014-1422-2).

[12] Hernández-Juárez M., López-Serrano J., Lara P., *et al.* (2015), Ruthenium(II) Complexes Containing Lutidine-Derived Pincer CNC Ligands: Synthesis, Structure, and Catalytic Hydrogenation of C=N bonds, *Chem. Eur. J.*, 21, 7540–7555 (https://doi.org/10.1002/chem.201406040).

[13] Younus H. A., Su W., Ahmad N., *et al.* (2015), Ruthenium Pincer Complexes: Synthesis and Catalytic Applications, *Adv. Synth. Catal.*, 357, 283–330 (https://doi.org/10.1002/adsc.201400777).

[14] Wei Z., Aguirre A. de, Junge K., *et al.* (2018), Benyzl Alcohol Dehydrogenative Coupling Catalyzed by Defined Mn and Re PNP Pincer Complexes – A Computational Mechanistic Study, *Eur. J. Inorg. Chem.*, 2018, 4643–4657 (https://doi.org/10.1002/ejic.201800674).

[15] Wang Z., Sugiarti S., Morales C. M., et al. (2006), Catalytic hydroxylation of 1-propanol by platinum NCN and PCP pincer complexes using $CuCl_2$ as oxidant, *Inorganica Chimica Acta*, 359, 1923–1928 (https://doi.org/10.1016/j.ica.2005.09.016).

[16] Ben-Ari E., Leitus G., Shimon L. J. W., Milstein D. (2006), Metal−Ligand Cooperation in C−H and H2 Activation by an Electron-Rich PNP Ir(I) System: Facile Ligand Dearomatization−Aromatization as Key Steps, *J. Am. Chem. Soc.*, 128, 15390–15391 (https://doi.org/10.1021/ja066411i).

[17] Benito-Garagorri D., Kirchner K. (2008), Modularly Designed Transition Metal PNP and PCP Pincer Complexes based on Aminophosphines: Synthesis and Catalytic Applications, *Acc. Chem. Res.*, 41, 201–213 (https://doi.org/10.1021/ar700129q).

[18] Fan L., Yang L., Guo C., *et al.* (2004), N−C Cleavage in Pincer PNP Complexes of Palladium, *Organometallics*, 23, 4778–4787 (https://doi.org/10.1021/om049651k).

[19] Takenaka K., Minakawa M., Uozumi Y. (2005), NCN Pincer Palladium Complexes: Their Preparation via a Ligand Introduction Route and Their Catalytic Properties, *J. Am. Chem. Soc.*, 127, 12273–12281 (https://doi.org/10.1021/ja052780n).

[20] Crabtree R. H. (2017), Homogeneous Transition Metal Catalysis of Acceptorless Dehydrogenative Alcohol Oxidation: Applications in Hydrogen Storage and to Heterocycle Synthesis, *Chem. Rev.*, 117, 9228–9246 (https://doi.org/10.1021/acs.chemrev.6b00556).

[21] Lawrence M. A. W., Green K.-A., Nelson P. N., Lorraine S. C. (2018), Review: Pincer ligands—Tunable, versatile and applicable, *Polyhedron*, 143, 11–27 (https://doi.org/10.1016/j.poly.2017.08.017).

[22] Younus H. A., Ahmad N., Su W., Verpoort F. (2014), Ruthenium pincer complexes: Ligand design and complex synthesis, *Coord. Chem. Rev.*, 276, 112–152 (https://doi.org/10.1016/j.ccr.2014.06.016).

[23] Poyatos M., Mata J. A., Falomir E., *et al.* (2003), New Ruthenium(II) CNC-Pincer Bis(carbene) Complexes: Synthesis and Catalytic Activity, *Organometallics*, 22, 1110–1114 (https://doi.org/10.1021/om020817w).

[24] Danopoulos A. A., Winston S., Motherwell W. B. (2002), Stable N-functionalised 'pincer' bis carbene ligands and their ruthenium complexes; synthesis and catalytic studies, *Chem. Commun.*, 1376–1377 (https://doi.org/10.1039/B202814J).

[25] Zhao Q., Meng G., Nolan S. P., Szostak M. (2020), *N*-Heterocyclic Carbene Complexes in C–H Activation Reactions, *Chem. Rev.*, 120, 1981–2048 (https://doi.org/10.1021/acs.chemrev.9b00634).

[26] Díez-González S., Marion N., Nolan S. P. (2009), *N*-Heterocyclic Carbenes in Late Transition Metal Catalysis, *Chem. Rev.*, 109, 3612–3676 (https://doi.org/10.1021/cr900074m).

[27] Andrew R. E., González-Sebastián L., Chaplin A. B. (2016) NHC-based pincer ligands: carbenes with a bite, *Dalton Trans.*, 45, 1299–1305 (https://doi.org/10.1039/C5DT04429D).

[28] Hopkinson M. N., Richter C., Schedler M., Glorius F. (2014), An overview of *N*-heterocyclic carbenes, *Nature*, 510, 485–496 (https://doi.org/10.1038/nature13384).

[29] Crudden C. M., Allen D. P. (2004), Stability and reactivity of *N*-heterocyclic carbene complexes, *Coord. Chem. Rev.*, 248, 2247–2273 (https://doi.org/10.1016/j.ccr.2004.05.013).

[30] Dorta R., Stevens E. D., Scott N. M., *et al.* (2005), Steric and Electronic Properties of *N*-Heterocyclic Carbenes (NHC): A Detailed Study on Their Interaction with $Ni(CO)_4$, *J. Am. Chem. Soc.*, 127, 2485–2495 (https://doi.org/10.1021/ja0438821).

[31] Albrecht M., Miecznikowski J. R., Samuel A., *et al.* (2002), Chelated Iridium(III) Bis-carbene Complexes as Air-Stable Catalysts for Transfer Hydrogenation, *Organometallics*, 21, 3596–3604 (https://doi.org/10.1021/om020338x).

[32] Taniguchi W., Ito J., Yamashita M. (2020), CNC-pincer iron complexes containing a bis(*N*-heterocyclic carbene)Amido ligand: Synthesis and application to catalytic hydrogenation of alkenes, *J. Organomet. Chem.*, 923, 121436 (https://doi.org/10.1016/j.jorganchem.2020.121436).

[33] Wang Y., Zhang B., Guo S. (2021), Transition Metal Complexes Supported by *N*-Heterocyclic Carbene-Based Pincer Platforms: Synthesis, Reactivity and Applications, *Eur. J. Inorg. Chem.*, 2021, 188–204 (https://doi.org/10.1002/ejic.202000911).

[34] Muñoz S. B., Fleischauer V. E., Brennessel W. W., Neidig M. L. (2018), Combined Effects of Backbone and N-Substituents on Structure, Bonding, and Reactivity of Alkylated Iron(II)-NHCs, *Organometallics*, 37, 3093–3101 (https://doi.org/10.1021/acs.organomet.8b00466).

[35] Nielsen D. J., Cavell K. J., Skelton B. W., White A. H. (2006), Methyl-palladium(II) complexes of pyridine-bridged bis(nucleophilic heterocyclic carbene) ligands: Substituent effects on structure, stability, and catalytic performanc, *Inorganica Chimica Acta*, 359, 1855–1869 (https://doi.org/10.1016/j.ica.2005.07.049).

[36] Piccirilli L., Lobo Justo Pinheiro D., Nielsen M. (2020), Recent Progress with Pincer Transition Metal Catalysts for Sustainability, *Catalysts,* 10, 773 (https://doi.org/10.3390/catal10070773).

[37] Gunanathan C., Milstein D. (2014), Bond Activation and Catalysis by Ruthenium Pincer Complexes, *Chem. Rev.,* 114, 12024–12087 (https://doi.org/10.1021/cr5002782).

[38] Younus H. A., Ahmad N., Su W., Verpoort F. (2014) Ruthenium pincer complexes: Ligand design and complex synthesis, *Coord. Chem. Rev.,* 276, 112–152 (https://doi.org/10.1016/j.ccr.2014.06.016).

[39] Serra D., Cao P., Cabrera J., *et al.* (2011), Development of Platinum(II) and -(IV) CNC Pincer Complexes and Their Application in a Hydrovinylation Reaction, *Organometallics,* 30, 1885–1895 (https://doi.org/10.1021/om101128f).

[40] Das S., Rodrigues R. R., Lamb R. W., *et al.* (2019), Highly Active Ruthenium CNC Pincer Photocatalysts for Visible-Light-Driven Carbon Dioxide Reduction, *Inorg. Chem.,* 58, 8012–8020 (https://doi.org/10.1021/acs.inorgchem.9b00791).

[41] Mrutu A., Goldberg K. I., Kemp R. A. (2010), Synthesis and characterization of a dinuclear Ni complex containing a bridging CNC pincer ligand, *Inorganica Chimica Acta,* 364, 115–119 (https://doi.org/10.1016/j.ica.2010.08.049).

[42] Kamdar J. M., Grotjahn D. B. (2019) An Overview of Significant Achievements in Ruthenium-Based Molecular Water Oxidation Catalysis, *Molecules,* 24, 494 (https://doi.org/10.3390/molecules24030494).

[43] Das B., Jia C., Ching K., *et al.* (2020) Ruthenium Complexes in Homogeneous and Heterogeneous Catalysis for

Electroreduction of CO_2, *ChemCatChem*, 12, 1292–1296 (https://doi.org/10.1002/cctc.201902020).

[44] Udvardy A., Joó F., Kathó Á. (2021), Synthesis and catalytic applications of Ru(II)-phosphaurotropine complexes with the use of simple water-soluble Ru(II)-precursors, *Coord. Chem. Rev.*, 438, 213871 (https://doi.org/10.1016/j.ccr.2021.213871).

[45] Sole R., Bortoluzzi M., Spannenberg A., *et al.* (2019), Synthesis, characterization and catalytic activity of novel ruthenium complexes bearing NNN click based ligands, *Dalton Trans.*, 48, 13580–13588 (https://doi.org/10.1039/C9DT01822K).

[46] Fleischauer V. E., Iii S. B. M., Neate P. G. N., *et al.* (2018), NHC and nucleophile chelation effects on reactive iron(II) species in alkyl–alkyl cross-coupling, *Chem. Sci.*, 9, 1878–1891 (https://doi.org/10.1039/C7SC04750A).

[47] Liu Y., Luo L., Xiao J., *et al.* (2015), Four-Coordinate Iron(II) Diaryl Compounds with Monodentate N-Heterocyclic Carbene Ligation: Synthesis, Characterization, and Their Tetrahedral-Square Planar Isomerization in Solution, *Inorg. Chem.*, 54, 4752–4760 (https://doi.org/10.1021/acs.inorgchem.5b00138).

[48] Zanardi A., Peris E., Mata J. A. (2008), Alkenyl-functionalized NHC iridium-based catalysts for hydrosilylation, *New J. Chem.*, 32, 120–126 (https://doi.org/10.1039/B707280E).

[49] Wang D., Astruc D. (2015), The Golden Age of Transfer Hydrogenation, *Chem. Rev.*, 115, 6621–6686 (https://doi.org/10.1021/acs.chemrev.5b00203).

[50] Albrecht M., Miecznikowski J. R., Samuel A., *et al.* (2002), Chelated Iridium(III) Bis-carbene Complexes as Air-Stable

Catalysts for Transfer Hydrogenation, *Organometallics*, 21, 3596–3604 (https://doi.org/10.1021/om020338x).

[51] Garg N., Paira S., Sundararaju B. (2020), Efficient Transfer Hydrogenation of Ketones using Methanol as Liquid Organic Hydrogen Carrier, *ChemCatChem*, 12, 3472–3476 (https://doi.org/10.1002/cctc.202000228).

[52] Murayama H., Heike Y., Higashida K., *et al.* (2020), Iridium-Catalyzed Enantioselective Transfer Hydrogenation of Ketones Controlled by Alcohol Hydrogen-Bonding and sp^3-C−H Noncovalent Interactions, *Adv. Synth. Catal.*, 362, 4655–4661 (https://doi.org/10.1002/adsc.202000615).

[53] Abubakar S., Bala M. D. (2020), Transfer Hydrogenation of Ketones Catalyzed by Symmetric Imino-N-heterocyclic Carbene Co(III) Complexes, *ACS Omega*, 5, 2670–2679 (https://doi.org/10.1021/acsomega.9b03181).

[54] Graauw C. F. de, Peters J. A., Bekkum H. van, Huskens J. (1994), Meerwein-Ponndorf-Verley Reductions and Oppenauer Oxidations: An Integrated Approach, *Synthesis*, 1994, 1007–1017 (https://doi.org/10.1055/s-1994-25625).

[55] Trocha-Grimshaw J., Henbest H. B. (1967) ,Catalysis of the transfer of hydrogen from propan-2-ol to αβ-unsaturated ketones by organoiridium compounds. A carbon–iridium compound containing a chelate keto-group, *Chem. Commun. (London)*, 544–544 (https://doi.org/10.1039/C19670000544).

[56] Wiesner T., Leypold M., Steinmaurer A., *et al.* (2020), Synthesis of Stable Dianionic Cyclic Silenolates and Germenolates, *Organometallics*, (https://doi.org/10.1021/acs.organomet.0c00385).

[57] Shahane S., Fischmeister C., Bruneau C. (2012), Acceptorless ruthenium catalyzed dehydrogenation of alcohols to ketones and esters, *Catal. Sci. Technol.*, 2, 1425–1428 (https://doi.org/10.1039/C2CY20066J).

[58] Chang W, Gong X., Wang S., *et al.* (2017), Acceptorless dehydrogenation and dehydrogenative coupling of alcohols catalysed by protic NHC ruthenium complexes, *Org. Biomol. Chem.*, 15, 3466–3471 (https://doi.org/10.1039/C7OB00542C)

[59] Pandey P., Dutta I., Bera J. K. (2016), Acceptorless Alcohol Dehydrogenation: A Mechanistic Perspective, *Proc. Natl. Acad. Sci., India, Sect. A Phys. Sci.*, 86, 561–579 (https://doi.org/10.1007/s40010-016-0296-7).

[60] Fuse H., Mitsunuma H., Kanai M. (2020), Catalytic Acceptorless Dehydrogenation of Aliphatic Alcohols, *J. Am. Chem. Soc.*, 142, 4493–4499 (https://doi.org/10.1021/jacs.0c00123).

[61] Wang Z., Pan B., Liu Q., et al. (2017), Efficient acceptorless dehydrogenation of secondary alcohols to ketones mediated by a PNN-Ru(II) catalyst, *Catal. Sci. Technol.*, 7, 1654–1661 (https://doi.org/10.1039/C7CY00342K).

[62] Zhang L., Raffa G., Nguyen D. H., *et al.* (2016), Acceptorless dehydrogenative coupling of alcohols catalysed by ruthenium PNP complexes: Influence of catalyst structure and of hydrogen mass transfer, *J. Catal.*, 340, 331–343 (https://doi.org/10.1016/j.jcat.2016.06.001).

[63] Siddiki S. M. A. H., Toyao T., Shimizu K. (2018), Acceptorless dehydrogenative coupling reactions with alcohols over heterogeneous catalysts, *Green Chem.*, 20, 2933–2952 (https://doi.org/10.1039/C8GC00451J).

[64] Nguyen D. H., Trivelli X., Capet F., *et al.* (2017), Manganese Pincer Complexes for the Base-Free, Acceptorless Dehydrogenative Coupling of Alcohols to Esters: Development, Scope, and Understanding, *ACS Catal.*, 7, 2022–2032 (https://doi.org/10.1021/acscatal.6b03554).

[65] Srimani D., Ben-David Y., Milstein D. (2013), Direct Synthesis of Pyrroles by Dehydrogenative Coupling of β-Aminoalcohols with Secondary Alcohols Catalyzed by Ruthenium Pincer Complexes, *Angew. Chem. Int. Ed.*, 52, 4012–4015 (https://doi.org/10.1002/anie.201300574).

[66] Ryabchuk P., Agapova A., Kreyenschulte C., *et al.* (2019), Heterogeneous nickel-catalysed reversible, acceptorless dehydrogenation of *N*-heterocycles for hydrogen storage, *Chem. Commun.*, 55, 4969–4972 (https://doi.org/10.1039/C9CC00918C).

[67] Pan B., Liu B., Yue E., et al. (2016), A Ruthenium Catalyst with Unprecedented Effectiveness for the Coupling Cyclization of γ-Amino Alcohols and Secondary Alcohols, *ACS Catal.*, 6, 1247–1253 (https://doi.org/10.1021/acscatal.5b02638).

[68] Peña-López M., Neumann H., Beller M. (2014), Ruthenium-Catalyzed Synthesis of Indoles from Anilines and Epoxides, *Chem. Eur. J.*, 20, 1818–1824 (https://doi.org/10.1002/chem.201304432).

[69] Mukherjee A., Nerush A., Leitus G., et al. (2016), Manganese-Catalyzed Environmentally Benign Dehydrogenative Coupling of Alcohols and Amines to Form Aldimines and H_2: A Catalytic and Mechanistic Study, *J. Am. Chem. Soc.*, 138, 4298–4301 (https://doi.org/10.1021/jacs.5b13519).

[70] Michlik S., Kempe R. (2013), Regioselectively Functionalized Pyridines from Sustainable Resources. *Angew. Chem. Int. Ed.*, 52, 6326–6329 (https://doi.org/10.1002/anie.2013019190).

[71] Fujita K., Tamura R., Tanaka Y., *et al.* (2017), Dehydrogenative Oxidation of Alcohols in Aqueous Media Catalyzed by a Water-Soluble Dicationic Iridium Complex Bearing a Functional *N*-Heterocyclic Carbene Ligand without Using Base, *ACS Catal.*, 7, 7226–7230 (https://doi.org/10.1021/acscatal.7b02560).

[72] Priecel P., Lopez-Sanchez J. A. (2019), Advantages and Limitations of Microwave Reactors: From Chemical Synthesis to the Catalytic Valorization of Biobased Chemicals, *ACS Sustainable Chem. Eng.*, 7, 3–21 (https://doi.org/10.1021/acssuschemeng.8b03286).

[73] Rong Z.-Q., Yu Z., Weng C., *et al.* (2020), Dynamic Kinetic Asymmetric Amination of Alcohols Assisted by Microwave: Stereoconvergent Access to Tetralin- and Indane-Derived Chiral Amines, *ACS Catal.*, 10, 9464–9475 (https://doi.org/10.1021/acscatal.0c02468).

[74] Rathi A. K., Gawande M. B., Zboril R., Varma R. S. (2015), Microwave-assisted synthesis – Catalytic applications in aqueous media, *Coord. Chem. Rev.*, 291, 68–94 (https://doi.org/10.1016/j.ccr.2015.01.011).

[75] Belowich M. E., Stoddart J. F. (2012), Dynamic imine chemistry, *Chem. Soc. Rev.*, 41, 2003–2024 (https://doi.org/10.1039/C2CS15305J).

[76] Reeves J. T., Visco M. D., Marsini M. A., *et al.* (2015), A General Method for Imine Formation Using $B(OCH_2CF_3)_3$, *Org. Lett.*, 17, 2442–2445 (https://doi.org/10.1021/acs.orglett.5b00949).

[77] Li R.-J., Ling C., Lv W.-R., *et al.* (2021), Cyclometalated Half-Sandwich Iridium(III) Complexes: Synthesis, Structure, and Diverse Catalytic Activity in Imine Synthesis Using Air as the Oxidant, *Inorg. Chem.,* 60, 5153–5162 (https://doi.org/10.1021/acs.inorgchem.1c00174).

[78] Chai H., Yu K., Liu B., *et al.* (2020), A Highly Selective Manganese-Catalyzed Synthesis of Imines under Phosphine-Free Conditions, *Organometallics,* 39, 217–226 (https://doi.org/10.1021/acs.organomet.9b00769).

[79] Huang M., Liu J., Li Y., *et al.* (2020), Recent advances on *N*-heterocyclic carbene transition metal complexes for dehydrogenative catalysis using alcohols, *Catalysis Today, (*https://doi.org/10.1016/j.cattod.2020.10.022).

[80] Schiff H. (1864), Mittheilungen aus dem Universitätslaboratorium in Pisa: Eine neue Reihe organischer Basen, *Justus Liebigs Annalen der Chemie,* 131, 118–119 (https://doi.org/10.1002/jlac.18641310113).

[81] Cheng C., Brookhart M. (2012), Iridium-Catalyzed Reduction of Secondary Amides to Secondary Amines and Imines by Diethylsilane, *J. Am. Chem. Soc.,* 134, 11304–11307 (https://doi.org/10.1021/ja304547s).

[82] Choudhury L. H., Parvin T. (2011), Recent advances in the chemistry of imine-based multicomponent reactions (MCRs), *Tetrahedron,* 67, 8213–8228 (https://doi.org/10.1016/j.tet.2011.07.020).

[83] Martin S. F. (2009) Recent applications of imines as key intermediates in the synthesis of alkaloids and novel nitrogen heterocycles, *Pure and Applied Chemistry,* 81, 195–204 (https://doi.org/10.1351/PAC-CON-08-07-03).

[84] Pavel O. D., Goodrich P., Cristian L., *et al.* (2015), Direct oxidation of amines to nitriles in the presence of ruthenium-terpyridyl complex immobilized on ILs/SILP, *Catal. Sci. Technol.,* 5, 2696–2704 (https://doi.org/10.1039/C5CY00011D).

[85] Sindhuja E., Ramesh R. (2014), Direct synthesis of imines from primary alcohols and amines using an active ruthenium(II) NNN–pincer complex, *Tetrahedron Lett.,* 55, 5504–5507 (https://doi.org/10.1016/j.tetlet.2014.08.035).

[86] Wu S., Zhang H., Cao Q., *et al.* (2021), Efficient imine synthesis via oxidative coupling of alcohols with amines in an air atmosphere using a mesoporous manganese–zirconium solid solution catalyst, *Catal. Sci. Technol.,* 11, 810–822 (https://doi.org/10.1039/D0CY02288H).

[87] Tseng K.-N. T., Rizzi A. M., Szymczak N. K. (2013), Oxidant-Free Conversion of Primary Amines to Nitriles, *J. Am. Chem. Soc.,* 135, 16352–16355 (https://doi.org/10.1021/ja409223a).

[88] Eizawa A., Nishimura S., Arashiba K., *et al.* (2018), Synthesis of Ruthenium Complexes Bearing PCP-Type Pincer Ligands and Their Application to Direct Synthesis of Imines from Amines and Benzyl Alcohol, *Organometallics,* 37, 3086–3092 (https://doi.org/10.1021/acs.organomet.8b00465).

[89] Cui X., Li W., Junge K., *et al.* (2020), Selective Acceptorless Dehydrogenation of Primary Amines to Imines by Core–Shell Cobalt Nanoparticles, *Angew. Chem. Int. Ed.,* 59, 7501–7507 (https://doi.org/10.1002/anie.201915526).

[90] Maggi A., Madsen R. (2012), Dehydrogenative Synthesis of Imines from Alcohols and Amines Catalyzed by a Ruthenium *N*-Heterocyclic Carbene Complex, *Organometallics,* 31, 451–455 (https://doi.org/10.1021/om201095m).

[91] Ke Z., Li Y., Hou C., Liu Y. (2018), Homogeneously catalyzed hydrogenation and dehydrogenation reactions – From a mechanistic point of view, *Phy. Sci. Rev. 3,* (https://doi.org/10.1515/psr-2017-0038).

[92] Filonenko G. A., Putten R. van, Hensen E. J. M., Pidko E. A. (2018), Catalytic (de)hydrogenation promoted by non-precious metals – Co, Fe and Mn: recent advances in an emerging field, *Chem. Soc. Rev.,* 47, 1459–1483 (https://doi.org/10.1039/C7CS00334J).

[93] Chen X., Yang X. (2016), Mechanistic Insights and Computational Design of Transition-Metal Catalysts for Hydrogenation and Dehydrogenation Reactions, *The Chemical Record*, 16, 2364–2378 (https://doi.org/10.1002/tcr.201600049).

[94] Zell T., Milstein D. (2015), Hydrogenation and Dehydrogenation Iron Pincer Catalysts Capable of Metal–Ligand Cooperation by Aromatization/Dearomatization, *Acc. Chem. Res.,* 48, 1979–1994 (https://doi.org/10.1021/acs.accounts.5b00027).

[95] Liu Y., Yue X., Luo C., *et al.* (2019), Mechanisms of Ketone/Imine Hydrogenation Catalyzed by Transition-Metal Complexes, *Energy & Environmental Materials,* 2, 292–312 (https://doi.org/10.1002/eem2.12050).

[96] Gunanathan C., Milstein D. (2011), Metal–Ligand Cooperation by Aromatization–Dearomatization: A New Paradigm in Bond Activation and "Green" Catalysis, *Acc. Chem. Res.,* 44, 588–602 (https://doi.org/10.1021/ar2000265).

[97] Ginsberg P. A. (1990), *Inorganic syntheses,* (https://doi.org/10.1002/9780470132586).

[98] Ohkuma T., Ooka H., Hashiguchi S., *et al.* (1995), Practical Enantioselective Hydrogenation of Aromatic Ketones, *J. Am. Chem. Soc.*, 117, 2675–2676 (https://doi.org/10.1021/ja00114a043).

[99] Noyori R., Ohkuma T. (2001), Asymmetric Catalysis by Architectural and Functional Molecular Engineering: Practical Chemo- and Stereoselective Hydrogenation of Ketones, *Angew. Chem. Int. Ed.*, 40, 40–73 (https://doi.org/10.1002/1521-3773(20010105)40:1<40::AID-ANIE40>3.0.CO;2-5).

[100] Sandoval C. A., Ohkuma T., Muñiz K., Noyori R. (2003), Mechanism of Asymmetric Hydrogenation of Ketones Catalyzed by BINAP/1,2-Diamine−Ruthenium(II) Complexes, *J. Am. Chem. Soc.*, 125, 13490–13503 (https://doi.org/10.1021/ja030272c).

[101] Corma A., Navas J., Sabater M. J. (2012), Coupling of Two Multistep Catalytic Cycles for the One-Pot Synthesis of Propargylamines from Alcohols and Primary Amines on a Nanoparticulated Gold Catalyst, *Chem. Eur. J.*, 18, 14150–14156 (https://doi.org/10.1002/chem.201201837).

[102] Yang Y., Qin A., Zhao K., *et al.* (2016), Design and Synthesis of Alanine Triazole Ligands and Application in Promotion of Hydration, Allene Synthesis and Borrowing Hydrogen Reactions, *Adv. Synth. Catal.*, 358, 1433–1439 (https://doi.org/10.1002/adsc.201600141).

[103] Tang C.-H., He L., Liu Y.-M., *et al.* (2011), Direct One-Pot Reductive *N*-Alkylation of Nitroarenes by using Alcohols with Supported Gold Catalysts, *Chem. Eur. J.*, 17, 7172–7177 (https://doi.org/10.1002/chem.2011003930).

[104] Yan T., Feringa B. L., Barta K. (2016), Benzylamines via Iron-Catalyzed Direct Amination of Benzyl Alcohols, *ACS Catal.*, 6:381–388 (https://doi.org/10.1021/acscatal.5b02160).

[105] Mehta A., Thaker A., Londhe V., Nandan S. R. (2014), Reinvestigating Raney nickel mediated selective alkylation of amines with alcohols via hydrogen autotransfer methodology, *Appl. Catal. Gen.*, 478, 241–251 (https://doi.org/10.1016/j.apcata.2014.04.009).

Chapter 2

Cationic Ru(II)-NHC Pincer Complexes: Synthesis and Characterization

2.1 Introduction

Pincer ligands have gained popularity due to their versatility and ease of application. Typically, pincer ligands are tridentate ligands that bind firmly to three adjacent coplanar sites of a metal centre in a meridional fashion. As a result, two stable cyclometallated rings are formed which can be five-membered, six-membered, or both five- and six-membered rings. Pincer-type compounds have become increasingly important in chemistry, since the pioneering work reported by Shaw and Van Koten in the 1970s using the PCP and NCN type tridentate ligands for the synthesis of pincer metal complexes,*[1-2]* Soon after, the field turned into an emerging class of new pincer ligand motifs, such as the NCN, PCP, PNN, PNP and CNC.*[3-6]* Pincer ligands containing NHCs' comprises strong electron-donating ability and give steric and electronic tunability which allows a wide range of structural modifications as well as high thermal stability.*[7-10]* Pincer complexes have made synthetic transformations feasible that were thought to be difficult at the time of their discovery. Several approaches have been investigated in the synthesis of target pincer metal complexes.*[11]*

In general, the synthetic pathways comprise either (i) metalation of the desired pincer ligand and coordination of remaining co-ligands occurs simultaneously in which, formation of metal-carbon σ-bond takes place in the final step or (ii) an initial metalation step where firstly only desired pincer ligand is coordinated to the metal to form metal-carbon σ-bond and then after coordination of the remaining co-ligands with metal centre takes place. These synthesis approaches

were referred to as "*metal introduction*" and "*ligand introduction*" routes, respectively.*[12]* It is worth mentioning that factors like steric effects at coordination sites, instability of particular functional groups, and regioselectivity control, play a curial role in determining the appropriate synthesis strategy.*[13–15]* Each method shows different advantages and drawbacks based on the nature of the pincer ligand, the metal precursor, and the reaction considerations. The pincer ligand platform provides robust transition metal complexes with high thermal stability. These metal complexes have been utilized for numerous catalytic reactions and small molecule activations, for example, dinitrogen activation, labilization of the N-H bonds in ammonia, carbon dioxide reduction, and water splitting. Among the variety of pincer ligands, pyridine–dicarbene pincer ligands with *N*-heterocyclic carbenes (CNC pincer ligands) have become popular ligands which enhance the electron density at the coordinated metal and increase the reactivity of the metal centre. For the synthesis of the CNC pincer complexes, four general types of methods are reported in the literature: (1) direct metalation, (2) oxidative addition, (3) transmetalation using metal transfer agents, and (4) transcyclometalation pathways.*[15]*

Ruthenium pincer complexes can be used as a significant catalyst due readily availability in different stable oxidation states and different coordination geometries viz. square pyramidal, trigonal-bipyramidal and octahedral. Ru-CNC type pincer complexes are widely communicated in the literature with various co-ligands including halides, CO and phosphines *[16-17]* however, the presence of different co-ligands can influence the electronic and steric properties and show interesting coordination chemistry.

1,5-cyclooctadiene (COD) is a well-known ligand in organometallic chemistry and generally form weak metal–COD bonds in complexes. While a few Ru-CNC pincer complexes with PPh_3, CO and halides as co-ligand are known (Figure **2.1**),*[18-20]* complexes with COD as co-ligand are rare.*[21]*

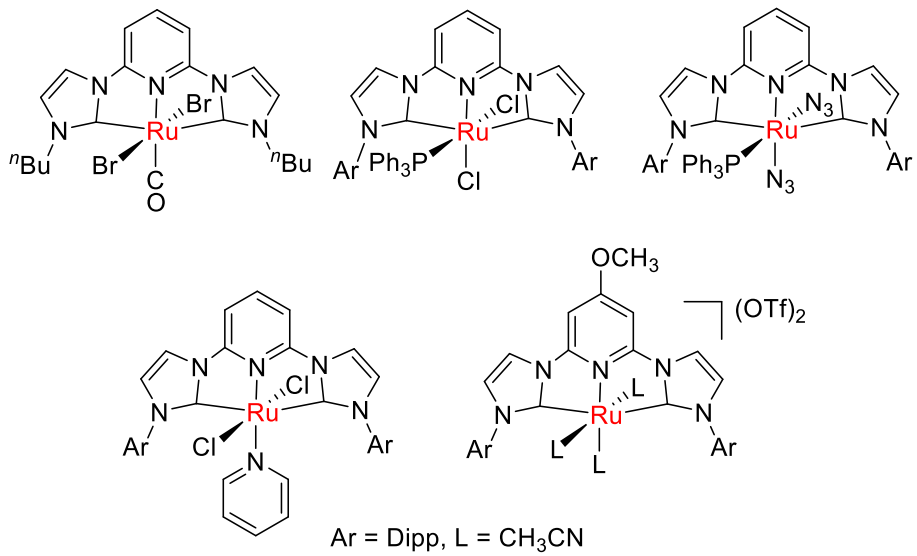

Figure 2.1 Reported CNC pincer ruthenium complexes with different co-ligands.

The high lability of the COD ligand makes metal-COD complexes as useful precursors in organometallic synthesis, as well as appears as a limiting factor in isolating metal-COD complexes in presence of other ligands. For example, a CO ligand has been speculated to originate from the ethanol solvent during the synthesis of Ru-CNC complex from $[Ru(COD)Cl_2]_n$ as Ru-precursor; however, the COD ligand was not bonded in the final complex.*[16]*

The molecular structures of majority of transition metal – COD complexes reveal a chelate type η^2:η^2-(Z,Z)-COD ligand, adopting a "boat" conformation or as a bridging η^2:η^2-(Z,Z)-COD ligand, with a "chair" conformation. Modifications of the metal-coordinated COD ligand involving C-H activation as well as insertion into metal-hydride bonds resulting into κ^1:η^3 binding modes (Figure **2.2**).*[22-29]* The "non-innocent" nature of a metal-bound COD ligand has also been documented during the synthesis of Ir-complexes with *N*-heterocyclic ligand.*[29]* However, examples of complexes with the non-chelating, non-bridging η^2-COD ligand are scarce.*[30]* The low coordination number Ni(0) complex reported by Hofmann et al. has been shown to

have an η^2-COD ligand with a significantly elongated alkene bond indicating a stronger Ni – (η^2-COD) bond.*[30]*

Different possible configurations and conformations of free COD molecules have been the subject of several experimental and theoretical investigations. Earlier the (Z,Z)-isomer has been shown to be the predominant configuration with the "twisted-boat" as the most stable conformer followed by the "chair" and "skew" conformations.*[31-37]* In 2015, Kunz and co-workers investigated the conformational interconversion of metal-bound COD ligand in an "encapsulated" Ir(I) complex using NMR and computational studies.*[38]*

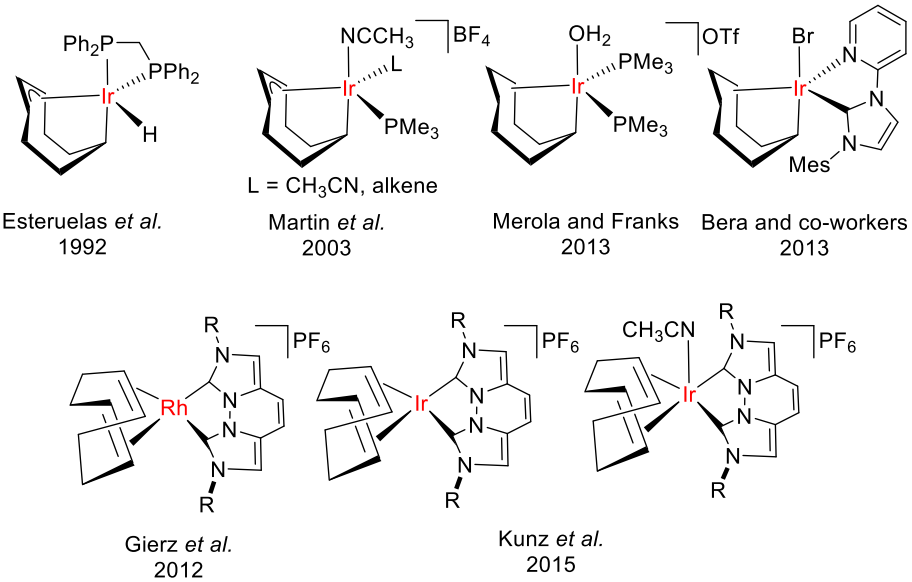

Figure 2.2 Reported κ^1,η^3-C_8H_{12} and COD complexes.

In general, the final composition and structure of Ru-CNC complexes depend on the Ru-precursor, reagents used for the carbene generation as well as the type of wing-tip substituents on the *N*-heterocycle. The substitution on the *N*-heterocycles of CNC pincer ligands can influence the steric environment around the central metal atom. Aromatic substituents are the most common examples reported in the literature, while smaller, alkyl substituents are somewhat less explored.

We have recently started investigating the synthesis and reactivities of complexes with pyridine–dicarbene CNC pincer ligands having smaller alkyl substituents. We aimed to utilise the robustness provided by the CNC pincer ligand, allowing the freedom to have a variety of bulkier co-ligands. In this series we have prepared cationic Ru(II)-CNC pincer complexes (CNC = 2,6-bis(1-methylimidazol-2-ylidene)-pyridine), [Ru(CNC)(CO)(PPh_3)Cl]X [X = Cl (**1a**), PF_6 (**1b**)], [Ru(CNC)(PPh_3)$_2$Cl]X [X = Cl (**2a**), PF_6 (**2b**)], [Ru(CNC)(PPh_3)$_2$H]X [X = Cl (**3a**), PF_6 (**3b**)] [Ru(CNC)(η^2:η^2-COD)Cl]X (COD = 1,5-cyclooctadiene), [X = Cl (**4a**), PF_6 (**4b**)], [Ru(CNC)(η^2-COD)Cl_2] (**5**), [Ru(CNC)(DMSO)$_2$Cl]X [X = Cl (**6a**) and PF_6 (**6b**)], where the COD ligand remains coordinated to the Ru in η^2:η^2- and η^2-fashion in **4a/b** and **5**, respectively.

2.2 Results and Discussion

2.2.1 Synthesis of Ru(II)-NHC Pincer complexes.

The imidazolium ligand precursor **CNC·2HBr** was prepared by the reported procedure in literature *[39]* and characterized by ^{1}H and ^{13}C NMR spectra. The reaction of imidazolium precursor with Ag_2O, in methanol, affords silver-carbene complex, which undergoes transmetallation with Ru-precursors in situ to give Ru-CNC complexes (Scheme **2.1**). When the silver-carbene complex was treated with the [RuHCl(CO)(PPh_3)$_3$] precursor (**Ru1**) for 24 h, **1a** was obtained. Spectroscopic data (^{31}P NMR and LC-MS) of the crude reaction mixture indicates that **2a** and **3a** are formed as a minor impurity during the synthesis of **1a**. The dissociation of the CO ligand and subsequent coordination of the PPh_3 ligand, present in the solution, may result in the formation of complex **2a**. The complex **2a**, subsequently, undergoes chloride ligand substitution by a methoxy ligand generated from methanol solvent followed by β-hydride elimination leading to the synthesis of the hydride complex **3a**. Compound **1b** was precipitated out by treating the crude reaction mixture of **1a** with

NH_4PF_6 in methanol. The minor impurities from **1a** and **1b** were removed upon precipitation followed by recrystallisation.

A similar reaction condition was used to synthesise **2a** from $[RuCl_2(PPh_3)_3]$ as the Ruthenium source (**Ru2**). However, the synthesis of compound **2a** is always accompanied by *in situ* generations of **3a**. Compound **2a** was attempted to purify in the form of **2b**, by precipitation using NH_4PF_6. However, we are unable to separate compound **3b** from **2b**, which also precipitated during the anion exchange. The mixture of complexes **2a** and **3a** can be converted to **3a**, cleanly, as shown in scheme 2 (vide infra). Spectroscopically pure **2a** was obtained by alumina-gel chromatography followed by recrystallization. Further, anion exchange of **2a** and **3a** by precipitation using NH_4PF_6 gives **2b** and **3b**, respectively.

Similarly, $[RuCl_2(COD)]_n$ and $[RuCl_2(DMSO)_4]$ was used as the Ruthenium source (**Ru3** and **Ru4**) for the synthesis of **4a** and **6a**. Complexes **4b** and **6b** were precipitated out by treating the crude reaction mixture of **4a** and **6a** with NH_4PF_6 in methanol, respectively. Complex **5** was also isolated during the crystallization of **4a** from the crude reaction mixture.

All the complexes are characterized by IR, Mass, and multinuclear NMR spectroscopic techniques. In the ^1H NMR spectrum, the ligand precursor **CNC·2HBr** exhibit a singlet at 10.59 ppm due to imidazolium proton and the disappearance of this peak indicated the carbene generation during complex formation.

The C=O stretching frequency of 1956 cm^{-1} and 1954 cm^{-1} in **1a** and **1b**, respectively, are significantly larger than 1922 cm^{-1} of Ru-CNC pincer *[17]* and comparable with previously reported CNC complexes 1952 cm^{-1} and 1954 cm^{-1}.*[40]* Complex **1a** showed signals for ESI^+ LC-MS at *m/z* 632.12 and 666.08 assigned to $[\mathbf{1a}\text{-}2Cl+H]^+$ and $[\mathbf{1a}\text{-}Cl]^+$, respectively. ^1H NMR of **1a** and **1b** are almost identical

with the pyridine protons appearing as a doublet at 8.44 and a triplet 8.11 ppm, while two doublets are observed at 7.77 and 7.56 ppm for the imidazol-2-ylidene protons. In the ^{13}C NMR spectra, the carbene carbon signals of **1a** and **1b** appear at 192 ppm. ^{31}P NMR spectrum of **1a** and **1b** showed peaks at 40.59 ppm and 43.27 ppm, respectively, for PPh_3 ligand, comparable with previously reported NNN pincer complexes.*[41]*

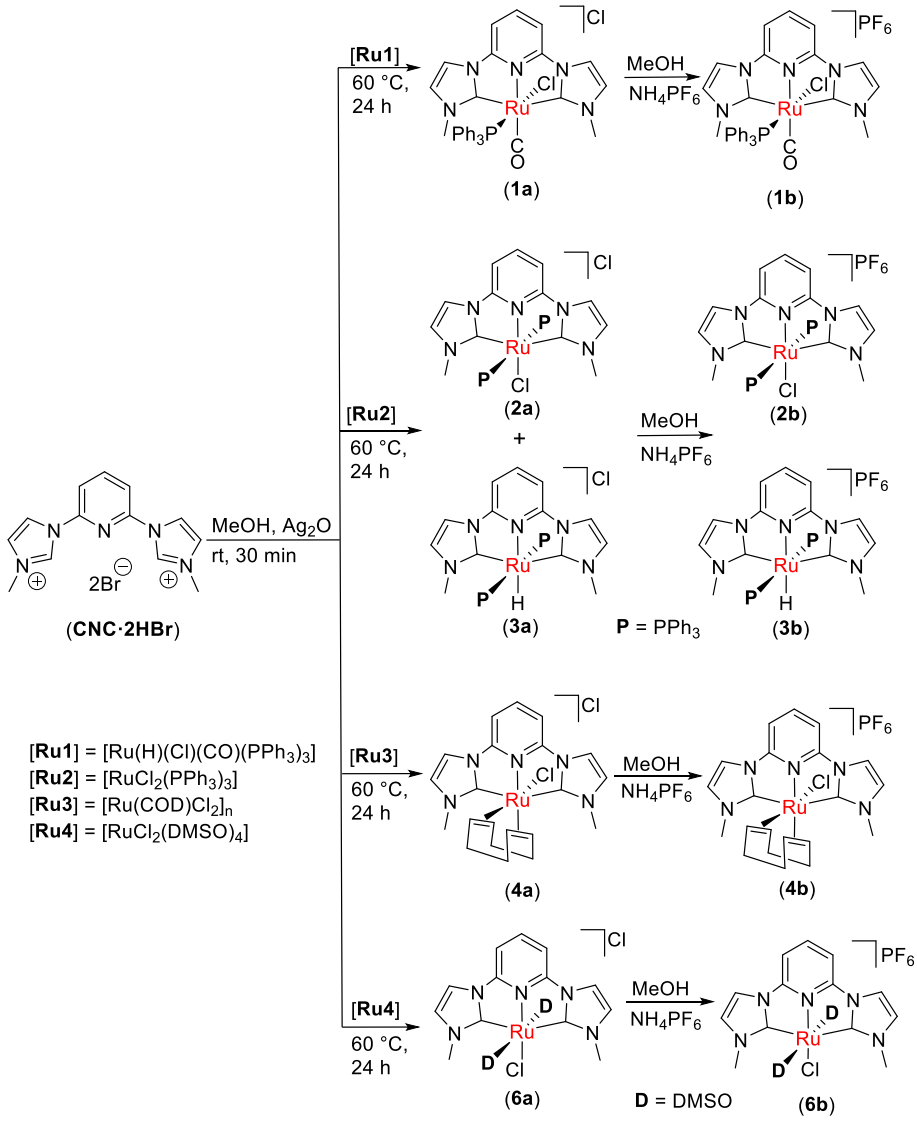

Scheme 2.1 Synthesis of CNC pincer ruthenium complexes **1–6**.

Compound **2a** and **2b** show ESI^+ LC-MS signal at *m/z* 900.00, assigned to $[\mathbf{2a/b\text{-}Cl}]^+$. In ^1H NMR of **2a**, one doublet and triplet appear at 8.31 and 7.36 ppm for pyridine protons, whereas imidazol-2-

ylidene protons were shown as two doublets at 7.49 and 7.06 ppm. In the case of **2b**, pyridine and imidazolium protons are slightly shifted to downfield than **2a,** however, methyl protons appear at the same value 3.59 ppm for both the complexes. Interestingly, ^{31}P NMR spectra of complexes **2a** and **2b** show two singlets at 31.79 ppm, 26.60 ppm and 31.70 ppm, 26.57 ppm, while no dissociation of PPh_3 was observed. The signal at 26.60 ppm was ruled out to be due to $O{=}PPh_3$ by recording the NMR after the addition of $O{=}PPh_3$ in the NMR sample of **2a** and **2b**. These complexes are expected to exhibit one singlet in the ^{31}P NMR considering the same chemical environment for the two phosphorus atoms. These two singlets in the ^{31}P NMR are attributed to the generation of two species in solution due to the dissociation of the coordinated chloride ligand. This assumption is confirmed by mass analysis where ESI$^+$ LC-MS signal at *m/z* 432.59 is observed and assigned to [**2a-Cl**]$^{2+}$/[**2b-Cl**]$^{2+}$.

ESI$^+$ LC-MS of the crude reaction mixture for the synthesis of **4a** displayed signals at *m/z* 484.08 and 528.03 assigned to [**4a**]$^+$ with a chloride or bromide ligand in the coordination sphere, respectively, indicating that a mixture of complexes with both types of halides coordinated to Ru is formed. Purification by crystallization gave pure **4a** with chloride ligand. Analysis of the mass data for crude reaction mixture also indicates no hydrogenation of the COD ligand under the reaction conditions and no evidence of a complex similar to [Ru(CNC)(Cyclooctene)(CO)(Cl)]Cl,*[25]* reported earlier. Mass spectrogram of **4b** is identical to that of **1a**, indicating identical cationic complex parts.

^{1}H NMR of complex **4a** and **4b** are nearly identical with six signals in the range 4.40-1.77 ppm for the COD ligand: two apparent singlets for the alkene hydrogens and four multiplets for the “axial” and “equatorial” hydrogens of two types of methylene groups. In addition, signals for imidazol-2-ylidene and pyridine ring hydrogens as well as *N*-methyl groups are also observed at expected chemical shifts.

The ^{13}C NMR of **4a** and **4b** are also the same containing the expected number of peaks with two signals for the methylene groups of the COD ligand and one for the *N*-methyl of NHC ligand in the alkyl region. The signal for carbene carbon is observed at 190.00 ppm for **4a** and 192.26 for **4b** respectively. The presence of PF_6^- counterion in **1b** is confirmed by ^{31}P NMR with a signal at 144 ppm.

Compound **6a** show ESI^+ LC-MS signal at *m/z* 532.01 and 454.00, assigned to [**6a**]$^+$and [**6a-DMSO**]$^{+,}$ respectively. In ^1H NMR of **6a**, one doublet and triplet appear at 8.11 and 7.89 ppm for pyridine protons whereas, imidazol-2-ylidene protons were shown as two doublets at 7.71 and 6.79 ppm, respectively. In the ^{13}C NMR spectra, the carbene carbon signal of **6a** appears at 184.66 ppm. Similarly, for **6b**, pyridine protons appear at 8.60 and 8.38 ppm as a doublet and triplet, respectively. Two imidazol-2-ylidene protons come as two doublets at 8.21 and 7.34 ppm, respectively. The carbene carbon signal of **6b** appears at 184.61 ppm in the ^{13}C NMR spectra.

Complex **5** is characterised in the solid-state as crystals of **4a** and **5** were obtained from the same solution. Therefore, we believe that a small fraction of **4a** is converted to **5** as a result of a change in the bonding mode of η^2:η^2-COD to η^2-COD and coordination of the chloride counterion to the ruthenium, by keeping several days in methanol/ether solvent (Scheme **2.2**). However, in solution, only **4a** is present with an η^2:η^2-COD ligand and chloride counterion.

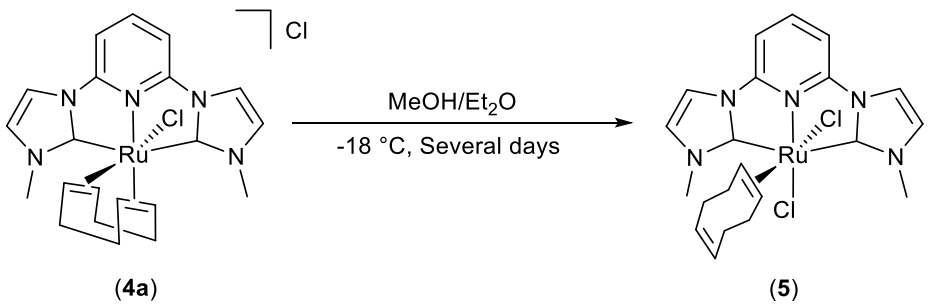

Scheme 2.2 Isolation of [Ru(CNC)(η^2-COD)Cl_2], (**5**) during crystallization.

Metal mediated alkene isomerisation, including *cis-trans* isomerisation, may be involved in solution during crystallisation. The COD ligand is known to undergo metal-mediated C-H activation and switch from η^2 to η^1 or an allylic η^3 and vice-versa.*[22-29]* Such a flip may be operational in this case too resulting in the isolation of the more crystalline **5** with η^2-(E,Z)-COD ligand. During our investigation of the mechanism (vide infra), the formation of η^1 or an allylic η^3 form of COD ligand is indicated in the LC-MS.

2.2.2 Description of the crystal structures

The molecular structures of complexes **1a, 2a, 4a, 4b** and **5** are confirmed by X-ray crystal diffraction analysis. Complex **1a** (Figure **2.1**) are crystallized in an orthorhombic system with a $P2_12_12_1$ space group while, **2a** (Figure **2.2**), **4a** (Figure **2.3**), **4b** (Figure **2.4**) and **5** (Figure **2.5**) are crystallised in a monoclinic system with *P*21/c space group and triclinic system with P-1 space group, respectively. The ruthenium metal centre in all the complexes displays distorted octahedral geometry. Selected bond lengths and angles of complexes **1a, 2a, 4a, 4b** and **5** are listed in Table **2.1**.

Complex **1a** crystallized with bromide ions from the crude reaction mixture while the mass data of the purified samples indicated chloride as the halide present in the coordination sphere. The molecular structure of **1a** consists of a six-coordinate Ru (II) centre with Br^- and triphenylphosphine at the axial positions, CO trans to the pyridine nitrogen atom, and CNC pincer ligand at the meridional site (Figure **2.1**). Another bromide ion is present in the lattice. The CNC pincer ligand occupies three meridional sites with a C1-Ru1-C10 angle of 152.3 (4), shorter than the previously reported complexes.*[40]* The bite angle (N3-Ru1-C10) of 76.8(4)$^\circ$ is similar to the complex reported by Peris *et. al.[44]* The bond distances of Ru1-C1 (2.051(9) Å) and Ru1-C10 (2.085(9) Å) are comparable to the reported ruthenium NHC carbene complexes 2.056(5) Å and 2.062(5) Å. The CO molecule is present *trans* to the pyridine ring, and Ru-C(CO) bond length of

1.875(13) Å is equivalent to those reported in the literature.*[17,40]* The C-O bond length of 1.114(13) Å (Table **2.3**) is comparable to NNN-pincer (C-O, 1.105(6)Å) *[41]* complex and slightly shorter than the previously reported CNC complex (C-O, 1.152(6) Å).*[17]*

Complex **2a** also has distorted octahedral geometry in which Ru (II) is surrounded by one CNC pincer ligand, two triphenylphosphines, and one chloride ion (Figure **2.4**). The two bulky triphenylphosphines are situated trans to each other. The N3-Ru1-C10 bite angle is 77.5(3)° and comparable to the previously reported complexes. The bond distance of Ru1-C1 (2.052 (6) Å) (Table **2.3**) is similar to that in the complex **1a** and comparable to the reported complex (2.056 (5) Å distance whereas Ru1-C10 (2.094 (7) Å was slightly larger than the complex **1a** and the previously reported complex (2.062(5) Å).*[17]* The Ru-P (Ru1-P1, 2.370(1) Å and Ru1-P2, 2.359(1) Å) bonds in the case of **2a** are slightly longer than the **1a** (Ru1-P1, 2.342 (2) Å) and previously reported complex (Ru1-P1, 2.318 (2) Å).*[39]*

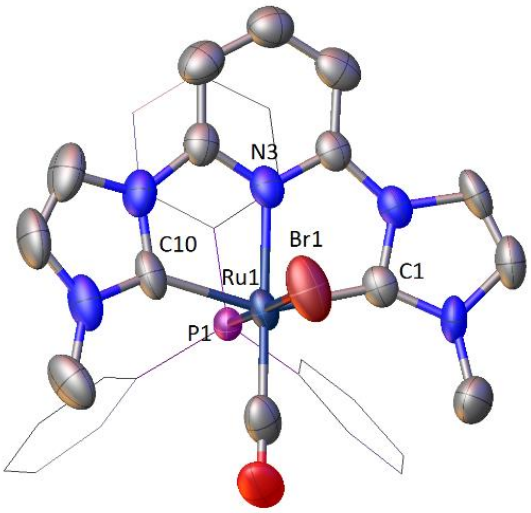

Figure 2.3 Molecular structure of **1a** with thermal ellipsoids drawn at the 50% level. All hydrogen atoms and a bromide counter anion are omitted for clarity. Selected bond lengths (Å) and angles (°): Ru1-N3, 2.077(8), Ru1-C1, 2.051(9); Ru1-C10, 2.085(9); Ru1-C14, 1.875(13); Ru1-P1, 2.342(2); Ru1-Br1, 2.5727(13); C1-Ru1-C10, 152.3(4); N3-Ru1-C10, 76.8(4); N3-Ru1-P1, 90.7(2); C10-Ru1-P1, 94.8(3);

C1-Ru1-Br1, 85.6(2); N3-Ru1-Br1, 87.2(2); C10-Ru1-Br1, 86.6(3); P1-Ru1-Br1, 177.20(6).

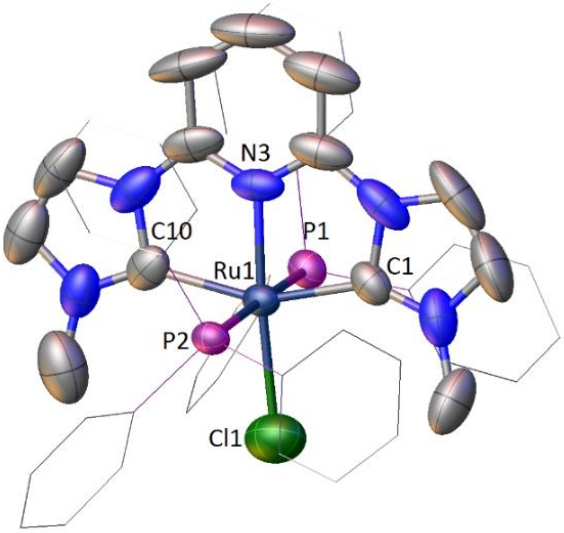

Figure 2.4 Molecular structure of **2a** with thermal ellipsoids drawn at the 50% level. All hydrogen atoms and a chloride counter anion are omitted for clarity. Selected bond lengths (Å) and angles (°): Ru1-N3, 2.020(5), Ru1-C1, 2.052(6); Ru1-C10, 2.094(7); Ru1-P1, 2.370(1); Ru1-P2, 2.359(1); Ru1-Cl1, 2.447(3); C1-Ru1-C10, 156.1(3); N3-Ru1-C10, 77.5(3); N3-Ru1-P1, 90.76(13); C10-Ru1-P1, 89.68(15); C1-Ru1-Cl1, 97.80(19); N3-Ru1-Cl1, 176.05(18); C10-Ru1-Br1, 106.1(2); P1-Ru1-Cl1, 87.73(7); P2-Ru1-Cl1, 89.12(7).

Table 2.1 Crystal data and structural refinement parameters for **1a, 2a, 4a, 4b** and **5.**

β/°	α/º	c/Å	b/Å	a/ Å	Space Group	Crystal System	T/K	Empirical formula	
90	90	14.5907(3)	21.8835(3)	9.8991(2)	$P2_12_12_1$	Orthorhombic	293	$C_{32}H_{28}Br_2N_5OPRu$	**1a**
94.111(7)	90	22.8232(17)	20.5547(19)	9.8223(7)	$P2_1/c$	Monoclinic	293	$C_{49}H_{43}Cl_2N_5P_2Ru$	**2a**
91.281(3)	90	13.0602(5)	22.7663(14)	8.1293(3)	$P2_1/c$	Monoclinic	293	$C_{22}H_{31}Cl_2N_5O_2Ru$	**4a**
89.220(6)	64.443(7)	13.5669(10)	13.4501(9)	8.2997(5)	P-1	Triclinic	293	$C_{23}H_{28}BrF_6N_6PRu$	**4b**
93.938(7)	90	18.0497(15)	12.9701(11)	11.3837(10)	$P2_1/c$	Monoclinic	293	$C_{21}H_{25}Cl_2N_5Ru$	**5**

GOF on F2	R indices (all data)	Final R indices [I>2σ(I)]	R (int)	Reflections Collected/unique	μ(Mo–Kα)/mm^{-1}	Z	V/Å^3	γ/°
1.051	R1 = 0.0558 wR2 = 0.1253	R1 = 0.0463 wR2 = 0.1170	0.0541	26686/5552	2.045	4	3160.74(10)	90
1.044	R1 = 0.1180 wR2 = 0.2474	R1 = 0.0783 wR2 = 0.2128	0.0668	10533/6814	0.566	4	4596.0(6)	90
1.085	R1 = 0.0896 wR2 = 0.1652	R1 = 0.0645 wR2 = 0.1498	0.0692	25926/5782	0.899	4	2416.5(2)	90
1.080	R1 = 0.0799 wR2 = 0.1381	R1 = 0.0540 wR2 = 0.1141	0.0637	17139/6388	2.162	2	1365.02(17)	87.524(5)
1.055	R1 = 0.1620 wR2 = 0.2775	R1 = 0.0975 wR2 = 0.2344	0.1324	24866/6412	0.805	4	2658.7(4)	90

Table 2.2 Selected bond lengths and bond angles of **1a, 2a, 4a, 4b** and **5**

Complex	**Bond lengths (Å)**		**Bond Angles (°)**	
1a	Ru1-C14	1.875(13)	C1-Ru1-N3	76.3(3)
	Ru1-C1	2.051(9)	C1-Ru1-C10	152.3(4)
	Ru1-N3	2.077(8)	C10-Ru1-N3	76.8(4)
	Ru1-C10	2.085(9)	C1-Ru1-P1	92.0(2)
	Ru1-P1	2.342(2)	N3-Ru1-P1	90.7(2)
	Ru1-Br1	2.5727(13)	C10-Ru1-P1	94.8(3)
			C1-Ru1-Br1	85.6(2)
			N3-Ru1-Br1	87.2(2)
			C10-Ru1-Br1	86.6(3)
			P1-Ru1-Br1	177.20(6)
2a	Ru1-P2	2.359(1)	P2-Ru1-P1	176.01(5)
	Ru1-P1	2.370(1)	P2-Ru1-Cl1	89.12(7)
	Ru1-Cl1	2.447(3)	P1-Ru1-Cl1	87.73(7)
	Ru1-N3	2.020(5)	N3-Ru1-P2	92.54(13)
	Ru1-C10	2.094(7)	N3-Ru1-P1	90.76(13)
	Ru1-C1	2.052(6)	N3-Ru1-Cl1	176.05(18)
			N3-Ru1-C10	77.5(3)
			N3-Ru1-C1	78.6(3)
			C10-Ru1-P2	88.84(15)
			C10-Ru1-P1	89.68(15)
			C10-Ru1-Cl1	106.1(2)
			C1-Ru1-P2	91.90(16)
			C1-Ru1-P1	90.96(16)
			C1-Ru1-Cl1	97.80(19)
			C1-Ru1-C10	156.1(3)
4a	Ru1-N3	2.045(4)	N3-Ru1-C1	76.39(2)
	Ru1-C1	2.098(5)	N3-Ru1-C10	75.84(2)
	Ru1-C10	2.100(5)	C1-Ru1-C10	149.0(2)
	Ru1-C19	2.209(5)	N3-Ru1-Cl1	97.70(1)
	Ru1-C14	2.210(5)	C1-Ru1-Cl1	84.73(2)
	Ru1-C18	2.214(6)	C10-Ru1-Cl1	85.66(1)
	Ru1-C15	2.226(5)	N3-Ru1-$C_{(COD)}$	171.51
	Ru1-Cl1	2.4741(13)	C1-Ru1-$C_{(COD)}$	104.34
			C10-Ru1-$C_{(COD)}$	105.16
			Cl1-Ru1-$C_{(COD)}$	90.78
			N3-Ru1-$C_{(COD)}$	87.89
			C1-Ru1-$C_{(COD)}$	97.46
			C10-Ru1-$C_{(COD)}$	94.95

			Cl1-Ru1-$C_{(COD)}$	174.34
			$C_{(COD)}$-Ru1-$C_{(COD)}$	100.40
4b	Ru1-N1	2.066(4)	N1-Ru1-C10	75.78(17)
	Ru1-C10	2.116(4)	N1-Ru1-C1	75.82(17)
	Ru1-C1	2.118(4)	C10-Ru1-C1	148.0(2)
	Ru1-C19	2.230(5)	N1-Ru1-Br1	99.61(11)
	Ru1-C15	2.231(5)	C10-Ru1-Br1	84.82(13)
	Ru1-C18	2.228(12)	C1-Ru1-Br1	85.71(13)
	Ru1-C14	2.224(5)	N1-Ru1-$C_{(COD)}$	171.35
	Ru1-Br1	2.5978(7)	C1-Ru1-$C_{(COD)}$	105.10
			C10-Ru1-$C_{(COD)}$	105.21
			Br1-Ru1-$C_{(COD)}$	89.05
			N1-Ru1-$C_{(COD)}$	87.43
			C1-Ru1-$C_{(COD)}$	97.08
			C10-Ru1-$C_{(COD)}$	96.03
			Br1-Ru1-$C_{(COD)}$	172.88
			$C_{(COD)}$-Ru1-$C_{(COD)}$	83.92
5	Ru1-Cl2	2.477(2)	N3-Ru1-C1	78.9(3)
	Ru1-C14	2.215(11)	N3-Ru1-C10	77.7(3)
	Ru1-Cl1	2.454(2)	N3-Ru1-Cl1	172.7(2)
	Ru1-C15	2.224(11)	N3-Ru1-Cl2	84.6(2)
	Ru1-N3	1.990(7)	Cl1-Ru1-Cl2	88.12(9)
	Ru1-C10	2.074(10)	C1-Ru1-Cl2	84.9(3)
	Ru1-C1	2.056(10)	C1-Ru1-Cl1	99.9(3)
			C1-Ru1-C10	155.9(4)
			Cl1-Ru1-$C_{(COD)}$	86.07
			Cl2-Ru1-$C_{(COD)}$	174.02
			C1-Ru1-$C_{(COD)}$	94.59
			C10-Ru1-$C_{(COD)}$	95.52
			N3-Ru1-$C_{(COD)}$	101.17

Complex **5** is a rare example of complexes in which COD is bound in a "non-bridging" η^2-mode (Figure **2.7**). The second chloride ligand is coordinated trans to pyridine occupying the coordination site after dissociation of one of the alkene bonds of the COD ligand. The C=C bond length of COD (coordinated) in **5** is 1.376(16) Å, comparable to the corresponding distance of 1.389(7) in a Ni (0) complex.*[20]* The free alkene C=C bond length is 1.474(16) Å and has E-configuration. Although there is some disorder in the non-coordinated end of the COD ligand in the crystal structure of **5**, the

other bond lengths and bond angles in the COD unit support the presence of an η^2-(E,Z)-COD. This occurrence may be due to the metal mediated *cis-trans* isomerization of Z to E-configuration. Additionally, a close look at the crystal packing diagram of **5** shows the η^2-(E,Z)-COD ligand oriented vertically from the CNC-pincer ligand and may be preferred in solid state due to better crystal packing.

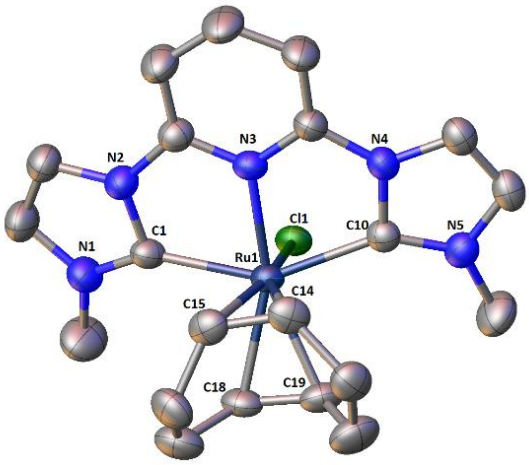

Figure 2.5 Molecular structure of **4a** with thermal ellipsoids drawn at the 50% level. Hydrogen atoms and one chloride anion are omitted for clarity. Selected bond lengths (Å) and angles (°): Ru1-N3, 2.045(4); Ru1-C1, 2.098(5); Ru1-C10, 2.100(5); C14-C15, 1.381(8); C18-C19, 1.392(8); Ru1-Cl1, 2.4741(13); N3-Ru1-C1, 76.40(2); N3-Ru1-C10, 75.84(2); C1-Ru1-C10, 149.0(2), N3-Ru1-Cl1, 97.70(1); C1-Ru1-Cl1, 84.73(2); C10-Ru1-Cl1, 85.66(1).

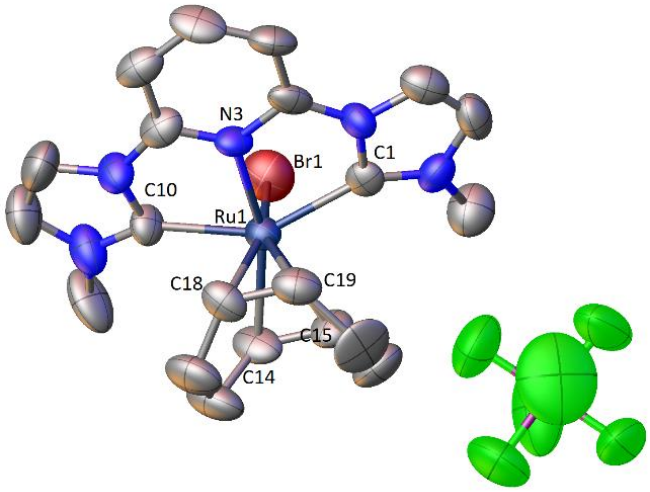

Figure 2.6 Molecular structure of **4b** with thermal ellipsoids drawn at the 50% level. Hydrogen atoms are omitted for clarity. Selected bond lengths (Å) and angles (°): Ru1-N3, 2.066(4); Ru1-C1, 2.118(4); Ru1-C10, 2.116(4); C14-C15, 1.399(7); C18-C19, 1.384(7); Ru1-Br1, 2.4741(13); N3-Ru1-C1, 75.82(17); N3-Ru1-C10, 75.78(17); C1-Ru1-C10, 148.0(2), N3-Ru1-Br1, 99.61(11); C1-Ru1-Br1, 85.71(13); C10-Ru1-Br1, 84.82(13).

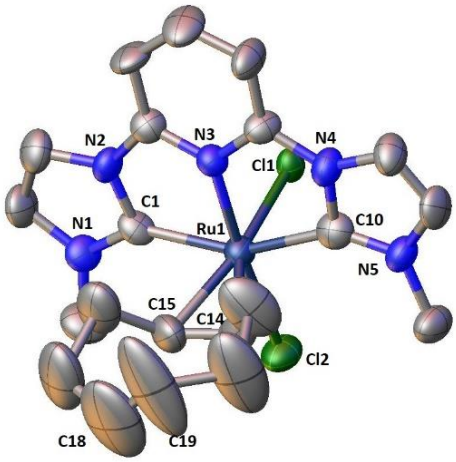

Figure 2.7 Molecular structure of **5** with thermal ellipsoids drawn at the 50% level. Hydrogen atoms are omitted for clarity. Selected bond lengths (Å) and angles (°): Ru1-N3, 1.990(7); Ru1-C1, 2.056(10); Ru1-C10, 2.074(10); C14-C15, 1.385(17); C18-C19, 1.329(17); Ru1-Cl1, 2.454(2); Ru1-Cl2, 2.477(2); N3-Ru1-C1, 78.9(3); N3-Ru1-C10, 77.7(3); C1-Ru1-C10, 155.9(4); N3-Ru1-Cl1, 84.6(2); N3-Ru1-Cl2, 172.7(2).

2.2.3 Computational Studies

Intrigued by structural similarities between the η^2-COD unit in the crystal structure of **5** and the calculated structure *[35]* of free (E,Z)-COD, we decided to investigate these structures using DFT. Geometry optimisations were carried out using B97-3c composite functional, which is a low-cost computational method and has been shown to produce good geometries for organometallic compounds, at par with other popular DFT methods.*[43]* In addition to the geometries starting from solid-state structures of **4a** and **5**, unconstrained geometry optimisations for several structures, isomeric to **5**, with different configurations and orientations for "twisted-boat" and"chair" η^2-(ZZ) -

COD ligand have also been carried out. The six calculated structures for isomeric forms of **5** are depicted in Figure **2.8**, along with their relative energies. As expected, the calculated structures **5-TB**, **5-TB'**, **5-C** and **5-C'** with "twisted-boat" and "chair" forms of η^2-(Z,Z)-COD ligand are energetically favoured compared to **5** and **5'** with η^2-(E,Z)-COD ligand.

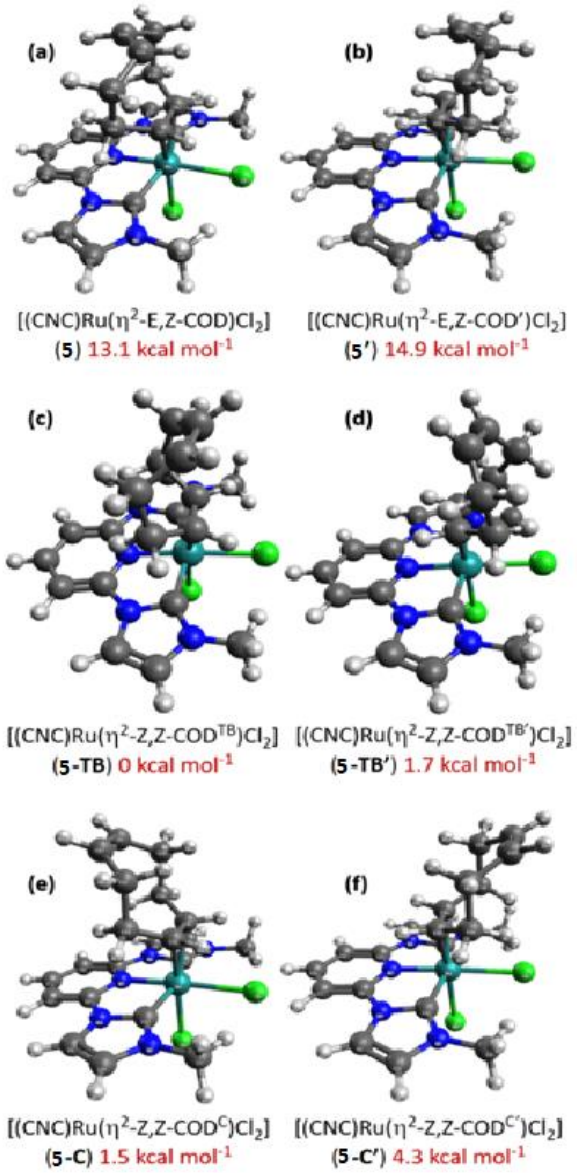

Figure 2.8 Calculated structures and relative Gibbs free energies (at 298.15 K) for isomeric forms of **5**. TB and C indicate "twisted boat" and "chair" conformers of the COD ligand, respectively. Structures **5'**,

5-TB' and **5**-C' have the COD ligand rotated, by 180°, along with the Ru-(C=C) bond axis.

The small difference in relative energies for structures **5-TB**, **5-TB'**, **5-C** and **5-C'** are in line with previous studies on different conformers of the free COD molecule. The interconversions of the twisted-boat and chair forms of (Z,Z)-COD have been investigated earlier with the estimated Gibbs free energy of activation for three distinct paths ranging between 4-6 kcal mol^{-1}.*[35]*

Table 2.3 Selected bond lengths (Å) and angles (°) for **4a** and **5** obtained from single-crystal X-ray diffraction and DFT studies.

Bond Parameter	**4a**		**5**	
	X-ray	**DFT**[a]	**X-ray**	**DFT**[a]
Ru1-N3	2.045(4)	2.038	1.990(7)	1.972
Ru1-C1	2.098(5)	2.084	2.056(10)	2.041
Ru1-C10	2.100(5)	2.086	2.074(9)	2.041
C14-C15	1.381(8)	1.400	1.385(17)	1.416
C18-C19	1.392(8)	1.393	1.329(17)	1.331
Ru1-Cl1	2.4741(13)	2.475	2.477(2)	2.494
Ru1-Cl2	--	--	2.454(2)	2.490
N3-Ru1-C1	76.40(2)	76.1	78.9(3)	78.4
N3-Ru1-C10	75.84(2)	75.8	77.3(3)	78.4
C1-Ru1-C10	149.0(2)	147.4	155.9(4)	154.8
N3-Ru1-Cl1	97.70(1)	98.5	84.6(2)	87.6
N3-Ru1-Cl2	--	--	172.7(2)	175.7
C1-Ru1-Cl1	84.73(2)	83.5	87.2(3)	84.6
C10-Ru1-Cl1	85.66(1)	84.6	84.9(3)	84.7
C1-Ru1-Cl2	--	--	102.6(2)	101.4
C10-Ru1-Cl2	--	--	99.9(3)	101.0

[a]Calculated with B97-3c composite functional.

Calculated structures of the cationic complex part of **4a** and **5-C'** are shown in Figure **2.9** with their relative Gibbs free energies. The zero-point corrected bond dissociation energy (BDE) for the dissociation of labile alkene (trans to pyridine nitrogen) in **4a**$^{+}$ to give **5-C'**$^{+}$ is obtained from these calculations as 24.8 kcal mol^{-1}. Similarly,

the bond dissociation energy for the dissociation of chloride ligand in **5-C'** to give the same species **5-C'**$^{+}$ is obtained as 23.3 kcal mol^{-1}.

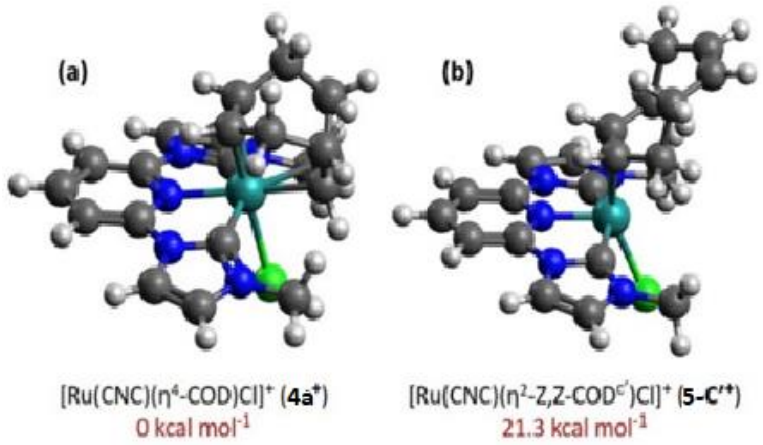

Figure 2.9 Calculated structures and relative Gibbs free energies (at 298.15 K) of cationic complex **4a**$^{+}$ and **5-C'**$^{+}$.

2.3 Conclusions

In summary, we have investigated the synthesis and characterisation of ruthenium pincer complexes [Ru(CNC)(CO)(PPh_3)Cl]X [X = Cl^- (**1a**), PF_6^- (**1b**)], [Ru(CNC)(PPh_3)$_2$Cl]X [X = Cl^- (**2a**), PF_6^- (**2b**)], and [Ru(CNC)(PPh_3)$_2$(H)]X [X = Cl^- (**3a**), PF_6^- (**3b**)], [Ru(CNC)(η^2:η^2-COD)Cl]X [X = Cl^- (**4a**), PF_6^- (**4b**)] [Ru(CNC)(DMSO)$_2$Cl]X [X = Cl^- (**6a**), PF_6^- (**6b**)] and [Ru(CNC)(η^2-COD)Cl_2] (**5**) with an η^2-(E,Z)-COD ligand. In the case of **4a**, Ru-C(COD) bond trans to pyridine is weaker and labile than the Ru-C(COD) bond trans to halide which allows the coordination of COD to the Ru in η^2:η^2-manners (**4a**) and η^2-manners (**5**). DFT studies indicate that the η^2-COD ligand should exist in (Z,Z) configuration in solution and (E,Z) configuration may only be favoured in solid state due to crystal packing. containing a "pyridine-dicarbene" pincer ligand.

2.4 Experimental

2.4.1 General procedure

All reactions and manipulations were carried out under an inert atmosphere using the standard Schlenk technique. Solvents were purchased from S. D. Fine-Chem Limited and purified by distillation under an inert atmosphere. $[RuHCl(CO)(PPh_3)_3]$,*[46]* $[RuCl_2(PPh_3)_3]$,*[47]* $[RuCl_2(COD)]_n$,*[48]* and$[RuCl_2(DMSO)_4]$ *[49]* were prepared by following the literature procedure using $RuCl_3 \cdot 3H_2O$. Deuterated dimethyl sulphoxide was purchased either from EURISOtop or Aldrich Chemical Co. NMR spectra were taken on Bruker Avance (III) spectrometer operating at 400 MHz (^1H), 162 MHz (^{31}P), and 100 MHz (^{13}C). NMR chemical shifts are reported in ppm and referenced to the solvent peaks for ^1H (DMSO-d^6, δ 2.54 ppm) and ^{13}C (natural abundance of ^{13}C in DMSO-d^6, δ 40.45 ppm) NMR. ^{31}P NMR chemical shifts are referenced to an external 85% H_3PO_4 standard as 0 ppm. The mass chromatograms were recorded on Bruker-Daltonics-microTOF-QII mass spectrometer. GC Samples were analysed in Shimadzu QP2010 Ultra, without an internal standard.

2.4.2 Synthesis of $[Ru(CNC)(CO)(PPh_3)Cl]Cl$, 1a

An oven dried Schlenk tube with the magnetic stirring bar was charged with the ligand precursor **CNC·2HBr** (0.200 g, 0.5 mmol) and dried under vacuum at 100 ˚C for 2 hours. The Schlenk tube was cooled to room temperature under the N_2 atmosphere. Dry methanol (10mL) was added, followed by Ag_2O (0.116 g, 0.5 mmol) and stirred at room temperature in the dark, covered with aluminium foil. After 30 min, a white precipitate had formed, and $[RuHCl(CO)(PPh_3)_3]$ (0.477 g, 0.5 mmol) was added to the reaction mixture. The reaction mixture was heated at 60 ˚C for 24 h, which results in a brown colour solution with some residue. The reaction mixture was filtered through celite, and the filtrate was reduced in volume (2 mL) followed by the addition of diethyl ether (5 mL). The compound precipitated out as a yellow solid.

The X-ray quality crystals of **1a** with bromide as the halide ligand were obtained by slow diffusion, at -18 ˚C, of diethyl ether in acetonitrile solution of the crude reaction mixture. Yield: 0.180 g (40 %). ^{1}H NMR (400 MHz, DMSO-d^{6}, δ in ppm): δ 8.44 (d, *J* = 2.2 Hz, 2H), 8.11 (t, *J* = 8.1 Hz, 1H), 7.77 (d, *J* = 8.1 Hz, 2H), 7.56 (d, *J* = 2.2 Hz, 2H), 7.39 – 7.31 (m, 3H), 7.25 (td, *J* = 7.7, 2.1 Hz, 6H), 6.94 (dd, *J* = 10.5, 7.8 Hz, 6H), 3.59 (s, 3H).; ^{13}C NMR (DMSO-D^{6}, δ in ppm): 192.34, 149.78, 140.41, 132.99, 132.59, 131.98, 129.77, 128.34, 124.54, 118.41, 106.33, 38.01; ^{31}P NMR (DMSO-d^{6}, δ in ppm): 42.94; IR (cm^{-1}): C=O (1955.77); LCMS: [M]$^{+}$ 666.08, [M-Cl+H] - 632.10, LCMS: [PF$_{6}$]$^{-}$ - 144.96, HRMS for [M]$^{+}$ [$C_{32}H_{28}ClN_{5}OPRu$] Calculated – 666.0763, Found – 666.0783; Anal. Calcd. For [$C_{32}H_{28}ClN_{5}OPRu$]Cl: C 59.12, H 4.34, N 10.77 Found: C 59.47, H 4.76, N 11.06.

2.4.3 Synthesis of [Ru(CNC)(CO)(PPh$_{3}$)Cl]PF$_{6}$, 1b

To a solution of **1a** (0.100 g, 0.13mmol) in 2 mL of methanol, add $NH_{4}PF_{6}$ (0.220 g, 0.13 mmol) and stirred for 30 min at room temperature. A yellow precipitate of **1b** slowly comes out and on cooling at 0˚C some more precipitation occurred. Yield: 0.035g (31%). ^{1}H NMR ((400 MHz, DMSO-d^{6}, δ in ppm): δ 8.37 (d, *J* = 2.4 Hz, 2H), 8.11 (t, *J* = 8.1 Hz, 1H), 7.72 (d, *J* = 8.2 Hz, 2H), 7.54 (d, *J* = 2.2 Hz, 2H), 7.36 (t, 3H), 7.25 (td, *J* = 7.7, 2.2 Hz, 6H), 6.96 (dd, 6H), 3.61 (s, 3H); ^{13}C NMR (DMSO-d^{6}, δ in ppm): 192.06, 149.50, 140.49, 132.78, 132.39, 131.93, 129.55, 127.93, 124.52, 118.02, 106.14, 37.82; ^{31}P NMR (DMSO-d^{6}, δ in ppm): 43.27, 143.87; IR (cm^{-1}): C=O (1954.21); LCMS: [M]$^{+}$ 666.08, [M-Cl+H] - 632.11, LCMS: [PF$_{6}$]$^{-}$ - 144.96, HRMS for [M]$^{+}$ [$C_{32}H_{28}ClN_{5}OPRu$] Calculated – 666.0763, Found – 666.0807; Anal. Calcd. For [$C_{32}H_{28}ClN_{5}OPRu$]PF$_{6}$: C 47.39, H 3.48, N 8.63 Found: C 47.74, H 3.87, N 8.95.

2.4.4 Synthesis of $[Ru(CNC)(PPh_3)_2Cl]Cl$, 2a and $[Ru(CNC)(PPh_3)_2H]Cl$, 3a

A similar procedure was followed as with **1a** except $[RuCl_2(PPh_3)_3]$ (0.480 g, 0.5 mmol) was added in place of $[RuHCl(CO)(PPh_3)_3]$. The solvent was reduced in volume (2 mL) followed by the addition of diethyl ether (5 mL) resulting in the precipitation of the compound which was filtered and dried under vacuum. Further, the crude solid was purified by column chromatography using neutral alumina with eluting solvent [(hexane/CH_2Cl_2)/CH_3OH] [(1:1):5] and [(hexane/CH_2Cl_2)/CH_3OH] [(1:1):7] affords **3a** and **2a** as a solid. The X-ray quality crystals of **2a** were obtained by slow diffusion of diethyl ether in acetonitrile solution at -18 ˚C.

Compound **2a**: Yield: 0.155 g (25%). ^{1}H NMR (DMSO-d^6, 500MHz, δ in ppm): δ 8.31 (d, *J* = 2.2 Hz, 2H), 7.49 (d, *J* = 2.1 Hz, 2H), 7.36 (t, *J* = 7.5 Hz, 1H), 7.29 (t, *J* = 7.4 Hz, 6H), 7.18 – 7.12 (m, 12H), 7.06 (d, *J* = 8.2 Hz, 2H), 7.04 – 7.00 (m, 12H), 3.59 (s, 3H).; ^{13}C NMR (DMSO-D^6, δ in ppm): 188.91, 152.10, 132.92, 132.13, 129.19, 127.69, 125.53, 117.83, 105.22, 48.28, 36.73; ^{31}P NMR (DMSO-d^6, δ in ppm): 31.79, 26.60. LCMS: $[M]^+$ 900.17, $[M-Cl]^{2+}$ 432.59, LCMS: $[M]^-$-144.9636, HRMS for $[M]^+$ $[C_{49}H_{43}ClN_5P_2Ru]$ Calculated – 900.1730, Found – 900.1714; Anal. Calcd. For $[C_{49}H_{43}ClN_5P_2Ru]Cl$: C 62.89, H 4.63, N 7.48 Found: C 63.14, H 4.89, N 7.72.

Compound **3a**: Yield: 0.058 g (10%).^{1}H NMR (400 MHz, DMSO-d^6): δ 8.35 (d, *J* = 2.3 Hz, 2H), 7.84 (t, *J* = 8.0 Hz, 1H), 7.61 (d, *J* = 7.9 Hz, 2H), 7.28 (t, *J* = 7.4 Hz, 6H), 7.25 (d, *J* = 2.2 Hz, 2H), 7.18 (t, *J* = 7.6 Hz, 12H), 6.85 – 6.70 (m, 12H), 2.46 (s, 6H), -8.88 (t, *J* = 27.0 Hz, 1H); ^{13}C NMR (DMSO-D^6, δ in ppm): 198.09, 149.75, 135.85, 131.66, 128.89, 127.71, 123.92, 117.19, 104.11, 48.43, 35.82; ^{31}P NMR (DMSO-d^6, δ in ppm): 52.10. LCMS: 866.17 $[M]^+$. HRMS for $[M]^+$ $[C_{49}H_{44}N_5P_2Ru]$ Calculated – 866.2123, Found – 866.2125; Anal. Calcd. For $[C_{49}H_{44}N_5P_2Ru]Cl$: C 65.29, H 4.92, N 7.77 Found: C 65.57, H 5.27, N 8.06.

2.4.5 Synthesis of $[Ru(CNC)(PPh_3)_2Cl]PF_6$, 2b

To a solution of **2a** (0.100 g, 0.11 mmol) in 2 mL of methanol, add NH_4PF_6 (0.190 g, 0.11 mmol) and stirred for 30 min at room temperature. A yellow precipitate of **2b** slowly comes out and on cooling at 0 ˚C some more precipitation occurred. Yield: 0.034 g (29 %).^{1}H NMR (DMSO-d^6, δ in ppm): ^{1}H NMR (500 MHz, DMSO-d^6) δ 8.22 (d, *J* = 2.2 Hz, 2H), 7.46 (d, *J* = 2.4 Hz, 2H), 7.36 (t, *J* = 8.1 Hz, 1H), 7.29 (t, *J* = 7.5 Hz, 6H), 7.19 – 7.12 (m, 12H), 7.06 – 6.99 (m, 12H), 6.98 (d, *J* = 4.00 Hz, 2H), 3.59 (s, 3H); ^{13}C NMR (DMSO-D^6, δ in ppm): 188.74, 152.09, 132.93, 132.13, 129.18, 127.55, 125.58, 117.75, 105.16, 48.29, 36.72; ^{31}P NMR (DMSO-d^6, δ in ppm): 31.70, 26.57, -144.18. LCMS: $[M]^+$ 900.18, $[M-Cl]^{2+}$ 432.60, LCMS: $[M]^-$-144.96, HRMS for $[M]^+$ $[C_{49}H_{43}ClN_5P_2Ru]$ Calculated – 900.1730, Found – 900.1739; Anal. Calcd. For $[C_{49}H_{43}ClN_5P_2Ru]PF_6$: C 56.30, H 4.15, N 6.70 Found: C 56.47, H 4.42, N 7.21.

2.4.6 Synthesis of $[Ru(CNC)(PPh_3)_2H]Cl$, 3a from 2a

Complex **2a** was added (0.200 g, 0.21 mmol) in a Schlenk tube followed by K_2CO_3 (0.029 g, 0.21 mmol), and then ^{i}PrOH was injected via the syringe. The reaction mixture was refluxed at 85 °C for 15 h. The colour of the reaction mixture was changed from greenish-brown to brown orange. After the completion of the reaction, the mixture was filtered, and the solvent was evaporated under a reduced vacuum to afford a brown solid. The Solid was washed with diethyl ether and dried under a vacuum. The complex was obtained with a 77.8% yield.

2.4.7 Synthesis of $[Ru(CNC)(PPh_3)_2H]PF_6$, 3b

To a solution of **3a** (0.100 g, 0.11 mmol) in methanol, NH_4PF_6 was added and stirred for 30 min at room temperature. A precipitate of **3b** slowly comes out and on cooling at 0 ˚C some more precipitation of $[Ru(CNC)(PPh_3)_2(H)]PF_6$ occurred. Yield: 0.060 g (54%). ^{1}H NMR (400 MHz, DMSO-d^6): δ 8.31 (d, *J* = 4.0 Hz, 2H), 7.85 (t, *J* = 8.1 Hz, 1H), 7.58 (d, *J* = 8.5 Hz, 2H), 7.28 (t, *J* = 7.5 Hz, 6H), 7.24 (d, *J* = 4.00

Hz 2H), 7.18 (t, J = 7.6 Hz, 12H), 6.90 – 6.64 (m, 12H), 2.47 (s, 2H), -8.86 (t, J = 27.0 Hz, 1H); ^{13}C NMR (DMSO-D^6, δ in ppm): 201.28, 149.43, 135.54, 131.38, 128.55, 127.41, 123.56, 116.80, 103.74, 47.11, 35.50; ^{31}P NMR (DMSO-d^6, δ in ppm): 51.91, -144.15. LCMS: 866.20 $[M]^+$. HRMS for $[M]^+$ $[C_{49}H_{44}N_5P_2Ru]$ Calculated – 866.2123, Found – 866.2168; Anal. Calcd. For $[C_{49}H_{44}N_5P_2Ru]PF_6$: C 58.22, H 4.39, N 6.93 Found: C 58.63, H 4.81, N 7.25.

2.4.8 Synthesis of [Ru(CNC)(η^2:η^2-COD)Cl]Cl, 4a

Similar procedure was followed as with **1a** except $[Ru(COD)Cl_2]_n$ (0.141 g, 0.5 mmol) was added in place of $[RuHCl(CO)(PPh_3)_3]$. The solvent was reduced in volume (2 mL) followed by the addition of diethyl ether (5 mL) resulting in the precipitation of dark brown colored compound which was filtered and dried under vacuum. Further, the resulting precipitate was dissolved in the minimum amount of methanol, layered with diethyl ether, and kept at -18 ˚C to afford X-ray quality brown crystals. Yield: 0.150 g (58%). ^{1}H NMR (DMSO-d^6, δ in ppm): 8.76 (d, J = 5.00 Hz, 2H), 8.31 (t, J = 10.00 Hz, 1H), 8.16 (d, J = 10.00 Hz, 2H), 7.90 (d, J = 5.00 Hz, 2H), 4.40-4.37 (m, 2H, COD), 4.32 (s, 6H), 2.67-2.34 (m, 2H, COD), 2.18-2.12 (m, 2H, COD), 1.98-1.81 (m, 4H, COD), 1.94-1.77 (m, 2H, COD); ^{13}C NMR (**1a**) (DMSO-d^6, δ in ppm): 190.05, 149.81, 141.47, 127.83, 118.30, 107.61, 81.81, 79.17, 37.07, 30.51, 30.23; LCMS: $[M(Cl)]^+$ - 484.08, $[M(Br)]^+$ - 528.03, HRMS for $[M(Cl)]^+$, $[C_{21}H_{25}ClN_5Ru]$ Calculated - 484.0839, Found – 484.0825.

2.4.9 Synthesis of [Ru(CNC)(η^2:η^2-COD)Cl]PF$_6$, 4b

To a solution of crude **4a** (0.100 g, 0.19 mmol) in 2 mL of methanol was added NH_4PF_6 (0.031 g, 0.19 mmol) and stirred for 30 min at room temperature. A brown precipitate of **4b** slowly comes out and on cooling at 0 ˚C some more precipitation occurred. The X-ray quality crystals of **4b** were obtained with bromide ligand by slow diffusion of diethyl ether in acetonitrile solution at -18 ˚C. Yield: 0.030g (24%). ^{1}H

NMR (DMSO-d^6, δ in ppm): 8.63 (d, *J* = 4.00 Hz, 2H), 8.31 (t, *J* = 8.00 Hz, 1H), 8.05 (d, *J* = 8.00 Hz, 2H), δ 7.85 (d, *J* = 4.00 Hz, 2H), 4.40 (m, 2H, COD), 4.32 (s, 6H), 2.71-2.80 (m, 2H, COD), 2.18-2.13 (m, 2H, COD), 1.95-1.92 (m, 4H, COD), 1.86-1.82 (m, 2H, COD); ^{13}C NMR (DMSO-d^6, δ in ppm): 192.26, 150.13, 141.63, 128.11, 118.24, 107.44, 81.90, 79.34, 37.22, 30.51, 30.24; ^{31}P NMR (DMSO-d^6, δ in ppm): 144.17. LCMS: $[M(Cl)]^+$- 484.08, $[M(Br)]^+$- 528.03, LCMS: $[PF_6]^-$-144.96, HRMS for $[M]^+$ $[C_{21}H_{25}ClN_5Ru]$ Calculated - 484.0839, Found - 484.0853.

2.4.10 Synthesis of $[Ru(CNC)(DMSO)_2Cl]Cl$, 6a

Similar procedure was followed as with **1a** except $[RuCl_2(DMSO)_4]$ (0.244 g, 0.5 mmol) was added in place of $[RuCl_2(COD)_n]$. The solvent was reduced in volume (2 mL) followed by the addition of diethyl ether (5 mL) resulting in the precipitation of yellow colored compound which was filtered and dried under vacuum. Yield: 0.138 g (49%). ^1H NMR (DMSO-d^6, δ in ppm): δ 8.11 (d, *J* = 5.00 Hz, 2H), 7.89 (t, *J* = 10.00 Hz, 1H), 7.71 (d, *J* = 10.00 Hz, 2H), 6.79 (d, *J* = 10.00 Hz, 2H), 3.60 (s, 3H), 3.52 (s, 3H), 2.81 (s, 6H), 2.69 (s, 6H).; ^{13}C NMR (DMSO-d^6, δ in ppm): δ 184.66, 153.95, 140.63, 125.80, 118.93, 106.78, 45.41, 45.24, 36.40, 34.82.; LCMS: $[M\text{-}DMSO]^+$ - 454.00, $[M]^+$ - 532.01, HRMS for $[M]^+$, $[C_{17}H_{25}ClN_5RuO_2S_2]$ Calculated - 532.0176, Found – 532.0201.

2.4.11 Synthesis of $[Ru(CNC)(DMSO)_2Cl]PF_6$, 6b

To a solution of crude **6a** (0.100 g, 0.17 mmol) in 2 mL of methanol was added NH_4PF_6 (0.029 g, 0.17 mmol) and stirred for 30 min at room temperature. A bright yellow precipitate of **6b** slowly comes out and on cooling at 0 ˚C some more precipitation occurred. Yield: 0.070g (21%). ^1H NMR (DMSO-d^6, δ in ppm): δ 8.60 (d, *J* = 5.00 Hz 2H), 8.38 (t, *J* = 10.00 Hz, 1H), 8.21 (d, *J* = 10.00 Hz, 2H), 7.34 (d, *J* = 10.00 Hz 2H), 4.18 (s, 3H), 4.01 (s, 3H), 2.81 (s, 6H), 2.60 (s, 6H).; ^{13}C NMR (DMSO-d^6, δ in ppm): 184.61, 153.78, 140.42, 124.65,

116.75, 118.81, 106.36, 45.20, 45.05, 36.23, 34.66; ^{31}P NMR (DMSO-d^6, δ in ppm): 144.18. $[M\text{-}DMSO]^+$ - 454.02, $[M]^+$ - 532.21, HRMS for $[M]^+$, $[C_{17}H_{25}ClN_5RuO_2S_2]$ Calculated - 532.0176, Found – 532.0211.

2.4.12 X-ray data collection and structure refinement

Single crystal X-ray data of compounds **1a, 2a, 4a, 4b** and **5** were collected on the Rigaku Oxford Diffractometer using graphite-monochromated Mo Kα radiation (λ = 0.7107 Å). The data collection was evaluated with the help of CrysAlisPro CCD software. Data collections for all complexes were carried out at room temperature. Final refinement included atomic positions for all the atoms, anisotropic thermal parameters for all the non-hydrogen atoms, and isotropic thermal parameters for all the hydrogen atoms. Full matrix least-squares refinement against |F2| was carried out using the WinGx package of programs.*[50]* In **5**, the disordered lattice chloride ion was refined by splitting them into two parts without fixing any site occupancy factor (sof). The occupancies of the split atoms were refined by means of a free variable. Details of the structural parameters and final refinements for the compounds are given in Table 1, 2, 3 and 4, respectively.

2.4.13 DFT calculations

DFT calculations were performed using ORCA 4.2.1 program package.*[51,52]* Geometry optimizations were carried out in methanol solution with SMD solvation model using B97-3c composite functional developed by Grimme and co-workers.*[53,54]* Default settings of ORCA program, i.e., def2-mTZVP basis set on all atoms with def2-ECP on Ru atom, the resolution of identity (RI) approximation to speed up the calculations with def2-mTZVP/J auxiliary basis set, and Grimme's D3, atom-pairwise dispersion correction with the Becke-Johnson damping scheme (D3BJ) dispersion corrections were used during the geometry optimizations. Analytical vibrational frequency calculations were carried out at the same level of

theory as for the optimizations to validate that the optimized structures correspond to minima or transition states of the potential energy surface. Enthalpies and Gibbs free energies at T=298.15 K were obtained from the frequency calculations. Single-point energy calculations were performed at the optimized geometry using B97M density functional and def2-TZVP all-electron basis set for all atoms except Ru for which def2-QZVP was used with def2-ECP.*[55–57]* The resolution of identity chain of sphere (RIJCOSX) was used with its corresponding auxiliary basis, def2/J, as implemented in ORCA to improve the calculations efficiency.*[58]* Dispersion effects were treated again in the Grimme's DFT-D3 framework with Becke–Johnson damping (D3BJ).*[59–61]* The grids used were “grid5” and the default “gridX” as implemented in ORCA for final single point energy calculations. The electronic energies obtained from single point energy calculations were converted to Gibbs free energies using the total corrections obtained for the thermochemical analysis performed at B97-3c level.

2.4.14 Characterization of metal complexes

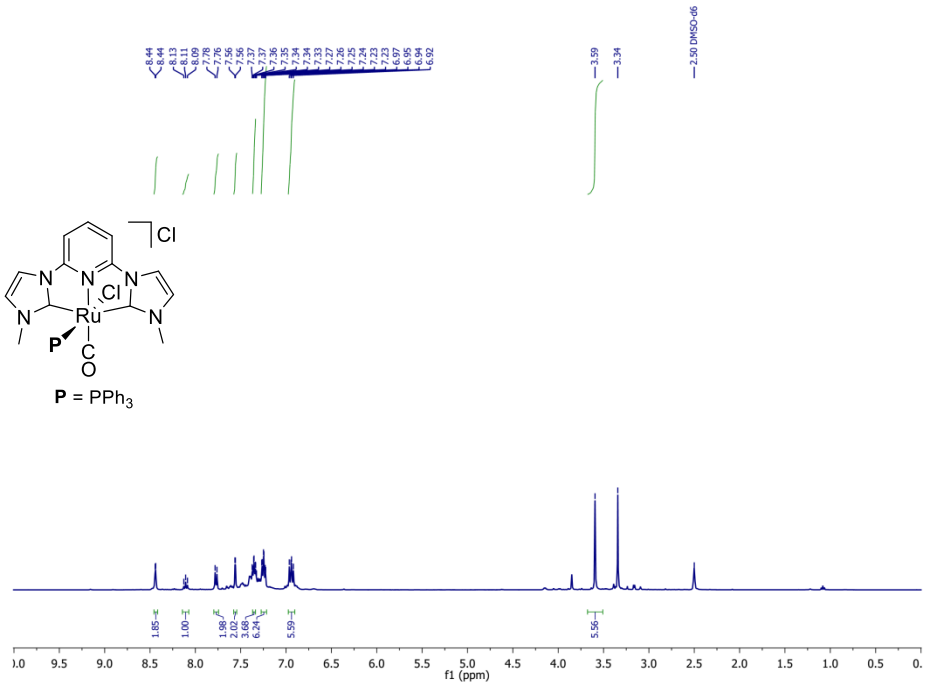

Figure 2.10 ^{1}H NMR spectrum of **1a**

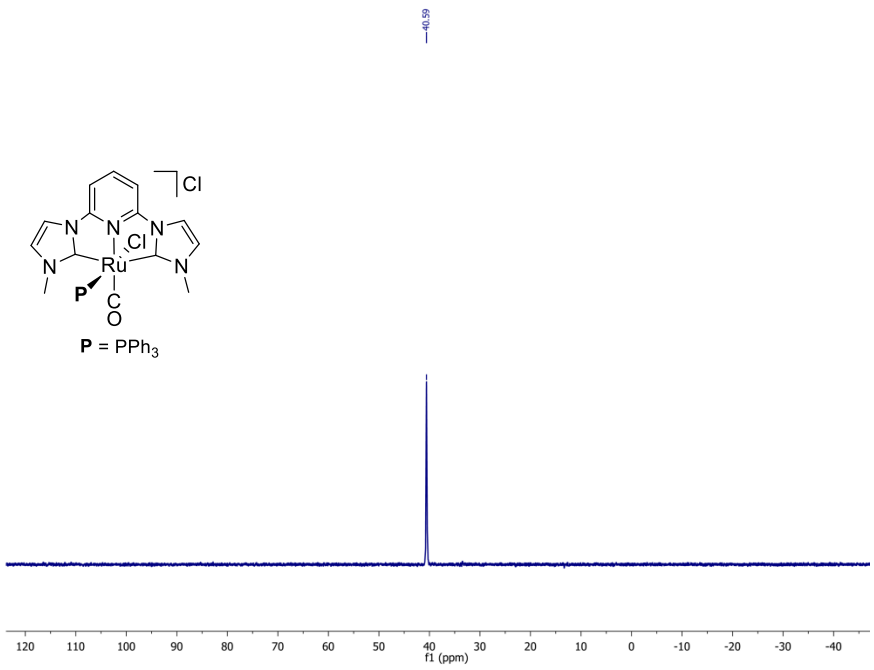

Figure 2.11 ^{31}P NMR spectrum of **1a**

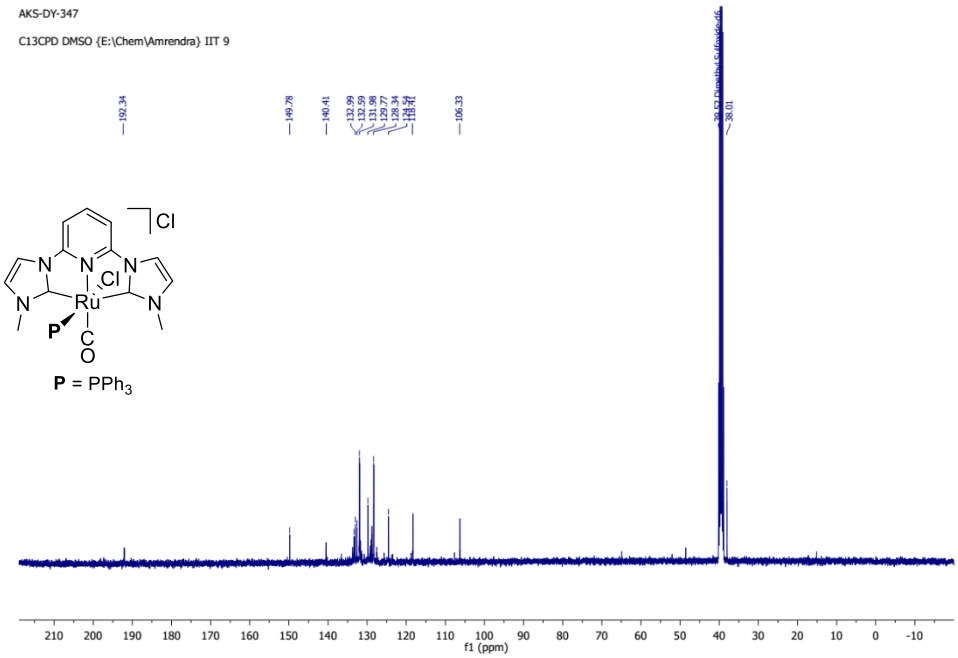

Figure 2.12 ^{13}C NMR spectrum of **1a**

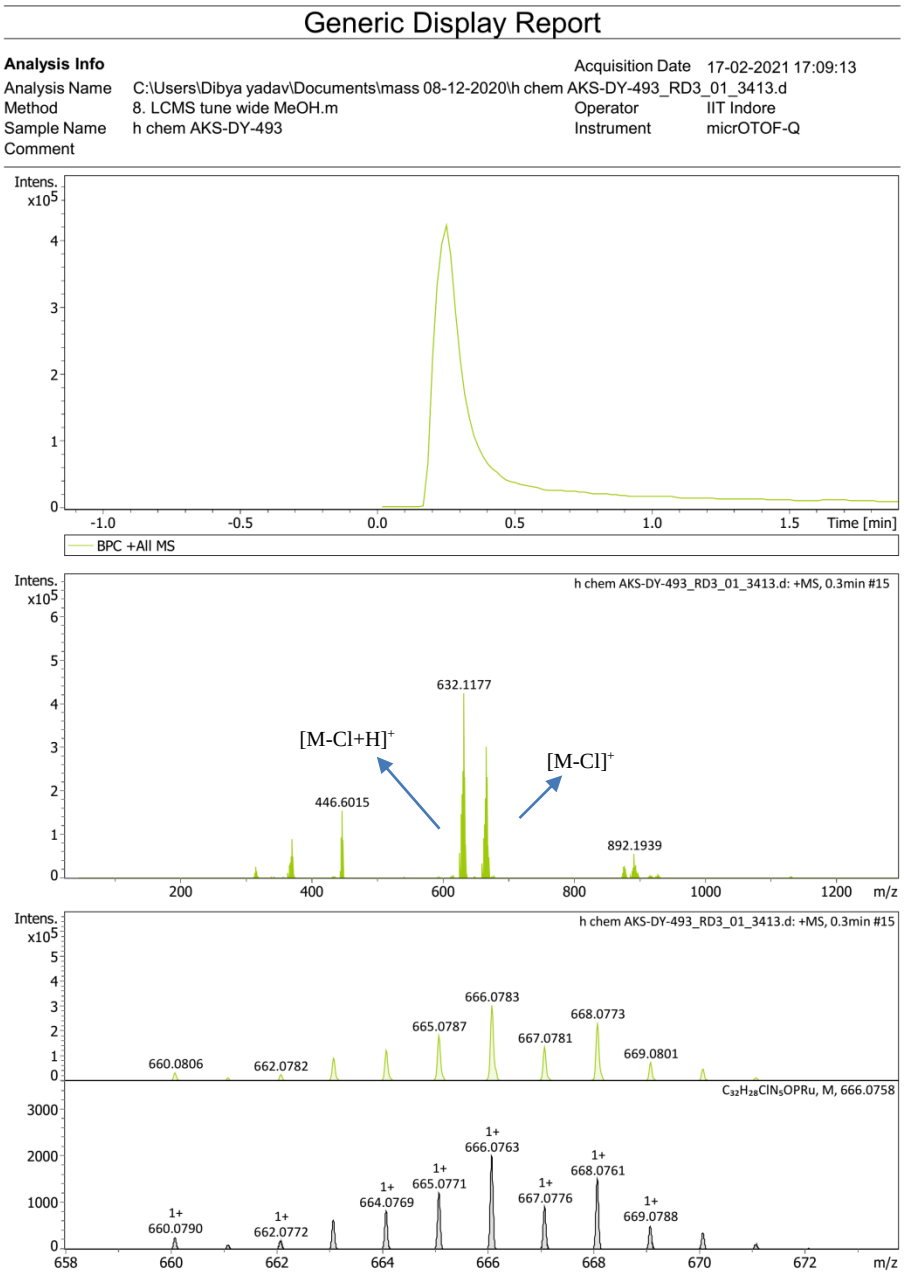

Figure 2.13 HRMS spectrum of **1a**

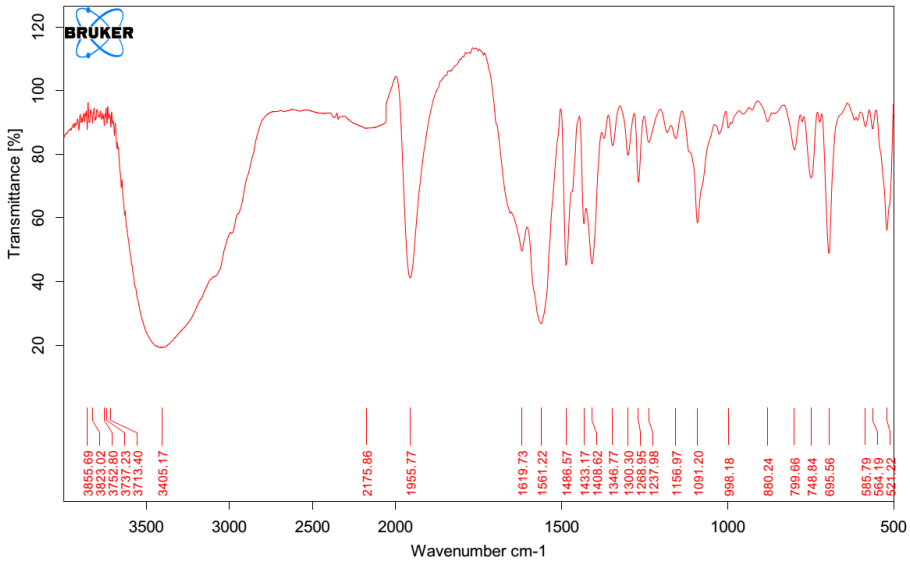

Figure 2.14 IR spectrum of **1a**

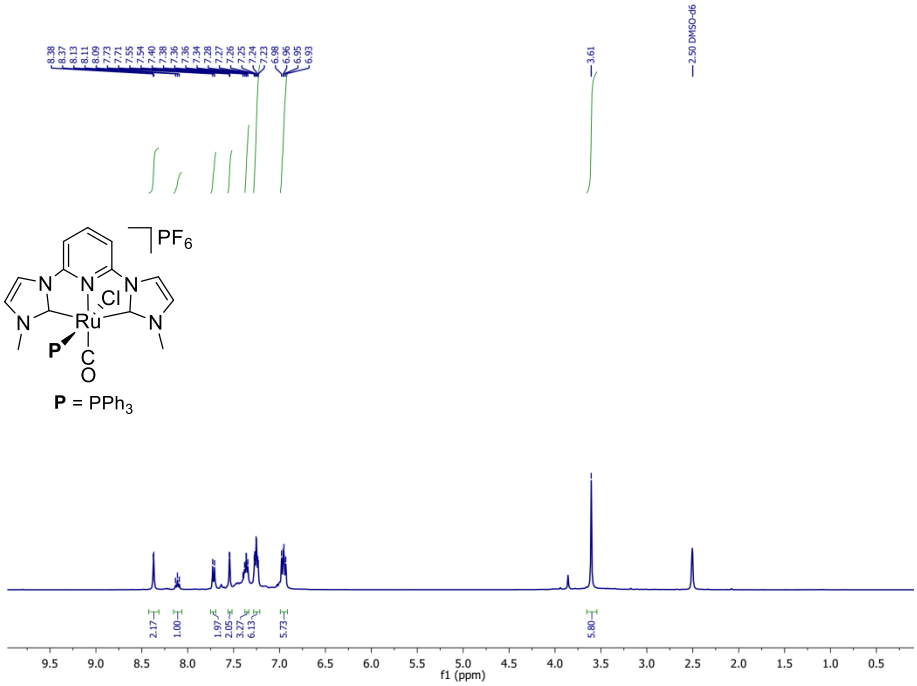

Figure 2.15 ^{1}H NMR spectrum of **1b**

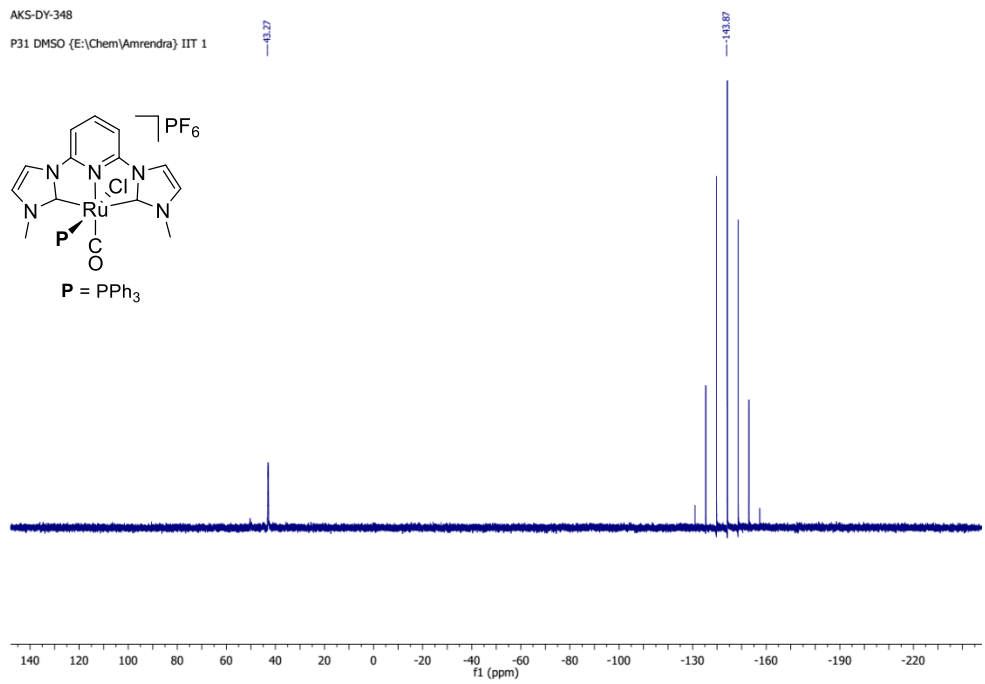

Figure 2.16 ^{31}P NMR spectrum of **1b**

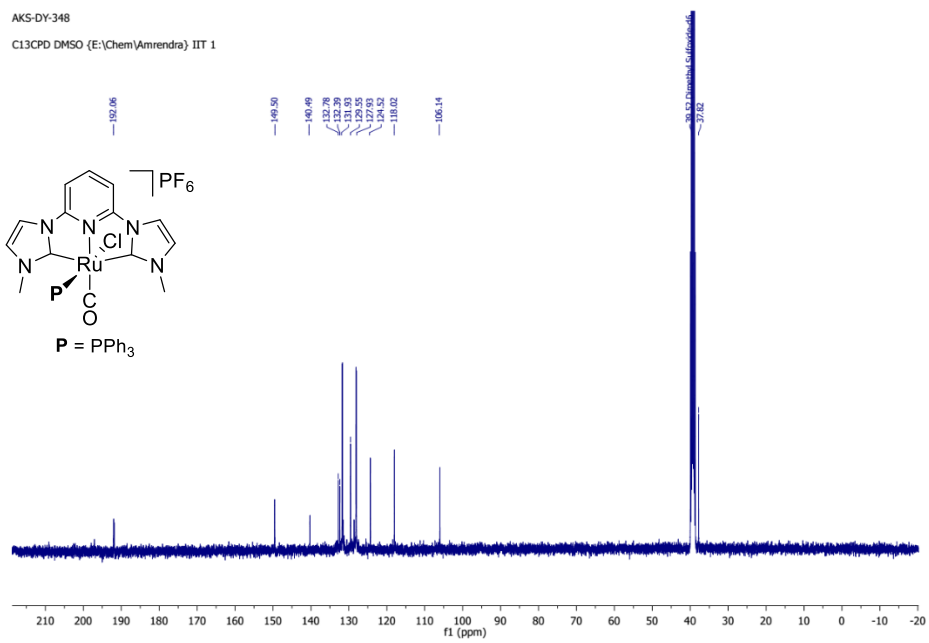

Figure 2.17 ^{13}C NMR spectrum of **1b**

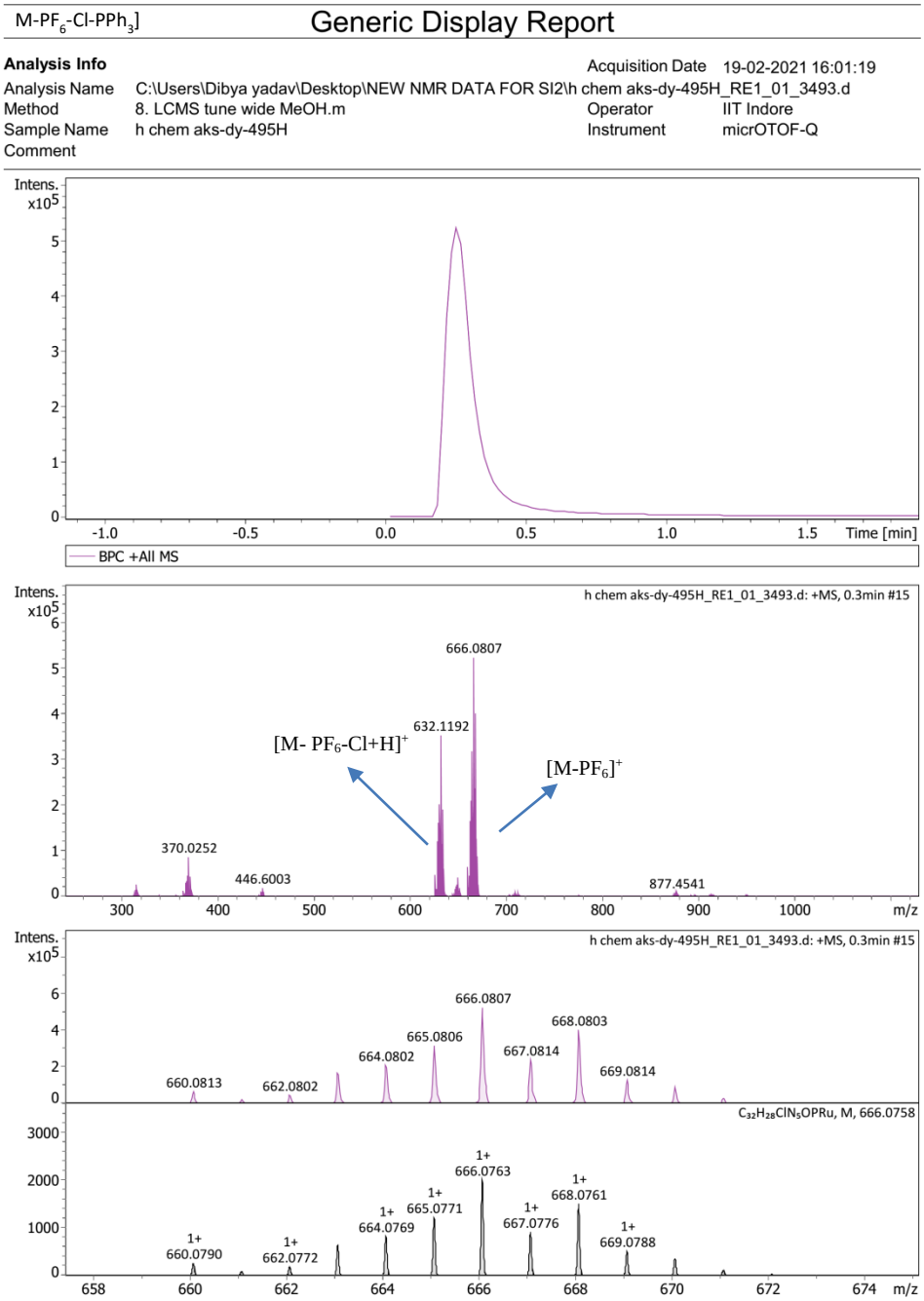

Figure 2.18 HRMS spectrum of **1b**

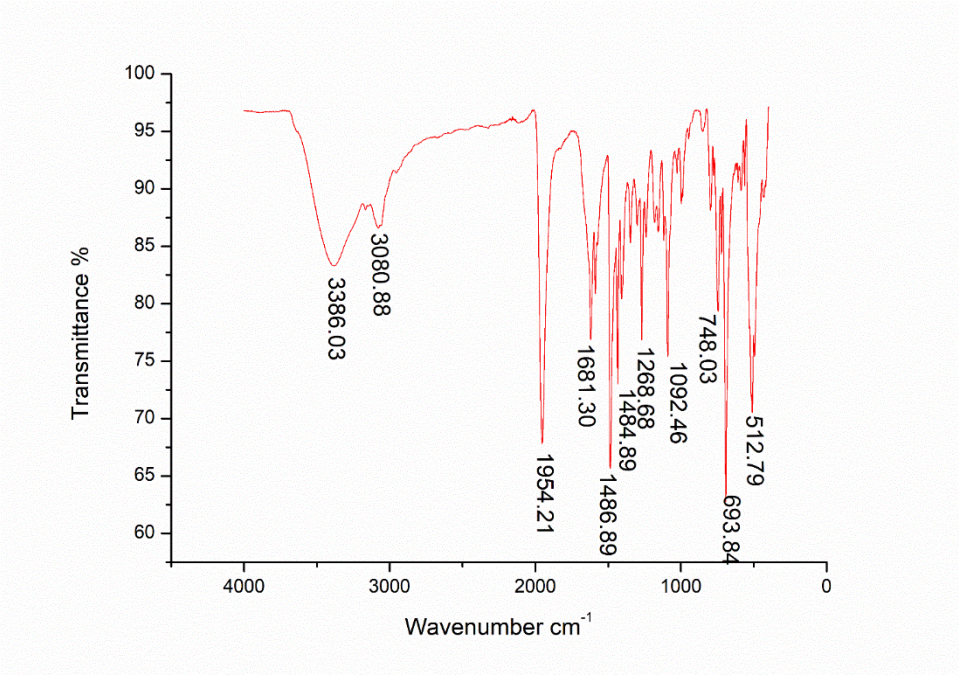

Figure 2.19 IR spectrum of **1b**

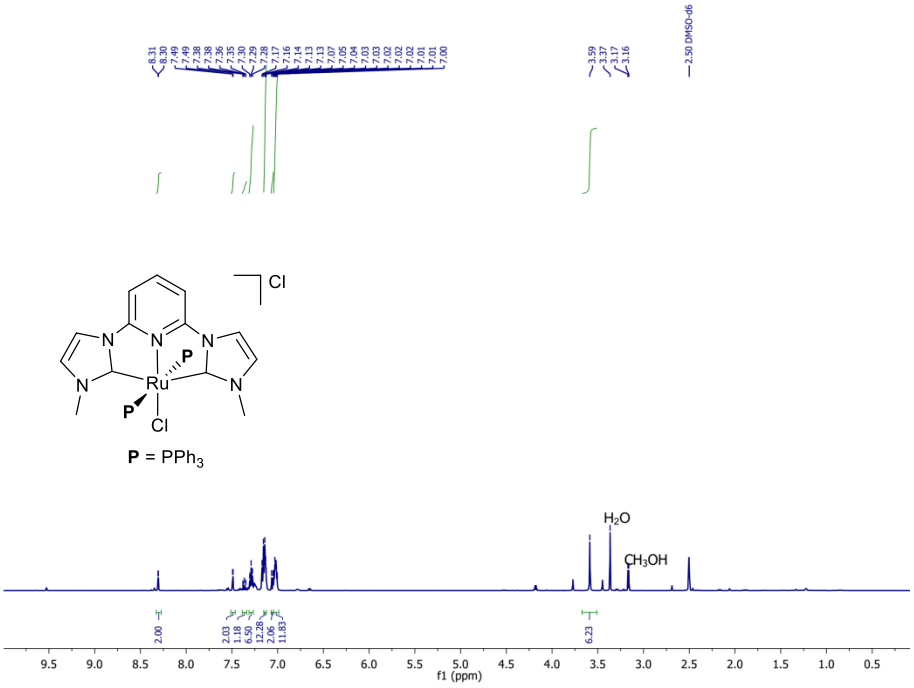

Figure 2.20 ^{1}H NMR spectrum of **2a**

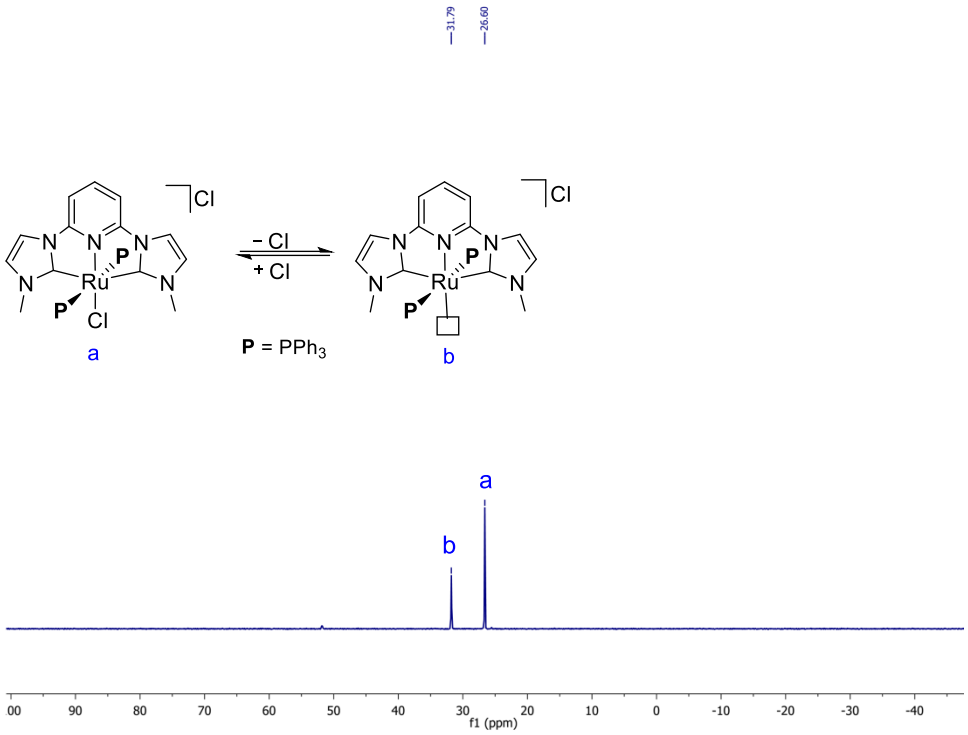

Figure 2.21 ^{31}P NMR spectrum of **2a**

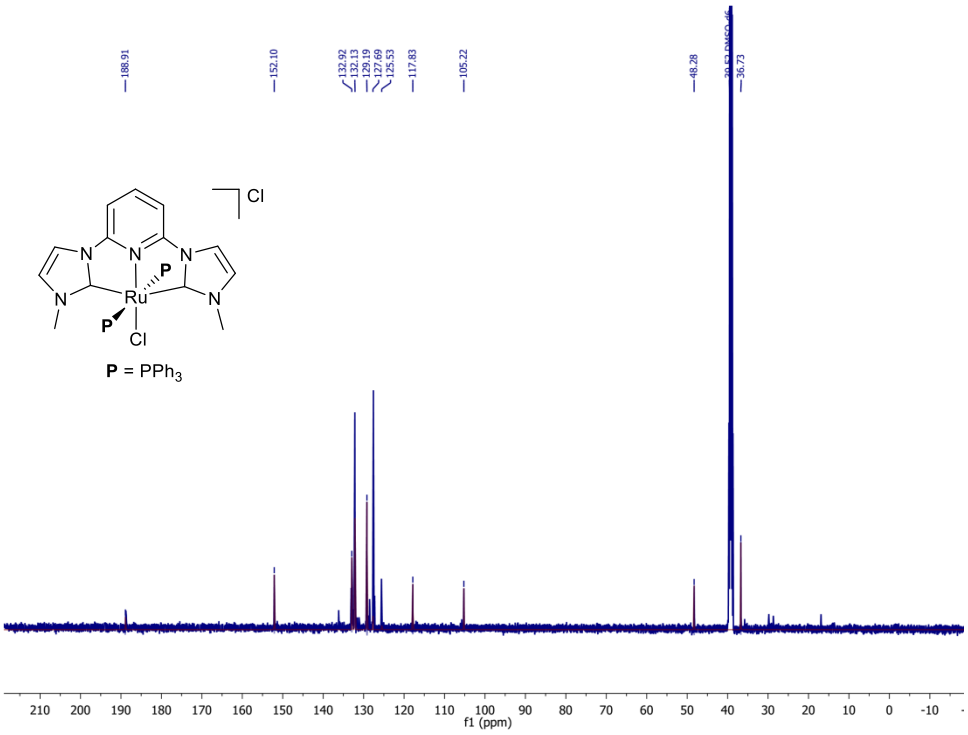

Figure 2.22 ^{13}C NMR spectrum of **2a**

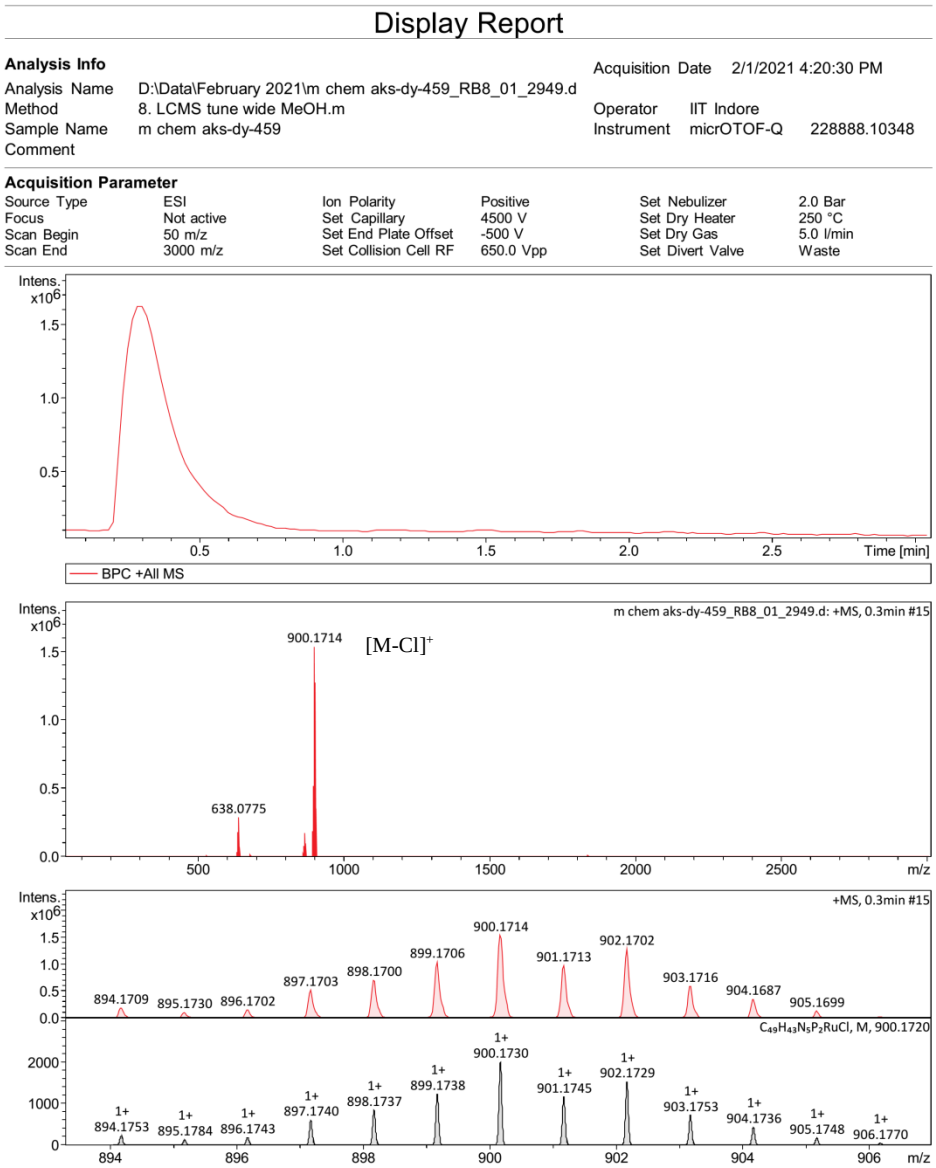

Figure 2.23 HRMS spectrum of **2a**

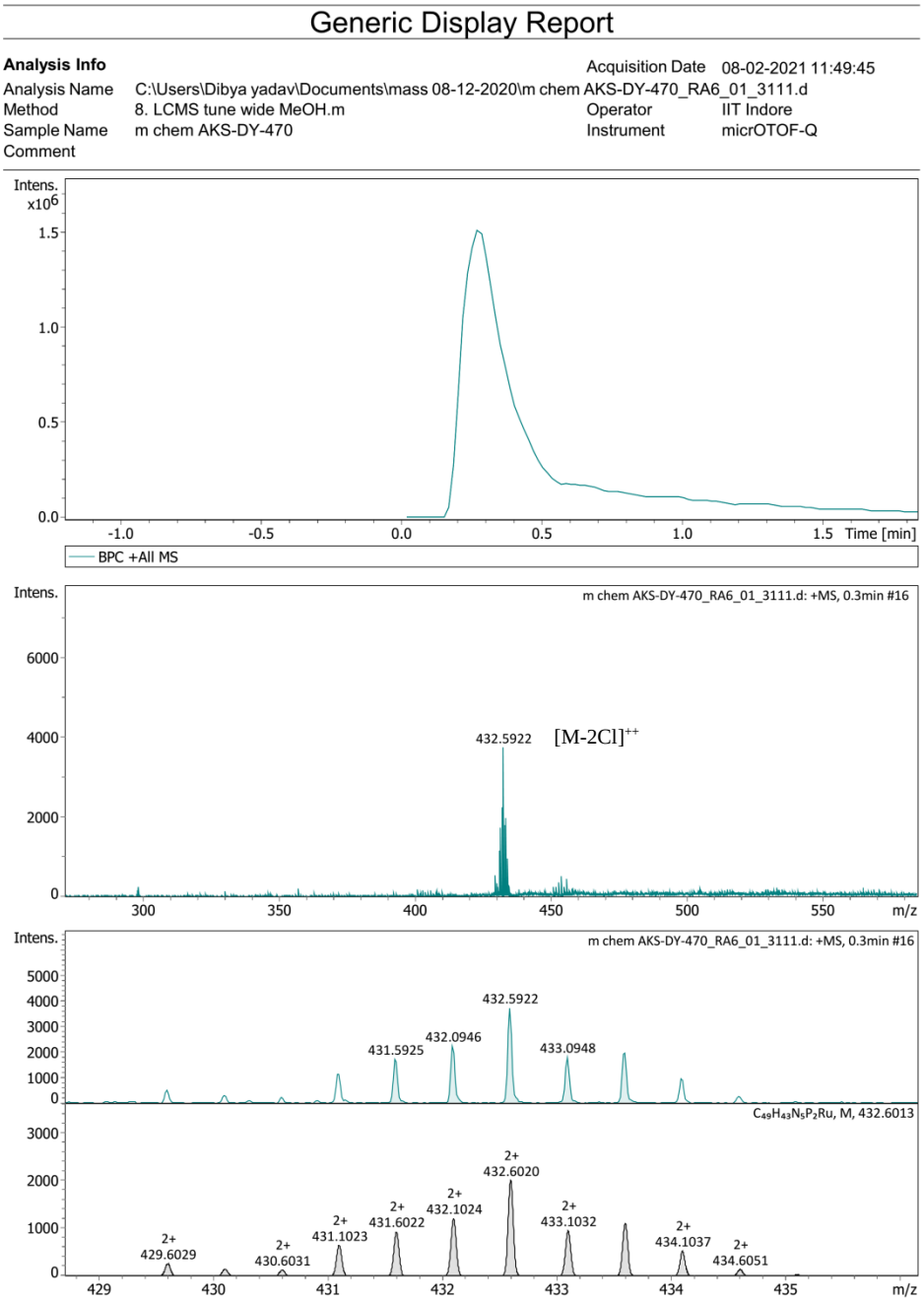

Figure 2.24 LCMS spectrum of **2a**

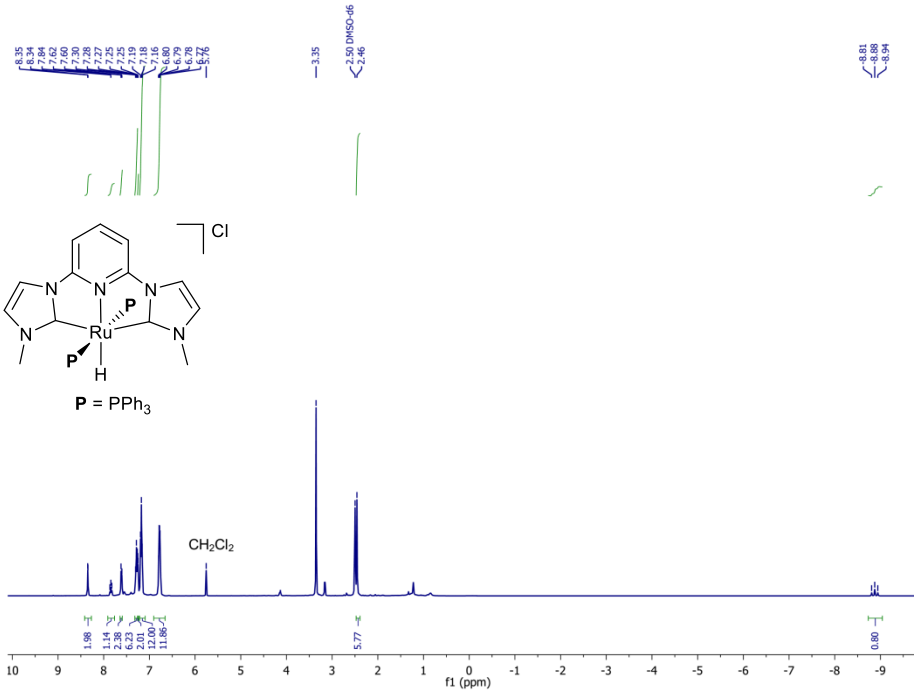

Figure 2.25 ^{1}H NMR spectrum of **3a**

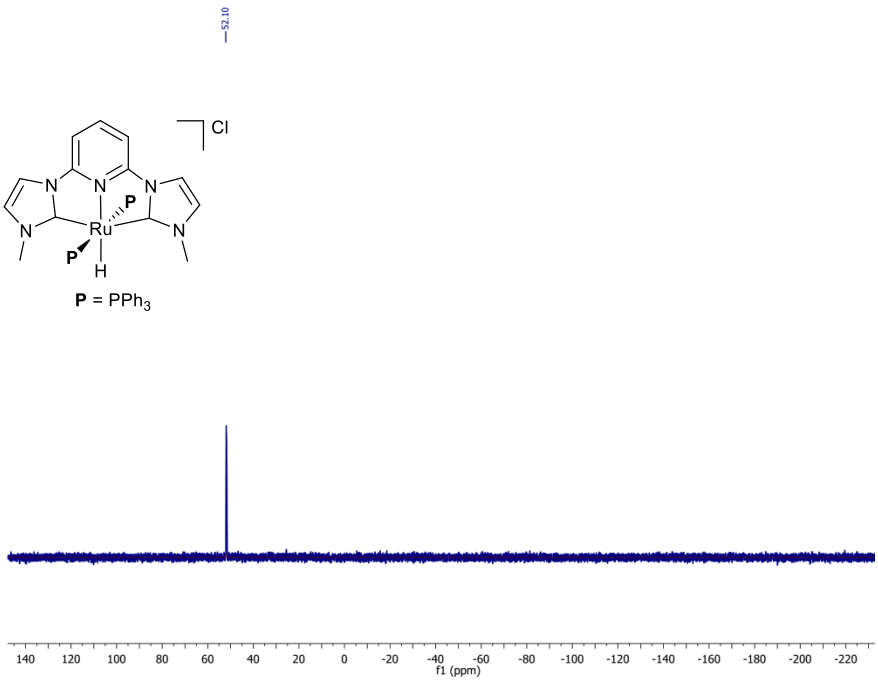

Figure 2.26 ^{31}P NMR spectrum of **3a**

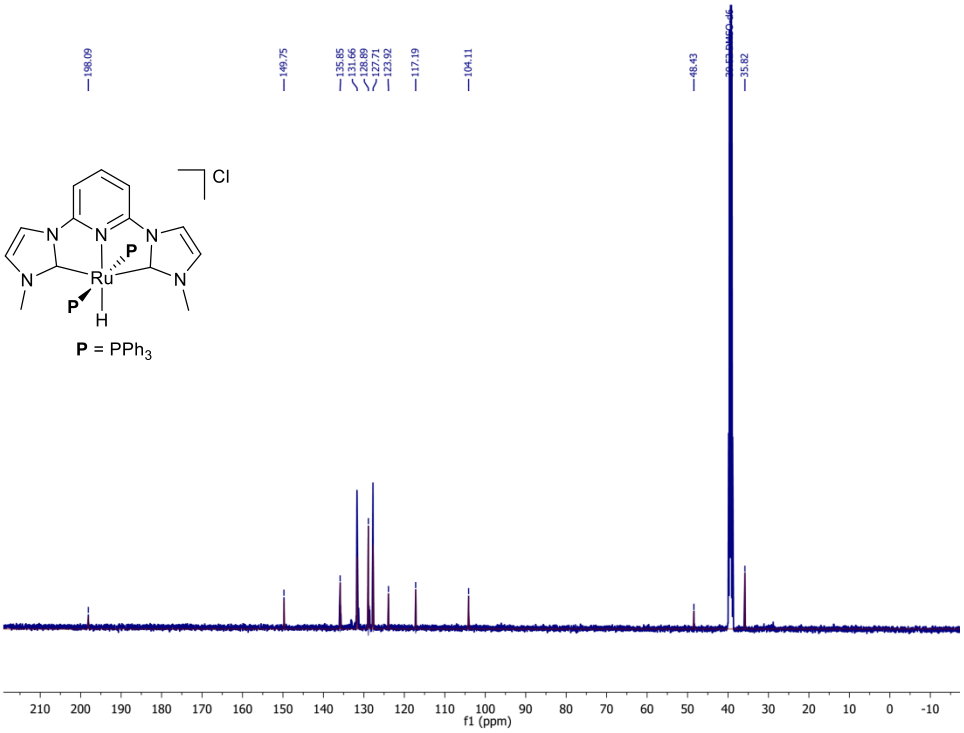

Figure 2.27 ^{13}C NMR spectrum of **3a**

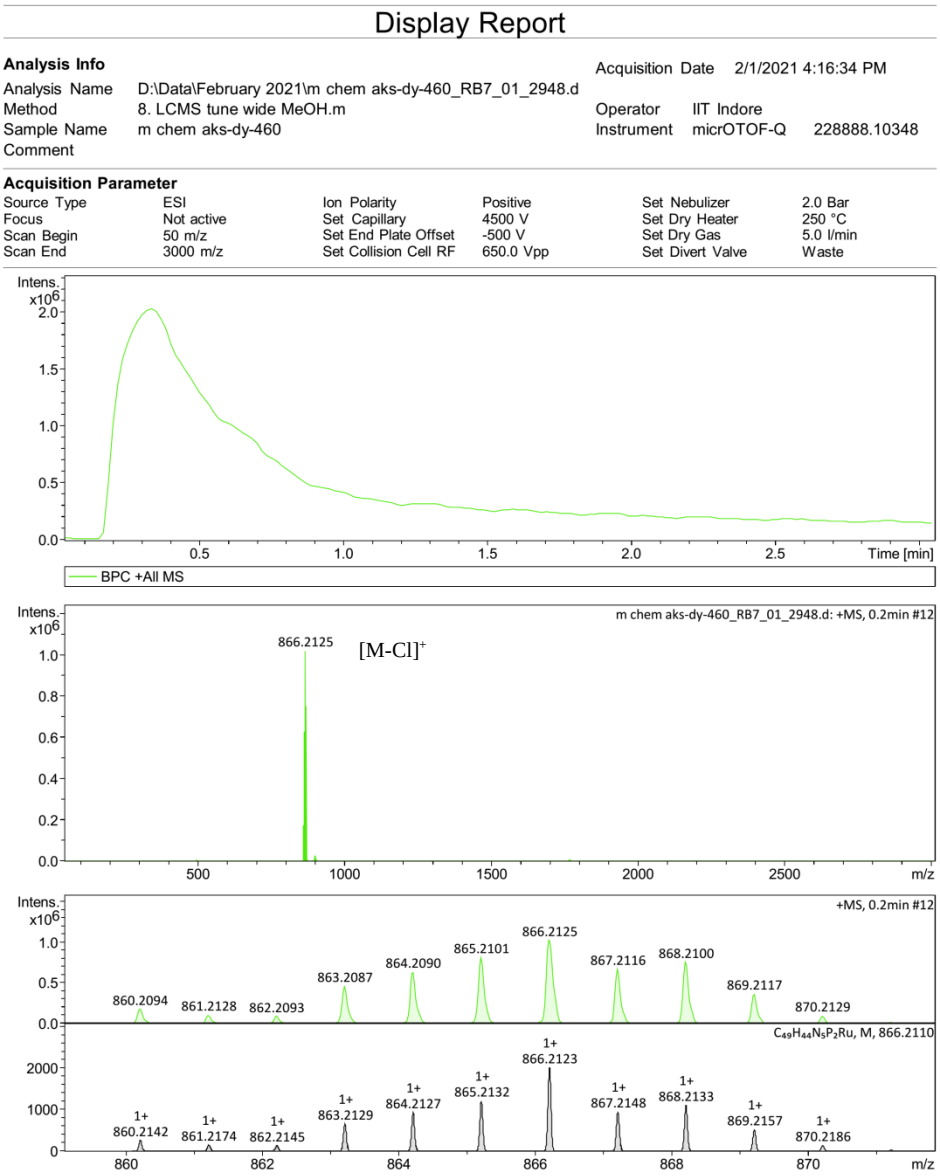

Figure 2.28 HRMS spectrum of **3a**

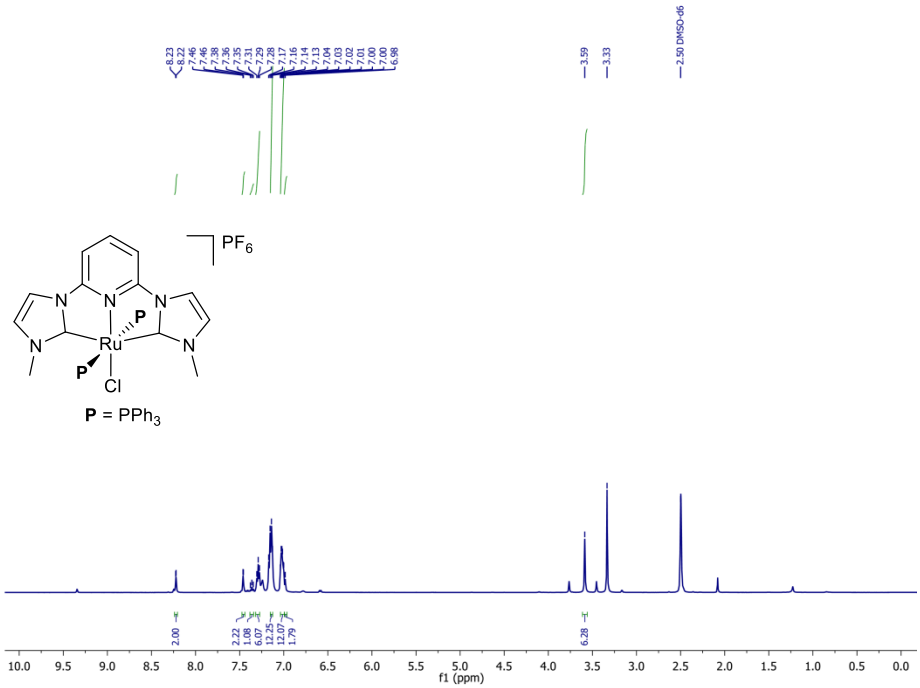

Figure 2.29 ^{1}H NMR spectrum of **2b**

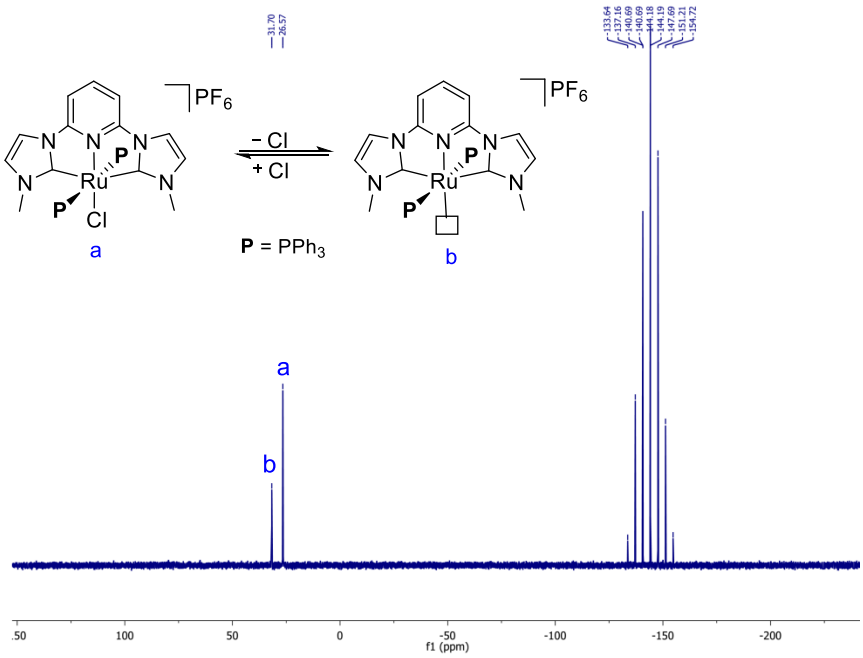

Figure 2.30 ^{31}P NMR spectrum of **2b**

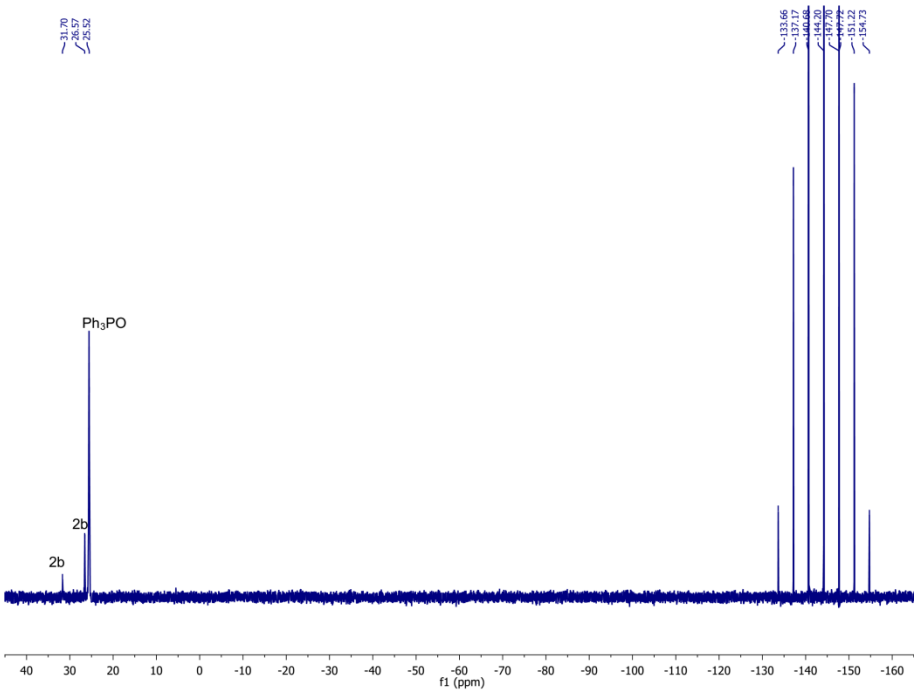

Figure 2.31 ^{31}P NMR spectrum of **2b** with PPh_3PO

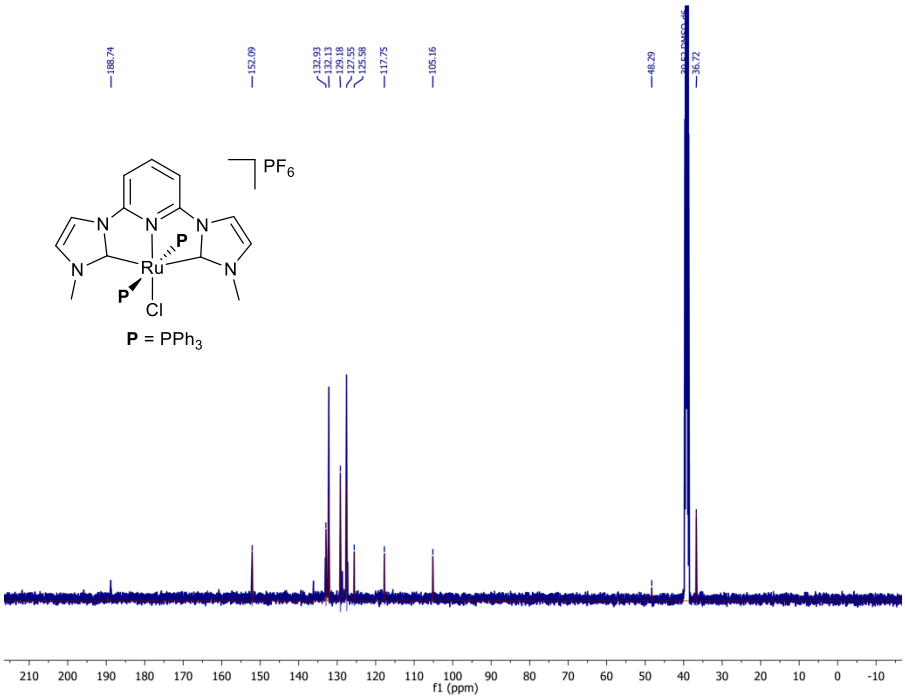

Figure 2.32 ^{13}C NMR spectrum of **2b**

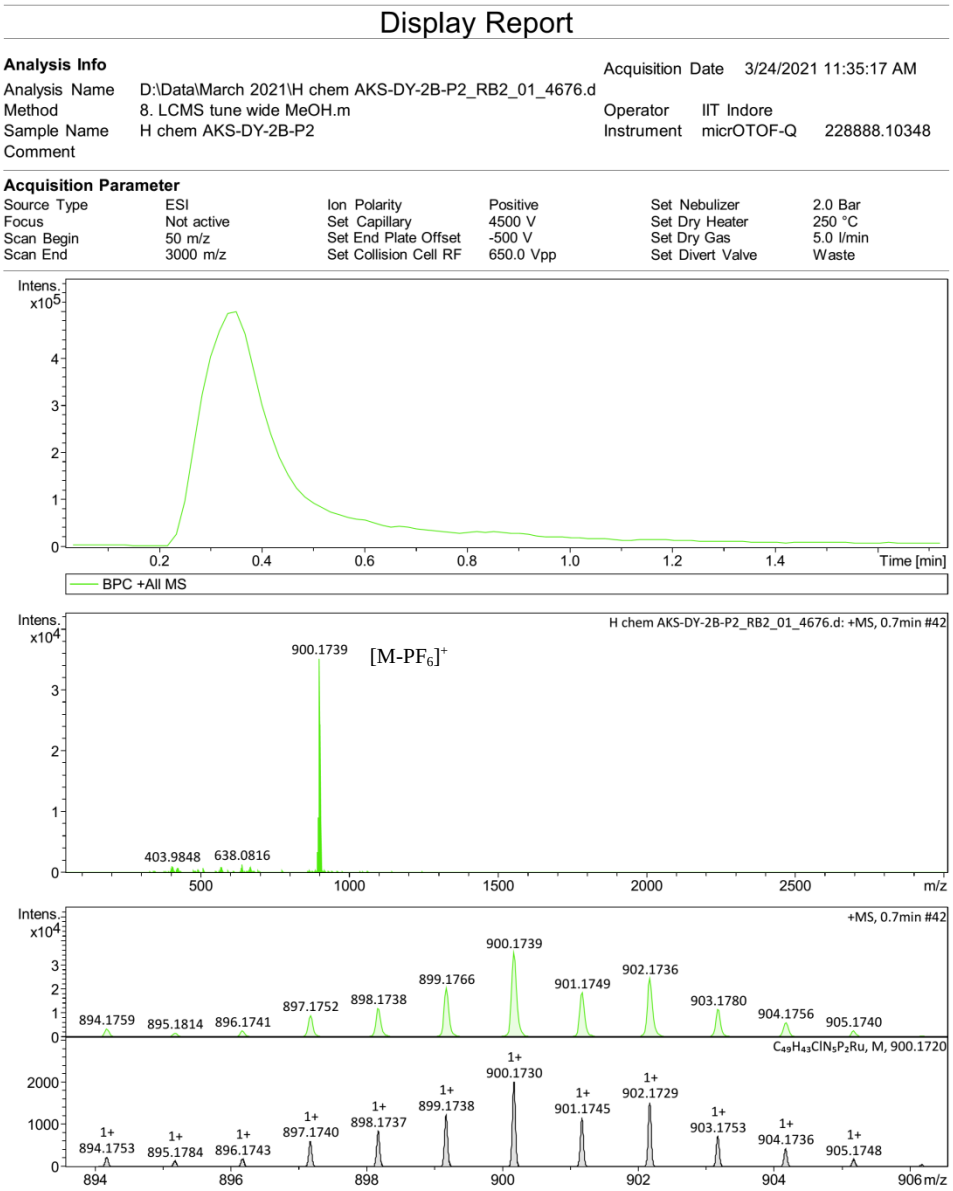

Figure 2.33 HRMS spectrum of **2b**

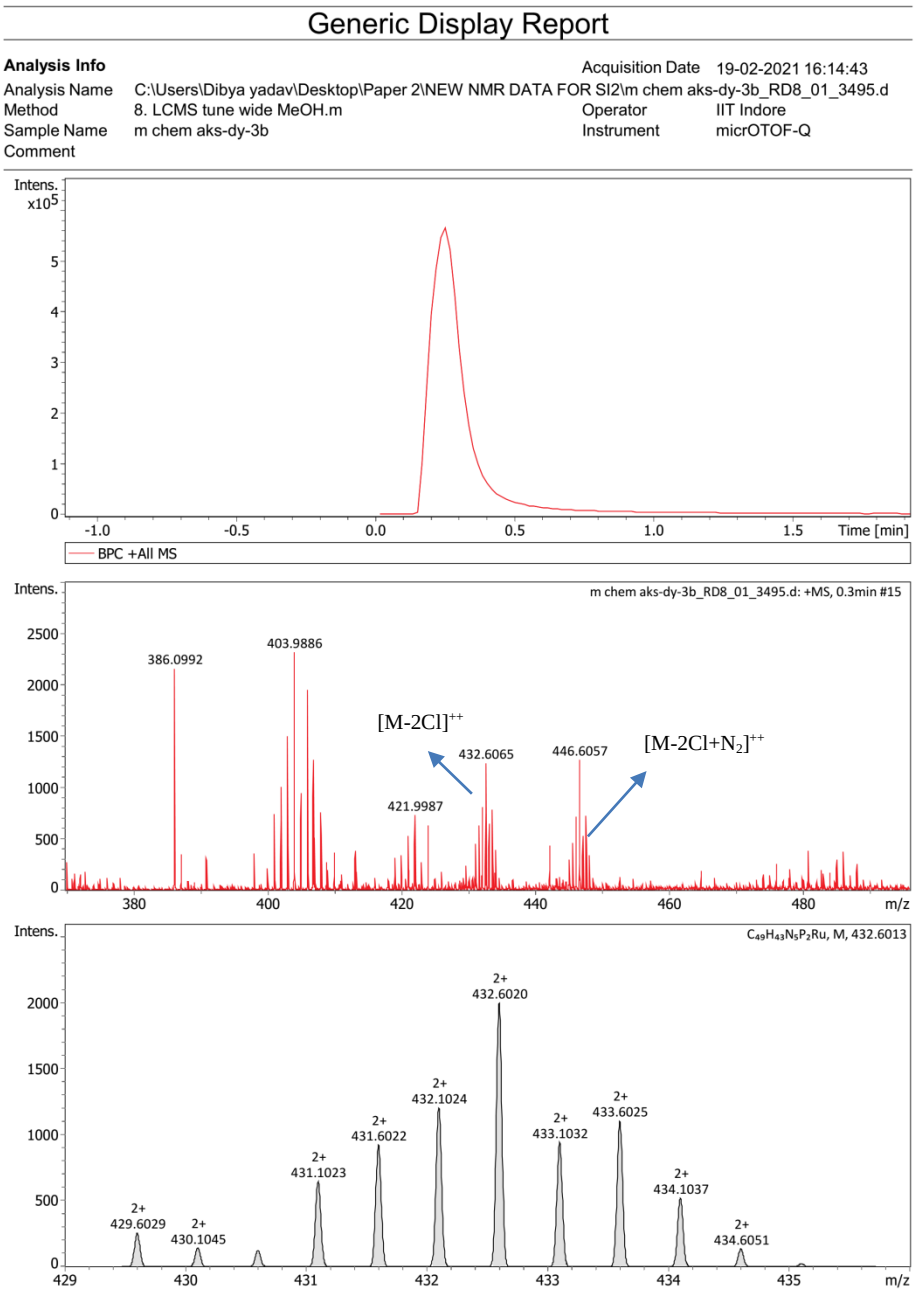

Figure 2.34 LCMS spectrum of **2b**

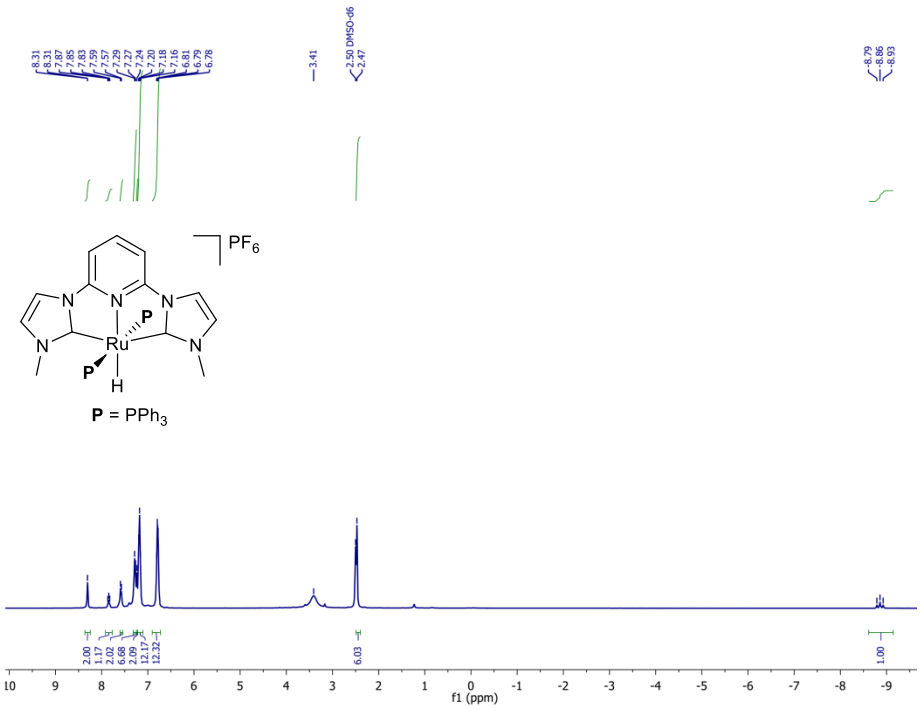

Figure 2.35 ^{1}H NMR spectrum of **3b**

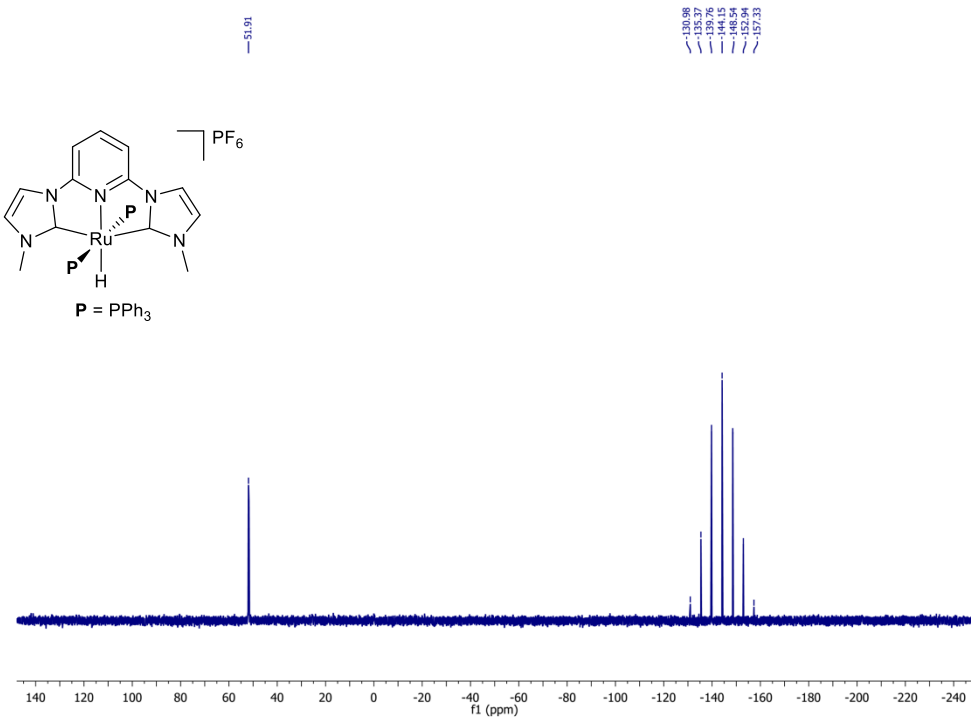

Figure 2.36 ^{31}P NMR spectrum of **3b**

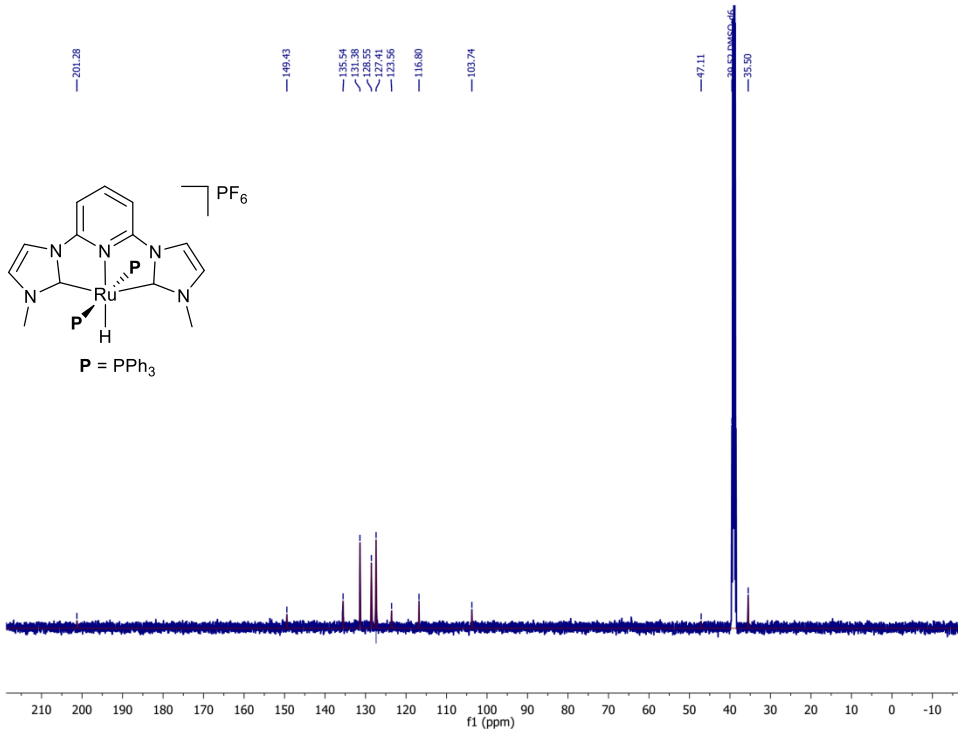

Figure 2.37 ^{13}C NMR spectrum of **3b**

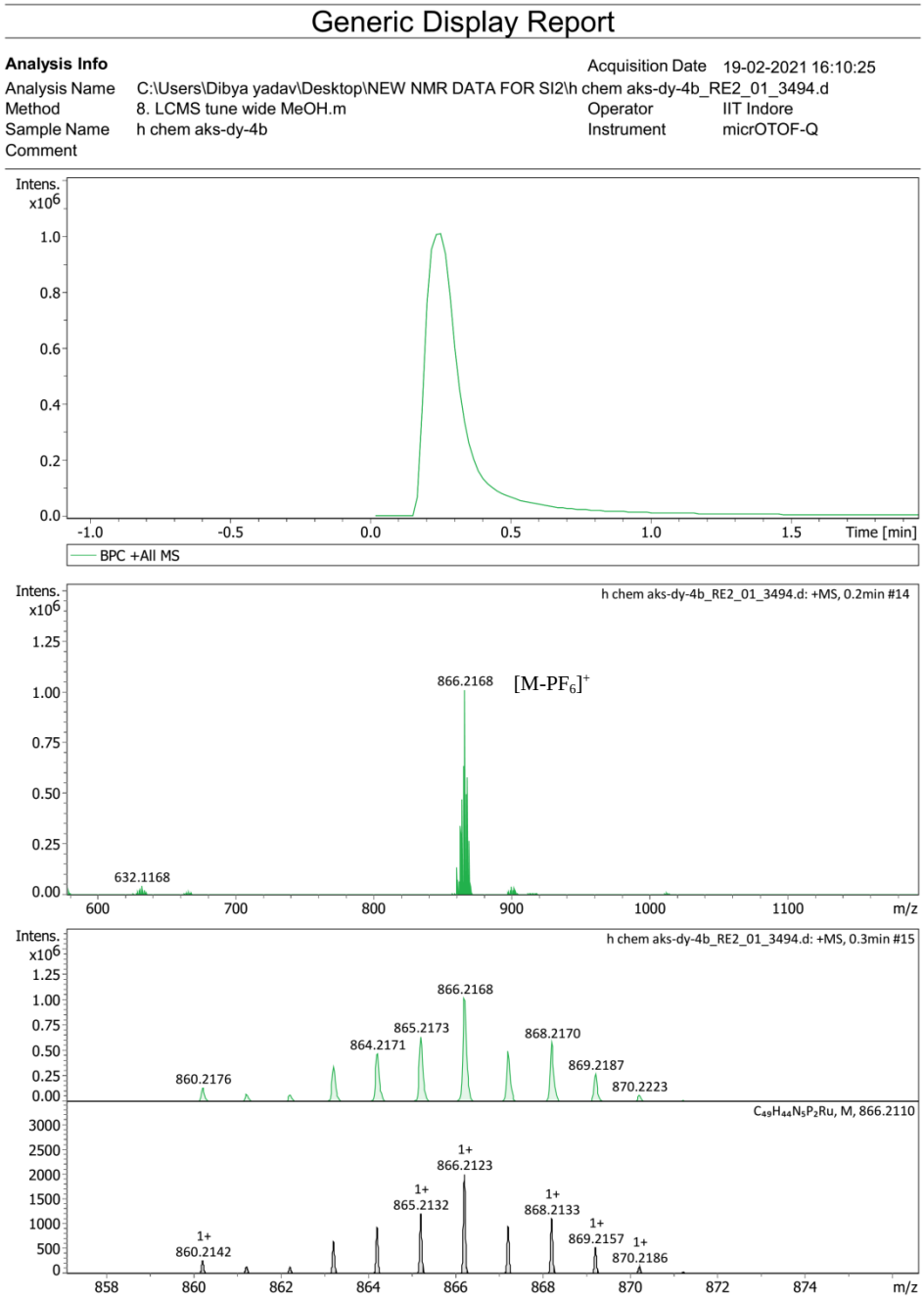

Figure 2.38 HRMS spectrum of **3b**

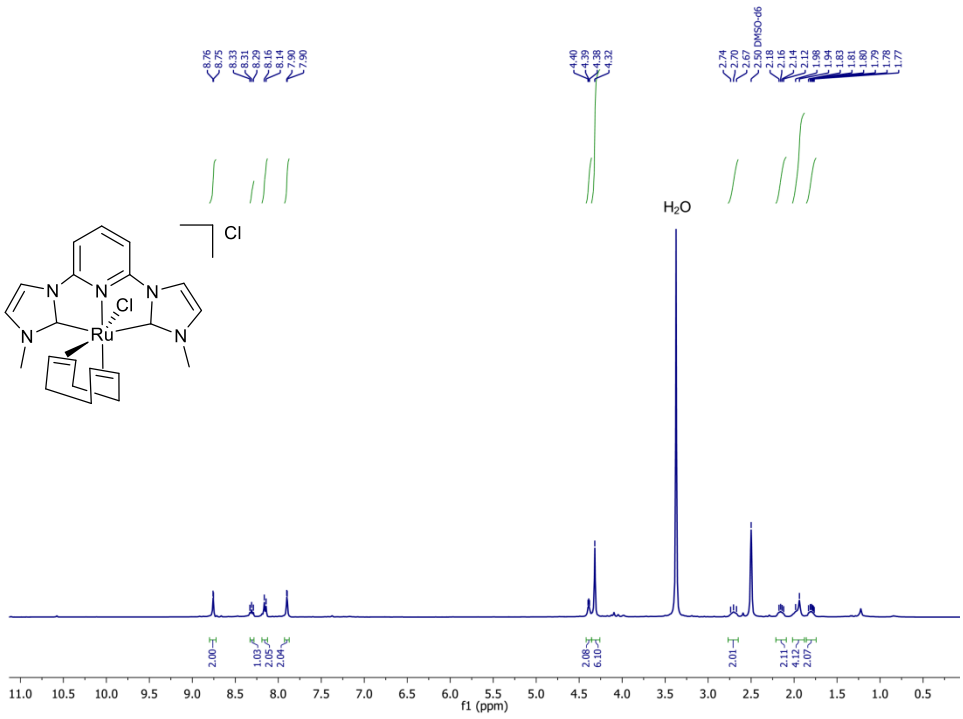

Figure 2.39 ^{1}H NMR spectrum of **4a**

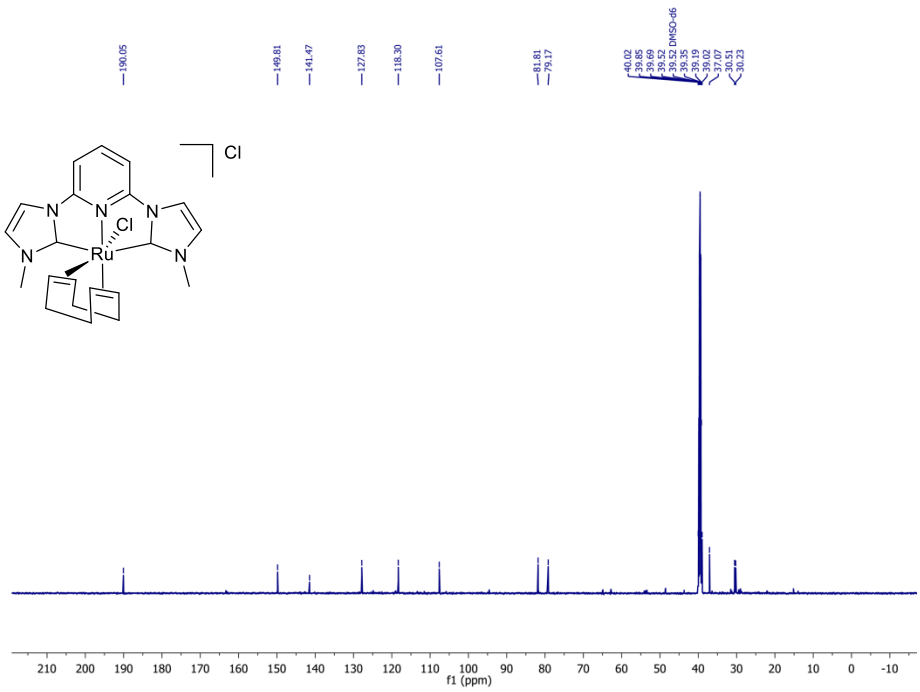

Figure 2.40 ^{13}C NMR spectrum of **4a**

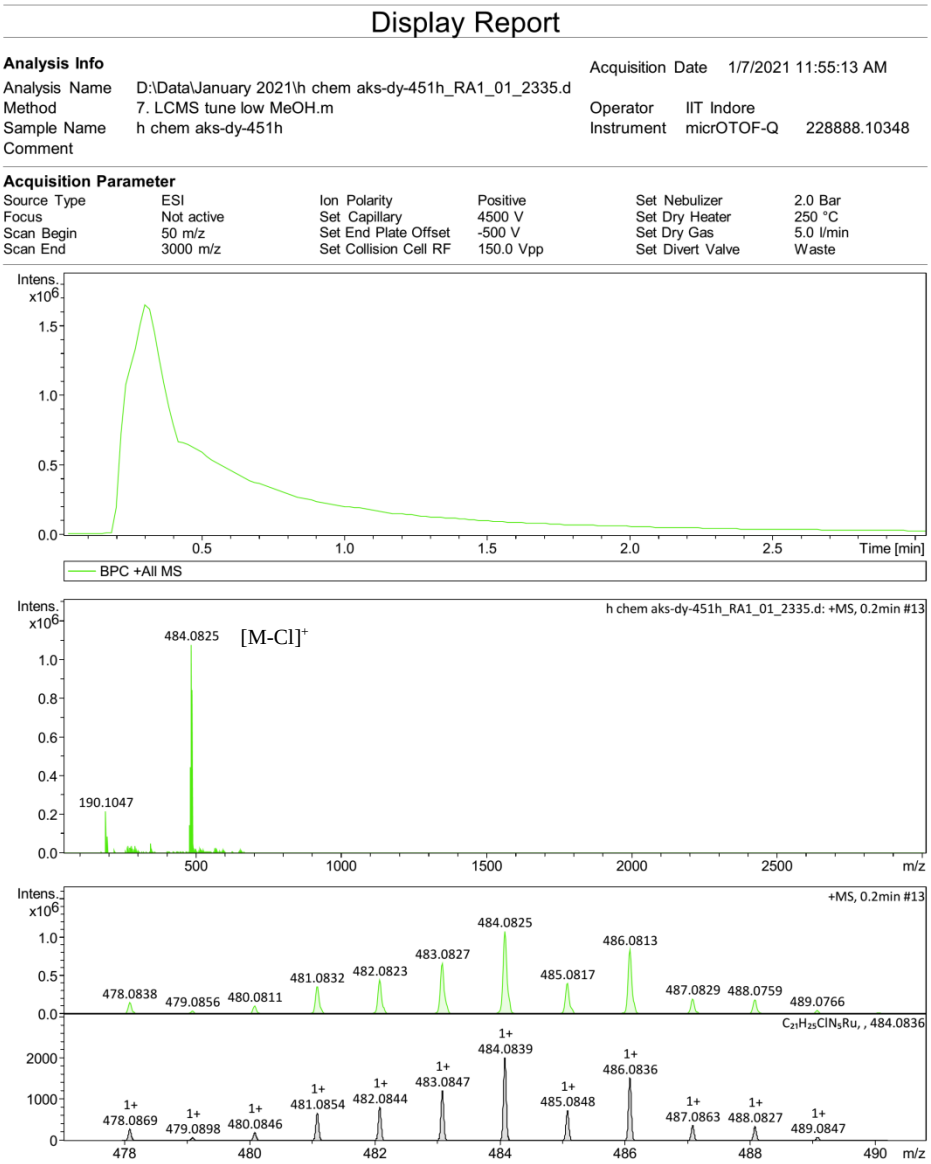

Figure 2.41 HRMS spectrum of **4a**

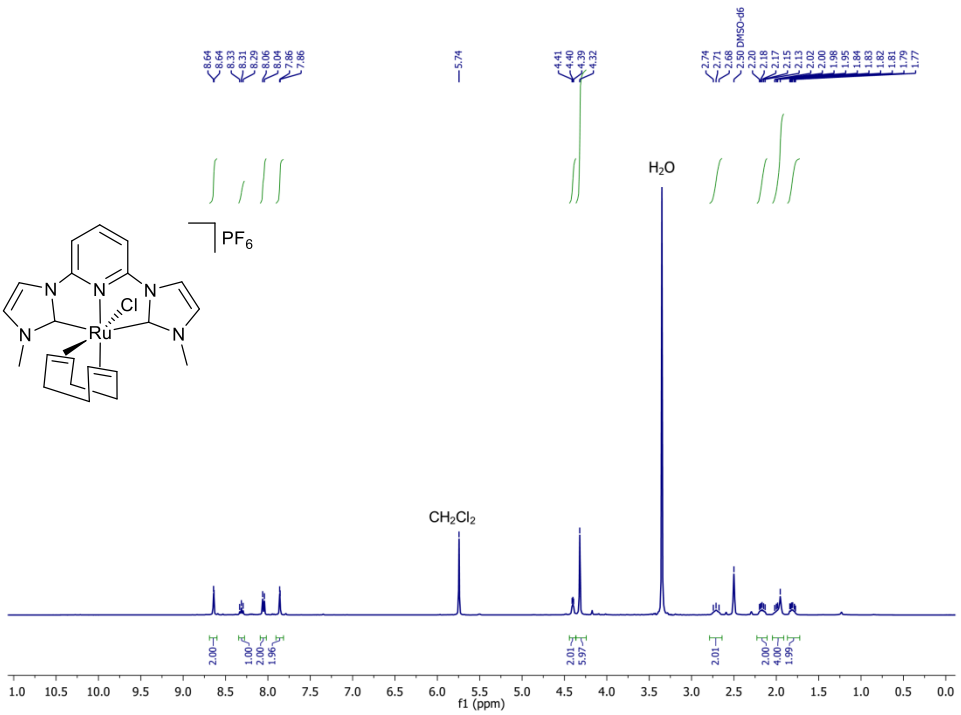

Figure 2.42 ^{1}H NMR spectrum of **4b**

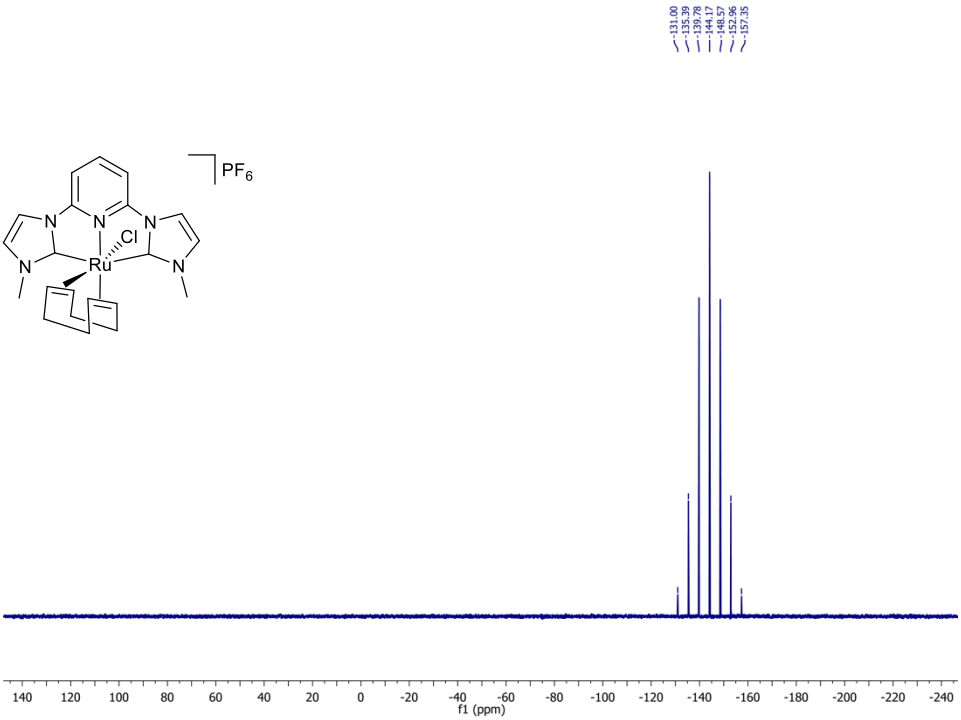

Figure 2.43 ^{31}P NMR spectrum of **4b**

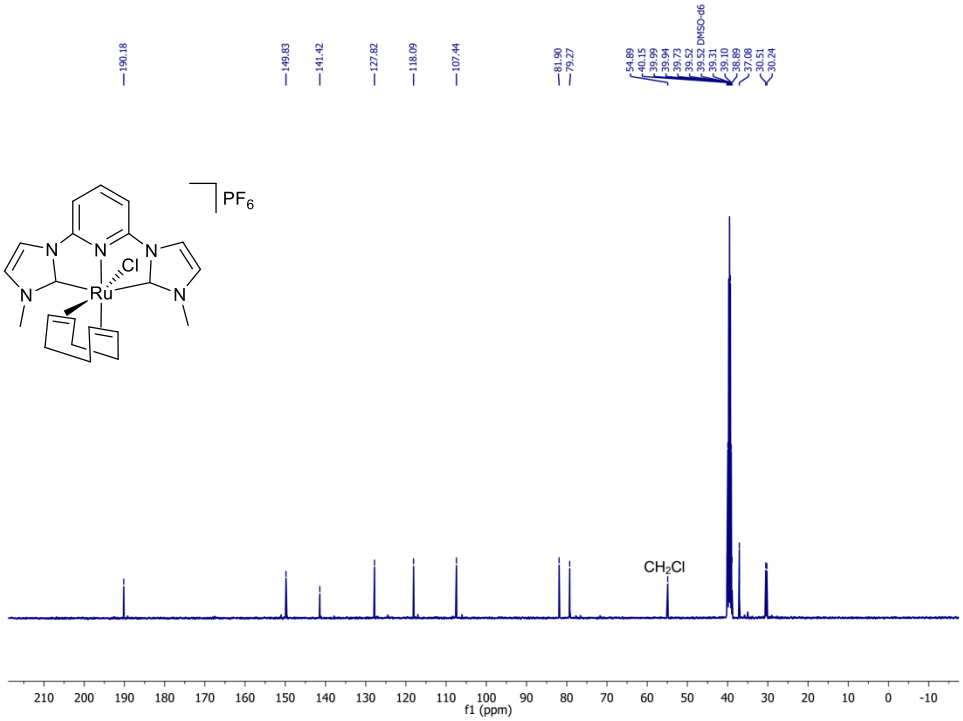

Figure 2.44 ^{13}C NMR spectrum of **4b**

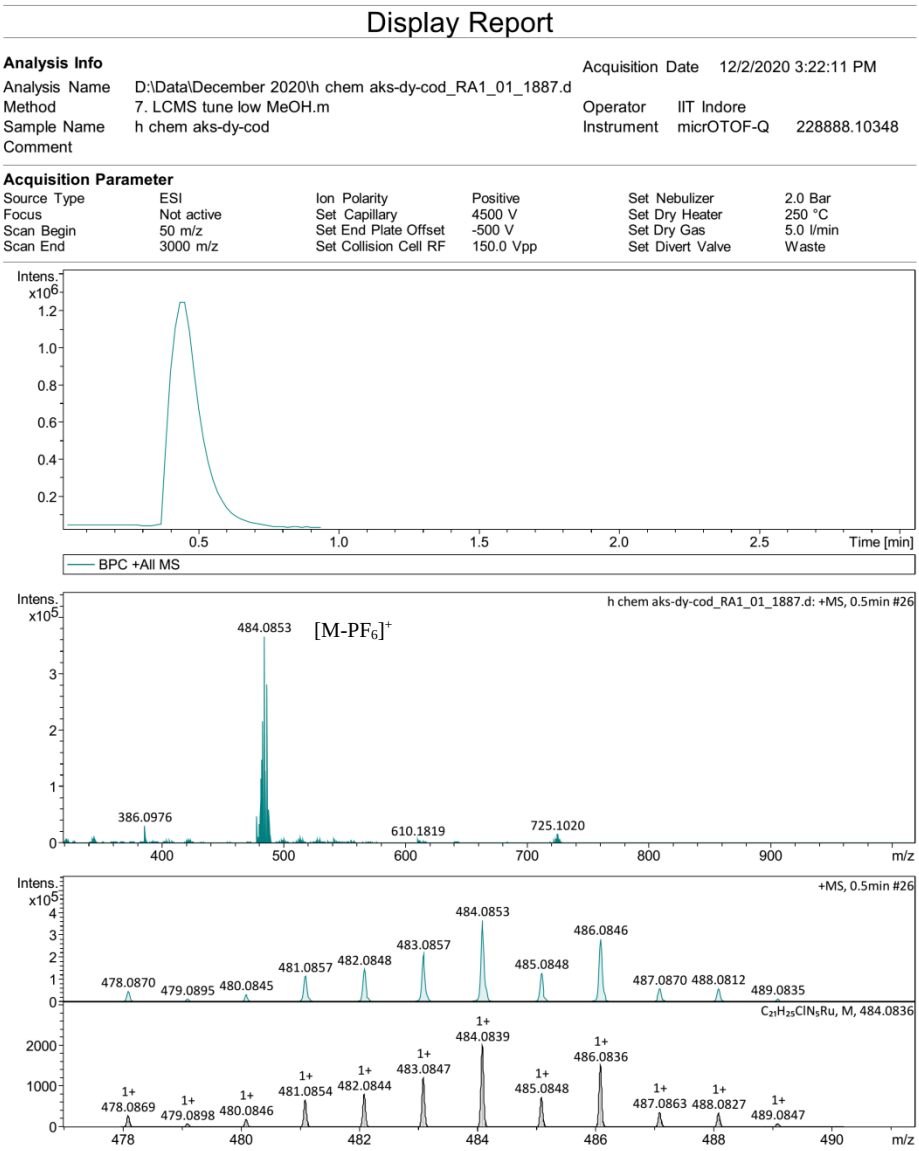

Figure 2.45 HRMS spectrum of **4b**

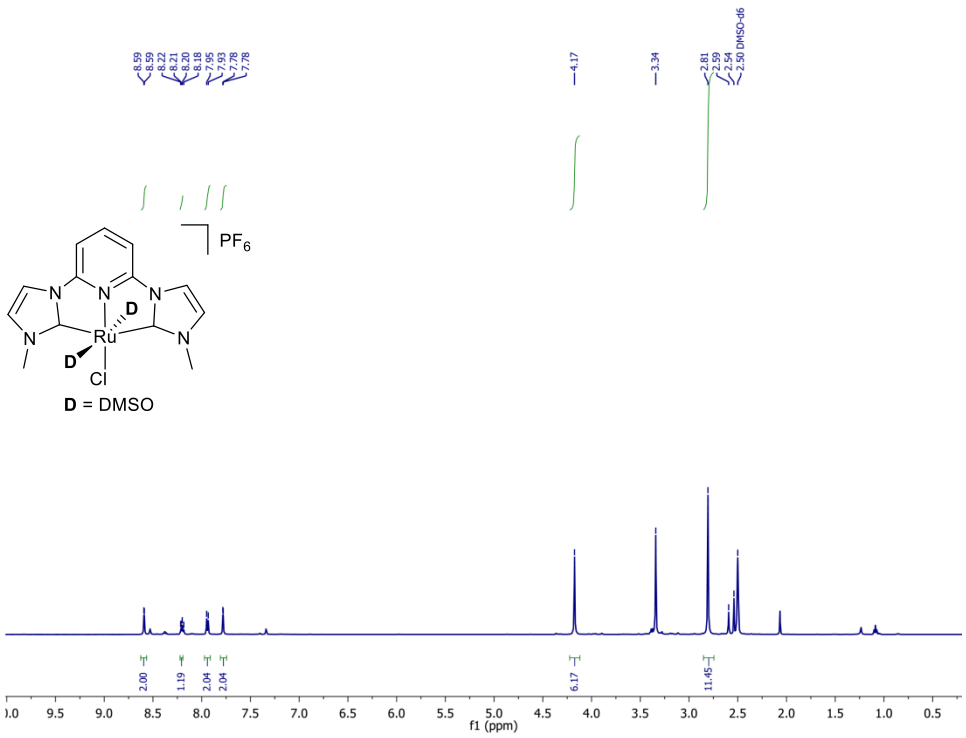

Figure 2.46 ^{1}H NMR spectrum of **6b**

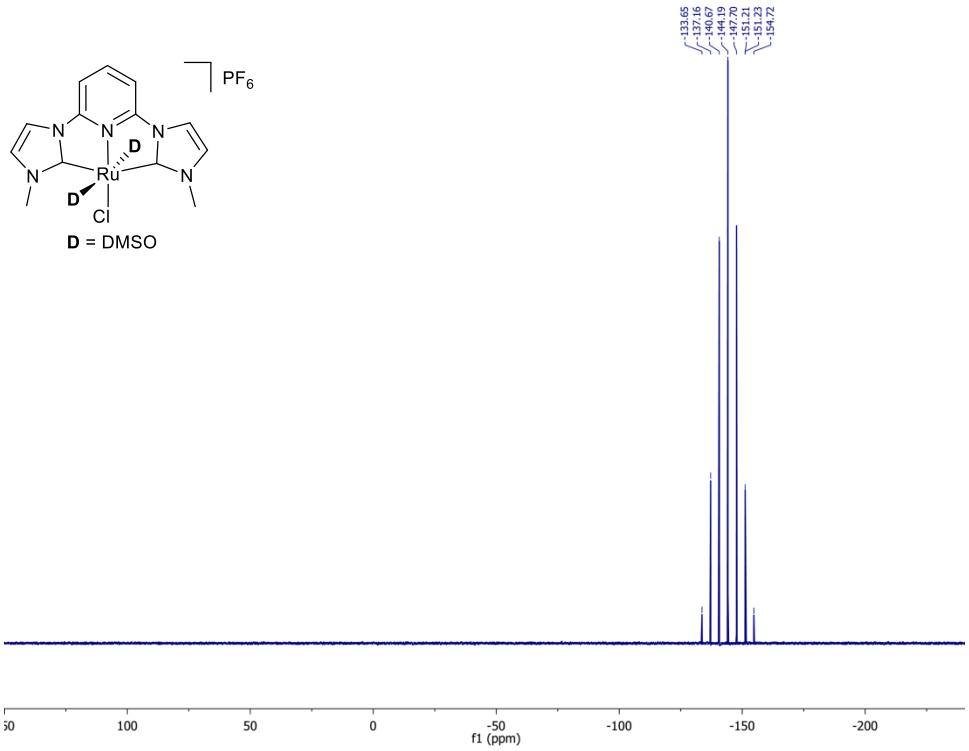

Figure 2.47 ^{31}P NMR spectrum of **6b**

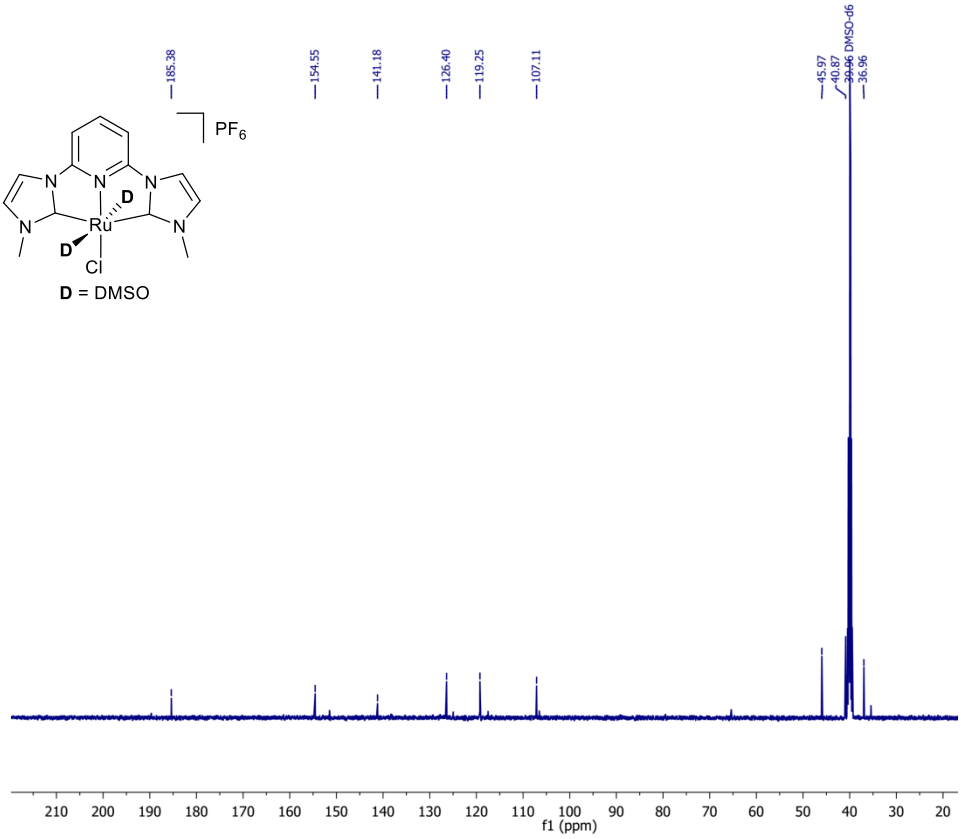

Figure 2.48 ^{13}C NMR spectrum of **6b**

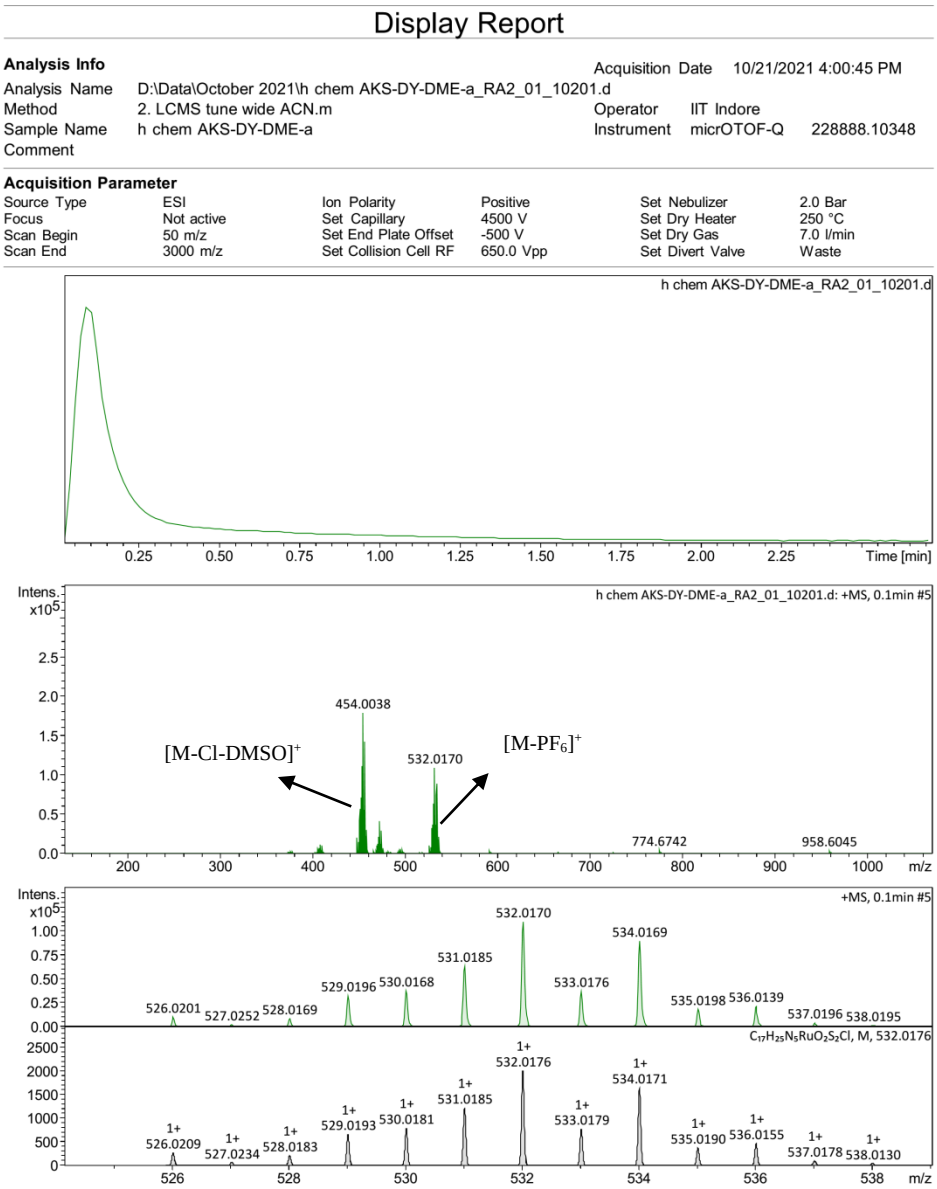

Figure 2.49 HRMS spectrum of **6b**

2.5 References

[1] Moulton C. J., Shaw B. L., (1976), Transition metal-carbon bonds. Part XLII. Complexes of nickel, palladium, platinum, rhodium and iridium with the tridentate ligand 2,6-bis[(di-t-butylphosphino)methyl]phenyl, *J. Chem. Soc., Dalton Trans.*, 1020–1024 (DOI: 10.1039/DT9760001020).

[2] Van Koten G., (1989), Tuning the reactivity of metals held in a rigid ligand environment, *Pure Appl. Chem.*, 61, 1681–1694 (DOI: 10.1351/pac198961101681).

[3] Van der Boom M. E., Milstein D., (2003), Cyclometalated Phosphine-Based Pincer Complexes: Mechanistic Insight in Catalysis, Coordination, and Bond Activation, *Chem. Rev.*, 103, 1759–1792 (DOI: 10.1021/cr960118r).

[4] Fan L., Yang L., Guo C., Foxman B. M., Ozerov O. V., (2004), N−C Cleavage in Pincer PNP Complexes of Palladium, *Organometallics*, 23, 4778–4787 (DOI: 10.1021/om049651k).

[5] Hahn C., (2004), Enhancing Electrophilic Alkene Activation by Increasing the Positive Net Charge in Transition-Metal Complexes and Application in Homogeneous Catalysis, *Chem. Eur. J.*, 10, 5888–5899 (DOI: 10.1002/chem.200400550).

[6] Arduengo III A. J., Harlow R. L., Kline M., (1991), A stable crystalline carbene, *J. Am. Chem. Soc.*, 113, 361–363 (DOI: 10.1021/ja00001a054).

[7] Chianese A. R., Mo A., Lampland N. L., Swartz R. L., Bremer P.T., (2010), Iridium Complexes of CCC-Pincer N-Heterocyclic Carbene Ligands: Synthesis and Catalytic C−H Functionalization, *Organometallics*, 29, 3019–3026 (DOI: 10.1021/om100302g).

[8] Lv K., Cui D., (2008), Tridentate CCC-Pincer Bis(carbene)-Ligated Rare-Earth Metal Dibromides. Synthesis and

Characterization, *Organometallics*, 27, 5438–5440 (DOI: 10.1021/om800801k).

[9] Danopoulos A.A., Winston S., Motherwell W.B., (2002), Stable N-functionalised 'pincer' bis carbene ligands and their ruthenium complexes; synthesis and catalytic studies, *Chem. Commun.*, 1376–1377 (DOI: 10.1039/B202814J).

[10] Danopoulos A.A., Braunstein P., Saßmannshausen J., Pugh D., Wright J.A., (2020), "Pincer" Pyridine–Dicarbene–Iridium and -Ruthenium Complexes and Derivatives Thereof, *Eur. J. Inorg. Chem.*, 2020, 3359–3569 (DOI: 10.1002/ejic.202000429).

[11] Younus H.A., Ahmad N., Su W., Verpoort F., (2014), Ruthenium pincer complexes: Ligand design and complex synthesis, *Coord. Chem. Rev.*, 276, 112–152 (DOI: 10.1016/j.ccr.2014.06.016).

[12] Takenaka K., Minakawa M., Uozumi Y., (2005), NCN Pincer Palladium Complexes: Their Preparation via a Ligand Introduction Route and Their Catalytic Properties, *J. Am. Chem. Soc.*, 127, 12273–12281 (DOI: 10.1021/ja052780n).

[13] Shelke Y. G., Yashmeen A., Gholap A. V. A., Gharpure S. J., Kapdi A. R., (2018), Homogeneous Catalysis: A Powerful Technology for the Modification of Important Biomolecules, *Chemistry – An Asian Journal*, 13, 2991–3013 (DOI: 10.1002/asia.201801020).

[14] Gunanathan C., Milstein D., (2014), Bond Activation and Catalysis by Ruthenium Pincer Complexes, *Chem. Rev.*, 114, 12024–12087 (DOI: 10.1021/cr5002782).

[15] Hernández-Juárez M., Vaquero M., Álvarez E., Salazar V., Suárez A., (2012), Hydrogenation of imines catalysed by ruthenium(II) complexes based on lutidine-derived CNC pincer

ligands, *Dalton Trans.*, 42, 351–354 (DOI: 10.1039/C2DT31907A).

[16] Danopoulos A.A., Winston S., Motherwell W.B., (2002**)**, Stable N-functionalised 'pincer' bis carbene ligands and their ruthenium complexes; synthesis and catalytic studies, *Chem. Commun.*, 1376-1377.(DOI: 10.1039/B202814J).

[17] Poyatos M., Mata J.A., Falomir E., Crabtree R.H., Peris E., (2003), New Ruthenium(II) CNC-Pincer Bis(carbene) Complexes: Synthesis and Catalytic Activity, *Organometallics*, *22*, 1110-1114 (DOI: 10.1021/om020817w).

[18] Hernμndez-Juμrez M., López-Serrano J., Lara P., Morales-Cerón J. P., Vaquero M., Álvarez E., Salazar V., Suμrez A., (2015), Ruthenium(II) Complexes Containing Lutidine-Derived Pincer CNC Ligands: Synthesis, Structure, and Catalytic Hydrogenation of C═N bonds, *Chem. Eur. J.*, 21, 7540-7555 (DOI: 10.1002/chem.201406040).

[19] Wu X., Ji L., Ji Y., Elageed E.H.M., Gao G., (2016), *Cat. Commun.*, 85, 7-60.

[20] Ng C. K., Wu J., Andy Hor T. S., Luo H. -K., (2016), A binary catalyst system of a cationic Ru–CNC pincer complex with an alkali metal salt for selective hydroboration of carbon dioxide, *Chem. Commun.*, 52, 11842-11845 (DOI: 10.1039/C6CC06278D).

[21] Vaquer L., Miró P., Sala X., Bozoglian F., Masllorens E., Benet-Buchholz J., Fontrodona X., Parella T., Romero I., Roglans A., Rodríguez M., Bo C., Llobet A., (2013), *ChemPlusChem*, 78, 235-243.

[22] Raible B., Gierz V. Kunz D., (2015), Identifying and Rationalizing the Conditions for the Isomerization of 1,5-

Cyclooctadiene in Iridium Complexes by Experimental and Theoretical Mechanistic Studies, *Organomettalics*, 34, 2018-2027. (DOI: 10.1021/acs.organomet.5b00267).

[23] Cotton F. A., Deeming A. J., Josty P. L., Ullah S. S., Domingos A. J. P., Johnson B. F. G., Lewis J., (1971), *J. Am. Chem. Soc.*, 93, 4624−4626.

[24] Bonnemann H., Goddard R., Grub J., Mynott R., Raabe E., Wendel S., (1989), Synthesis and Properties of Some New (η6-Arene)cobaIt Complexes, *Organometallics*, 8, 1941−1958.

[25] Esteruelas M. A., Olivan M., Oro L. A., Schulz M., Sola E., Werner H., (1992), Synthesis, molecular structure and reactivity of the octahedral iridium(III) compound [IrH(.eta.1,.eta.3-C_8H_{12})(dppm)] [dppm = bis(diphenylphosphino)methane], *Organometallics*, 11, 3659−3664 (DOI: 10.1021/om00059a031).

[26] Martín M., Sola E., Torres O., Plou P., Oro L.A., (2002), *Organometallics*, 22, 5406−5417.

[27] Martín M., Torres O., Oñate E., Sola E., Oro L. A., (2005), C−H Activations at Iridium(I) Square-Planar Complexes Promoted by a Fifth Ligand, *J. Am. Chem. Soc.*, 127, 18074 −18084 (DOI: 10.1021/ja0557233).

[28] Merola J. S., Franks M. A., (2013), The basicity of [tris-(trimethylphosphine)(cyclooctadiene)iridium(I)], *J. Organomet. Chem.*, 723, 49-55 (DOI: 10.1016/j.jorganchem.2012.09.020).

[29] Rahaman S. M. W., Dinda S., Sinha A., Bera J. K., (2013), A Noninnocent Cyclooctadiene (COD) in the Reaction of an "Ir(COD)(OAc)" Precursor with Imidazolium Salts, *Organometallics*, 32, 192 −201 (DOI: 10.1021/om300982q).

[30] Tauchert M. E., Kaiser T. R., Göthlich A. P. V., Rominger F., Warth D. C. M., Hofmann P., (2010), Phosphonite Ligand Design

for Nickel-Catalyzed 2-Methyl-3-butenenitrile Isomerization and Styrene Hydrocyanation, *ChemCatChem*, 2, 674–682.

[31] Cope A.C., Howell C.F., Bowers John., Lord R.C., Whitesides G. M., (1987), *J. Am. Chem. Soc.*, 89, 4024–4027.

[32] Hedburg L., Hedburg K., (1971), *Perspect. Struct. Chem.* 60.

[33] Anet F. A. L., Kozerski L., (1973), Determination of conformational barriers in 1,5-cyclooctadiene by proton and carbon-13 nuclear magnetic resonance, *J. Am. Chem. Soc.*, 95, 3407-3408 (DOI: 10.1021/ja00791a068).

[34] Ermer O., (1976), Conformational interconversions of cis,cis-cyclooctadiene-1,5, *J. Am. Chem. Soc.*, 98, 3964–3970 (DOI: 10.1021/ja00429a036).

[35] Yavari I., Kabiri-Fard H., Moradi S., (2004), An Ab Initio Study Of Conformational Properties Of (Z,Z)-, (E,Z)-And (E,E)-Cycloocta-1,5-Diene, *JICS*, 1, 71-78.

[36] Favinni G., Zuccerallo F., Beumi G., (1969), Molecular conformation of cyclenes: II. cyclohexadienes, cycloheptadienes and cyclooctadienes, *J. Mol. Struct.*, 3, 385-394 (DOI: 10.1016/0022-2860(69)87035-3).

[37] Shimizu T., Iwata K., Kamigata N., Ikuta S., (1997), Conformational Strains of (Z,Z)-, (E,Z)- and (E,E)-1,2,5,6-Tetrathiacycloocta-3,7-dienes based on ab initio Molecular Orbital Calculations, *J. Chem. Res. S*, 38-39 (DOI: 10.1039/A605304A).

[38] Korom S., Martin E., Serapian S. A., Bo C., Ballester P., (2016), Molecular Motion and Conformational Interconversion of IrI·COD Included in Rebek's Self-Folding Octaamide Cavitand, *J. Am. Chem. Soc.*, 138, 2273–2279 (DOI: 10.1021/jacs.5b12646).

[39] Nielsen D. J., Cavell K. J., Skelton B. W., White A. H., (2006), Methyl-palladium(II) complexes of pyridine-bridged bis(nucleophilic heterocyclic carbene) ligands: Substituent effects on structure, stability, and catalytic performance, *Inorg. Chim. Acta*, 359, 1855-1869 (DOI: 10.1016/j.ica.2005.07.049).

[40] Li X. W., Chen F., Xu W. F., Li Y. Z., Chen X. T., Xue Z. L., (2011), *Inorg. Chem. Comm.*, 14, 1673-1676.

[41] Zhang B., Wang H., Yan X., Duan Y.A., Guo S., Luo F.X., (2020), *Transition Metal Chemistry*, *45*, 99-110.

[42] Zhong Y. Q., Xiao H. Q., Yi X. Y., (2016), Synthesis, structural characterization and catalysis of ruthenium(ii) complexes based on 2,5-bis(2′-pyridyl)pyrrole ligand, *Dalton Trans.*, 45, 18113-18119 (DOI: 10.1039/C6DT03464K).

[43] Zagermann J., Klein K., Merz K., Molon M., Metzler-Nolte N., (2011), Synthesis and Characterization of the Azido-Functionalized Ruthenocene Analogue [TpmRu(p-$N_3C_6H_4$)Tp]Cl and Its Attachment to Biomolecules by Copper-Catalyzed Azide–Alkyne Cycloaddition, *Eur. J. Inorg. Chem.*, 2011, 4212-4219 (DOI: 10.1002/ejic.201100433).

[44] Mardirossian N., Head-Gordon M., (2016), ωB97M-V: A combinatorially optimized, range-separated hybrid, meta-GGA density functional with VV10 nonlocal correlation, *J. Chem. Phys.*, 144, 214110 (DOI: 10.1063/1.4952647).

[45] Braundenburg J. G., Bannwarth C., Hansen A., Grimme S., (2018), B97-3c: A revised low-cost variant of the B97-D density functional method, *J. Chem. Phys.*, 148, 064104 (DOI: 10.1063/1.5012601).

[46] Ahmad N., Lavison J.J., Robinson S. D., Uttley M. F., *Inorganic Syntheses*, 15, 48.

[47] Hallman P. S., Stephenson T. A., Wilkinson G., (1970), Tetrakis(triphenylphosphine)dichlororuthenium(II) and Tris(triphenylphosphine)dichlororuthenium(II), *Inorganic Syntheses*, 12, 238-239 (DOI: 10.1002/9780470132432.ch40).

[48] Albers M. O., Singleton E., Yates J.E., *Inorganic Syntheses*, 26, 253.

[49] Evans I. P., Spencer A., Wilkinso G., (1973), Dichlorotetrakis(dimethyl sulphoxide)ruthenium(II) and its use as a source material for some new ruthenium(II) complexes, *J. Chem. Soc. Dalton Trans.*, 204-209 (DOI: 10.1039/DT9730000204).

[50] Farrugia L. J. (2012), WinGX and ORTEP for Windows: an update, *J. Appl. Cryst.*, 45, 849–854 (https://doi.org/10.1107/S0021889812029111).

[51] F. Neese (2012), The ORCA program system, *WIREs Comput. Mol. Sci.* 2, 73–78 (https://doi.org/10.1002/wcms.81).

[52] F. Neese (2018), Software update: the ORCA program system, version 4.0, *WIREs Comput. Mol. Sci.* 8, e1327 (https://doi.org/10.1002/wcms.1327).

[53] A.V. Marenich, C.J. Cramer, D.G. Truhlar (2009), Universal Solvation Model Based on Solute Electron Density and on a Continuum Model of the Solvent Defined by the Bulk Dielectric Constant and Atomic Surface Tensions, *J. Phys. Chem. B.* 113, 6378–6396 (https://doi.org/10.1021/jp810292n).

[54] J.G. Brandenburg, C. Bannwarth, A. Hansen, S. Grimme (2018), B97-3c: A revised low-cost variant of the B97-D density functional method, *J. Chem. Phys.* 148, 064104 (https://doi.org/10.1063/1.5012601).

[55] N. Mardirossian, M. Head-Gordon (2016), ωB97M-V: A combinatorially optimized, range-separated hybrid, meta-GGA density functional with VV10 nonlocal correlation, *J. Chem. Phys.* 144, 214110 (https://doi.org/10.1063/1.4952647).

[56] F. Weigend, R. Ahlrichs (2005), Balanced basis sets of split valence, triple zeta valence and quadruple zeta valence quality for H to Rn: Design and assessment of accuracy, *Phys. Chem. Chem. Phys.* 7, 3297–3305 (https://doi.org/10.1039/B508541A).

[57] F. Weigend (2006), Accurate Coulomb-fitting basis sets for H to Rn, *Phys. Chem. Chem. Phys.* 8, 1057–1065 (https://doi.org/10.1039/B515623H).

[58] R. Izsák, F. Neese (2011), An overlap fitted chain of spheres exchange method, *J. Chem. Phys.* 135, 144105 (https://doi.org/10.1063/1.3646921).

[59] A.D. Becke, E.R. Johnson (2005), A density-functional model of the dispersion interaction, *J. Chem. Phys.* 123, 154101 (https://doi.org/10.1063/1.2065267).

[60] S. Grimme, J. Antony, S. Ehrlich, H. Krieg (2010), A consistent and accurate ab initio parametrization of density functional dispersion correction (DFT-D) for the 94 elements H-Pu, *J. Chem. Phys.* 132, 154104 (https://doi.org/10.1063/1.3382344).

[61] S. Grimme, S. Ehrlich, L. Goerigk (2011), Effect of the damping function in dispersion corrected density functional theory, J. Comput. Chem. 32, 1456–1465 (https://doi.org/10.1002/jcc.21759).

Chapter 3

Catalytic Transfer Hydrogenation and Dehydrogenation of ketones and alcohols using Ru(II)-NHC Pincer Complexes

3.1 Introduction

Hydrogenation/dehydrogenation reactions play an important role in synthetic organic chemistry, and such reactions involving oxygenated compounds are particularly useful for manufacturing agrochemicals, pharmaceuticals, foods, and fuels.*[1-2]* Metal-catalyzed hydrogenations are a potent and practical approach for reducing ketones to secondary alcohols.*[3–13]* While hydrogenation with H_2 is a non-polluting reaction, however, takes a long time to complete. Transfer hydrogenation (TH) is an atom-efficient catalytic process and does not require the use of dangerous molecular hydrogen or high-pressure equipment. The catalyst can construct a hydride and abstract proton from the hydrogen donor and transfer it to the ketone's carbonyl moiety.*[3,4-6]*

From an economic and environmental perspective, catalytic processes have a clear advantage over stoichiometric reactions. Traditionally, which reactions have been carried out using high hydrogen pressure or a stoichiometric amount of hazardous reagents, various additives, and co-catalysts, often eliminate copious waste.*[2]* On the other hand, transfer hydrogenation and acceptorless dehydrogenation are two of the most atom-efficient ways to access valuable intermediates and various organic transformations.*[11–13]*

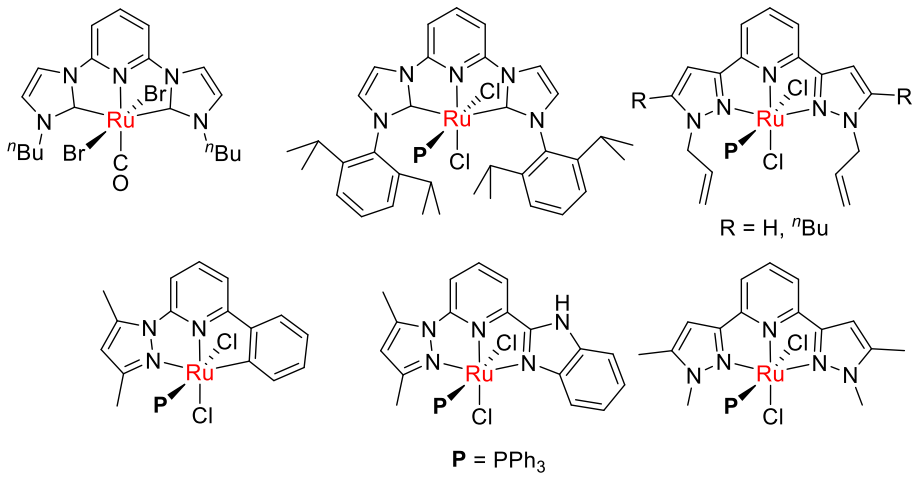

Figure 3.1 Reported ruthenium pincer complexes for Transfer hydrogenation of ketones.

Typically, these reactions require high temperatures, in the range of 100-140 °C, and long reaction times of 24-72 h, although milder reaction conditions have also been reported recently.*[16–18]* In 2004, Milestein and co-workers reported an electron-rich, bulky ruthenium PNP pincer complex (Figure **2.2**), which was found to be very efficient for catalytic acceptorless alcohol dehydrogenation (AAD). Similarly, ruthenium and osmium CNN pincer complexes can also be used for the dehydrogenation of secondary alcohol under acceptorless reaction conditions at 130 °C (Figure **2.2)**.

The high temperature required for these reactions are generally detrimental to the selectivity of the reactions, e.g., at higher temperatures, the selectivity between primary and secondary alcohol present in the same molecule is lost. Therefore, there is a need to explore active catalysts or new processes that can work at low temperatures with a range of substrates. Microwave radiation has revolutionized chemical reactions and is widely exploited in various organic syntheses, to reduce the reaction time drastically.*[19–21]* Condensation between an aldehyde or/and ketone with amines to synthesize imines using microwave heating has been described in the literature; however, microwave-assisted AAD reaction has not been explored.

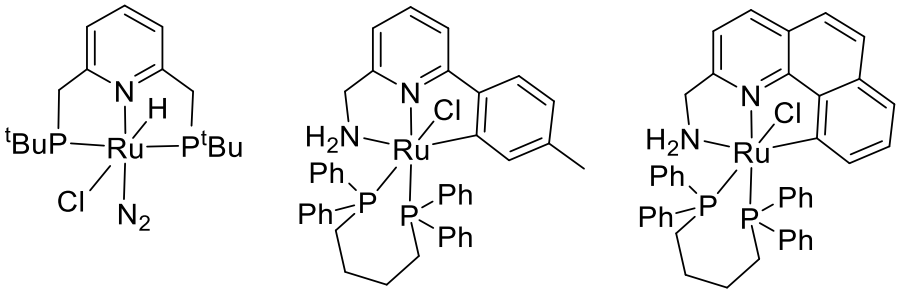

Figure 3.2 Reported ruthenium pincer complexes for aceptorless dehydrogenation of alcohols

Ruthenium pincer complexes are of significant interest as catalysts as they are readily available in different stable oxidation states and coordination geometries viz. square pyramidal, trigonal-bipyramidal, and octahedral.*[25-28]*

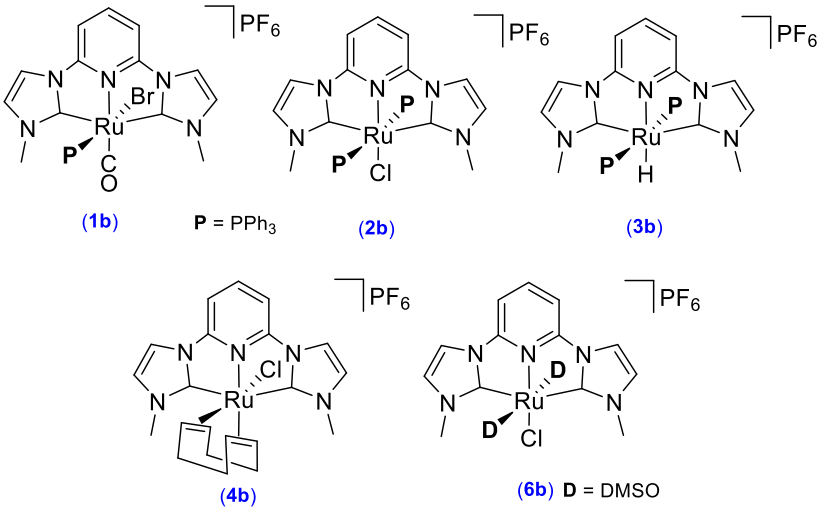

Figure 3.3 Cationic Ru(II)–CNC pincer complexes in this study.

Ru(II) complexes bearing pincer ligands have been well studied, however, complexes with CNC-pincer ligands are less explored for the transfer hydrogenation of ketones and acceptorless dehydrogenation of alcohols.*[1,22]* Therefore, it is worth exploring the reactivity of Ru(II) CNC pincer complexes for these transformations. Herein, we report the application of Ruthenium-CNC pincer complexes $[Ru(CNC)(CO)(PPh_3)Cl]PF_6$ (**1b**), $[Ru(CNC)(PPh_3)_2Cl]PF_6$ (**2b**), $[Ru(CNC)(PPh_3)_2H]PF_6$ (**3b),** $[Ru(CNC)(\eta^2{:}\eta^2\text{-COD})Cl]PF_6$

(**4b**), and [Ru(CNC)(DMSO)$_2$Cl]PF$_6$ (**6b**) for transfer hydrogenation of ketones and acceptorless dehydrogenation of alcohols.

3.2 Results and Discussion

3.2.1 Catalytic application in transfer hydrogenation

Ruthenium complexes **1b**, **2b**, **3b**, **4b,** and **6b** were used as catalysts for the transfer hydrogenation (TH) of ketones using isopropanol, and the reaction was monitored by gas chromatography without internal standard. Initially, the transfer hydrogenation of cyclohexanone in refluxing isopropanol was selected as a model reaction to evaluate the catalytic activity of complexes. Using 2 mmol of ketone, 1 mol% of catalyst, and 1 equivalent of sodium iso-propoxide (NaO^{i}Pr) as base complex **1b** showed higher catalytic activity than other complexes viz: **2b**, **3b**, **4b,** and **6b** resulting in >99 % conversion of cyclohexanone in 30 min (Table **3.1**, entry 2).

Table 3.1 Optimisation table of different catalysts

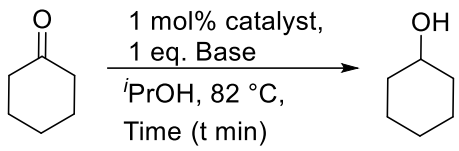

Entry[a]	Catalyst	Base	Time (min)	Conversion[b](%)	TON/TOF (h^{-1})
1.	**1b**	NaO^{i}Pr	15	85	85/340
2.	**1b**	NaO^{i}Pr	30	>99	99/198
3.	**2b**	NaO^{i}Pr	30	61	61/122
4.	**3b**	NaO^{i}Pr	30	72	72/144
5.	**4b**	NaO^{i}Pr	30	80	80/160
6.	**6b**	NaO^{i}Pr	30	56	56/112
7.	**1b**	NaOH	15	55	55/220
8.	**1b**	NaOH	30	79	79/158

9.	**1b**	KOH	15	71	71/284
10.	**1b**	KOH	30	74	74/148
11.	**1b**	KO^{t}Bu	15	-	-
12.	**1b**	KO^{t}Bu	30	78	78/156
13.	**1b**	NaO^{i}Pr	15	48^c	96/384
14.	**1b**	NaO^{i}Pr	30	51^c	102/204

[a]Reaction conditions: Ketone (2.0 mmol), Catalyst([**Ru**] 1 mol%),NaO^{i}Pr(1 eq.), ^{i}PrOH (5 mL), at 82 ^{o}C under a slow N_2 flow. [b]Determined by gas chromatography without internal standard. [c]Catalyst([**Ru**] 0.5 mol%). TON = (Number of moles of substrate converted)/(Number of moles of catalyst), at the end of the reaction. TOF = [(TON)/ hour].

Under similar conditions, complex **2b, 3b, 4b** and **6b** exhibited slightly lower catalytic activity with 61%, 72%, 80%, and 56% conversions, respectively (Table **3.1**, entries 3, 4, 5 and 6). Further, the effect of various bases e.g., NaOH, KOH, KO^{t}Bu in different time intervals (15 min and 30 min) with complex **1b** were also studied (Table **3.1**, entries 7-12). The conversion of cyclohexanone to corresponding alcohol was achieved in 79%, 74%, and 78% in 30 min (Table **3.1**, entries 6, 8, and 10) and 55%, 71%, and 0% in 15 min (Table **3.1**, entries 5, 7 and 9) using the bases NaOH, KOH, and KO^{t}Bu, respectively, indicating there is a significant induction period for catalysis with KO^{t}Bu. As the results, ruthenium complex **1b** (1 mol%) as catalyst and NaO^{i}Pr as a base in isopropanol under reflux temperature were chosen as suitable reaction conditions.

The scope of catalyst **1b** was then examined using various ketone substrates to establish the generality of the reaction. Several ketone derivatives with aliphatic and aromatic substituents, as well as both the electron-donating and withdrawing substituents were investigated (Table **3.2**). Aliphatic cyclic ketones (Table **3.2**, entries 1,3) gave good to moderate conversions in 30 min and 1 hour, however, the reaction proceed comparatively slowly in the case of

aliphatic acyclic ketone (Table **3.2**, entry 2). For aromatic ketones, the yield varies from 58-99% in one hour (Table **3.2**, entries 4-10). The electron-withdrawing substituents like Br at the para position (Table **3.2**, entry 5) showed comparable conversion to acetophenone but in the case of chloro (Table **3.2**, entry 5) reactivity of reaction was slightly decreased.

Table 3.2 Transfer hydrogenation of various ketones with catalyst **1b**

Entry[a]	Reactant	Product	% Conv.[b] at the time (Isolated yield[c]) 0.5h	1h	TON/TOF(h^{-1})
1.	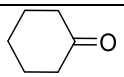	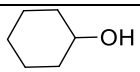	>99 (98)	-	98/196
2.	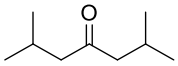	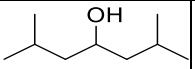	24	37 (30)	30/30
3.	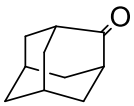	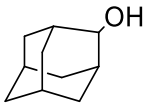	65	80 (62)	62/62
4.	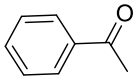	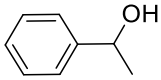	80	>99 (95)	95/95
5.	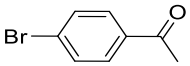	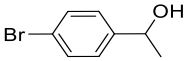	60	97 (75)	75/75
6.	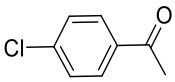	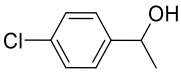	58	84 (80)	80/80
7.	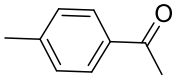	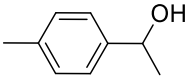	32	58 (45)	45/45
8.	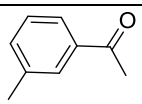	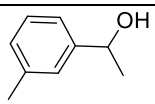	24	68 (53)	53/53
9.	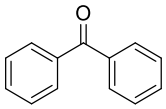	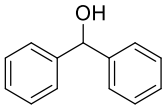	12	73 (67)	67/67
10.	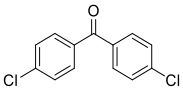	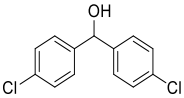	70	83 (64)	64/64

[a]Reaction conditions: Ketone (2.0 mmol), **1b** ([Ru] 1 mol%),NaO^{i}Pr(1 eq.), ^{i}PrOH (5 mL), at 82 ^{o}C under a slow N_2 flow for 0.5 and 1h. [b]Determined by gas chromatography without internal standard. [c]Isolated yields. TON = (Number of moles of substrate converted)/(Number of moles of catalyst), at the end of the reaction. TOF = [(TON)/ hour].

Subsequently, the electron-donating methyl substituents at para and meta positions (Table **3.2**, entries 7, 8) relatively decelerated the rate of transfer hydrogenation. Benzophenone was reduced in 1h with 73% conversion, whereas 4,4'-dichlorobenzophenone gave 83% conversion (Table **3.2**, entries 9, 10). For the unexpected high reactivity of benzophenone, we believe that after the dissociation of one PPh_3 ligand the steric environment around Ru-center is not so crowded to prevent its coordination to the Ru. Further, the bulkiness of the product may be helpful in the dissociation from the catalyst which can, then, start another catalytic cycle. The alcohols were isolated in good to excellent yield after column chromatography as reported in Table **3.2**.

A plausible mechanism for transfer hydrogenation is shown in Scheme **3.2**, with complex **2b** as the catalyst precursor and **3b** as the Ru-hydride intermediate. A similar mechanism may also be suggested to be operating during the catalysis with **1b**. It is worth mentioning that the corresponding Ru-hydride species for **1b** is observed in the fragmentation pattern of **1a** in LC-MS as [**1a**-2Cl+H]$^+$, however,attempts to synthesize or identify this Ru-hydride intermediate under catalytic conditions have been unsuccessful, probably due to its high reactivity. Therefore, mechanistic studies were performed on catalysis with complexes **2b** and **3b**. ^{31}P NMR of an NMR scale experiment with 1 equivalent each of **2b**, base, and isopropanol indicates the presence of free PPh_3 ligand as well as the generation of the hydride complex **3b** in the catalytic reaction mixture.

Based on the ^{31}P NMR and mass analyses of the catalytic samples, it is proposed that in the presence of NaO^{i}Pr, complex **2b** generates the ruthenium alkoxide species **A**. The Ru-H intermediate

3b' is formed from **A** via β-H elimination by releasing one molecule of acetone, or by dissociation of a PPh_3 ligand if starting from **3b**. The addition of a ketone to the intermediate **3b'** produces another ruthenium alkoxide intermediate **B**, which releases the hydrogenated product upon protonation from ^{i}PrOH resulting in the formation of **A** again.

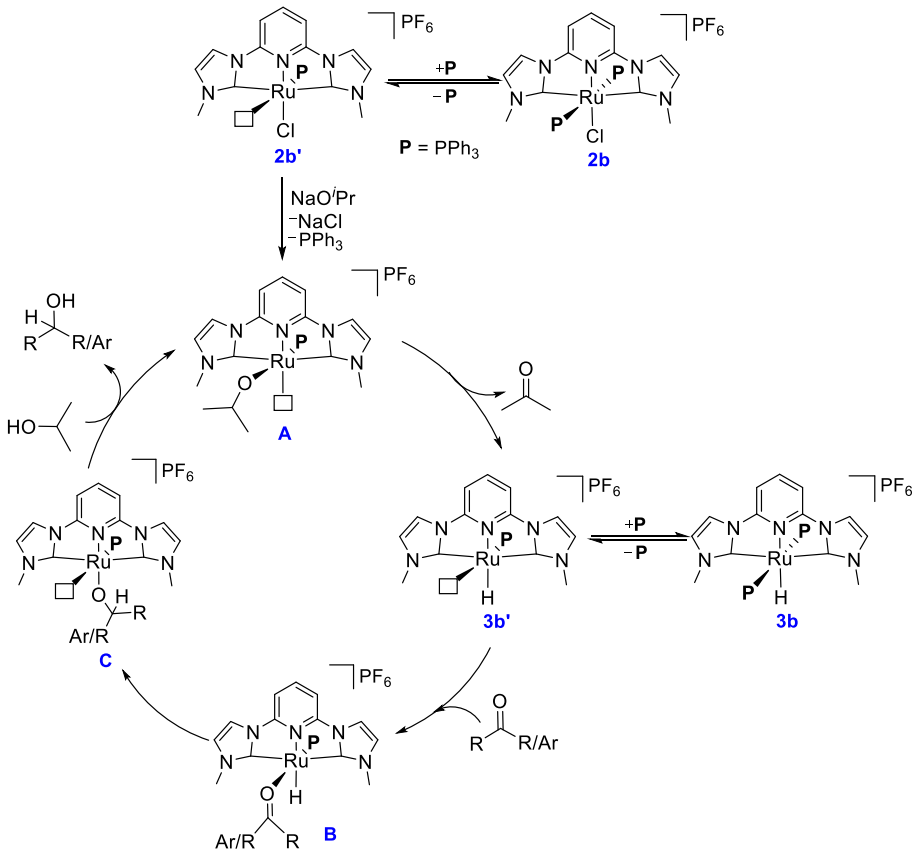

Scheme 3.1 Plausible mechanism for transfer hydrogenation catalysis by **2b**.

To further confirm our proposed mechanism, we have synthesized **3b** from **2a** and performed a catalytic test run starting from **3b**. The reaction of complex **3a** with K_2CO_3 in refluxing ^{i}PrOH for 15 h, affords clean synthesis of hydride intermediate complex **3a** (Scheme **3.2**).

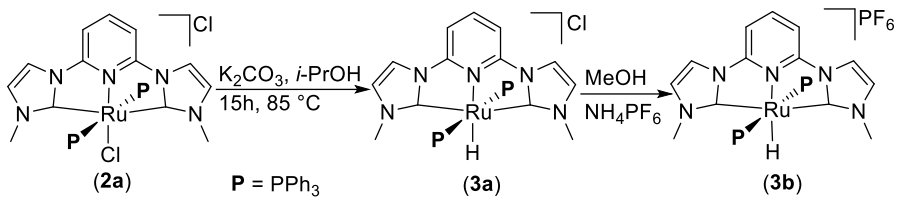

Scheme 3.2 Synthesis of CNC pincer ruthenium complexes **3a** and **3b** from **2a.**

The pure hydride complex **3a** was characterized by ^{1}H, ^{13}C, IR, and mass spectrometry. ESI^{+} LC-MS of **3a** displayed signal at *m/z* 866.2 assigned to [**3a**]$^{+}$, matching with the catalytic sample mass. Anion exchange of complex **3a** with NH_4PF_6 was carried out to obtain the cleaner data of **3b**. In ^{1}H NMR of **3b**, the hydrido signal gives a triplet at δ = -8.86 ppm, which is indicative of the Ru-H complex with two phosphines. Similarly, signals assignable to the pyridine protons and imidazol-2-ylidene protons appeared at δ = 8.31 as a doublet, δ = 7.85 ppm as a triplet and two doublets at δ = 7.58 ppm and δ = 7.24 ppm. All the aromatic protons are slightly shifted to the downfield in comparison to **2a**, though methyl protons show a significant upfield shift at δ = 2.47 ppm. ^{31}P NMR spectrum of **3b** showed peaks at δ = 51.96 for PPh_3 and δ = 144.16 ppm for PF_6, respectively. Encouraged by excellent conversions of transfer hydrogenation reactions, we also examined the dehydrogenation reactions of primary alcohols with all the synthesized catalysts.

3.2.2 Catalytic application in Aceptorless alcohol dehydrogenation

3.2.2.1 Acceptorless alcohol dehydrogenation under thermal conditions.

The dehydrogenation of benzyl alcohol was examined as a model reaction to investigate the applicability of these complexes (**1b**, **2b, 4b,** and **6b**) for catalytic AAD reactions. Complex **1b** in toluene with KO^{t}Bu at 110 °C for 3h afforded >99% conversion to benzaldehyde (Table **3.3**, entry 1) while complex **2b, 4b** and **6b** gave 47%, 89% and 60% conversions, respectively (Table **3.3**, entry 2, 3 and 4). The

catalytic activity of complex **1b** with different bases was then studied under a similar reaction condition, and screening suggested that KO^{t}Bu is the best option (Table **3.3**, entry 1). Keeping the other conditions same, a decrease in catalyst loading from 3 mol% to 1 mol% resulted in a drop in the catalytic activity with 30% conversion in 3h (Table **3.3**, entry 6). Therefore, the complex **1** (3 mol%) and KO^{t}Bu was then chosen as a suitable catalyst system for AAD of a range of primary and secondary alcohols under these optimized reaction conditions (Table **3.4**).

Table 3.3 Screening of catalyst with different bases.

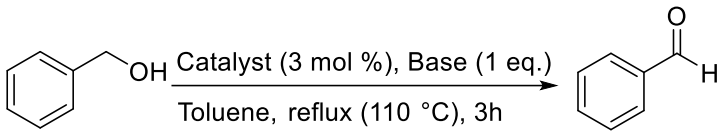

Entry[a]	Catalyst	Base	% Conversion[b]	TON[c]/TOF[d]
1.	**1b**	KO^{t}Bu	>99	33/11
2.	**2b**	KO^{t}Bu	47	15/5
3.	**4b**	KO^{t}Bu	89	29/10
4.	**6b**	KO^{t}Bu	60	20/6
3.	**1b**	NaO^{t}Bu	20	6/2
4.	**1b**	NaOH	51	17/5
5.	**1b**	KOH	65	21/7
6.	**1b**	KO^{t}Bu	30[e]	10/3

[a]Reaction conditions: Benzyl alcohol (1 mmol), Catalyst (3 mol %), Base (1 eq.), Toluene (5 ml), at 110 ^{o}C under a slow N_2 flow under thermal condition. [b]Determined by gas chromatography without an internal standard. TON = [(Number of moles of substrate converted)/(Number of moles of catalyst)] at the end of the reaction. [c]TON = [(Number of moles of substrate converted)/(Number of moles of catalyst)] at the end of the reaction. [d]TOF = [(TON)/hour]. [e]Catalyst loading, 1 mol%.

3.2.2.2. Acceptorless alcohol dehydrogenation under microwave conditions.

Taking inspiration from excellent improvements, in terms of reduced reaction temperature and time, reported for several organic syntheses

reactions,*[16–18,23]* the dehydrogenation of benzyl alcohol using Ru-complexes **1b** and **2b** was further explored under microwave irradiation at low temperatures using optimized conditions for the thermal reaction. Thus, a toluene solution of benzyl alcohol and KO^{t}Bu was heated at 50 °C in the presence of 3 mol% catalysts for 10 min under microwave radiation to obtain benzaldehyde. Ruthenium-CNC pincer complexes (**1b** and **2b**) showed moderate to excellent conversion, while ruthenium complex **1b** again performs better than complex **2b** (33%) (Table **3.4**). In contrast, when benzyl alcohol was treated at 80 ^{o}C under microwave conditions, >99% conversion to the benzaldehyde was observed after 5 min. (Table **3.4**, entry 3).

Table 3.4 Screening of catalyst under microwave conditions.

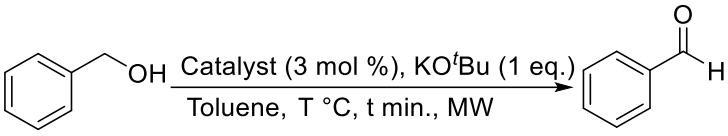

Entry[a]	Catalyst	Temp.(^{o}C) (Time)	% Conversion[b]	TON[c]/TOF[d]
1.	**1b**	50 (10 min)	>99	33/193
2.	**2b**	50 (10 min)	33	11/68
3.	**1b**	80 (5 min)	>99	33/412

[a]Reaction conditions: Benzyl alcohol (1 mmol), Catalyst (3 mol %), KO^{t}Bu (1 eq.), Toluene (5 ml), at 50 ^{o}C and 80 ^{o}C, respectively under a slow N_2 flow under microwave condition. [b]Determined by gas chromatography without an internal standard. [c]TON = [(Number of moles of substrate converted)/(Number of moles of catalyst)] at the end of the reaction. [d]TOF = [(TON)/hour].

3.2.2.3. Substrate scope for acceptorless alcohol dehydrogenation under thermal and microwave conditions.

The dehydrogenation reaction of various alcohols to examine the substrate scope has been studied using the optimized conditions (Table **3.5** and **3.6**). The complex **1b** (3 mol%), with KO^{t}Bu, was found to be an efficient precatalyst for acceptorless dehydrogenation with a range

of primary benzylic alcohols under thermal and microwave conditions. The dehydrogenation proceeded well with both the electron-donating and withdrawing substituents and gave the desired aldehydes in good to excellent yields.

Table 3.5 Acceptorless alcohol dehydrogenation of various alcohols with Ru catalyst **1b** under conventional heating

Entry[a]	Reactant	Product	Thermal (110 °C, 3 h)	
			% Conversion[b] (Isolated yield)	TON[c]/ TOF[d]
1.	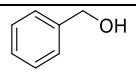	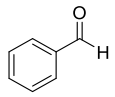	>99 (95)	31/10
2.	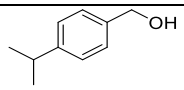	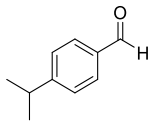	59 (52)	17/5
3.	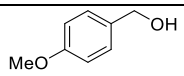	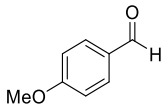	>99 (90)	29/10
4.	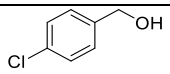	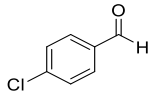	72 (67)	22/7
5.	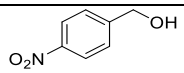	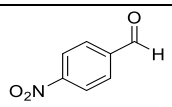	20 (14)	4/1
6.	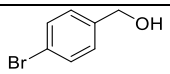	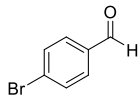	>99 (90)	30/10
7.	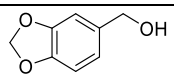	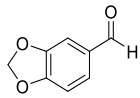	92 (84)	28/9
8.	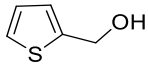	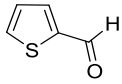	>99 (95)	31/10

[a]Reaction conditions: Alcohols (1 mmol), Catalyst (3 mol %), KO^{t}Bu (1 eq.), Toluene (5 mL), under a slow N_2 flow under thermal condition (110 ^{o}C/3h). [b]Determined by gas chromatography without internal standard. [c]TON = [(Number of moles of substrate converted)/(Number of moles of catalyst)] at the end of the reaction. [d]TOF = [(TON)/hour].

Benzyl alcohol with isopropyl- and chloro-groups underwent a smooth reaction and resulted in the corresponding aldehyde in excellent yield (>80%) in 10 min under the microwave, while in thermal conditions, low conversion was observed (Table **3.5** and **3.6**, entries 2 and 4). The catalytic efficiency increases to >99% (Table **3.5** and **3.6**, entry 3) for 4-methoxy substituent under thermal and microwave conditions, respectively.

Table 3.6 Acceptorless alcohol dehydrogenation of various alcohols with Ru catalyst **1b** under the microwave.

Entry[a]	Reactant	Product	Microwave (50 °C, 10 min)	
			% Conversion[b] (Isolated yield)	TON[c]/ TOF[d]
1.	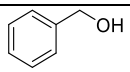	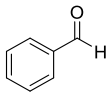	>99 (93)	31/193
2.	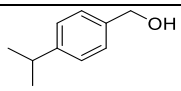	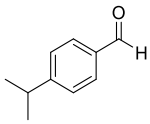	82 (76)	25/158
3.	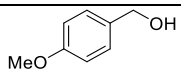	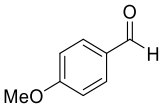	>99 (87)	29/181
4.	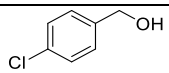	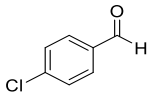	>99 (90)	30/187
5.	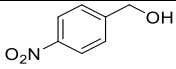	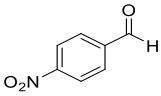	>99 (92)	30/191
6.	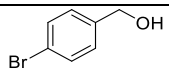	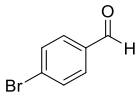	61 (54)	18/112
7.	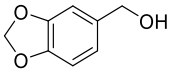	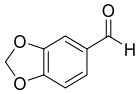	>99 (86)	28/179
8.	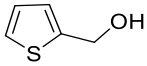	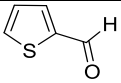	>99 (92)	30/191

[a]Reaction conditions: Alcohols (1 mmol), Catalyst (3 mol %), KO^{t}Bu (1 eq.), Toluene (5 mL), under a slow N_2 flow under microwave (50 ^{o}C/10min). [b]Determined by gas chromatography without internal standard. [c]TON = [(Number of moles of

substrate converted)/(Number of moles of catalyst)] at the end of the reaction. [d]TOF = [(TON)/hour].

Benzyl alcohol with p-nitro substituent performed well using microwave condition and gave >99% conversion (Table **3.5** and **3.6**, entry 5), whereas a little drop was observed with Bromo substituent under microwave condition (Table **3.5** and **3.6**, entry 6). Piperonyl alcohol and 2-thiophene methanol were also effective substrates to dehydrogenate in >99% conversions under thermal and microwave conditions, respectively (Table **3.5** and **3.6**, entries 7 and 8).

Based on our investigation for transfer hydrogenation catalysis, a plausible mechanism for acceptorless dehydrogenation of alcohols has been proposed (Scheme **3.4**). The reaction begins with the synthesis of ruthenium alkoxide species **A** by the reaction of complex **2b** with alcohol in the presence of KO^{t}Bu. Further, the Ru-H intermediate **3b'**, considered as the catalytically active species, is generated via β-H elimination, releasing one molecule of aldehyde. The Ru-H intermediate **3b'** can also be formed by dissociation of a PPh_3 ligand if starting from the Ru-hydride complex **3b**. Finally, the addition of alcohol to the intermediate **3b'** produces another ruthenium alkoxide intermediate **C**, which liberates the H_2 and regenerates the ruthenium alkoxide species **A**. ESI^+ mass analysis of the catalytic mixture confirms the presence of ruthenium hydride complex **3b** in the reaction mixture.

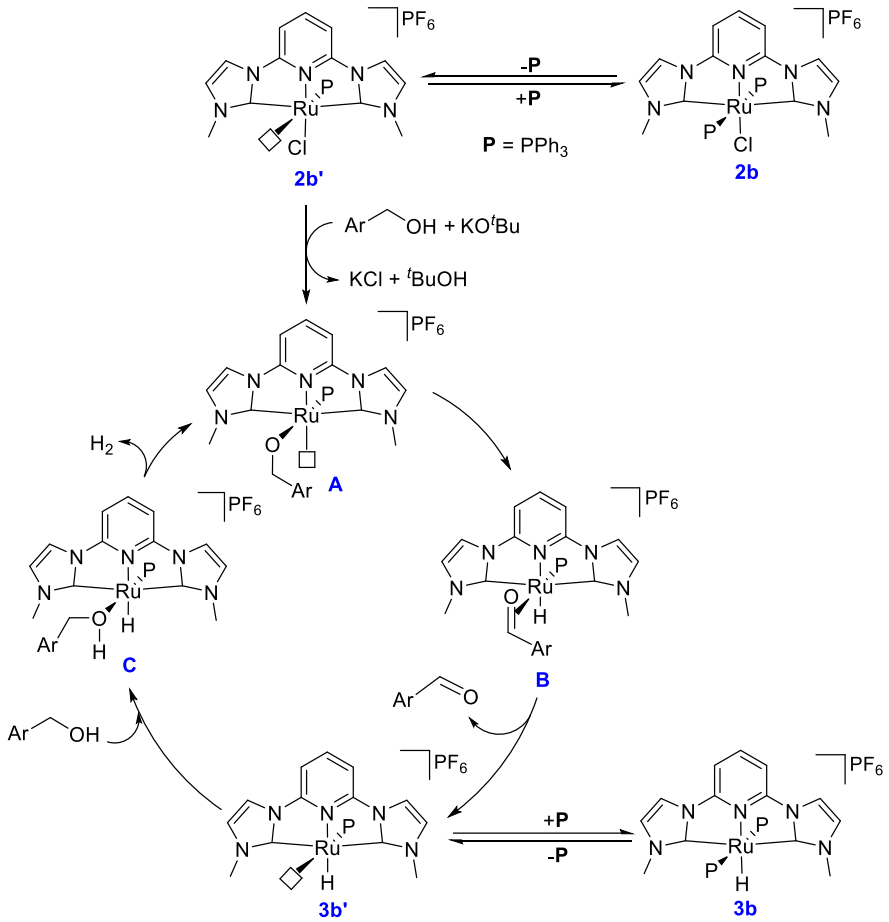

Scheme 3.3 Plausible mechanism for acceptorless dehydrogenation of alcohols catalysis by **2b**.

3.3 Conclusions

In summary, we have studied the catalytic activity of Ru(II)-CNC complexes viz; $[Ru(CNC)(CO)(PPh_3)Cl]PF_6$ (**1b**), $[Ru(CNC)(PPh_3)_2Cl]$ PF_6 (**2b**), $[Ru(CNC)(\eta^2{:}\eta^2\text{-COD})Cl]PF_6$ (**4b**) and $[Ru(CNC)(DMSO)_2Cl]PF_6$ (**6b**) for transfer hydrogenation of ketones and AAD of alcohols. All the ruthenium complexes were found catalytically active for both types of reactions. Complex **1b** was found to be catalytically more active than its analogous complexes **2b, 4b, 6b** for transfer hydrogenation of ketones and AAD, respectively under the optimised conditions. The *in-situ* transformations of these complexes during their synthesis were also observed, which helps in understanding their behaviour during catalysis. Subsequently, the substrate scope for transfer hydrogenation catalysis with a range of

substituted ketones was studied with complex **1b** as the catalyst precursor. Compared to conventional "oil-bath" heating, microwave irradiation resulted in faster catalysis under milder conditions. Substrate scope for AAD with complex **1b** has been explored with various electron-donating and withdrawing alcohol substrates.

3.4 Experimental

3.4.1 General procedure for catalytic hydrogen transfer reaction

Typically, the ketone (2 mmol) and catalyst (1 mol %) were dissolved in ^{i}PrOH (5 ml), under an inert atmosphere in two neck 25 ml R.B. flask equipped with a reflux condenser, followed by the addition of Na (1 eq., 2 mmol) to generate NaO^{i}Pr, in situ. After all the sodium metal had dissolved, the reaction mixture was quickly heated to reflux by lowering into a preheated oil bath. The conversion of the corresponding product at 15 min time intervals was determined by the relative peak area of the substrate and the product in GC without an internal standard. After the reaction was completed, the solution was cooled quickly in an ice bath and analysed by GC-MS. The product was purified by silica gel column chromatography using hexane/ethyl acetate (typically 8:2) as an eluent to determine the isolated yield. NMR data for alcohol products match the reported values.

3.4.2 General procedure for acceptorless dehydrogenation reaction under thermal condition

Typically, catalyst (3 mol%) was added to the solution of alcohol (1 mmol), KO^{t}Bu (1 eq.) in toluene under an inert atmosphere in toluene in a 2-neck R.B. flask equipped with a reflux condenser and heated at 110 ^{o}C for 3h by lowering into a preheated oil bath. The conversion of the corresponding product was determined by the relative peak area of the substrate and the product in GC without an internal standard. After completion of the reaction, the product was extracted with chloroform and dried in a vacuum. The product was purified by silica gel column

chromatography using hexane/ethyl acetate (typically 8:2) as eluent. ^{1}H NMR data for the aldehyde products match the reported values.

3.4.3 General procedure for acceptorless dehydrogenation reaction under microwave conditions.

Typically, catalyst (3 mol %) was added to the solution of alcohol (1 mmol), KO^{t}Bu (1 eq.) in toluene under an inert atmosphere in a 2-neck R.B. flask equipped with a straight-tube air condenser and heated at the required temperature under microwave radiation for the specified time. The conversion of the corresponding product was determined by the relative peak area of the substrate and the product in GC without an internal standard. After completion of the reaction, the product was extracted with chloroform and dried in a vacuum. The product was purified by silica gel column chromatography using hexane/ethyl acetate (8:2) as eluent. ^{1}H NMR data for the aldehyde products match the reported values.

3.4.3 Characterization data and Mechanistic studies

3.4.3.1 Characterization data for Transfer hydrogenation of ketone products

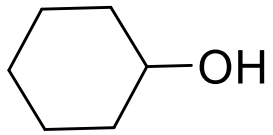

Cyclohexanol; ^{1}H NMR (500 MHz, $CDCl_3$, δ in ppm): δ 3.72 – 3.47 (m, 1H), 2.62 (d, *J* = 8.7 Hz, 1H), 1.99 – 1.84 (m, 2H), 1.81 – 1.66 (m, 2H), 1.39 – 1.20 (m, 5H), 1.20 – 1.06 (m, 2H).

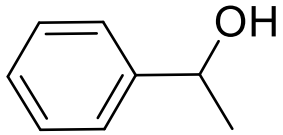

1-Phenylethanol; ^{1}H NMR (500 MHz, $CDCl_3$, δ in ppm): δ 7.27 (d, *J* = 7.9 Hz, 1H), 7.17 (d, *J* = 8.2 Hz, 1H), 4.86 (q, *J* = 6.5 Hz, 1H), 2.43 (s, 1H), 2.36 (s, 1H), 1.49 (d, *J* = 6.5 Hz, 3H).

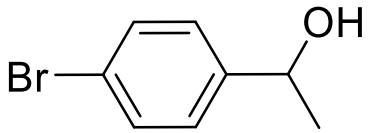

1-(4-Bromophenyl) ethanol; ^{1}H NMR (500 MHz, $CDCl_3$, δ in ppm): δ 7.46 (d, *J* = 8.4 Hz, 1H), 7.23 (d, *J* = 8.4 Hz, 1H), 4.84 (q, *J* = 6.5 Hz, 1H), 2.10 (s, 1H), 1.45 (d, *J* = 6.5 Hz, 3H).

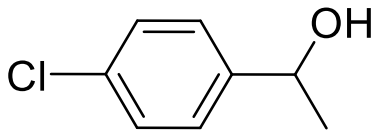

1-(4-Chlorophenyl) ethanol; ^{1}H NMR (500 MHz, $CDCl_3$, δ in ppm): δ 7.30 (d, *J* = 1.9 Hz, 1H), 4.86 (q, *J* = 6.4 Hz, 1H), 2.07 (s, 1H), 1.46 (d, *J* = 6.5 Hz, 3H).

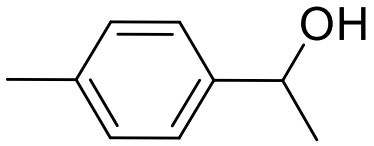

1-(4-Methylphenyl) ethanol; ^{1}H NMR (500 MHz, $CDCl_3$, δ in ppm): δ 7.27 (d, *J* = 7.9 Hz, 1H), 7.17 (d, *J* = 8.2 Hz, 1H), 4.86 (q, *J* = 6.5 Hz, 1H), 2.43 (s, 1H), 2.36 (s, 3H), 1.49 (d, *J* = 6.5 Hz, 3H).

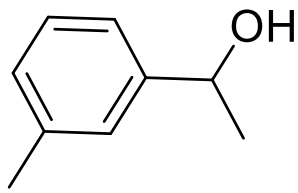

1-(3-Methylphenyl) ethanol; ^{1}H NMR (500 MHz, $CDCl_3$, δ in ppm): δ 7.28 – 7.21 (m, 1H), 7.22 – 7.14 (m, 2H), 7.09 (d, *J* = 7.4 Hz, 1H), 4.86 (q, *J* = 6.5 Hz, 1H), 2.37 (s, 3H), 1.93 (s, 1H), 1.49 (d, *J* = 6.5 Hz, 3H).

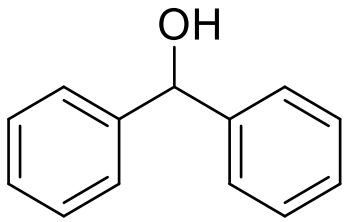

Diphenyl methanol; ^{1}H NMR (500 MHz, $CDCl_3$, δ in ppm): δ 7.43 – 7.38 (m, 4H), 7.34 (t, *J* = 7.6 Hz, 4H), 7.30 – 7.24 (m, 2H), 5.85 (d, *J* = 2.1 Hz, 1H), 2.24 (d, *J* = 3.2 Hz, 1H).

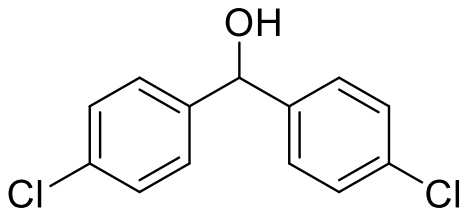

4,4'-Dichloro-diphenyl methanol; ^{1}H NMR (500 MHz, $CDCl_3$, δ in ppm): δ 7.29 (q, *J* = 8.6 Hz, 8H), 5.77 (s, 1H), 2.34 (d, *J* = 7.8 Hz, 1H).

3.4.3.2 Characterization data for Acceptorless dehydrogenation of alcohol products

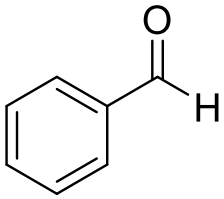

Benzaldehyde; ^{1}H NMR (500 MHz, $CDCl_3$, δ in ppm):10.04 (s, 1H), 7.91 (d, *J*=7.91 Hz, 2H), 7.65 (t, *J*=7.65 Hz, 1H), 7.56 (d, *J*=7.56 Hz, 2H).

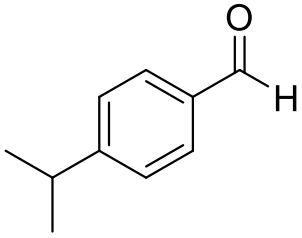

4-Isopropylbenzaldehyde; ^{1}H NMR (500 MHz, $CDCl_3$, δ in ppm):9.97 (s, 1H), 7.81 (d, *J*=7.81 Hz, 2H), 7.39 (d, *J*=7.39 Hz, 2H), 4.12 (q, 3H), 3.55 (d, *J*=3.55 Hz, 6H).

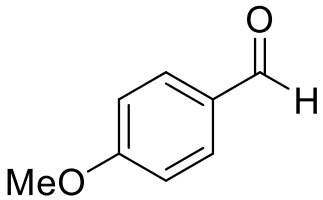

4-Methoxybenzaldehyde; ^{1}H NMR (500 MHz, $CDCl_3$, δ in ppm):9.88 (s, 1H), 7.84 (d, *J*=7.84 Hz, 2H), 7.09 (d, *J*=7.09 Hz, 2H), 3.89 (s, 3H).

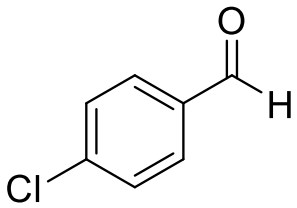

4-Chlorobenzaldehyde; ^{1}H NMR (500 MHz, $CDCl_3$, δ in ppm):9.98 (s, 1H), 7.82 (d, *J*=7.82 Hz, 2H), 7.52 (d, *J*=7.52 Hz, 2H).

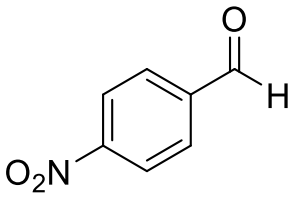

4-Nitrobenzaldehyde; ^{1}H NMR (500 MHz, $CDCl_3$, δ in ppm):10.16 (s, 1H), 8.40 (d, *J*=8.40 Hz, 2H), 8.08 (d, *J*=8.08 Hz, 2H).

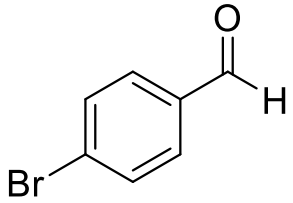

4-Bromobenzaldehyde; ^{1}H NMR (500 MHz, $CDCl_3$, δ in ppm):9.96 (s, 1H), 7.81 (d, *J*=7.81 Hz, 2H), 7.50 (d, *J*=7.50 Hz, 2H).

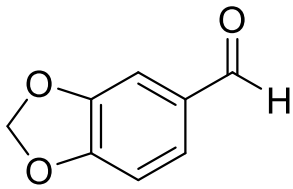

Piperonaldehyde; ^{1}H NMR (500 MHz, $CDCl_3$, δ in ppm):9.80 (s, 1H), 7.41 (d, *J*=7.41 Hz, 1H), 7.33 (s, 1H), 6.93 (d, *J*=6.93 Hz, 1H), 6.07 (s, 2H).

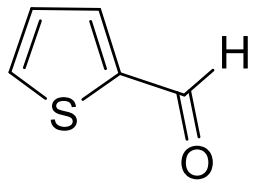

2-Thiophenecarboxaldehyde; ^{1}H NMR (500 MHz, $CDCl_3$, δ in ppm):10.04 (s, 1H), 8.16 (d, *J*=8.00 Hz, 1H), 7.65 (d, *J*=4.00 Hz, 1H), 7.50 (d, *J*=8.00 Hz, 1H).

3.4.3.2 Mechanistic studies

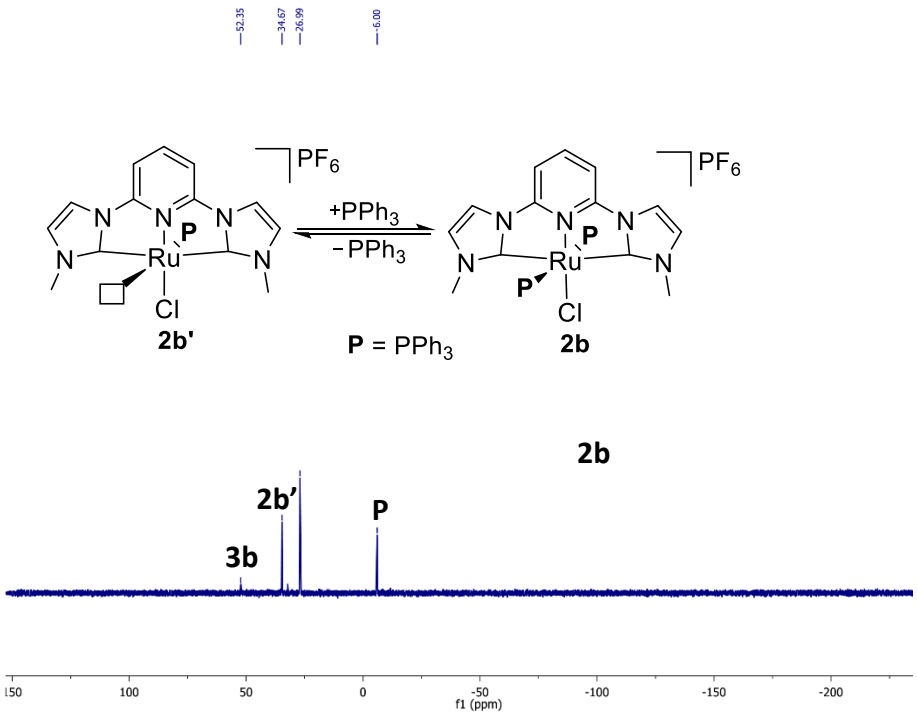

Figure 3.4 ^{31}P NMR of **2b** in the presence of base and isopropanol.

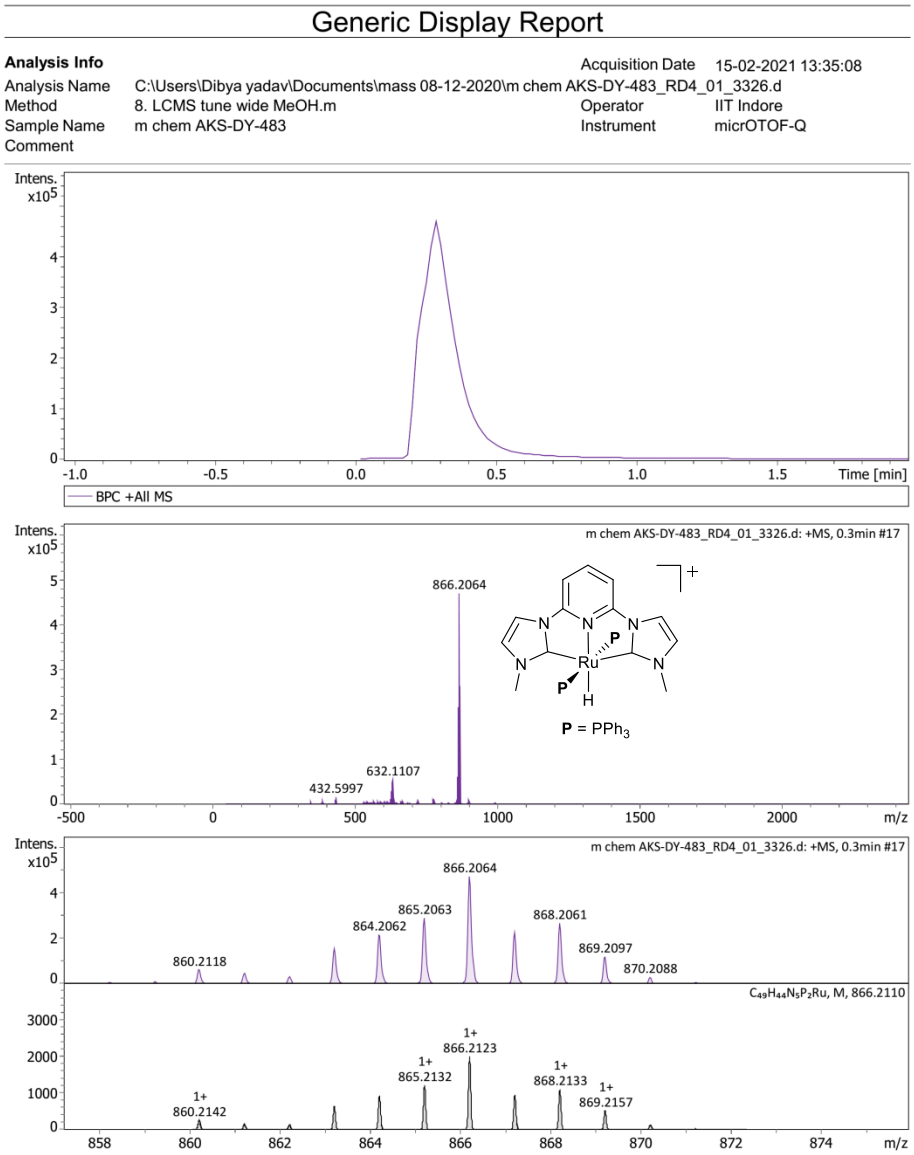

Figure 3.5 LC-MS spectrum of catalytic sample from **2b**.

3.5 References

[1] Meyer N., Lough A. J., Morris R. H., (2009), Iron(II) Complexes for the Efficient Catalytic Asymmetric Transfer Hydrogenation of Ketones, *Chem. Eur. J.*, 15, 5605-5610 (DOI: 10.1002/chem.200802458).

[2] Gavriilidis A., Constantinou A., Hellgardt K., Hii K. K. (Mimi), Hutchings G. J., Brett G. L., Kuhn S., Marsden S. P., (2016), Aerobic oxidations in flow: opportunities for the fine chemicals and pharmaceuticals industries, *React. Chem. Eng.*, 1, 595-612 (DOI: 10.1039/c6re00155f).

[3] Poyatos M., Mata J. A., Falomir E., Crabtree R. H., Peris E., (2003), New Ruthenium(II) CNC-Pincer Bis(carbene) Complexes: Synthesis and Catalytic Activity, *Organometallics*, *22*, 1110-1114 (DOI: 10.1021/om020817w).

[4] Albrecht M., Miecznikowski J. R., Samuel A., Faller J. W., Crabtree R. H., (2002), Chelated Iridium(III) Bis-carbene Complexes as Air-Stable Catalysts for Transfer Hydrogenation, *Organometallics*, 21, 3596–3604 (DOI: 10.1021/om020338x).

[5] Wang D., Astruc D., (2015), The Golden Age of Transfer Hydrogenation, *Chem. Rev.*, 115, 6621–6686 (DOI: 10.1021/acs.chemrev.5b00203).

[6] Castellanos-Blanco N., Arévalo A., García J. J., (2016), Nickel-catalyzed transfer hydrogenation of ketones using ethanol as a solvent and a hydrogen donor, *Dalton Trans.* 45, 13604–13614 (DOI: 10.1039/C6DT02725C).

[7] Garg N., Paira S., Sundararaju B., (2020), Efficient Transfer Hydrogenation of Ketones using Methanol as Liquid Organic Hydrogen Carrier, *ChemCatChem*, 12, 3472–3476 (DOI: 10.1002/cctc.202000228).

[8] Murayama H., Heike Y., Higashida K., Shimizu Y., Yodsin N., Wongnongwa Y., Jungsuttiwong S., Mori S., Sawamura M.,

(2020), Iridium-Catalyzed Enantioselective Transfer Hydrogenation of Ketones Controlled by Alcohol Hydrogen-Bonding and sp^3-C−H Noncovalent Interactions, *Advanced Synthesis & Catalysis*, 362, 4655–4661 (DOI: 10.1002/adsc.202000615).

[9] Wiesner T., Leypold M., Steinmaurer A., Schnalzer D., Fischer R. C., Torvisco A., Haas M., (2020), Synthesis of Stable Dianionic Cyclic Silenolates and Germenolates *Organometallics*, 39, 2878–2887 (DOI: 10.1021/acs.organomet.0c00385).

[10] Segizbayev M., Öztopçu Ö., Hayrapetyan D., Shakhman D., Lyssenko K. A., Khalimon A. Y., (2020), Transfer hydrogenation of aldehydes and ketones catalyzed using an aminophosphinite POCNH pincer complex of Ni(II), *Dalton Trans.*, 49, 11950–11957 (DOI: 10.1039/D0DT02264K).

[11] Wang R., Han X., Xu J., Liu P., Li F., (2020), Transfer Hydrogenation of Ketones and Imines with Methanol under Base-Free Conditions Catalyzed by an Anionic Metal–Ligand Bifunctional Iridium Catalyst, *J. Org. Chem.* 85, 2242–2249 (DOI: 10.1021/acs.joc.9b02957).

[12] Abubakar S., Bala M. D., (2020), Transfer Hydrogenation of Ketones Catalyzed by Symmetric Imino-*N*-heterocyclic Carbene Co(III) Complexes, *ACS Omega*, 5, 2670–2679 (DOI: 10.1021/acsomega.9b03181).

[13] Gunanathan C., Milstein D., (2014), Bond Activation and Catalysis by Ruthenium Pincer Complexes, *Chem. Rev.*, 114, 12024–12087 (DOI: 10.1021/cr5002782).

[14] Fuse H., Mitsunuma H., Kanai M., (2020), Catalytic Acceptorless Dehydrogenation of Aliphatic Alcohols, *J. Am. Chem. Soc.*, 142, 4493–4499 (DOI: 10.1021/jacs.0c00123).

[15] Crabtree R. H., (2017), Homogeneous Transition Metal Catalysis of Acceptorless Dehydrogenative Alcohol Oxidation: Applications in Hydrogen Storage and to Heterocycle Synthesis, *Chem. Rev.*, 117, 9228–9246 (DOI: 10.1021/acs.chemrev.6b00556).

[16] Wang Z., Pan B., Liu Q., Yue E., Solan G. A., Maa Y., Sun W. -H., (2017), Efficient acceptorless dehydrogenation of secondary alcohols to ketones mediated by a PNN-Ru(ii) catalyst, *Catal. Sci. Technol.*, 7, 1654-1661 (DOI: 10.1039/C7CY00342K).

[17] Borah D., Saha B., Sarma B., Das P., (2020), A cyclometalated Ir(III)–NHC complex as a recyclable catalyst for acceptorless dehydrogenation of alcohols to carboxylic acids, *Dalton Trans.* 49 16866–16876 (DOI: 10.1039/D0DT02341H).

[18] Elangovan S., Neumann J., Sortais J.-B., Junge K., Darcel C. and Beller M. 2016 Efficient and selective N -alkylation of amines with alcohols catalysed by manganese pincer complexes *Nat. Commun.*, 7, 12641.

[19] Tan D. -W., Li H. -X., Zhang M. -J., Yao J. -L., Lang J. -P., (2017), Acceptorless Dehydrogenation of Alcohols Catalyzed by CuI *N*-Heterocycle Thiolate Complexes, *ChemCatChem*, 9, 1113–1118 (DOI: 10.1002/cctc.201601459).

[20] Wu S., Wang Y., Cao Q., Zhao Q., Fang W., (2021), Efficient Imine Formation by Oxidative Coupling at Low Temperature Catalyzed by High-Surface-Area Mesoporous CeO2 with Exceptional Redox Property, *Chem. Eur. J.*, *27*, 3019–3028 (DOI: 10.1002/chem.202004909).

[21] Rathi A. K., Gawande M. B., Zboril R., Varma R. S., (2015), Microwave-assisted synthesis – Catalytic applications in aqueous

media, *Coord. Chem. Rev.*, 291, 68–94 (DOI: 10.1016/j.ccr.2015.01.011).

[22] Kokel A., Schäfer C., Török B., (2017), Application of microwave-assisted heterogeneous catalysis in sustainable synthesis design, *Green Chem.*, 19, 3729–3751 (DOI: 10.1039/C7GC01393K).

[23] Priecel P., Lopez-Sanchez J. A., (2019), Advantages and Limitations of Microwave Reactors: From Chemical Synthesis to the Catalytic Valorization of Biobased Chemicals *ACS Sustainable Chem. Eng.*, 7, 3–21 (DOI: 10. 10.1021/acssuschemeng.8b03286).

[24] Danopoulos A. A., Winston S., Motherwell W. B., (2002), Stable N-functionalised 'pincer' bis carbene ligands and their ruthenium complexes; synthesis and catalytic studies, *Chem. Commun*, 1376–1377 (DOI: 10.1039/B202814J).

[25] Trincado M., Bösken J., Grützmacher H., (2021), Homogeneously catalyzed acceptorless dehydrogenation of alcohols: A progress report, *Coord. Chem. Rev.*, 443, 213967 (DOI: 10.1016/j.ccr.2021.213967).

Chapter 4

Dehydrogenative coupling reactions under conventional and microwave heating using Ru(II)-NHC Pincer Complexes

4.1 Introduction

The development of atom efficient and environment-friendly strategies for the construction of C-N bonds is a highly desirable and extensively studied area of chemistry.*[1–19]* Transition metal-catalyzed acceptorless dehydrogenation of alcohols and their dehydrogenative coupling can be used to convert alcohols to a range of compounds in a green and atom-efficient manner. Alcohols could be, for example, converted to aldehydes or acids, ketones, esters, and amides, or C=N bonds created via acceptorless alcohol dehydrogenation (AAD) or related dehydrogenative coupling processes. The alcohols could also be used to form C-N and C-C bonds by coupling with amines or ketones/secondary alcohols using the borrowing hydrogen (BH) or hydrogen autotransfer (HA) methods. (Scheme **4.1**).*[20–31]* AAD and other dehydrogenative coupling processes AAD of primary alcohol can give an aldehyde or an ester formed via nucleophilic attack by another alcohol molecule on the aldehyde followed by a second dehydrogenation step.*[32–35]* Similarly, acceptorless dehydrogenative coupling (ADC) of an alcohol with an amine can give an imine, an amide or a substituted amine (after rehydrogenation of the imine) depending on the nature of the catalyst.*[36,37]* Amine double dehydrogenation (ADD) to give nitriles is a closely related class of reactions that have attracted considerable interest in recent times.*[38–40]* In addition to the atom economy and reaction safety (without the need for an oxidant altogether), the AAD to form a carbonyl compound (e.g., a ketone or an aldehyde) or ADD to form nitriles are also crucial towards the

development of Liquid Organic Hydrogen Carriers (LOHCs) for the so-called hydrogen economy.*[41–43]*

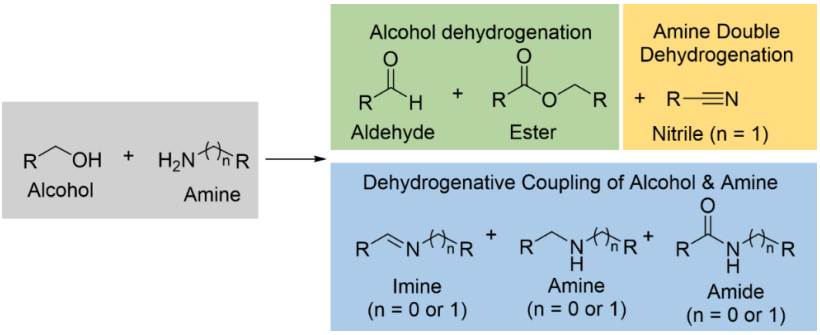

Scheme 4.1 Possible products from acceptorless alcohol dehydrogenation, amine double dehydrogenation or dehydrogenative coupling of alcohols and amines.

In recent years, transition metal complexes have been shown as efficient catalysts for these related reactions.*[24–27]* Tremendous progress has been made in this field with contributions from Milstein,*[24,25,28,44–47]* Kempe,*[48]* Beller,*[49–52]* Fujita,*[53,54]* Sun,*[55,56]* Williams,*[57]* and many other groups (Figure **4.1**).*[30,58–62]* There are several transition metal complexes known to accomplish the key reaction step, i.e., the AAD reaction *[22,26,27,29,63]* as well as subsequent dehydrogenative coupling reactions.*[18,64,65]* Although most of the complexes reported in the earlier studies were those of the "precious" metals,*[5,8–12,19,66–70]* "base" metal complexes have also emerged as efficient catalysts in recent years.*[13–16]*

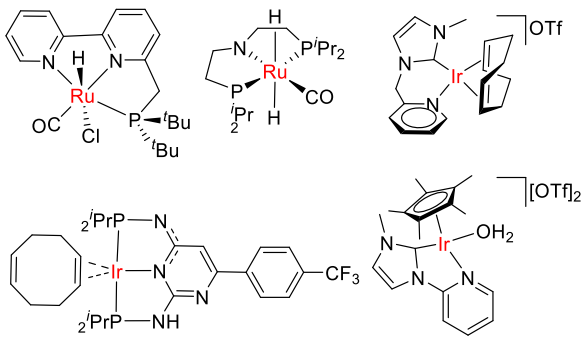

Figure 4.1 Ru and Ir complexes for AAD and dehydrogenative coupling reactions.

NHC-Ru complexes were also used in the dehydrogenative coupling of alcohols with amines to produce imines (Figure **4.1**).*[71–73]* For example, Madsen *et al.* reported the [$RuCl_2$(liPr)(p-cymene)] compound for direct imine synthesis from alcohols and amines. Similarly, NHC-diruthenium(I) complex with a hydroxy appendage on the naphthyridine unit showed good activity for the acceptorless dehydrogenative coupling under mild condition.*[36]* Later, Nishibayashi *et al.* have reported two Ru complexes with NHC and phosphine-based PCP-type pincer ligands, were excellent catalysts in the direct synthesis of imines from amine and benzyl alcohol.*[72]*

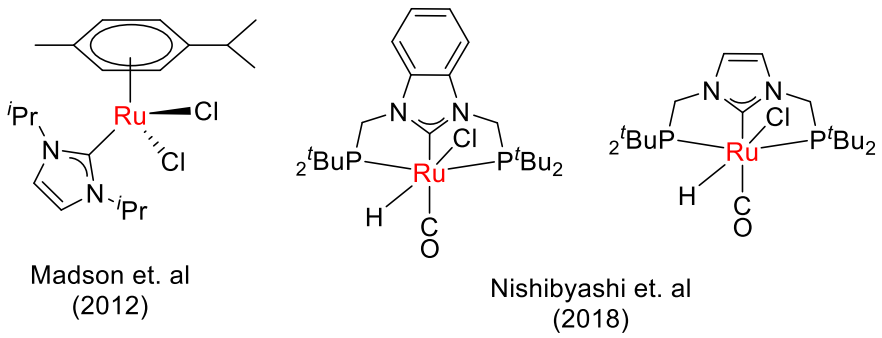

Figure 4.2 Reported ruthenium NHC complexes for dehydrogenative coupling of alcohols and amines

The use of microwaves over conventional heating has various advantages viz; enhancement of reactions rate, production of higher yields, uniform and selective heating, less energy usage, improve reaction repeatability and many more.*[74,75]* Microwave heating differs from conventional heating as it involves correlation of electromagnetic radiation with matter, resulting in an energetic coupling at the molecular level. Microwave-assisted heterogeneous catalysis has been extensively studied, however homogenous catalysis using microwave is not well explored till date.*[76]*

Ruthenium-CNC type pincer complexes have shown high efficiency in a broad range of transformations.*[77–80]* Recently, transfer hydrogenation of a wide range of ketones and aldehydes was explored by our group using the Ruthenium-CNC pincer complexes **1**

and **2** as the catalyst precursors (Figure **4.3**).*[81]* Further, the hydride complex **3** was synthesized from **2** and confirmed to be the active catalyst formed during catalysis with the precatalyst **2**. Herein, we report the application of Ruthenium-CNC pincer complexes $[Ru(CNC)(CO)(PPh_3)Cl]PF_6$ (**1**) and $[Ru(CNC)(PPh_3)_2Cl]PF_6$ (**2**), for acceptorless dehydrogenative coupling of alcohols and amines under conventional heating and microwave. Interestingly, Ruthenium complex **2b** shows excellent efficiency for ADC under thermal and microwave conditions than Ruthenium complex **1b**, resulting in the imine synthesis with various amines and benzyl alcohol.

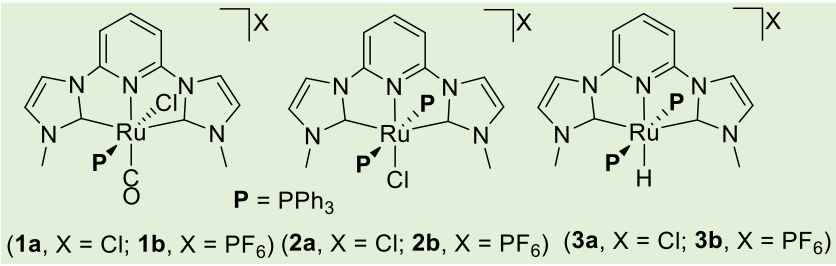

Figure 4.3 Cationic Ru(II)–CNC pincer complexes in this study.

4.2 Results and discussion

4.2.1 Dehydrogenative coupling of alcohols and amines

4.2.1.1 Catalyst screening for dehydrogenative coupling of alcohols and amines under thermal and microwave conditions.

Encouraged by the excellent dehydrogenation results earlier, the dehydrogenative coupling of aniline with benzyl alcohol, resulting in the imine synthesis, was explored as a model system. Aniline was chosen during the catalyst screening to exclude the possibilities of side reactions like amine dehydrogenation. The optimized conditions for the alcohol dehydrogenation reactions, viz., solvent, temperature, base, and catalyst amount, were borrowed as the key initial step in this case, too, is the alcohol dehydrogenation. In catalyst screening experiments, it was observed that the Ru-catalyst **2b** performs better than catalyst **1b** for the ADC of alcohols and amines under both thermal and microwave

conditions (Table **4.1**). This interesting reverse trend in catalytic activity indicates involvement of the Ru-metal centre in the dehydrogenative coupling step as, otherwise, the catalyst better at alcohol dehydrogenation should also have been better at the imine formation.

Table 4.1 Catalyst screening under thermal and microwave conditions.

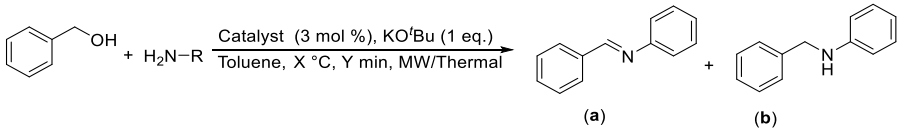

Entry[a]	Catalyst	TH/ MW	Temp. (°C) (Time)	% Conversion[b]	TON[c]/TOF[d]	Selectivity a:b
1.	**1b**	TH	110 (3 h)	60	20/6	75:25
2.	**1b**	MW	80 (30 min)	58	19/38	100:0
3.	**2b**	TH	110 (3 h)	68	22/7	100:0
4.	**2b**	MW	80 (30 min)	>99	33/66	100:0
5.	**2b**	MW	80 (15 min)	56	18/74	100:0

[a]Reaction conditions: Benzyl alcohol (1 mmol), Catalyst (3 mol %), KO^{t}Bu (1 eq.), Toluene (5 mL) under a slow N_2 flow under thermal condition (110 °C/3h) and microwave condition (80 °C/30 min). [b]Determined by gas chromatography without an internal standard. [c]TON = [(Number of moles of substrate converted)/(Number of moles of catalyst)] at the end of the reaction. [d]TOF = [(TON)/hour].

4.2.1.2 Substrate scope for dehydrogenative coupling of alcohols and amines under thermal and microwave conditions.

ADC of several amines, including benzylic, heterocyclic, cyclic, and acyclic aliphatic amines, was explored with benzyl alcohol for the direct synthesis of imines under the optimized reaction condition (Table **4.2** and **4.3**). It was found that complex **2b** serves as an efficient pre-catalyst for a range of substrates and gives excellent conversion in most cases. n-hexylamine and 2-aminopyridine are suitable substrates for imination with >99% conversions (Table **4.2** and **4.3**, entries 3 and 4).

Table 4.2. Imine synthesis reaction from various amines and benzene methanol with catalyst **2b** under conventional heating.

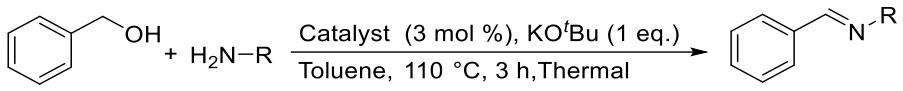

Entry[a]	Reactant	Product	Thermal[b] (110 °C, 3 h)	
			% Conversion[c] (Isolated yield)	TON[d]/TOF[e]
1.	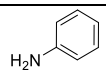	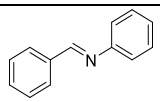	68(65)	21/7
2.	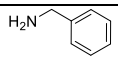	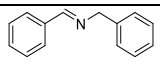	>99(90)	30/10
3.		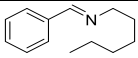	>99(93)	31/10
4.	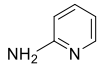	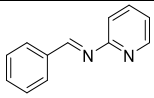	>99(85)	28/9
5.	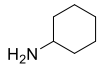	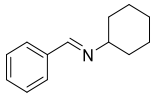	86(73)	24/8
6.	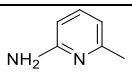	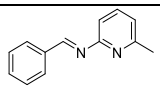	83(71)	23/7
7.	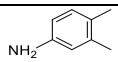	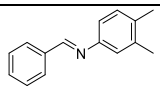	95(85)	28/9
8.	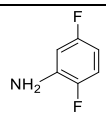	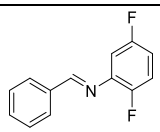	NR	-

[a]Reaction conditions: Amines (1 mmol), Benzyl alcohol (1 mmol), Catalyst (3 mol %), KO^{t}Bu (1 eq.), Toluene (5 mL) under a slow N_2 flow under thermal[b] condition (110 ^{o}C/3h). [c]Determined by gas chromatography without internal standard. [d]TON = [(Number of moles of substrate converted)/(Number of moles of catalyst)] at the end of the reaction. [e]TOF = [(TON)/hour].

Table 4.3. Imine synthesis reaction from various amines and benzene methanol with catalyst **2b** under microwave.

Entry[a]	Reactant	Product	Microwave[b] (80 °C, 30 min)	
			% Conversion[c] (Isolated yield)	TON[d]/TOF[e]
1.	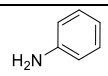	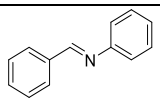	>99(82)	27/54
2.	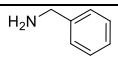	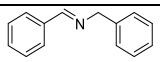	>99(91)	30/60
3.		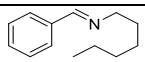	>99(84)	28/56
4.	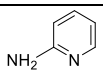	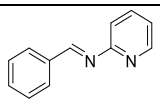	>99(86)	28/57
5.	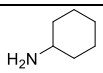	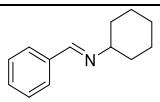	>99(90)	29/59
6.	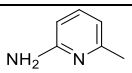	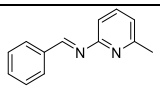	85(80)	26/59
7.	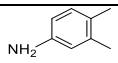	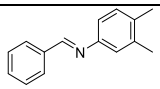	47(38)	12/25
8.	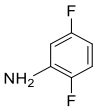	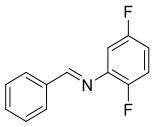	33(18)	6/12

[a]Reaction conditions: Amines (1 mmol), Benzyl alcohol (1 mmol), Catalyst (3 mol %), KO^{t}Bu (1 eq.), Toluene (5 mL) under a slow N_2 flow under microwave[b] condition (80 ^{o}C/30min). [c]Determined by gas chromatography without internal standard. [d]TON = [(Number of moles of substrate converted)/(Number of moles of catalyst)] at the end of the reaction. [e]TOF = [(TON)/hour].

However, reaction with cyclohexylamine gave slightly reduced conversion, 86% under thermal condition (Table **4.2**, entry 5). 6-Methyl-2-aminopyridine and 3,4 dimethylaniline gave 83%, 85% and 95%, 47%

under thermal and microwave conditions, respectively (Table **4.2** and **4.3**, entries 6 and 7). In the case of 2,5-difluoro aniline, no conversion under thermal conditions and a low yield of 33% in the case of microwave conditions was observed (Table **4.2** and **4.3**, entry 8).

4.2.1.3 Synthesis of pharmaceutically important scaffolds under microwave conditions.

To further evaluate the applicability of the reaction, different biologically active imine precursors were assembled. The reaction of 4-aminostilbene with benzyl alcohol and 4-methoxy benzyl alcohol under microwave for 10 min gave >99% conversions for Resveratrol precursors in both cases (Table **4.4**, entries 1 and 2). Resveratrol derived imines are active precursors for the resveratrol drugs which is used for Alzheimer's disease.

Table 4.4 Synthesis of biologically active imine precursors with catalyst **2b**

Entry[a]	Reactant (Alcohol)	Reactant (Amine)	Product	%Conversion[b] (Isolated yield)	TON[c]/ TOF[d]
1.		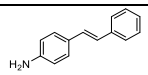	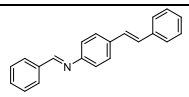	>99(90)	30/60
2.	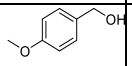	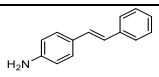	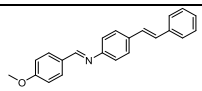	>99(87)	29/58
3.	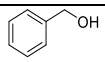		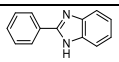	>99(95)	31/63
4.	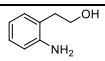	-		>99(91)	30/60

[a]Reaction conditions: Amines (1 mmol), Alcohols (1 mmol), Catalyst (3 mol %), KO^{t}Bu (1 eq.), Toluene (5 mL) under a slow N_2 flow for 30 min at 80 ^{o}C under microwave. [b]Determined by gas chromatography without internal standard. [c]TON = [(Number of moles of substrate converted)/(Number of moles of catalyst)] at the end of the reaction. [d]TOF = [(TON)/hour].

On the other hand, the reaction of 1,2-diaminobenzene with benzyl alcohol results in 2-phenylbenzimidazole and intermolecular

reactions of 2-amino-phenylethanol) delivered indole in >99% conversion (Table **4.4**, entries 3 and 4).

4.2.2 Mechanisms for dehydrogenative coupling of alcohols and amines.

The mechanisms for AAD and ADC catalysed by transition metal complexes have been studied thoroughly earlier.*[24–28,37,82,83]* Based on the earlier studies reported in literature and our recent investigation of the mechanism of transfer hydrogenation and acceptorless dehydrogenation of alcohols using these complexes,*[81]* a plausible mechanism for acceptorless dehydrogenative coupling of alcohols and amines has been proposed involving the Ru-hydride complex **3** as an intermediate (Scheme **4.2**). The presence of ruthenium hydride complexes **3** and **3'** in the reaction mixture of ADC reactions starting from the precatalyst **2** was again confirmed through mass spectrometry. Dissociation of a PPh_3 ligand and the formation of complexes **3** and **3'** was also observed during our investigation for transfer hydrogenation catalysis in a previous report.*[81]* The reaction begins with the formation of a ruthenium alkoxide species **A** by the reaction of complex **2'** with alcohol in the presence of KO^tBu. Further, the Ru-H intermediate **B** is formed via β-H elimination resulting in the generation of the metal-bound aldehyde. Release of the aldehyde molecule produces Ru-H intermediate **3'**, which can also be formed by dissociation of a PPh_3 ligand, starting from the Ru-hydride complex **3**. Finally, the addition of an alcohol molecule to the intermediate **3'** produces another intermediate **C**, which liberates H_2 gas and regenerates the ruthenium alkoxide species **A**, completing the alcohol dehydrogenation step.

For the imine formation, the dehydrogenative coupling step can be considered to proceed via nucleophilic attack of an amine on the metal-bound aldehyde in the intermediate **B**, which generates the intermediate **D**. A similar mechanism for ADC of amines and alcohols by ruthenium catalysts has been studied and reported earlier.*[36]* This

nucleophilic attack should be facilitated in a metal-bound aldehyde due to decreased electron density at the metal-bound carbon atom. Further, a weaker trans effect of PPh_3 ligand allows the aldehyde intermediate to remain metal-bound and facilitates the coupling with an amine. Proton transfer from the ammonium nitrogen to the oxygen atom then generates intermediate **E** with the coordinated hemiaminal species. Dissociation of the hemiaminal generates Ru-hydride intermediate **3'**, which can participate further in another alcohol dehydrogenation step. Dehydration of the hemiaminal generates the final imine product.

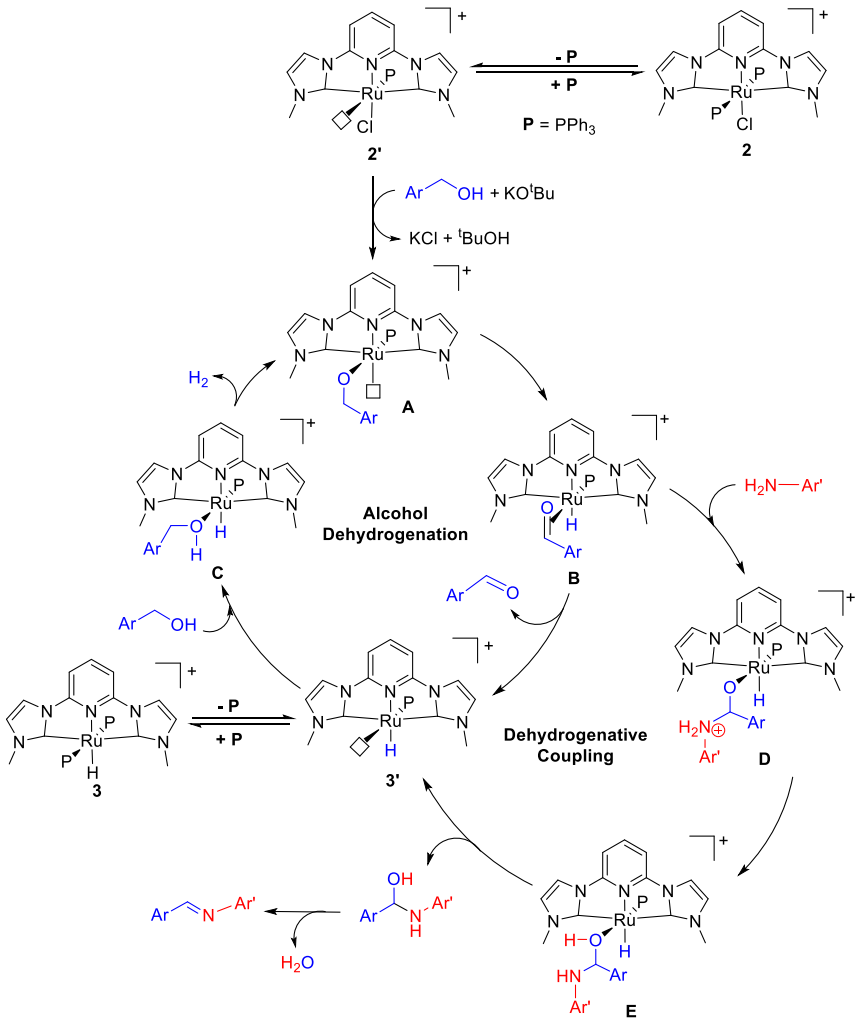

Scheme 4.2 Plausible mechanism for aceptorless alcohol dehydrogenation and dehydrogenative coupling of amines by complexes **2** and **3**.

The role of *trans* effect of an ancillary ligand in the selectivity of the type of reaction is an important feature of these complexes. A similar

observation has recently been reported for the role of metal nanoparticles in the photo dehydrogenative coupling of amines, where stronger adsorption over the metal nanoparticle results in dehydrogenative homocoupling of amines while the weaker adsorption results in imine formation.*[84]*

4.3 Conclusion

In summary, we have studied the catalytic activity of Ru(II)-CNC complexes viz; $[Ru(CNC)(CO)(PPh_3)Cl]PF_6$ (**1b**) and $[Ru(CNC)(PPh_3)_2Cl]\ PF_6$ (**2b**) for ADC of benzyl alcohol and amines. Both the ruthenium complexes were found catalytically active for both types of reactions. Compared to conventional "oil-bath" heating, microwave irradiation resulted in faster catalysis under milder conditions. Further, an unexpected reversal in the catalytic activity of the two complexes has been observed. In our earlier reports, complex **1b** was found to be catalytically more active than its analogous complex **2b** for acceptorless dehydrogenation of alcohols, but now, complex **2b** was found more active for direct synthesis of imines than complex **1b**. A mechanism is proposed involving the role of Ru-center to explain this reversal in catalytic activity. This report highlights, for the first time, the enhancement in catalytic activity for ADC reactions under microwave radiation and potential electronic effects of other ligands present on the metal complex in the selectivity control of dehydrogenation over the dehydrogenative coupling. The results reported in this study can lead to the design of more selective catalysts.

4.4 Experimental

4.4.1 General considerations

All reactions and manipulations were carried out under an inert atmosphere using the standard Schlenk technique. Solvents were purchased from S. D. Fine-Chem Limited and purified by distillation under N_2 atmosphere. The metal complexes were synthesized according to our previous work. Microwave experiments were performed in Milestone Start S microwave reactor equipped with a straight-tube air

condenser connected to an inert-gas line and oil bubbler, a magnetic stirrer bar and a non-contact infrared feedback temperature system which allows continuous stirring and constant temperature control. The microwave reactor has a maximum power output of 1200W while the required power output is controlled electronically to maintain the reaction temperature. NMR spectra were taken on Bruker Avance (III) spectrometer operating at 400 MHz (^{1}H). NMR chemical shifts are reported in ppm and referenced to the solvent peaks for ^{1}H ($CDCl_3$, δ 7.26 ppm). The mass chromatograms were recorded on Bruker-Daltonics-microTOF-QII mass spectrometer. GC Samples were analysed in Shimadzu QP2010 Ultra.

4.4.2 General procedure for imination reaction under thermal condition.

Typically, catalyst (3 mol %) was added to the solution of alcohol (1 mmol), amine (1 mmol), KO^{t}Bu (1 eq.) in toluene under an inert atmosphere in a 2-neck R.B. flask equipped with reflux condenser and heated at 110 ^{o}C for 3h by lowering into a preheated oil bath. The conversion of the corresponding product was determined by the relative peak area of the substrate and the product in GC without an internal standard. After completion of the reaction, the product was extracted with chloroform and dried in vacuum. The product was purified by alumina gel column chromatography using hexane/ethyl acetate (typically 7.7:0.3) as eluent. ^{1}H NMR data for the aldehyde products match the reported values.

4.4.3 General procedure for imination reaction under microwave condition.

Typically, catalyst (3 mol %) was added to the solution of alcohol (1 mmol), amine (1 mmol), KO^{t}Bu (1 eq.) in toluene under an inert atmosphere in a 2-neck R.B. flask equipped with a straight-tube air condenser and heated at 80 ^{o}C for 30 min under microwave radiation. The conversion of the corresponding product was determined by the relative peak area of the substrate and the product in GC without an

internal standard. After completion of the reaction, the product was extracted with chloroform and dried in vacuum. The product was purified by silica gel column chromatography using hexane/ethyl acetate (typically 7.7:0.3) as eluent. ^{1}H NMR data for the aldehyde products match the reported values.

4.4.3 Characterization data and Mechanistic studies

4.4.3.1 Characterization data for Dehydrogenative coupling products

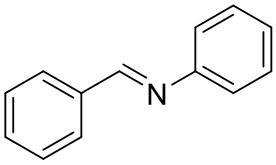

***N*-1-diphenylmethanimine;** ^{1}H NMR ($CDCl_3$, δ in ppm): 8.50 (s, 1H), 7.72-7.69 (m, 2H), 7.63-7.58 (m, 1H), 7.55-7.50 (m, 1H), 7.47-7.33 (m, 4H), 7.20-7.17 (m, 2H).

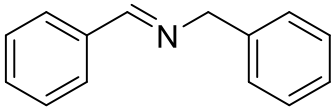

***N*-benzyl-1-phenylmethanimine;** ^{1}H NMR ($CDCl_3$, δ in ppm): 8.31 (s, 1H), 7.70-7.67 (m, 2H), 7.61-7.56 (m, 1H), 7.47-7.43 (m, 1H), 7.38-7.34 (m, 4H), 7.20-7.16 (m, 2H), 4.74 (s, 2H).

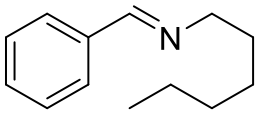

***N*-hexyl-1-phenylmethanimine;** ^{1}H NMR ($CDCl_3$, δ in ppm): 8.27 (s, 1H), 7.71-7.66 (m, 2H), 7.55-7.53 (m, 1H), 7.47-7.40 (m, 2H), 3.62-3.59 (m, 2H), 2.05-1.96 (m, 2H), 1.32-1.25 (m, 6H), 0.88-0.83 (m, 2H).

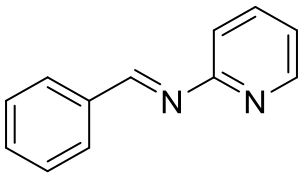

***N*-(pyridin-2-yl)-1-phenylmethanimine;** ^{1}H NMR ($CDCl_3$, δ in ppm): 8.86 (s, 1H), 8.49 (d, *J*=8.00 Hz, 1H), 7.70-7.67 (m, 3H), 7.64-7.58 (m, 1H), 7.54-7.47 (m, 2H), 6.68 (d, *J*=8.00 Hz, 1H), 6.45 (d, *J*=8.00 Hz, 1H).

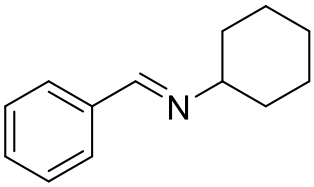

***N*-cyclohexyl-1-phenylmethanimine;** ^{1}H NMR ($CDCl_3$, δ in ppm): 8.20 (s, 1H), 7.79-7.65 (m, 2H), 7.54-7.46 (m, 2H), 7.35-7.23 (m, 1H), 1.80-1.76 (m, 1H), 1.40-1.24 (m, 10 H).

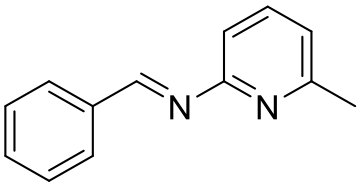

***N*-(6-methylpyridin-2-yl)-1-phenylmethanimine;** ^{1}H NMR ($CDCl_3$, δ in ppm): 8.58 (s, 1H), 7.68-7.63 (m, 3H), 7.54-7.52 (m, 1H), 7.48-7.45 (m, 2H), 6.50 (d, *J*=8.00 Hz, 1H), 6.34 (d, *J*=8.00 Hz, 1H), 2.37 (s, 3H).

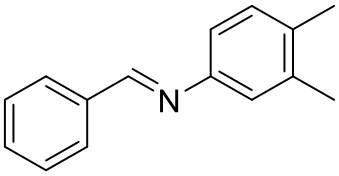

***N*-(3,4-dimethylphenyl)-1-phenylmethanimine;** ^{1}H NMR ($CDCl_3$, δ in ppm): 8.51 (s, 1H), 7.93-7.87 (m, 2H), 7.74-7.69 (m, 1H), 7.57-7.50 (m, 2H), 7.21 (s, 1H), 7.19 (s, 1H), 7.09 (s, 1H), 2.33 (s, 3H), 1.30 (s, 3H).

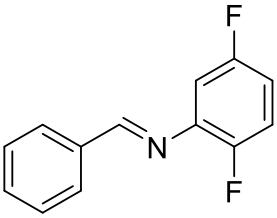

***N*-(2,5-difluorophenyl)-1-phenylmethanimine;** ^{1}H NMR ($CDCl_3$, δ in ppm): 8.22 (s, 1H), 7.69-7.64 (m, 2H), 7.57-7.53 (m, 1H), 7.48-7.45 (m, 2H), 7.36 (s, 1H), 7.26 (s, 1H), 7.10 (s, 1H).

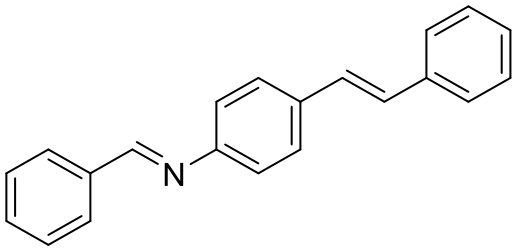

***N*-(4-styryl)-1-phenylmethanimine;** ^{1}H NMR ($CDCl_3$, δ in ppm): 8.52 (s, 1H), 7.88-7.76 (m, 2H), 7.75-7.71 (m, 2H), 7.70-7.66 (m, 2H), 7.65-7.58 (m, 1H), 7.56-7.51 (m, 1H), 7.50-7.49 (m, 2H), 7.48-7.43 (m, 2H), 7.41-7.38 (m, 2H), 6.89 (d, *J*=8.00 Hz, 2H).

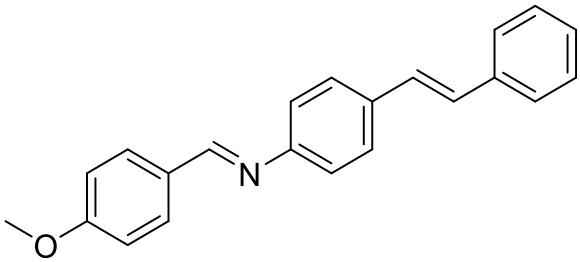

***N*-(4-styryl)-1-(4-methoxyphenylmethanimine;** ^{1}H NMR ($CDCl_3$, δ in ppm): 8.53 (s, 1H), 7.89-7.80 (m, 2H), 7.76-7.72 (m, 2H), 7.70-7.66 (m, 2H), 7.65-7.57 (m, 1H), 7.56-7.49 (m, 2H), 7.48-7.42 (m, 2H), 7.40-7.39 (m, 2H), 6.90 (d, *J*=8.00 Hz, 2H), 3.83 (s, 3H).

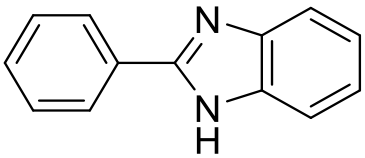

2-phenylbenzimidazole; ^{1}H NMR ($CDCl_3$, δ in ppm): 12.54 (s, 1H), 8.23-8.20 (t, *J*=8.00 Hz 2H), 7.65-7.41 (m, 5H), 7.24-7.19 (m, 2H).

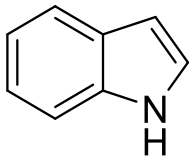

Indole; ^{1}H NMR ($CDCl_3$, δ in ppm): 9.98 (s, 1H), 7.52-7.48 (m, 1H), 7.47-7.41 (m, 1H), 7.32-7.27 (m, 1H), 7.18-7.07 (m, 1H), 7.00-7.66 (m, 1H), 6.57 (d, *J*=8.00 Hz, 1H).

4.4.3.2 Mechanistic studies

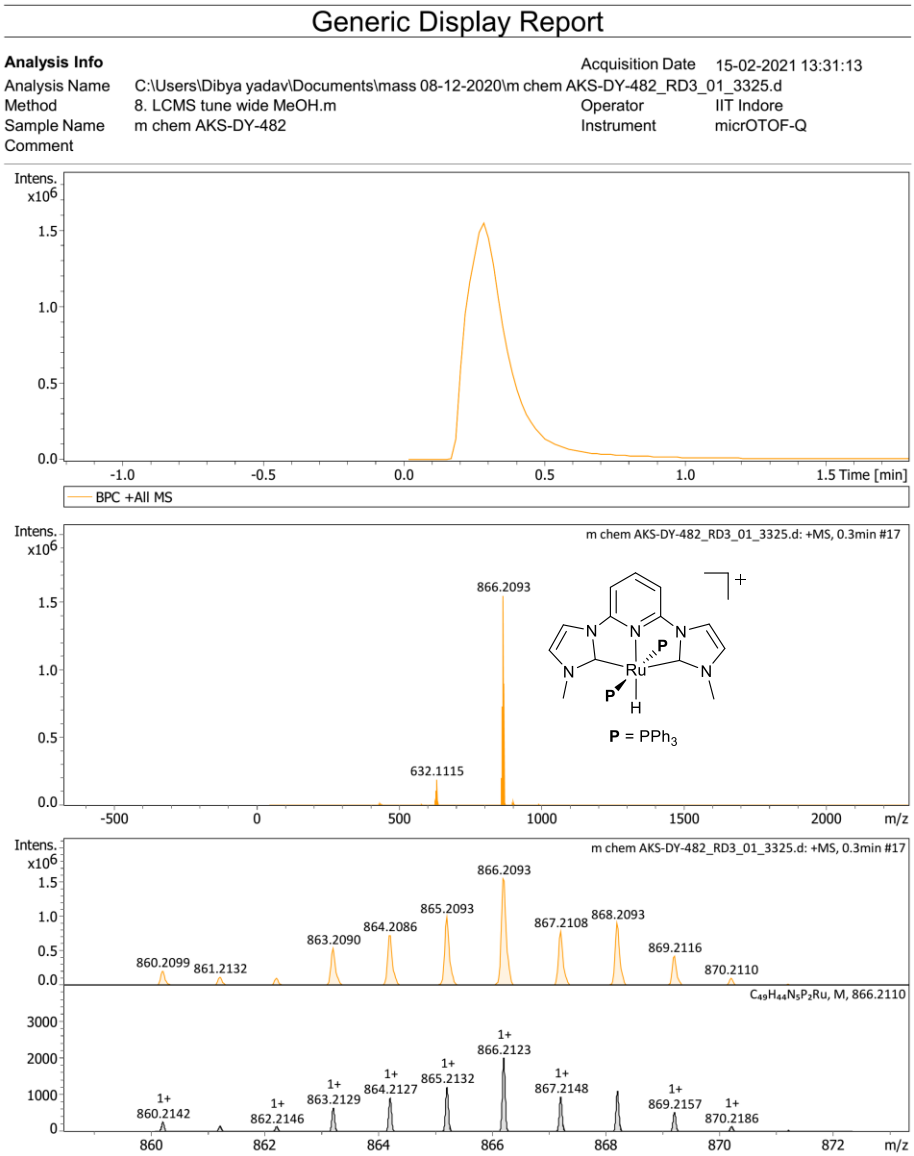

Figure 4.4 LC-MS spectrogram of catalytic sample of imination reaction of complex **2b**

4.5 References

[1] Jumde V. R., Gonsalvi L., Guerriero A., et al. (2015), A Ruthenium-Based Catalytic System for a Mild Borrowing-Hydrogen Process, *Eur. J. Org. Chem.*, 2015, 1829–1833 (https://doi.org/10.1002/ejoc.201403636).

[2] Santoro F., Psaro R., Ravasio N., Zaccheria F. (2013), *N*-Alkylation of amines through hydrogen borrowing over a heterogeneous Cu catalyst, *RSC Adv.*, 4, 2596–2600 (https://doi.org/10.1039/C3RA44364G).

[3] Broomfield L. M., Wu Y., Martin E., Shafir A. (2015), Phosphino-amine (PN) Ligands for Rapid Catalyst Discovery in Ruthenium-Catalyzed Hydrogen-Borrowing Alkylation of Anilines: A Proof of Principle, *Adv. Synth. Catal.*, 357, 3538–3548 (https://doi.org/10.1002/adsc.201500562).

[4] Mastalir M., Glatz M., Pittenauer E., *et al.* (2019), Rhenium-Catalyzed Dehydrogenative Coupling of Alcohols and Amines to Afford Nitrogen-Containing Aromatics and More, *Org. Lett.*, 21, 1116–1120 (https://doi.org/10.1021/acs.orglett.9b00034).

[5] Marichev K. O., Takacs J. M. (2016), Ruthenium-Catalyzed Amination of Secondary Alcohols Using Borrowing Hydrogen Methodology, *ACS Catal.*, 6, 2205–2210 (https://doi.org/10.1021/acscatal.6b00175).

[6] Leonard J., Blacker A. J., Marsden S. P., *et al.* (2015), A Survey of the Borrowing Hydrogen Approach to the Synthesis of some Pharmaceutically Relevant Intermediates, *Org. Process Res. Dev.*, 19, 1400–1410 (https://doi.org/10.1021/acs.oprd.5b00199).

[7] Shan S. P., Xiaoke X., Gnanaprakasam B., *et al.* (2014), Benzimidazolin-2-ylidene N-heterocyclic carbene complexes of ruthenium as a simple catalyst for the *N*-alkylation of amines using

alcohols and diols, *RSC Adv.*, 5, 4434–4442 (https://doi.org/10.1039/C4RA15398G).

[8] Hikawa H., Koike T., Izumi K., *et al.* (2016),, Borrowing Hydrogen Methodology for N-Benzylation using a π-Benzylpalladium System in Water, *Adv. Synth. Catal.*, 358, 784–791 (https://doi.org/10.1002/adsc.201501041).

[9] Yang Y., Qin A., Zhao K., *et al.* (2016), Design and Synthesis of Alanine Triazole Ligands and Application in Promotion of Hydration, Allene Synthesis and Borrowing Hydrogen Reactions, *Adv. Synth. Catal.*, 358, 1433–1439 (https://doi.org/10.1002/adsc.201600141).

[10] Corma A., Navas J., Sabater M. J. (2012), Coupling of Two Multistep Catalytic Cycles for the One-Pot Synthesis of Propargylamines from Alcohols and Primary Amines on a Nanoparticulated Gold Catalyst, *Chem. Eur. J.*, 18, 14150–14156 (https://doi.org/10.1002/chem.201201837).

[11] Liu H., Chuah G.-K., Jaenicke S. (2012), *N*-alkylation of amines with alcohols over alumina-entrapped Ag catalysts using the "borrowing hydrogen" methodology, *J. Catal.*, 292, 130–137 (https://doi.org/10.1016/j.jcat.2012.05.007).

[12] Satyanarayana P., Reddy G. M., Maheswaran H., Kantam M. L. (2013), Tris(acetylacetonato)rhodium(III)-Catalyzed α-Alkylation of Ketones, β-Alkylation of Secondary Alcohols and Alkylation of Amines with Primary Alcohols, *Adv. Synth. Catal.*, 355, 1859–1867 (https://doi.org/10.1002/adsc.201300061).

[13] Yan T., Feringa B. L., Barta K. (2016), Benzylamines via Iron-Catalyzed Direct Amination of Benzyl Alcohols, *ACS Catal.*, 6, 381–388 (https://doi.org/10.1021/acscatal.5b02160).

[14] Quintard A., Rodriguez J. (2016), A Step into an eco-Compatible Future: Iron- and Cobalt-catalyzed Borrowing Hydrogen Transformation, *ChemSusChem*, 9, 28–30 (https://doi.org/10.1002/cssc.201501460).

[15] Elangovan S., Neumann J., Sortais J.-B., *et al.* (2016), Efficient and selective *N*-alkylation of amines with alcohols catalysed by manganese pincer complexes, *Nat. Commun.*, 7, 12641 (https://doi.org/10.1038/ncomms12641).

[16] Mehta A., Thaker A., Londhe V., Nandan S. R. (2014), Reinvestigating Raney nickel mediated selective alkylation of amines with alcohols via hydrogen autotransfer methodology, *Appl. Catal. Gen.*, 478, 241–251 (https://doi.org/10.1016/j.apcata.2014.04.009).

[17] Abdukader A., Jin H., Cheng Y., Zhu C. (2014), Rhenium-catalyzed amination of alcohols by hydrogen transfer process, *Tetrahedron Lett.*, 5, 4172–4174 (https://doi.org/10.1016/j.tetlet.2014.05.068).

[18] Wu S., Zhang H., Cao Q., *et al.* (2021), Efficient imine synthesis via oxidative coupling of alcohols with amines in an air atmosphere using a mesoporous manganese–zirconium solid solution catalyst, *Catal. Sci. Technol.*, 11, 810–822 (https://doi.org/10.1039/D0CY02288H).

[19] Rong Z.-Q., Zhang Y., Chua R. H. B., *et al.* (2015), Dynamic Kinetic Asymmetric Amination of Alcohols: From A Mixture of Four Isomers to Diastereo- and Enantiopure α-Branched Amines, *J. Am. Chem. Soc.*, 137, 4944–4947 (https://doi.org/10.1021/jacs.5b02212).

[20] Shahane S., Fischmeister C., Bruneau C. (2012), Acceptorless ruthenium catalyzed dehydrogenation of alcohols to ketones and

esters, *Catal. Sci. Technol.*, 2, 1425–1428 (https://doi.org/10.1039/C2CY20066J).

[21] Pandey P., Dutta I., Bera J. K. (2016), Acceptorless Alcohol Dehydrogenation: A Mechanistic Perspective, *Proc. Natl. Acad. Sci. India, Sect. A Phys. Sci.*, 86, 561–579 (https://doi.org/10.1007/s40010-016-0296-7).

[22] Fuse H., Mitsunuma H., Kanai M. (2020), Catalytic Acceptorless Dehydrogenation of Aliphatic Alcohols, *J. Am. Chem. Soc.*, 142, 4493–4499 (https://doi.org/10.1021/jacs.0c00123).

[23] Chang W., Gong X., Wang S., *et al.* (2017), Acceptorless dehydrogenation and dehydrogenative coupling of alcohols catalysed by protic NHC ruthenium complexes, *Org. Biomol. Chem.*, 15, 3466–3471 (https://doi.org/10.1039/C7OB00542C).

[24] Mastalir M., Glatz M., Gorgas N., *et al.* (2016), Divergent Coupling of Alcohols and Amines Catalyzed by Isoelectronic Hydride MnI and FeII PNP Pincer Complexes, *Chem. Eur. J.*, 22, 12316–12320 (https://doi.org/10.1002/chem.201603148).

[25] Zhang J., Gandelman M., Shimon L. J. W., *et al.* (2004), Electron-Rich, Bulky Ruthenium PNP-Type Complexes. Acceptorless Catalytic Alcohol Dehydrogenation, *Organometallics*, 23, 4026–4033 (https://doi.org/10.1021/om049716j).

[26] Zell T., Milstein D. (2015), Hydrogenation and Dehydrogenation Iron Pincer Catalysts Capable of Metal–Ligand Cooperation by Aromatization/Dearomatization, *Acc. Chem. Res.*, 48, 1979–1994 (https://doi.org/10.1021/acs.accounts.5b00027).

[27] Masdemont J., Luque-Urrutia J. A., Gimferrer M., *et al.* (2019), Mechanism of Coupling of Alcohols and Amines To Generate Aldimines and H_2 by a Pincer Manganese Catalyst, *ACS Catal.*, 9, 1662–1669 (https://doi.org/10.1021/acscatal.8b04175).

[28] Luque-Urrutia J. A., Solà M., Milstein D., Poater A. (2019), Mechanism of the Manganese-Pincer-Catalyzed Acceptorless Dehydrogenative Coupling of Nitriles and Alcohols, *J. Am. Chem. Soc.*, 141, 2398–2403 (https://doi.org/10.1021/jacs.8b11308).

[29] Weber S., Kirchner K. (2021), The Role of Metal-Ligand Cooperation in Manganese(I)-Catalyzed Hydrogenation/Dehydrogenation Reactions. In: van Koten G, Kirchner K, Moret M-E (eds) Metal-Ligand Co-operativity: Catalysis and the Pincer-Metal Platform. *Springer International Publishing*, Cham, pp 227–261.

[30] Miao Y., Samuelsen S. V., Madsen R. (2021), Vanadium- and Chromium-Catalyzed Dehydrogenative Synthesis of Imines from Alcohols and Amines, *Organometallics*, 40, 1328–1335 (https://doi.org/10.1021/acs.organomet.1c00123).

[31] Li R.-J., Ling C., Lv W.-R., *et al.* (2021), Cyclometalated Half-Sandwich Iridium(III) Complexes: Synthesis, Structure, and Diverse Catalytic Activity in Imine Synthesis Using Air as the Oxidant, *Inorg. Chem.*, 60, 5153–5162 (https://doi.org/10.1021/acs.inorgchem.1c00174).

[32] Zhang L., Raffa G, Nguyen D. H., *et al.* (2016) Acceptorless dehydrogenative coupling of alcohols catalysed by ruthenium PNP complexes: Influence of catalyst structure and of hydrogen mass transfer, *J. Catal.*, 340, 331–343 (https://doi.org/10.1016/j.jcat.2016.06.001).

[33] Siddiki S. M. A. H., Toyao T., Shimizu K. (2018), Acceptorless dehydrogenative coupling reactions with alcohols over heterogeneous catalysts, *Green Chem.*, 20, 2933–2952 (https://doi.org/10.1039/C8GC00451J).

[34] Nguyen D. H., Trivelli X., Capet F., *et al.* (2017) Manganese Pincer Complexes for the Base-Free, Acceptorless

Dehydrogenative Coupling of Alcohols to Esters: Development, Scope, and Understanding, *ACS Catal.*, 7, 2022–2032 (https://doi.org/10.1021/acscatal.6b03554).

[35] Wei Z., Aguirre A. de, Junge K., et al. (2018), Benyzl Alcohol Dehydrogenative Coupling Catalyzed by Defined Mn and Re PNP Pincer Complexes – A Computational Mechanistic Study, *Eur. J. Inorg. Chem.*, 2018, 4643–4657 (https://doi.org/10.1002/ejic.201800674).

[36] Maggi A., Madsen R. (2012), Dehydrogenative Synthesis of Imines from Alcohols and Amines Catalyzed by a Ruthenium *N*-Heterocyclic Carbene Complex, *Organometallics*, 31, 451–455 (https://doi.org/10.1021/om201095m).

[37] Chai H., Yu K., Liu B., *et al.* (2020), A Highly Selective Manganese-Catalyzed Synthesis of Imines under Phosphine-Free Conditions, *Organometallics*, 39, 217–226 (https://doi.org/10.1021/acs.organomet.9b00769).

[38] Olivares M., Knörr P., Albrecht M. (2020), Aerobic dehydrogenation of amines to nitriles catalyzed by triazolylidene ruthenium complexes with O_2 as terminal oxidant, *Dalton Trans.*, 49, 1981–1991 (https://doi.org/10.1039/C9DT04873A).

[39] Pavel O. D., Goodrich P., Cristian L., *et al.* (2015), Direct oxidation of amines to nitriles in the presence of ruthenium-terpyridyl complex immobilized on ILs/SILP, *Catal. Sci. Technol.*, 5, 2696–2704 (https://doi.org/10.1039/C5CY00011D).

[40] Tseng K.-N. T., Rizzi A. M., Szymczak N. K. (2013), Oxidant-Free Conversion of Primary Amines to Nitriles, *J. Am. Chem. Soc.*, 135, 16352–16355 (https://doi.org/10.1021/ja409223a).

[41] Preuster P., Papp C., Wasserscheid P. (2017), Liquid Organic Hydrogen Carriers (LOHCs): Toward a Hydrogen-free Hydrogen

Economy, *Acc. Chem. Res.*, 50, 74–85 (https://doi.org/10.1021/acs.accounts.6b00474).

[42] Jaiswal G., Landge V. G., Jagadeesan D., Balaraman E. (2017), Iron-based nanocatalyst for the acceptorless dehydrogenation reactions, *Nat. Commun.*, 8, 2147 (https://doi.org/10.1038/s41467-017-01603-3).

[43] Crabtree R. H. (2017), Homogeneous Transition Metal Catalysis of Acceptorless Dehydrogenative Alcohol Oxidation: Applications in Hydrogen Storage and to Heterocycle Synthesis, *Chem. Rev.*, 117, 9228–9246 (https://doi.org/10.1021/acs.chemrev.6b00556).

[44] Srimani D., Ben-David Y., Milstein D. (2013), Direct Synthesis of Pyrroles by Dehydrogenative Coupling of β-Aminoalcohols with Secondary Alcohols Catalyzed by Ruthenium Pincer Complexes, *Angew. Chem. Inter. Ed.*, 52, 4012–4015 (https://doi.org/10.1002/anie.201300574).

[45] Mukherjee A., Nerush A., Leitus G., *et al.* (2016), Manganese-Catalyzed Environmentally Benign Dehydrogenative Coupling of Alcohols and Amines to Form Aldimines and H_2: A Catalytic and Mechanistic Study, *J. Am. Chem. Soc.*, 138, 4298–4301 (https://doi.org/10.1021/jacs.5b13519).

[46] Espinosa-Jalapa N. A., Kumar A., Leitus G., *et al.* (2017), Synthesis of Cyclic Imides by Acceptorless Dehydrogenative Coupling of Diols and Amines Catalyzed by a Manganese Pincer Complex, *J. Am. Chem. Soc.*, 139, 11722–11725 (https://doi.org/10.1021/jacs.7b08341)

[47] Daw P., Kumar A., Espinosa-Jalapa N. A., *et al.* (2018), Synthesis of Pyrazines and Quinoxalines via Acceptorless Dehydrogenative Coupling Routes Catalyzed by Manganese Pincer Complexes, *ACS Catal.*, 8, 7734–7741 (https://doi.org/10.1021/acscatal.8b02208).

[48] Michlik S., Kempe R., (2013), Regioselectively Functionalized Pyridines from Sustainable Resources, *Angew. Chem. Inter. Ed.*, 52, 6326–6329 (https://doi.org/10.1002/anie.201301919).

[49] Peña-López M., Neumann H., Beller M. (2014), Ruthenium-Catalyzed Synthesis of Indoles from Anilines and Epoxides, *Chem. Eur. J.*, 20, 1818–1824 (https://doi.org/10.1002/chem.201304432).

[50] Alberico E., Lennox A. J. J., Vogt L. K., *et al.* (2016), Unravelling the Mechanism of Basic Aqueous Methanol Dehydrogenation Catalyzed by Ru–PNP Pincer Complexes, *J. Am. Chem. Soc.*, 138, 14890–14904 (https://doi.org/10.1021/jacs.6b05692).

[51] Ryabchuk P., Agapova A., Kreyenschulte C., *et al.* (2019), Heterogeneous nickel-catalysed reversible, acceptorless dehydrogenation of *N*-heterocycles for hydrogen storage, *Chem. Commun.*, 55, 4969–4972 (https://doi.org/10.1039/C9CC00918C).

[52] Cui X., Li W., Junge K, *et al.* (2020), Selective Acceptorless Dehydrogenation of Primary Amines to Imines by Core–Shell Cobalt Nanoparticles, *Angew. Chem. Inter. Ed.*, 59, 7501–7507 (https://doi.org/10.1002/anie.201915526).

[53] Kawahara R., Fujita K., Yamaguchi R. (2012), Dehydrogenative Oxidation of Alcohols in Aqueous Media Using Water-Soluble and Reusable Cp*Ir Catalysts Bearing a Functional Bipyridine Ligand, *J. Am. Chem. Soc.*, 134, 3643–3646 (https://doi.org/10.1021/ja210857z).

[54] Fujita K., Tamura R., Tanaka Y., *et al.* (2017), Dehydrogenative Oxidation of Alcohols in Aqueous Media Catalyzed by a Water-Soluble Dicationic Iridium Complex Bearing a Functional *N*-Heterocyclic Carbene Ligand without Using Base, *ACS Catal.*, 7, 7226–7230 (https://doi.org/10.1021/acscatal.7b02560).

[55] Pan B., Liu B., Yue E., *et al.* (2016), A Ruthenium Catalyst with Unprecedented Effectiveness for the Coupling Cyclization of γ-Amino Alcohols and Secondary Alcohols, *ACS Catal.,* 6, 1247–1253 (https://doi.org/10.1021/acscatal.5b02638).

[56] Wang Z., Pan B., Liu Q., *et al.* (2017), Efficient acceptorless dehydrogenation of secondary alcohols to ketones mediated by a PNN-Ru(II) catalyst, *Catal. Sci. Technol.,* 7, 1654–1661 (https://doi.org/10.1039/C7CY00342K).

[57] Cherepakhin V., Williams T. J. (2018), Iridium Catalysts for Acceptorless Dehydrogenation of Alcohols to Carboxylic Acids: Scope and Mechanism, *ACS Catal.,* 8, 3754–3763 (https://doi.org/10.1021/acscatal.8b00105).

[58] Musa S., Fronton S., Vaccaro L., Gelman D. (2013), Bifunctional Ruthenium(II) PCP Pincer Complexes and Their Catalytic Activity in Acceptorless Dehydrogenative Reactions, *Organometallics,* 32, 3069–3073 (https://doi.org/10.1021/om400285r).

[59] Luque-Urrutia J. A., Pèlachs T., Solà M., Poater A. (2021), Double-Carrousel Mechanism for Mn-Catalyzed Dehydrogenative Amide Synthesis from Alcohols and Amines, *ACS Catal.,* 11, 6155–6161 (https://doi.org/10.1021/acscatal.1c00693).

[60] Khalafi-Nezhad A., Panahi F. (2014), Ruthenium-Catalyzed Synthesis of Benzoxazoles Using Acceptorless Dehydrogenative Coupling Reaction of Primary Alcohols with 2-Aminophenol under Heterogeneous Conditions, *ACS Catal.,* 4, 1686–1692 (https://doi.org/10.1021/cs5000872).

[61] Bhattacharyya D., Sarmah B. K., Nandi S., *et al.* (2021), Selective Catalytic Synthesis of α-Alkylated Ketones and β-Disubstituted Ketones via Acceptorless Dehydrogenative Cross-Coupling of Alcohols, *Org. Lett.,* 23, 869–875 (https://doi.org/10.1021/acs.orglett.0c04098).

[62] He X., Li Y., Fu H., *et al.* (2019), Synthesis of Unsymmetrical N-Heterocyclic Carbene–Nitrogen–Phosphine Chelated Ruthenium(II) Complexes and Their Reactivity in Acceptorless Dehydrogenative Coupling of Alcohols to Esters, *Organometallics*, 38, 1750–1760 (https://doi.org/10.1021/acs.organomet.9b00071).

[63] Gunanathan C., Milstein D. (2014), Bond Activation and Catalysis by Ruthenium Pincer Complexes, *Chem. Rev.*, 114, 12024–12087 (https://doi.org/10.1021/cr5002782).

[64] Sindhuja E., Ramesh R. (2014), Direct synthesis of imines from primary alcohols and amines using an active ruthenium(II) NNN–pincer complex, *Tetrahedron Lett.*, 55, 5504–5507 (https://doi.org/10.1016/j.tetlet.2014.08.035).

[65] Eizawa A., Nishimura S., Arashiba K., *et al.* (2018), Synthesis of Ruthenium Complexes Bearing PCP-Type Pincer Ligands and Their Application to Direct Synthesis of Imines from Amines and Benzyl Alcohol, *Organometallics*, 37, 3086–3092 (https://doi.org/10.1021/acs.organomet.8b00465).

[66] Santoro F., Psaro R., Ravasio N., Zaccheria F. (2013), *N*-Alkylation of amines through hydrogen borrowing over a heterogeneous Cu catalyst, *RSC Adv.*, 4, 2596–2600 (https://doi.org/10.1039/C3RA44364G).

[67] Babón J. C., Esteruelas M. A., Fernández I., *et al.* (2020), Dihydroboration of Alkyl Nitriles Catalyzed by an Osmium-Polyhydride: Scope, Kinetics, and Mechanism, *Organometallics*, 39, 3864–3872 (https://doi.org/10.1021/acs.organomet.0c00582).

[68] Tang C.-H., He L., Liu Y.-M., *et al.* (2011), Direct One-Pot Reductive *N*-Alkylation of Nitroarenes by using Alcohols with Supported Gold Catalysts, *Chem. Eur. J.*, 17, 7172–7177 (https://doi.org/10.1002/chem.201100393).

[69] Peña-López M., Neumann H., Beller M. (2016), (Enantio)selective Hydrogen Autotransfer: Ruthenium-Catalyzed Synthesis of Oxazolidin-2-ones from Urea and Diols, *Angew. Chem. Inter. Ed.*, 55, 7826–7830 (https://doi.org/10.1002/anie.201600698).

[70] Pan Y., You Y., He D., *et al.* (2020), Asymmetric Synthesis of γ-Secondary Amino Alcohols via a Borrowing-Hydrogen Cascade, *Org. Lett.*, 22, 7278–7283 (https://doi.org/10.1021/acs.orglett.0c02614).

[71] Huang M., Liu J., Li Y., *et al.* (2021), Recent advances on *N*-heterocyclic carbene transition metal complexes for dehydrogenative catalysis using alcohols, *Catalysis Today*, 370, 114–141 (https://doi.org/10.1016/j.cattod.2020.10.022).

[72] Eizawa A., Nishimura S., Arashiba K., *et al.* (2018), Synthesis of Ruthenium Complexes Bearing PCP-Type Pincer Ligands and Their Application to Direct Synthesis of Imines from Amines and Benzyl Alcohol, *Organometallics*, 37, 3086–3092 (https://doi.org/10.1021/acs.organomet.8b00465).

[73] Saha B., Wahidur Rahaman S. M., Daw P., *et al.* (2014), Metal–Ligand Cooperation on a Diruthenium Platform: Selective Imine Formation through Acceptorless Dehydrogenative Coupling of Alcohols with Amines, *Chem. Eur. J.*, 20, 6542–6551 (https://doi.org/10.1002/chem.201304403).

[74] Priecel P., Lopez-Sanchez J. A. (2019), Advantages and Limitations of Microwave Reactors: From Chemical Synthesis to the Catalytic Valorization of Biobased Chemicals, *ACS Sustainable Chem. Eng.*, 7, 3–21 (https://doi.org/10.1021/acssuschemeng.8b03286).

[75] Rathi A. K., Gawande M. B., Zboril R., Varma R. S. (2015), Microwave-assisted synthesis – Catalytic applications in aqueous

media, *Coord. Chem. Rev.*, 291, 68–94 (https://doi.org/10.1016/j.ccr.2015.01.011).

[76] Kokel A., Schäfer C., Török B. (2017), Application of microwave-assisted heterogeneous catalysis in sustainable synthesis design, *Green Chem.*, 19, 3729–3751 (https://doi.org/10.1039/C7GC01393K).

[77] Danopoulos A. A., Braunstein P., Saßmannshausen J., *et al.* (2020), "Pincer" Pyridine–Dicarbene–Iridium and -Ruthenium Complexes and Derivatives Thereof, *Eur. J. Inorg. Chem.*, 2020, 3359–3369 (https://doi.org/10.1002/ejic.202000429).

[78] Peris E., Loch J.A., Mata J., Crabtree R. H. (2001), A Pd complex of a tridentate pincer CNC bis-carbene ligand as a robust homogenous Heck catalyst, *Chem. Commun.*, 201–202 (https://doi.org/10.1039/B008038L).

[79] Poyatos M., Mata J. A., Falomir E., *et al.* (2003), New Ruthenium(II) CNC-Pincer Bis(carbene) Complexes: Synthesis and Catalytic Activity, *Organometallics*, 22, 1110–1114 (https://doi.org/10.1021/om020817w).

[80] Danopoulos A. A., Winston S., Motherwell W. B. (2002), Stable *N*-functionalised 'pincer' bis carbene ligands and their ruthenium complexes; synthesis and catalytic studies, *Chem. Commun.*, 1376–1377 (https://doi.org/10.1039/B202814J).

[81] Yadav D., Misra S., Kumar D., *et al.* Cationic ruthenium(II)–NHC pincer complexes: Synthesis, characterisation and catalytic activity for transfer hydrogenation of ketones, *Appl. Organomet. Chem.*, 35, e6287 (https://doi.org/10.1002/aoc.6287).

[82] Eizawa A., Nishimura S., Arashiba K., *et al.* (2018), Synthesis of Ruthenium Complexes Bearing PCP-Type Pincer Ligands and Their Application to Direct Synthesis of Imines from Amines and

Benzyl Alcohol, *Organometallics*, 37, 3086-3092 (https://doi.org /10.1021/acs.organomet.8b00465).

[83] Li H., Lupp D., Das P. K., *et al.* (2021), Redox-Neutral Imination of Alcohol with Azide: A Sustainable Alternative to the Staudinger/Aza-Wittig Reaction, *ACS Catal.*, 11, 4071–4076 (https://doi.org/10.1021/acscatal.1c00379).

[84] Yu J., Liu Q., Qiao W., *et al.* (2021), Catalytic Role of Metal Nanoparticles in Selectivity Control over Photodehydrogenative Coupling of Primary Amines to Imines and Secondary Amines, *ACS Catal.*, 11, 6656–6661 (https://doi.org/10.1021/acscatal.1c01519).

Chapter 5

Role of Ancillary Ligands in Selectivity for Catalytic Applications

5.1 Introduction

Transition metal pincer complexes have attracted great attention because of their vast application in organic transformations.*[1,2]* Pincer complexes exhibit high thermal stability, robust nature, and variable oxidation states which proves them a significant catalyst for high temperature and pressure reactions without catalyst decomposition.*[3,4]* A large number of commercially available organometallic precatalysts and ligands have been developed till now, because of their tendency to synthetically alter the ligand additives for catalysis.*[5–14]* *N*-heterocyclic carbenes (NHCs) are the common class of ligand additives that have been employed as organocatalysts and also used in a wide range of catalytic processes with transition metals and Group 13 elements.*[15,16]* NHCs are readily available as stable salts with a variety of *N*-substituents, central ring size, and central ring functionalization, making them versatile ligands to carry out several reactions.*[17,18]*

Among the variety of pincer ligands, CNC pincer ligands have become gradually popular due to the increase the electron density at the coordinated metal as well as enhance the reactivity of the metal centre.*[19–22]* Additionally, the development of ligand construction with NHCs, in comparison to other functional groups gave an opportunity to tune the catalytic activity. Furthermore, the advantage of combining steric and electronic effects with pincer ligands has led to the construction of ruthenium pincer complexes, with a wide variety of applications in catalysis.*[1,23]*

Hydrogenation and transfer hydrogenation of carbonyl compounds by ruthenium complexes are industrially accepted processes

to produce alcohols via H_2 or isopropanol as reducing agents rather than $NaBH_4$ and $LiAlH_4$.*[12–14,24–27]* Metal complexes give high control of selectivity with atom economy than the classical methods, which makes this approach a viable pathway for carbonyl compound reduction in organic synthesis.

Likewise, dehydrogenation reactions are also one of the most fundamental transformations in organic chemistry reactions to synthesize aldehydes or ketones.*[6,28–31]* Typically, stoichiometric or excess of additional oxidants is used for conventional dehydrogenation operations. on the other hand, acceptorless dehydrogenation reaction is an atom-efficient and ecologically friendly technique for alcohol dehydrogenation. Subsequently, dehydrogenative coupling of alcohols and amines, imines are formed *[32–35]* which is used as electrophilic reagents in a variety of processes, including additions, condensations, multi-component reactions, asymmetric organocatalysis, cross-dehydrogenative couplings, and cycloadditions. Because of their high reactivity, they have been employed in synthetic, biological, medicinal, and industrial applications as nitrogen sources. Several metal complexes were investigated for these transformations,*[10,11,36–38]* with some limitations, therefore, synthesis of selective catalyst is desirable at present.

Wing-tip substituents on the *N*-heterocyclic carbene can modulate the steric environment around the central metal atom. This is an important structural feature of CNC-based metal complexes. Therefore, we have explored the CNC pincer ligands with smaller wingtips at *N*-heterocycle. We report herein the synthesis, structure and catalytic activity of Ru(II)-CNC complexes, namely $[Ru(CNC^{iPr})(CO)(PPh_3)Cl]X$ [X = Cl^- (**7a**), PF_6^- (**7b**)], $[Ru(CNC^{iPr})(PPh_3)_2Cl]X$ [X = Cl^- (**8a**), PF_6^- (**8b**)] and $[Ru(CNC^{iPr})(DMSO)_2Cl]X$ [X = Cl^- (**10a**) and PF_6^- (**10b**)].

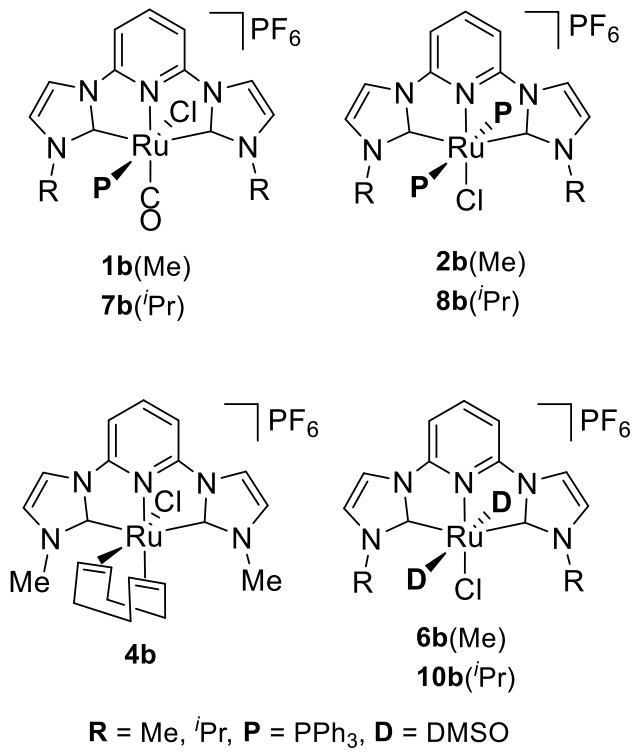

Figure 5.1 Cationic Ru(II)-CNC pincer complexes in this study.

The comparative reactivities of complexes **7b**, **8b**, and **10b** with our previously synthesized *N*-methyl complexes **1b**, **2b**, **4b,** and **6b** (Figure **5.1**) have been investigated for the transfer hydrogenation of cyclohexanone, acceptorless dehydrogenation of benzyl alcohol and acceptorless dehydrogenative coupling of benzyl alcohol with aniline, respectively.

5.2 Results and Discussion

5.2.l Synthesis of CNC pincer ruthenium complexes

The imidazolium ligand precursor **CNC^{iPr}·2HBr** was easily synthesized by the reported procedure in literature *[39]* in gram-scale and characterised by ^{1}H. The synthesis of new metal complexes done using our previously optimised method, in which treatment of imidazolium precursor with Ag_2O, in methanol, promptly affords the silver-carbene complex, followed by transmetallation with Ru-precursors *in situ* to afford Ru-CNC complexes (Scheme **5.1**). The disappearance of the imidazolium proton peak at 10.72 ppm in the ^{1}H NMR spectrum of

ligand precursor **CNC^{iPr}·2HBr** indicated the carbene generation during complex formation.

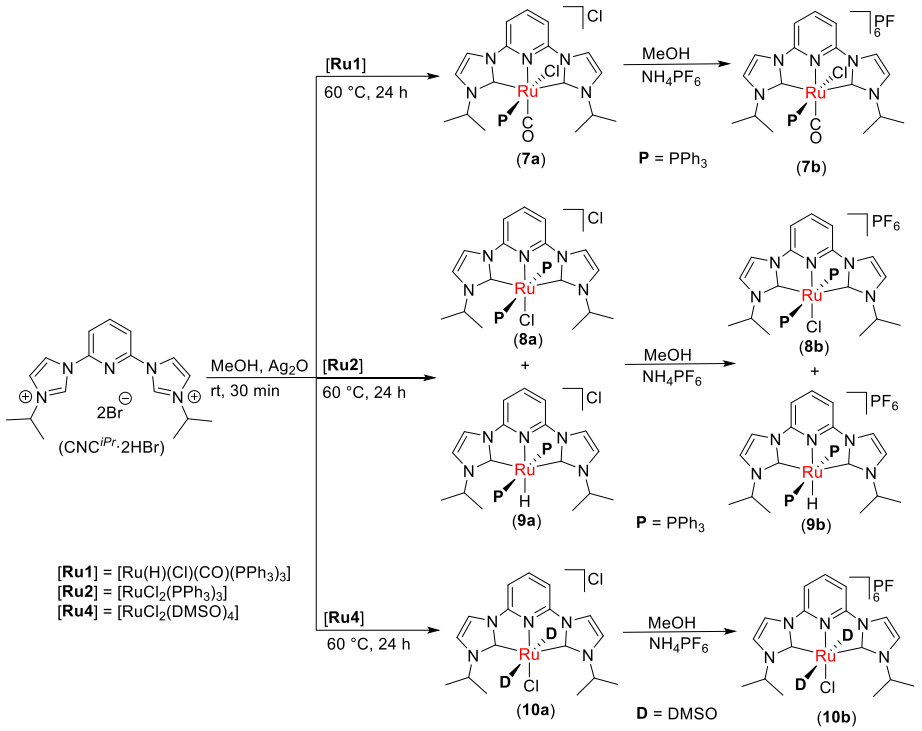

Scheme 5.1 Synthesis of CNC pincer ruthenium complexes **7–10**.

The reaction of the silver-carbene complex with the [RuHCl(CO)(PPh$_3$)$_3$] precursor (**Ru1**) for 24 h, gave **7a**. Compound **7b** was precipitated out by treating **7a** with NH_4PF_6 in methanol. ^{1}H NMR of **7b** showed signals as a doublet at 8.46 and a triplet at 8.21 ppm for the pyridine protons, while two doublets are observed at 7.82 and 7.70 ppm for the imidazol-2-ylidene protons. Isopropyl protons come at 4.70 ppm for C-H protons and 1.49, 1.35 and 1.31 ppm for attached CH_3 protons, respectively. In the ^{13}C NMR spectra, the carbene carbon signal of **7b** appears at 188 ppm. ^{31}P NMR spectrum of **7b** showed peaks at 49.01 ppm for PPh_3 ligand which is slightly higher than our previously reported CNC pincer complexes.*[40]*

Alternatively, **8a** is prepared by the same reaction condition as **7a** rather than [RuCl$_2$(PPh$_3$)$_3$] is used as the Ruthenium source (**Ru2**). Though, during the synthesis of compound **8a**, **9a** is also generated *in situ* as like our methyl *N*-methyl analogous complexes. Later,

compounds **8a** and **9a** were purified by using alumina gel column chromatography.

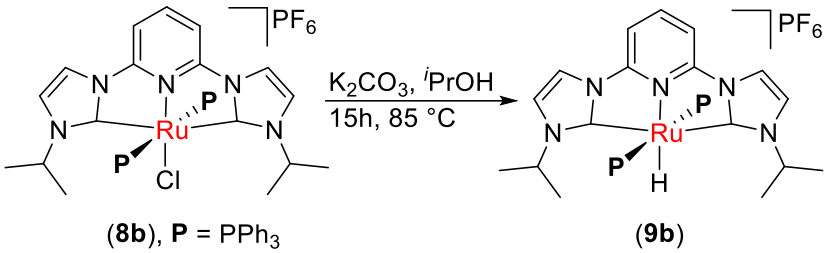

Scheme 5.2 Synthesis of CNC pincer ruthenium complex **9b** from **8b.**

Spectroscopically pure **8a** was isolated by recrystallization. Furthermore, anion exchange with NH_4PF_6 gives **8b**. Compound **8b** show ESI^+ LC-MS signal at *m/z* 956.14, assigned to [**8b-Cl**]$^+$. In ^1H NMR of **8b**, imidazol-2-ylidene protons were shown as two doublets at 10.41 and 8.26 ppm whereas, one doublet and triplet appear at 8.84 and 8.60 ppm for pyridine protons. ^{31}P NMR spectra of complex **8b** show two singlets at 28.38 ppm and 20.69 ppm, while no dissociation of PPh_3 was observed. Complex **8b** is expected to exhibit one singlet in the ^{31}P NMR considering the same chemical environment for the two phosphorus atoms. These two singlets in the ^{31}P NMR are attributed to the generation of two species in solution due to dissociation of the coordinated PPh_3 ligand. This assumption is confirmed by mass analysis where ESI^+ LC-MS signal at *m/z* 694.14 is observed and assigned to [**8b-PPh3**]$^+$. Furthermore, on treatment with K_2CO_3 in isopropanol, the mixture of complexes **8b** and **9b** can be converted to **9b**, as shown in scheme **5.2**.

Followed by a similar reaction condition, **10a** was also synthesized from [$RuCl_2(DMSO)_4$] as the Ruthenium source (**Ru3**). Pure **10a** was obtained by precipitation followed by recrystallization of the crude reaction mixture. Furthermore, anion exchange with NH_4PF_6 gives **10b**. Compound **10b** show ESI^+ LC-MS signal at *m/z* 588.08 and 510.06, assigned to [**10b-Cl**]$^+$ and [**10b-DMSO**]$^{+,}$ respectively. In ^1H NMR of **10b**, one doublet and triplet appear at 8.61 and 8.25 ppm for pyridine protons whereas, imidazol-2-ylidene protons were shown as

two doublets at 8.03 and 7.96 ppm, which is slightly shifted to lower ppm than the respective analogous complexes **7b** and **8b**, respectively. Isopropyl protons come at 5.54 ppm for C-H protons and 1.53 ppm for attached CH_3 protons, respectively. In the ^{13}C NMR spectra, the carbene carbon signal of **10b** appears at 183 ppm.

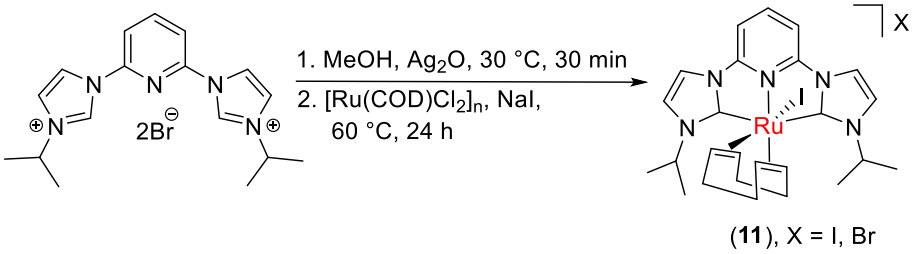

Scheme 5.3 Synthesis of CNC-COD pincer ruthenium complex.

Several attempts were also made for synthesizing Ru-COD pincer complex by using Ru precursor $[RuCl_2(COD)]_n$ (Scheme **5.3**) Although mass spectrogram indicates the formation of the desired complex, dissociation of COD ligand was also observed, which was not observed in our previously synthesized analogous Ru-COD pincer complex.*[41]* This is probably due to the steric hindrance of the *N*-isopropyl which is somewhat bulkier than the *N*-methyl. We were not able to successfully isolate the complex probably due to the dissociation of COD ligand from the desired complex and subsequent decomposition (Figure **5.20**).

5.2.2 Description of the crystal structures

The molecular structures of complexes **9a** and **10a** are confirmed by X-ray crystal diffraction analysis. Complexes **9a** (Figure **5.2**) and **10a** (Figure **5.3**) crystallised in a monoclinic system with a *P*21/c space group, respectively. The ruthenium metal centre in both complexes displays distorted octahedral geometry. Selected bond lengths and angles of complexes **9a** and **10a** are listed in table **5.5**.

The molecular structure of **9a** consists of a six-coordinate Ru (II) centre with one CNC pincer ligand, two triphenylphosphines, and one hydride (Figure **5.2**). The two bulky triphenylphosphines are situated

trans to each other. The N3-Ru1-C10 bite angle is 77.7(3)° and comparable to our previously reported complexes. The bond distances of Ru1-C1 (2.015(7) Å and Ru1-C11 (2.045(7) Å was slightly shorter than the previously reported complex (with chloride) (2.052 (6) Å) and (2.094 (7) Å, respectively. The Ru-P (Ru1-P1, 2.3502 (18) Å and Ru1-P2, 2.3334(19) Å) bonds in the case of **9a** are slightly shorter than the previously reported complex (with chloride) (Ru1-P1, 2.370(1) Å and Ru1-P2, 2.359(1) Å).*[40]*

The molecular structure of **10a** has distorted octahedral geometry, consists of a six-coordinate Ru(II) centre with two dimethyl sulphoxide *trans* to each other, one chloride ion trans to the pyridine nitrogen atom, and a CNC pincer ligand (Figure **5.3**). One chloride ion is present in the lattice. The CNC pincer ligand occupies three meridional sites with a C1-Ru1-C10 angle of 101.34 (13) shorter than the previously reported complexes 152.3 (4).*[19,40,41]* The bite angle (N3-Ru1-C10) of 77.99(17)° is similar to the complex reported by Peris *et. al.[19]* and our previously reported complexes. The bond distances of Ru1-C1 (2.073(5) and Ru1-C11 (2.062(5) Å are comparable to the reported ruthenium NHC carbene complexes 2.056(5) Å and 2.062(5) Å and (2.051(9) Å and (2.085(9) Å.*[19,40]*

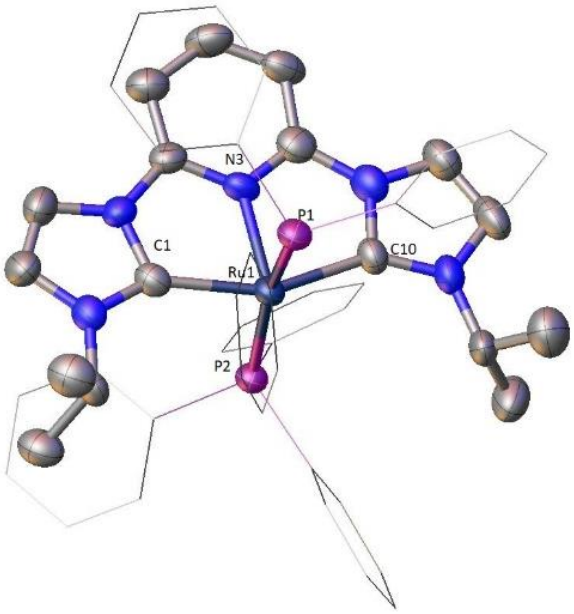

Figure 5.2 Molecular structure of **9a** with thermal ellipsoids drawn at the 50% level. All hydrogen atoms and one chloride counter-anion are omitted for clarity. Selected bond lengths (Å) and angles (°): Ru1-N1, 2.052(6), Ru1-C1, 2.015(7); Ru1-C11, 2.045(7); Ru1-P1, 2.3502(18); Ru1-P2, 2.3334(19)N1-Ru1-P1, 100.71(18); C11-Ru1-P1, 94.5(2).

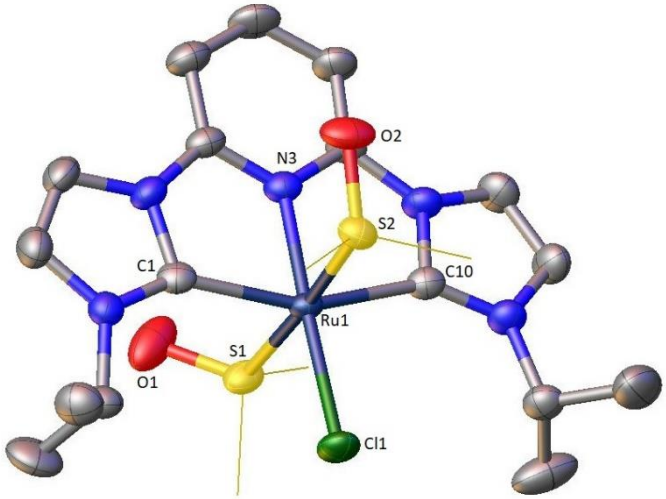

Figure 5.3 Molecular structure of **10a** with thermal ellipsoids drawn at the 50% level. All hydrogen atoms and one chloride counter-anion are omitted for clarity. Selected bond lengths (Å) and angles (°): Ru1-N1, 1.996(4), Ru1-C1, 2.073(5); Ru1-C11, 2.062(5); Ru1-S1, 2.2936(11); Ru1-S2, 2.3130(12); Ru1-Cl1, 2.4300(11); C1-Ru1-C11, 101.34(13); N1-Ru1-C1, 77.99(17); N1-Ru1-S1, 89.79(11); N1-Ru1-S2, 89.28(11); C10-Ru1-S1, 91.83(12); C1-Ru1-Cl1, 97.80(19); N1-Ru1-Cl1, 101.34(13).

Table 5.4 Crystal data and structural refinement parameters for **9a** and **10a**

	9a	**10a**
Empirical formula	$C_{53}H_{51}N_5P_2Ru$	$C_{21}H_{39}Cl_2N_5O_5RuS_2$
T/K	300	300
Crystal System	Monoclinic	Monoclinic
Space Group	$P2_1/n$	$P2_1/c$
a/ Å	12.3384(3)	11.3897(2)
b/Å	26.5703(15)	11.0142(2)
c/Å	14.8808(6)	24.3549(5)
α/º	90	90
β/°	92.582(3)	96.689(2)
γ/°	90	90
V/Å³	4873.5(4)	3034.49(10)
Z	4	4
Reflections Collected/unique	21984/9229	13716/5766
R (int)	0.0908	0.0825
Final R indices [I>2σ(I)]	R1 = 0.1032 wR2 = 0.2955	R1 = 0.0756 wR2 = 0.1989
R indices (all data)	R1 = 0.1253 wR2 = 0.3274	R1 = 0.0814 wR2 = 0.2083
GOF on F2	1.162	1.014

5.2.2 Catalytic application in transfer hydrogenation of cyclohexanone

The ruthenium complexes **7b**, **8b**, and **10b** have been investigated for the reduction of cyclohexanone via transfer hydrogenation (TH) with isopropanol in the presence of a base. The reaction was monitored by gas chromatography with n-decane as an internal standard. Using 2 mmol of cyclohexanone, 1 mol% of catalyst, and 1 equivalent of sodium iso-propoxide (NaO^iPr) as base complex **7b** (81%) showed higher catalytic activity than other complexes viz: **8b** and **10b** (64 and 70%, respectively, Table **5.1**, entries 5, 6 and 7) while, lower than the

previously synthesized *N*-methyl complex **1b** (>99%, Table **5.1**, entry 1). Complexes **2b**, **4b** and **6b** gave 61, 80 and 56%, conversions, respectively (Table **5.1**, entries 2, 3 and 4). Catalyst **11b** is *in situ* generated from $[RuCl_2(COD)]_n$+CNC^{iPr}2PF_6 in catalysis reaction conditions and gave 54% conversion (Table **5.1**, entry 8).

Table 5.1 Transfer hydrogenation with different catalysts

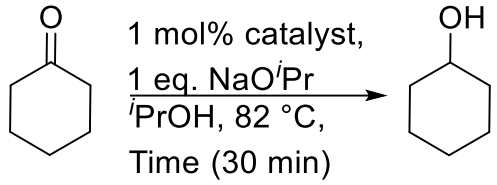

[a]Entry	Catalyst	Ancillary ligand (L) & *N*-wingtip (R)	Conversion[b] (%)	TON[c]/TOF[d] (h^{-1})
1.	**1b**[e]	L = CO R = Me	>99	99/198
2.	**2b**[e]	L = PPh_3 R = Me	61	61/122
3.	**4b**[e]	L = COD R = Me	80	80/160
4.	**6b**[e]	L = DMSO R = Me	56	56/112
5.	**7b**	L = CO R = ^{i}Pr	81	81/162
6.	**8b**	L = PPh_3 R = ^{i}Pr	64	64/128
7.	**10b**	L= DMSO	70	70/140

		R = ^{i}Pr		
8.	**11b**[f]	L = COD R = ^{i}Pr	54	54/108

[a]Reaction conditions: Cyclohexanone (2.0 mmol), Catalyst (1 mol%), NaO^{i}Pr (1 eq.), ^{i}PrOH (5 mL), at 82 ^{o}C under a slow N_2 flow. [b]Determined by gas chromatography with n-decane as an internal standard. [c]TON = (Number of moles of substrate converted)/(Number of moles of catalyst), at the end of the reaction. [d]TOF = [(TON)/ hour]. [e]*[40, 41]*. [f]*In situ* generated from $[RuCl_2(COD)]_n$+CNC^{iPr}2PF_6.

We assume that, with *N*-isopropyl, the catalytic performance will increase, but it does not give the expected reactivity. This decrease in reactivity is probably due to the steric hindrance at the ruthenium centre, which is not allowed to substrate to approach efficiently as like with *N*-methyl. The steric factor is dominating here rather than the electronic factor with isopropyl *N*-isopropyl complexes. As a result, ruthenium complex **1b** with methyl *N*-methyl (1 mol%) as catalyst and NaO^{i}Pr as a base in isopropanol under reflux temperature was more efficient than its respective newly synthesized *N*-isopropyl analogous complexes.

5.2.3 Catalytic application in acceptorless dehydrogenation of benzyl alcohol

After transfer hydrogenation, dehydrogenation of benzyl alcohol was also examined to investigate the applicability of complexes **7b, 8b** and **10b** for catalytic AAD reactions. Complexes **7b** and **10b** in toluene in the presence of KO^{t}Bu at 110 °C for 3h afforded >99% conversion to benzaldehyde (Table **5.2**, entries 5 and 7) while, complex **8b** gave much lower conversion, 38% (Table **5.2**, entry 6). The observed catalytic trend is also similar with the analogous *N*-methyl complexes, where CO containing complex **1b** shows higher conversion >99% (Table **5.2**, entry 1) than the PPh_3 (**2b,** 47%, Table **5.2**, entry 2) and DMSO (**6b,** 60%, Table **5.2**, entry 4) complexes, respectively.

Table 5.2 Acceptorless dehydrogenation of benzyl alcohol with different catalysts

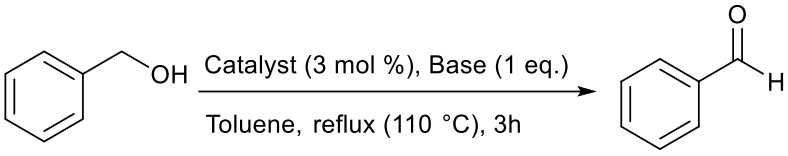

[a]Entry	Catalyst	Ancillary ligand (L) & *N*-wingtip (R)	Conversion[b] (%)	TON[c]/TOF[d] (h^{-1})
1.	**1b**	L = CO R = Me	>99	33/11
2.	**2b**	L = PPh_3 R = Me	47	15/5
3.	**4b**	L = COD R = Me	89	29/10
4.	**6b**	L = DMSO R = Me	60	20/6
5.	**7b**	L = CO R = ^{i}Pr	>99	33/11
6.	**8b**	L = PPh_3 R = ^{i}Pr	38	12/4
7.	**10b**	L= DMSO R = ^{i}Pr	>99	33/11
8.	**11b**[e]	L = COD R = ^{i}Pr	8	3/0.8

[a]Reaction conditions: Benzyl alcohol (1 mmol), Catalyst (3 mol %), KO^{t}Bu (1 eq.), Toluene (5 mL) under a slow N_2 flow at 110 ^{o}C for 3h. [b]Determined by gas chromatography without an internal standard. [c]TON = [(Number of moles of substrate converted)/(Number of moles of catalyst)] at the end of the reaction. [d]TOF = [(TON)/hour]. [e]*In situ* generated from $[RuCl_2(COD)]_n$+CNC^{iPr}2PF_6.

The observed catalytic performance is owing to the higher trans effect of CO than PPh_3 and DMSO, but in the case of *N*-isopropyl, DMSO complex also gave >99% conversion (Table **5.2**, entry 7), due to the steric effect of *N*-isopropyl along with trans effect. In situ generated ruthenium COD catalyst (**11b**) performs very poor (Table **5.2**, entry 8), probably because of lower solubility of ligand and metal precursor in toluene, therefore generation of precatalyst was not so feasible.

5.2.4 Catalytic application in acceptorless dehydrogenative coupling of benzyl alcohol and aniline

The acceptorless dehydrogenative coupling (ADC) of aniline with benzyl alcohol was explored, resulting in imine synthesis. In a comparison of all the synthesized ruthenium complexes, it was observed that the Ru-complexes with *N*-isopropyl performs better than Ru-complexes with *N*-methyl for the ADC of alcohols and amines.

Table 5.3 Dehydrogenative coupling of benzyl alcohol and aniline with different catalysts

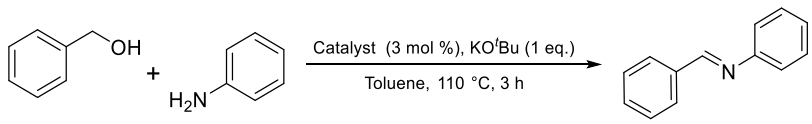

Entry[a]	Catalyst	Ancillary ligand (L) & *N*-wingtip (R)	Conversion[b] (%)	TON[c]/TOF[d] (h^{-1})
1.	**1b**	L = CO R = Me	60	20/6

2.	**2b**	L = PPh_3 R = Me	68	22/7
3.	**4b**	L = COD R = Me	71	23/8
4.	**6b**	L = DMSO R = Me	97	32/10
5.	**7b**	L = CO R = ^{i}Pr	90	29/10
6.	**8b**	L = PPh_3 R = ^{i}Pr	96	31/10
7.	**10b**	L= DMSO R = ^{i}Pr	92	30/10

[a]Reaction conditions: Aniline (1 mmol), Benzyl alcohol (1 mmol), Catalyst (3 mol %), KO^{t}Bu (1 eq.), Toluene (5 mL) under a slow N_2 flow at 110 ^{o}C for 3h. [b]Determined by gas chromatography with n-decane as an internal standard. [c]TON = [(Number of moles of substrate converted)/(Number of moles of catalyst)] at the end of the reaction. [d]TOF = [(TON)/hour].

Although ruthenium complexes with PPh_3 and DMSO as a co-ligand shows higher conversions of 96 and 92%, respectively (Table **5.3**, entries 4, 6 and 7) than the other analogous complex, CO as a co-ligand (Table **5.3**, entries 1 and 5). The remarkable reverse trend in catalytic activity indicates involvement of the Ru-metal centre in the dehydrogenative coupling step as, otherwise, the catalyst better at alcohol dehydrogenation (CO and COD as a co-ligand) should also have been better at the imine formation.

5.4 Conclusions

In summary, a straightforward synthesis of a series of pincer ruthenium complexes viz: [Ru(CNC^{iPr})(CO)(PPh$_3$)Cl]X [X = Cl$^-$ (**7a**), PF$_6^-$ (**7b**)], [Ru(CNC^{iPr})(PPh$_3$)$_2$Cl]X [X = Cl$^-$ (**8a**), PF$_6^-$ (**8b**)], [Ru(CNC^{iPr})(PPh$_3$)$_2$(H)]X [X = Cl$^-$ (**9a**), PF$_6^-$ (**9b**)] and [Ru(CNC^{iPr})(DMSO)$_2$(Cl)]X [X = Cl$^-$ (**10a**), PF$_6^-$ (**10b**)] reported from a "pyridine-dicarbene" pincer ligand. These complexes were found catalytically active for the transfer hydrogenation of cyclohexanone, acceptorless dehydrogenation of benzyl alcohol and dehydrogenative coupling of benzyl alcohol and aniline, respectively. The in-situ transformations of these complexes during their synthesis were also observed, which helps in understanding their behaviour during catalytic transformations. Complexes containing CO and COD proved to be better catalysts for transfer hydrogenation and acceptorless dehydrogenation reactions, whereas complexes with PPh$_3$ and DMSO showed more efficiency for imine synthesis under the optimised conditions, respectively.

5.5 Experimental

5.5.1 General procedure

All reactions were carried out under an inert atmosphere using the standard Schlenk technique. Solvents were purchased from S. D. Fine-Chem Limited and purified by distillation under an inert atmosphere. [RuHCl(CO)(PPh$_3$)$_3$],*[42]* [RuCl$_2$(PPh$_3$)$_3$],*[43]* [RuCl$_2$(DMSO)$_4$],*[44]* and [RuCl$_2$(COD)]$_n$ *[45]* were prepared by following the literature procedure using RuCl$_3$·3H$_2$O. Deuterated dimethyl sulphoxide was purchased either from EURISOtop or Aldrich Chemical Co. NMR spectra were taken on Bruker Avance (III) spectrometer operating at 400 MHz (^{1}H), 162 MHz (^{31}P), and 100 MHz (^{13}C). NMR chemical shifts are reported in ppm and referenced to the solvent peaks for ^{1}H (DMSO-d^6, δ 2.54 ppm) and ^{13}C (natural abundance of ^{13}C in DMSO-d^6, δ 40.45 ppm) NMR. ^{31}P NMR chemical shifts are referenced to an external 85% H$_3$PO$_4$ standard as 0 ppm. The mass chromatograms were recorded on

Bruker-Daltonics-microTOF-QII mass spectrometer. GC Samples were analysed in Shimadzu QP2010 Ultra, with an internal standard.

Synthesis of [Ru(CNC^{iPr})(CO)(PPh$_3$)Cl]PF$_6$, 7b

An oven dried Schlenk tube with the magnetic stirring bar was charged with the ligand precursor **CNC^{iPr}·2HBr** (0.227 g, 0.5 mmol) and dried under vacuum at 100 ˚C for 2 hours. The Schlenk tube was cooled to room temperature under N_2 atmosphere. Dry methanol (10 mL) was added, followed by Ag_2O (0.115 g, 0.5 mmol) and stirred at room temperature in the dark, covered with aluminium foil. After 30 min, a white precipitate had formed, and [RuHCl(CO)(PPh$_3$)$_3$] (0.475 g, 0.5 mmol) was added to the reaction mixture. The reaction mixture was heated at 60 ˚C for 24 h, which results in a brown colour solution with some residue. The reaction mixture was filtered through celite, and the filtrate was reduced in volume (2 mL) followed by the addition of diethyl ether (5 mL). The compound precipitated out as yellowish brown solid. The resulting precipitate was dissolved in 2 mL of methanol, add 1 equivalent NH_4PF_6 and stirred for 30 min at room temperature. A yellow precipitate of **7b** slowly comes out on cooling at 4 ˚C. Yield: 0.180 g (40 %). ^{1}H NMR (DMSO-d^6, 500MHz, δ in ppm): δ 8.46 (d, *J* = 6.4 Hz, 2H), 8.21 (t, *J* = 7.8 Hz, 1H), 7.82 (d, *J* = 4.1 Hz, 2H), 7.70 (d, *J* = 8.1 Hz, 2H), 7.44 (t, *J* = 7.6 Hz, 3H), 7.34 (t, *J* = 7.7 Hz, 6H), 6.96 (t, *J* = 9.4 Hz, 6H), 4.70 (dh, *J* = 13.1, 6.6 Hz, 2H), 1.49 (t, *J* = 7.4 Hz, 6H), 1.35 (d, *J* = 6.6 Hz, 3H), 1.31 (d, *J* = 6.8 Hz, 3H).; ^{13}C NMR (DMSO-D^6, δ in ppm): 188.83, 150.61, 144.82, 132.53, 132.38, 131.92, 131.11, 129.32, 121.08, 119.66, 107.89, 54.45, 26.24, 20.74; ^{31}P NMR (DMSO-d^6, δ in ppm): 49.01, 48.60, -144.17; LCMS: [M(Br)]$^+$- 768.02, [M(Cl)]$^+$- 722.13 [M-Cl+H] - 688.12, HRMS for [M]$^+$ [$C_{36}H_{36}BrN_5OPRu$] Calculated – 668.0878, Found – 666.0841.

Synthesis of [Ru(CNC^{iPr})(PPh$_3$)$_2$Cl]PF$_6$, 8b

Similar procedure was followed as with **7b** except [RuCl$_2$(PPh$_3$)$_3$] (0.478 g, 0.5 mmol) was added in place of [RuHCl(CO)(PPh$_3$)$_3$]. The solvent was reduced in volume (2 mL) followed by the addition of

diethyl ether (5 mL) resulting in the precipitation of compound which was filtered and dried under vacuum. Further, resulting precipitate was dissolved in 2 mL of methanol, add one equivalent of NH_4PF_6 (0.190 g, 0.11 mmol) and stirred for 30 min at room temperature. A yellowish-green precipitate of **8b** slowly comes out and on cooling at 4 ˚C some more precipitation occurred. Yield: 0.155 g (25%). ^{1}H NMR (DMSO-d^6, 500MHz, δ in ppm): δ 8.84 (d, *J* = 8.1 Hz, 2H), 8.60 (t, *J* = 8.1 Hz, 1H), 8.26 (d, *J* = 8.1 Hz, 2H), 8.26 (d, *J* = 8.1 Hz, 2H), 4.79 (p, *J* = 6.9 Hz, 2H), 1.61 (d, *J* = 6.7 Hz, 12H); ^{13}C NMR (DMSO-D^6, δ in ppm): 186.15, 154.21, 145.88, 145.14, 135.33, 133.93, 133.02, 129.35, 122.31, 120.16, 114.81, 106.68, 54.07, 22.68; ^{31}P NMR (DMSO-d^6, δ in ppm): 50.70, -144.17. LCMS: $[M]^+$ 956.14, $[M\text{-}Cl]^{2+}$ 460.60, HRMS for $[M]^+$ $[C_{53}H_{51}ClN_5P_2Ru]$ Calculated – 956.2357, Found – 956.2398.

Synthesis of $[Ru(CNC^{iPr})(PPh_3)_2H]PF_6$, 9b from 8b

Complex **8b** (0.200 g, 0.18 mmol) was taken in an oven dried Schlenk tube followed by the addition of K_2CO_3 (0.025 g, 0.18 mmol), and then ^{i}PrOH was injected via the syringe. The reaction mixture was refluxed at 85 °C for 15 h. The colour of the reaction mixture was changed from green to yellowish green. After the completion of the reaction, the mixture was filtered, and the solvent was evaporated under a reduced vacuum to afford yellowish green solid. Solid was washed with diethyl ether and dried under vacuum. The X-ray quality crystals of **9b** were obtained by slow diffusion of diethyl ether in methanol solution at -18 ˚C. Yield: 0.155 g (25%). ^{1}H NMR (DMSO-d^6, 500MHz, δ in ppm): δ 8.31 (d, 2H), 7.73 (t, *J* = 8.1 Hz, 1H), 7.48 (d, 2H), 7.43 (d, *J* = 8.1 Hz, 2H), 7.27 (t, *J* = 6.7 Hz, 6H), 7.15 (t, *J* = 7.7 Hz, 12H), 6.78 (dt, *J* = 9.0, 5.0 Hz, 12H), 4.30 (p, *J* = 6.9 Hz, 2H), 0.16 (d, *J* = 6.7 Hz, 12H), -8.66 (t, *J* = 24.5 Hz, 1H); ^{13}C NMR (DMSO-D^6, δ in ppm): 196.75, 150.28, 136.70, 135.91, 132.53, 132.04, 129.62, 129.33, 128.46, 120.29, 118.79, 104.95, 53.01, 21.40; ^{31}P NMR (DMSO-d^6, δ in ppm): 31.79, 26.60. LCMS: $[M]^+$ 922.18, HRMS for $[M]^+$ $[C_{53}H_{52}N_5P_2Ru]$ Calculated – 922.2750, Found – 922.2773.

Synthesis of [Ru(CNC^{iPr})(DMSO)$_2$Cl]PF$_6$, 10b

Similar procedure was followed as with **7a** except [$RuCl_2(DMSO)_4$] (0.241 g, 0.5 mmol) was added in place of [$RuHCl(CO)(PPh_3)_3$]. The solvent was reduced in volume (2 mL) followed by the addition of diethyl ether (5 mL) resulting in the precipitation of compound which was filtered and dried under vacuum. The X-ray quality crystals of **10a** were obtained by slow diffusion of diethyl ether in methanol solution at -18 ˚C. The resulting precipitate of **10a** (0.100 g, 0.11 mmol) was dissolved in 2 mL of methanol, add NH_4PF_6 (0.190 g, 0.11 mmol) and stirred for 30 min at room temperature. A bright yellow precipitate of **10b** slowly comes out and on cooling at 4 ˚C some more precipitation occurred. Yield: 0.034 g (29 %). ^{1}H NMR (DMSO-d^6, 400MHz, δ in ppm): δ 8.61 (d, *J* = 2.3 Hz, 2H), 8.25 (t, *J* = 8.1 Hz, 1H), 8.03 (d, *J* = 2.3 Hz, 2H), 7.96 (d, *J* = 8.2 Hz, 2H), 5.54 (p, *J* = 6.7 Hz, 2H), 2.69 (s, 9H), 2.54 (s, 3H), 1.53 (d, *J* = 6.7 Hz, 12H).; ^{13}C NMR (DMSO-D^6, δ in ppm): 183.85, 154.82, 145.91, 141.58, 135.25, 122.32, 121.49, 120.20, 114.85, 107.59, 54.10, 51.61, 49.16, 45.77, 40.93, 22.70; ^{31}P NMR (DMSO-d^6, δ in ppm):-144.18 ppm. LCMS: $[M]^+$ 588.08, $[M\text{-}DMSO]^+$ 510.06, HRMS for $[M]^+$ [$C_{21}H_{33}ClN_5O_2S_2Ru$] Calculated – 588.0803, Found – 588.0822.

5.5.2 X-ray data collection and structure refinement

Single crystal X-ray data of compounds **9a** and **10a** were collected on the Rigaku Oxford Diffractometer using graphite-monochromated Mo Kα radiation (λ = 0.7107 Å). The data collection was evaluated with the help of CrysAlisPro CCD software. Data collections for all complexes were carried out at room temperature. Final refinement included atomic positions for all the atoms, anisotropic thermal parameters for all the non-hydrogen atoms, and isotropic thermal parameters for all the hydrogen atoms. Full matrix least-squares refinement against |F2| was carried out using the WinGx package of programs.*[46]* Details of the structural parameters and final refinements for the compounds are given in Table **5.4**.

Table 5.4 Crystal data and structural refinement parameters for **9a** and **10a**

Complex	Bond lengths (Å)		Bond Angles (°)	
9a	Ru1-C1	2.015(7)	C1-Ru1-C10	154.6(3)
	Ru1-C10	2.045(7)	C1-Ru1-N3	77.7(3)
	Ru1-N3	2.052(6)	C10-Ru1-N3	76.9(3)
	Ru1-P1	2.350(18)	C1-Ru1-P1	91.5(2)
	Ru1-P2	2.333(19)	C1-Ru1-P2	91.8(2)
			C10-Ru1-P1	94.5(2)
			C10-Ru1-P2	88.7(2)
			N3-Ru1-P2	100.71(18)
10a	Ru1-S1	2.293(11)	S1-Ru1-Cl1	87.57(4)
	Ru1-S2	2.313(12)	S1-Ru1-S2	175.97(5)
	Ru1-N3	1.996(4)	S2-Ru1-Cl1	93.40(5)
	Ru1-Cl1	2.430(11)	N3-Ru1-S1	89.79(11)
	Ru1-C10	2.062(5)	N3-Ru1-S2	89.28(11)
	Ru1-C1	2.073(5)	N3-Ru1-Cl1	177.26(12)
			N3-Ru1-C1	77.99(17)
			N3-Ru1-C10	78.15(18)
			C1-Ru1-S1	91.83(12)
			C1-Ru1-Cl1	101.34(13)

5.5.3 General procedure for catalytic hydrogen transfer reaction

Cyclohexanone (2 mmol) and catalyst (1 mol %) were dissolved in ^{i}PrOH (5 ml), under an inert atmosphere in Schlenk tube, followed by the addition of Na (1 eq., 2 mmol) to generate NaO^{i}Pr, in situ. After all the sodium metal had dissolved, the reaction mixture was quickly heated to reflux by lowering into a preheated oil bath. The conversion of the corresponding product was determined by the relative peak area of the substrate and the product in GC with n-decane as an internal standard. The product was purified by silica gel column chromatography using

hexane/ethyl acetate (typically 8:2) as an eluent. NMR data for alcohol product match the reported values.

5.5.4 General procedure for catalytic acceptorless dehydrogenation reaction

Typically, catalyst (3 mol%) was added to the solution of alcohol (1 mmol), KO^{t}Bu (1 eq.) in toluene under an inert atmosphere in toluene in a 2-neck R.B. flask equipped with a reflux condenser and heated at 110 ^{o}C for 3h by lowering into a preheated oil bath. The conversion of the corresponding product was determined by the relative peak area of the substrate and the product in GC without an internal standard. After completion of the reaction, the product was extracted with chloroform and dried in a vacuum. The product was purified by silica gel column chromatography using hexane/ethyl acetate (8:2) as eluent. ^{1}H NMR data for the aldehyde product match the reported values.

5.5.5 General procedure for the catalytic dehydrogenative coupling reaction

Typically, catalyst (3 mol %) was added to the solution of alcohol (1 mmol), amine (1 mmol), KO^{t}Bu (1 eq.) in toluene under an inert atmosphere in a 2-neck R.B. flask equipped with a reflux condenser and heated at 110 ^{o}C for 3h by lowering into a preheated oil bath. The conversion of the corresponding product was determined by the relative peak area of the substrate and the product in GC with n-decane as an internal standard. After completion of the reaction, the product was extracted with chloroform and dried in a vacuum. The product was purified by alumina gel column chromatography using hexane/ethyl acetate (7.7:0.3) as eluent. ^{1}H NMR data for the imine product match the reported values.

5.5.6 Characterization data of metal complexes

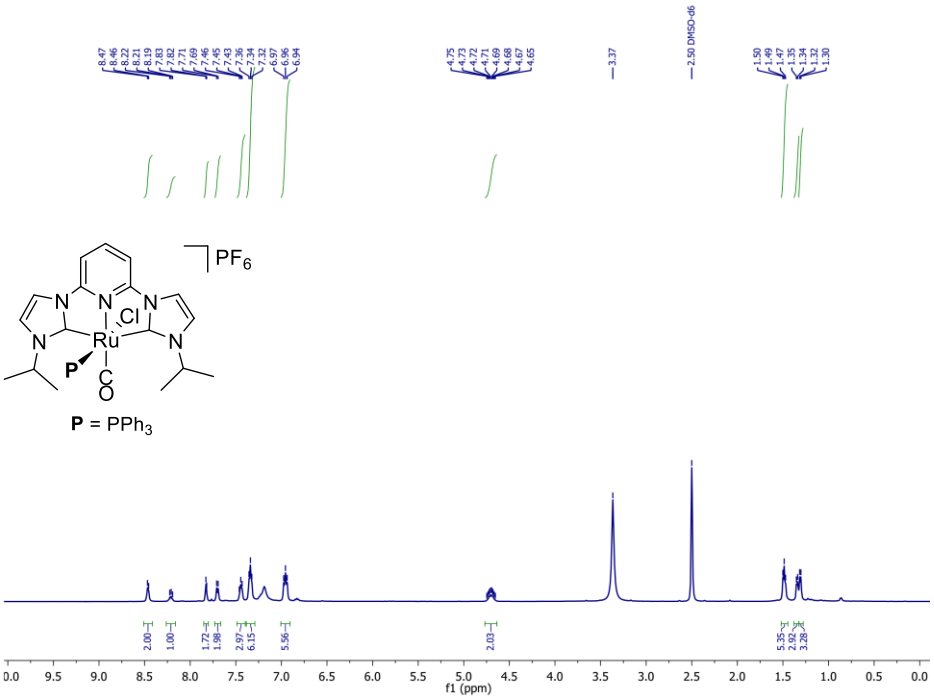

Figure 5.4 ^{1}H NMR spectrum of **7b**

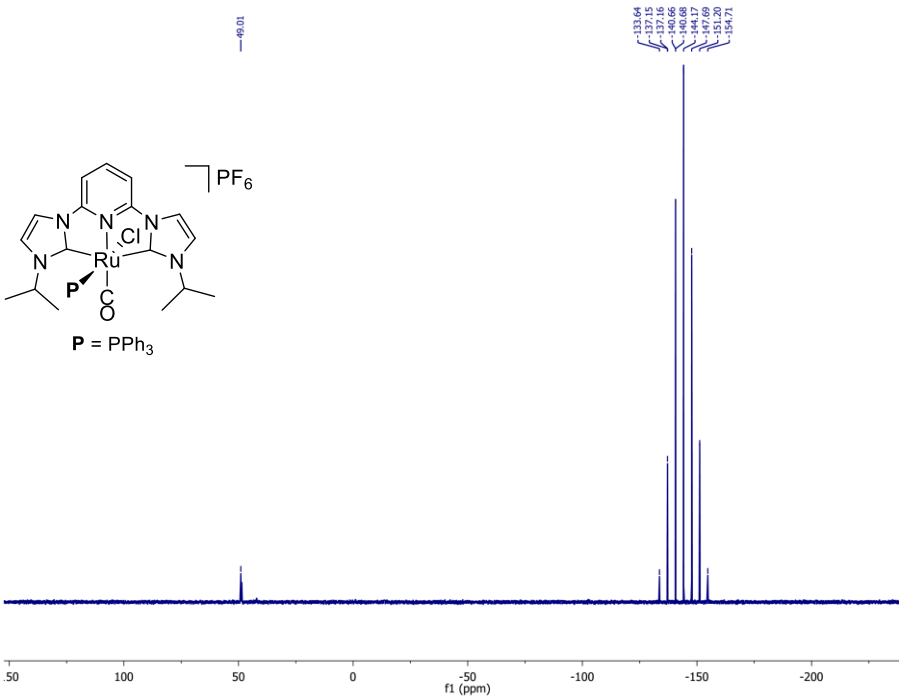

Figure 5.5 ^{31}P NMR spectrum of **7b**

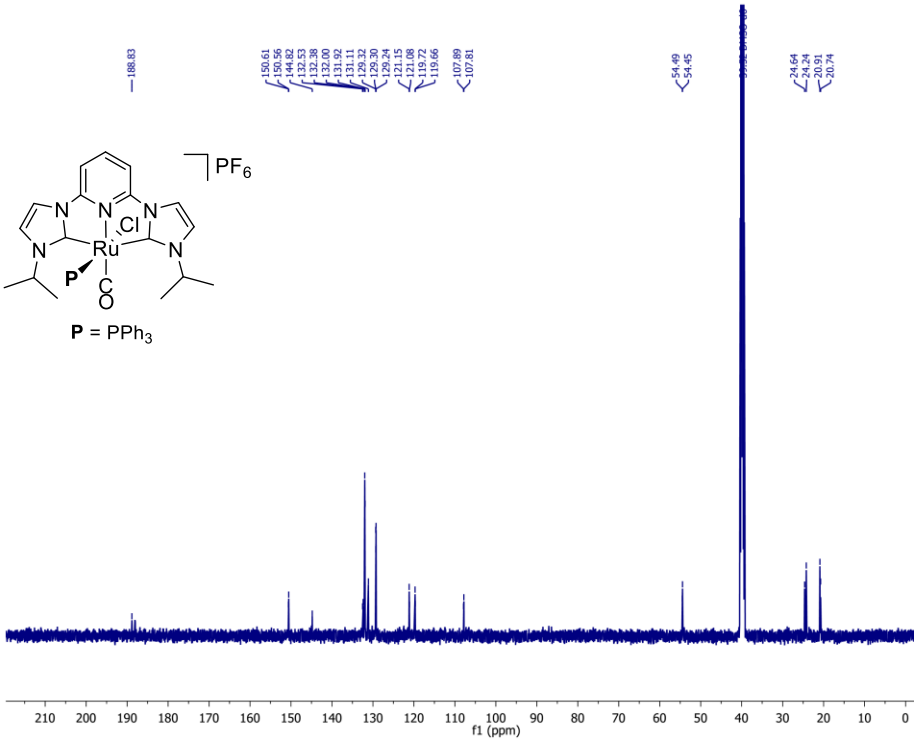

Figure 5.6 ^{13}C NMR spectrum of **7b**

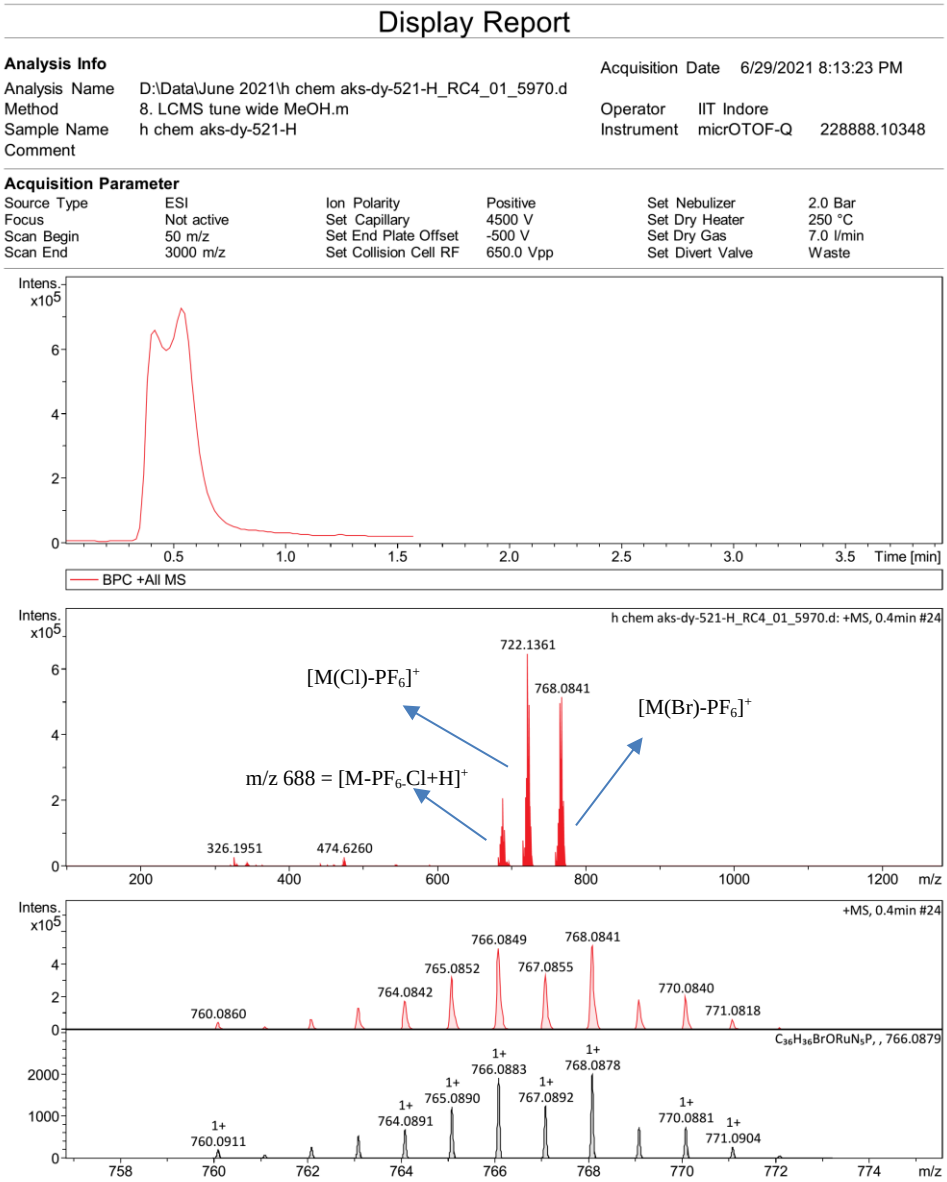

Figure 5.7 HRMS spectrum of **7b**

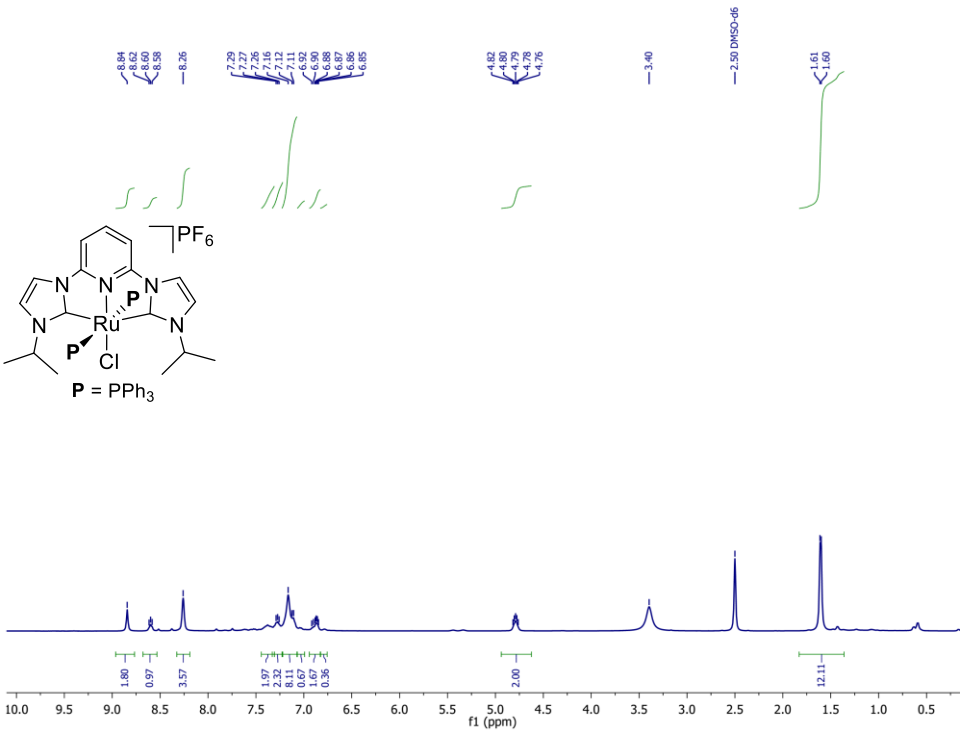

Figure 5.8 ^{1}H NMR spectrum of **8b**

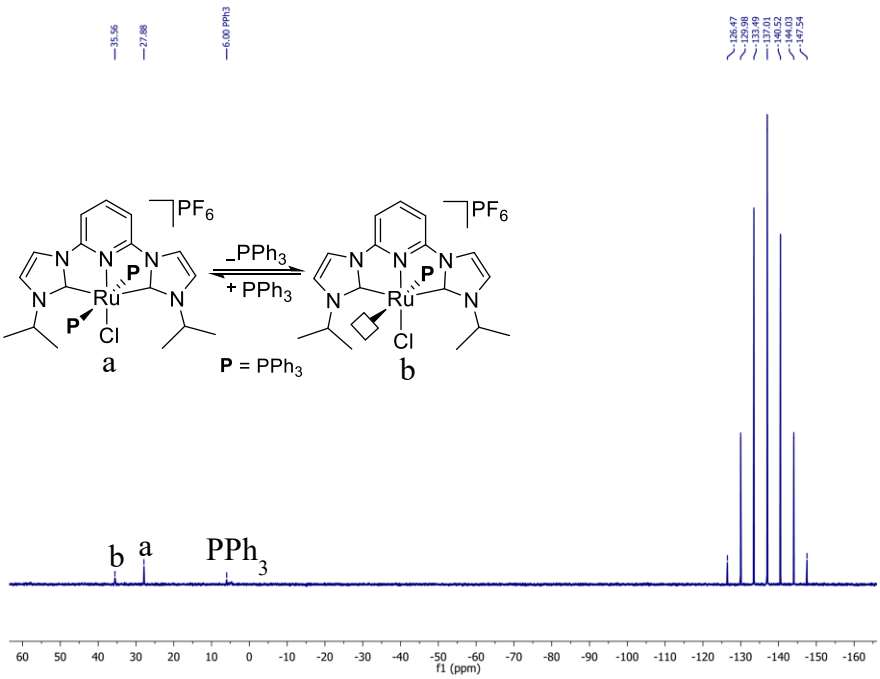

Figure 5.9 ^{31}P NMR spectrum of **8b**

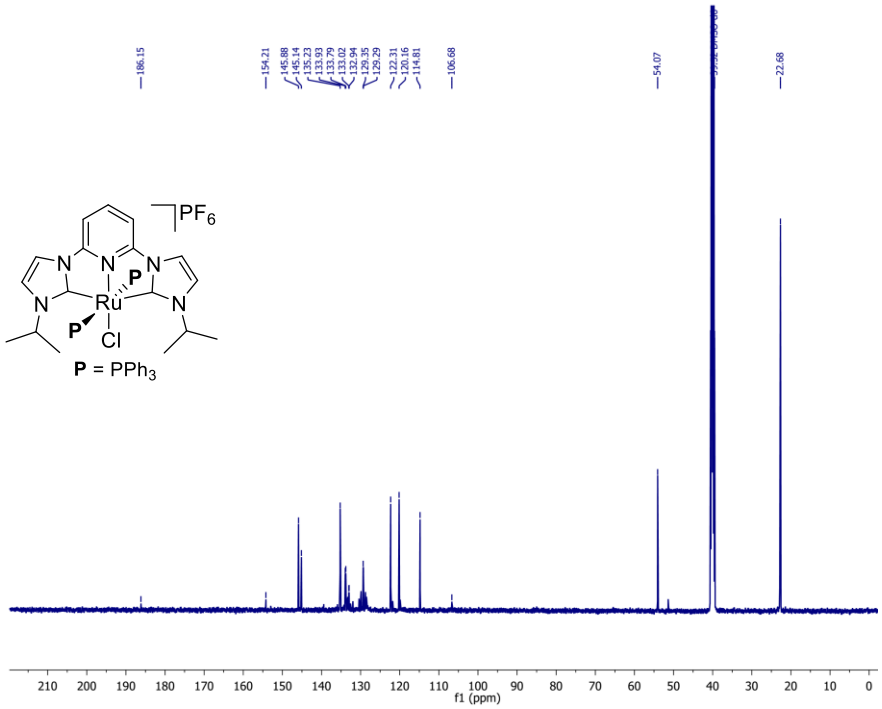

Figure 5.10 ^{13}C NMR spectrum of **8b**

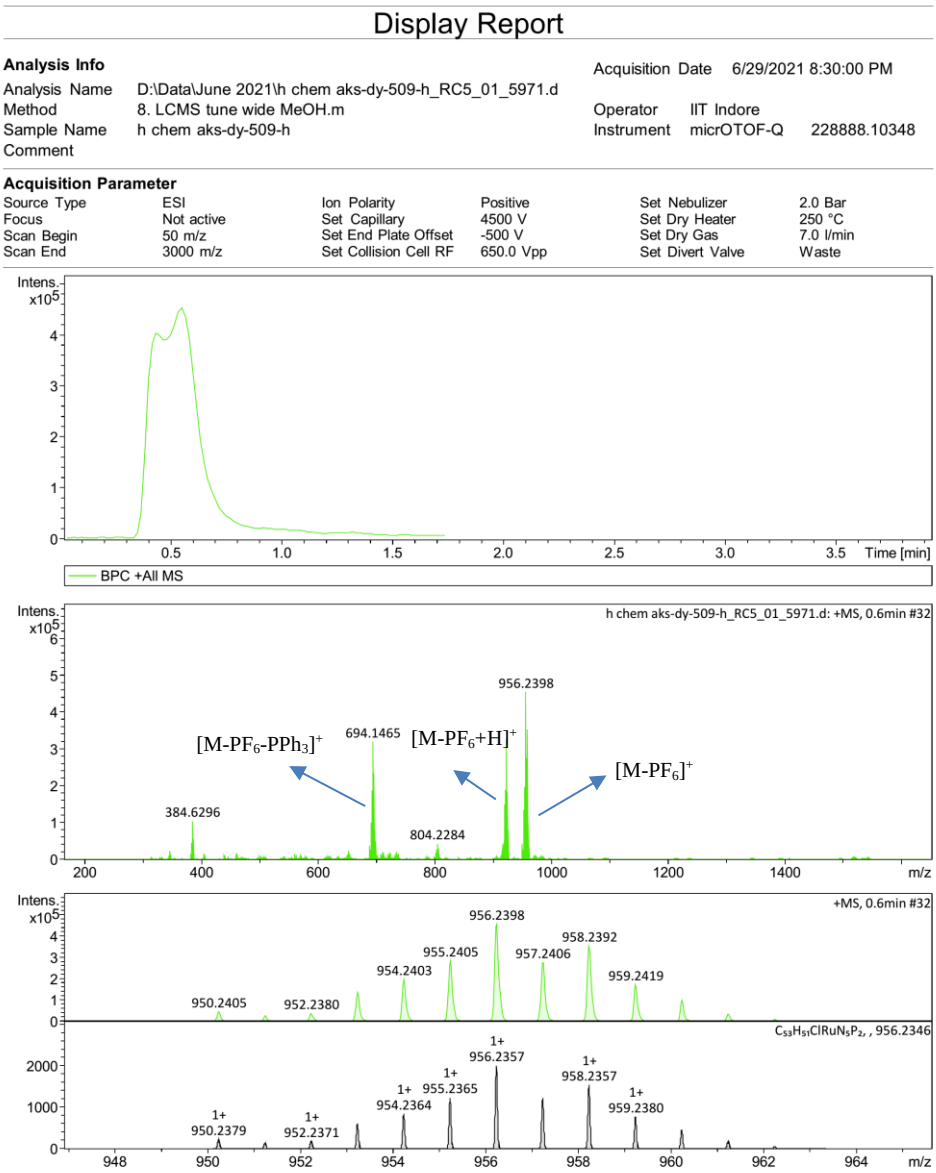

Figure 5.11 HRMS spectrum of **8b**

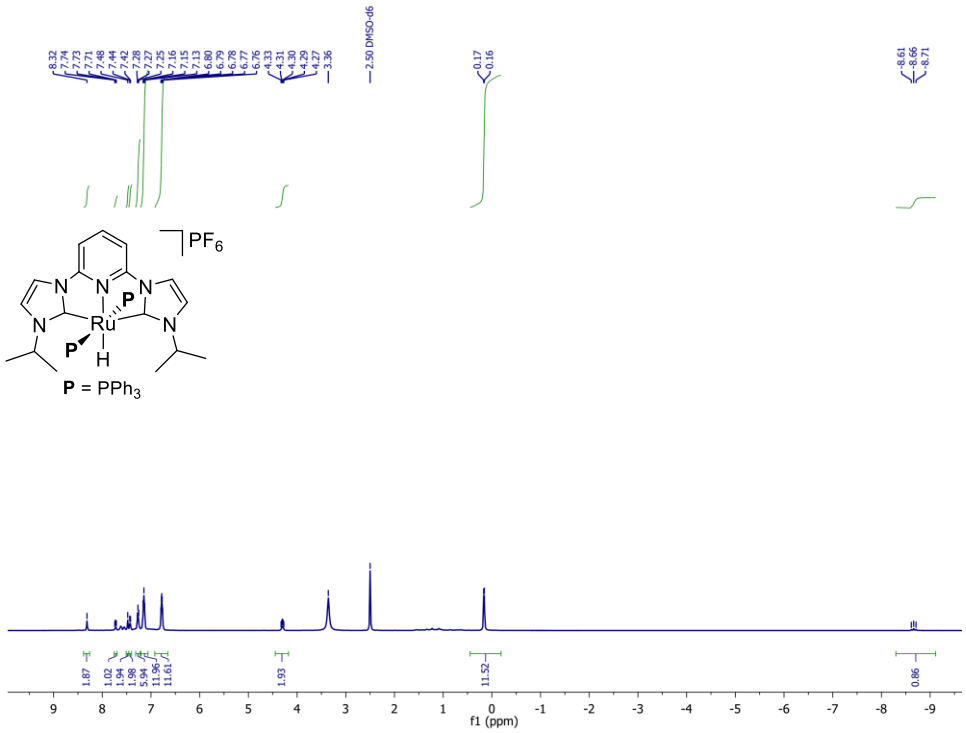

Figure 5.12 ^{1}H NMR spectrum of **9b**

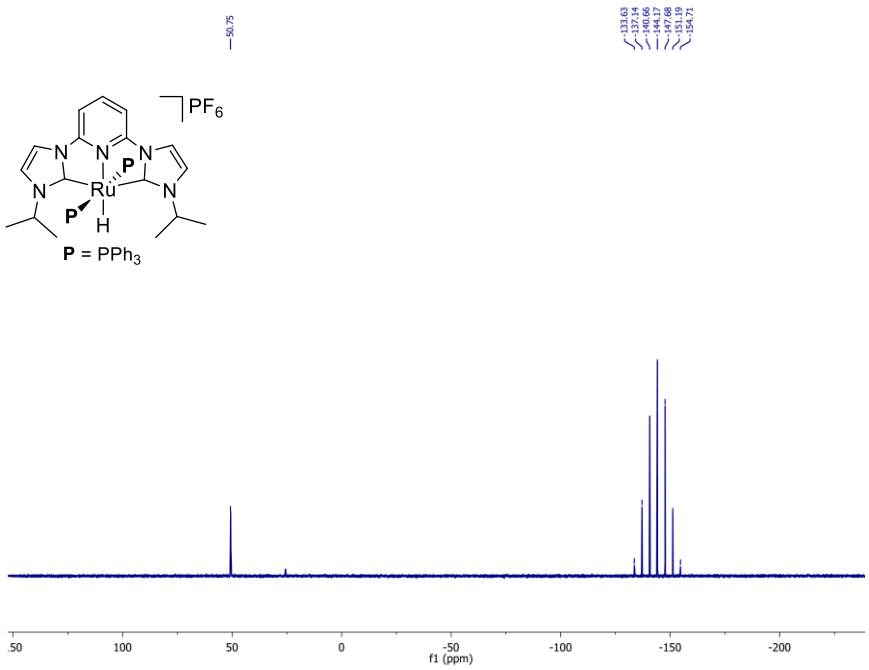

Figure 5.13 ^{31}P NMR spectrum of **9b**

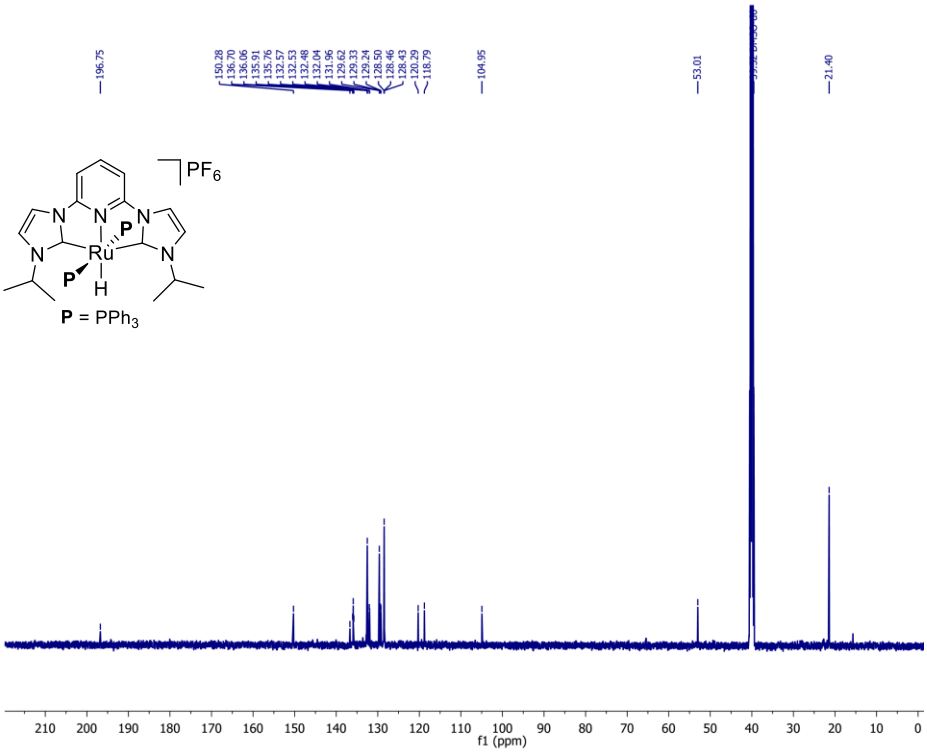

Figure 5.14 ^{13}C NMR spectrum of **9b**

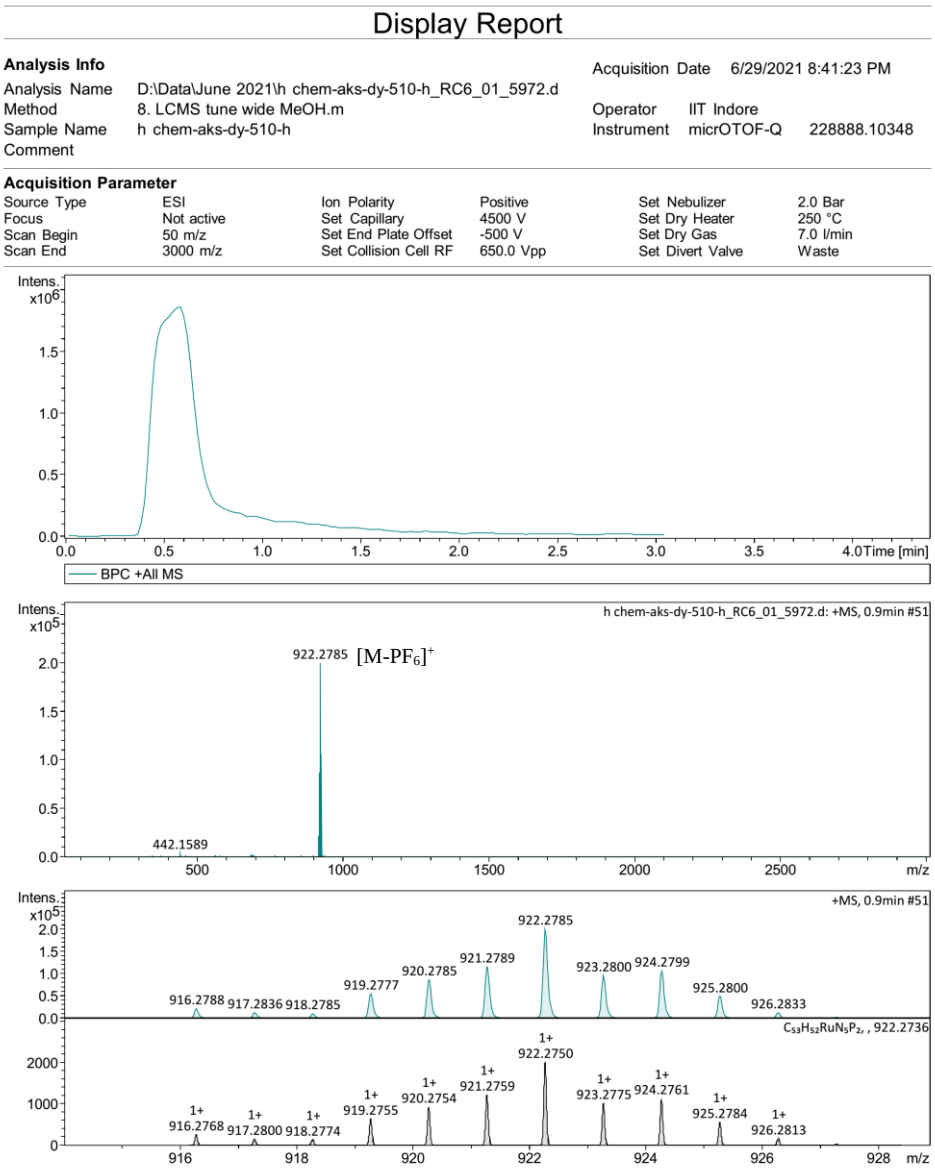

Figure 5.15 HRMS spectrum of **9b**

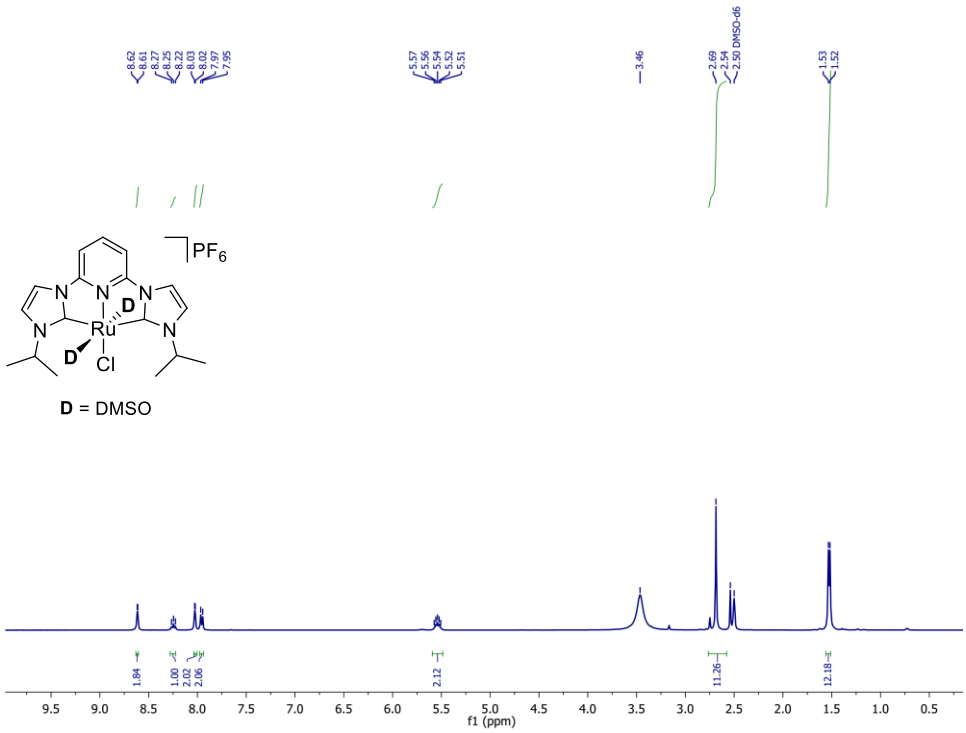

Figure 5.16 ^{1}H NMR spectrum of **10b**

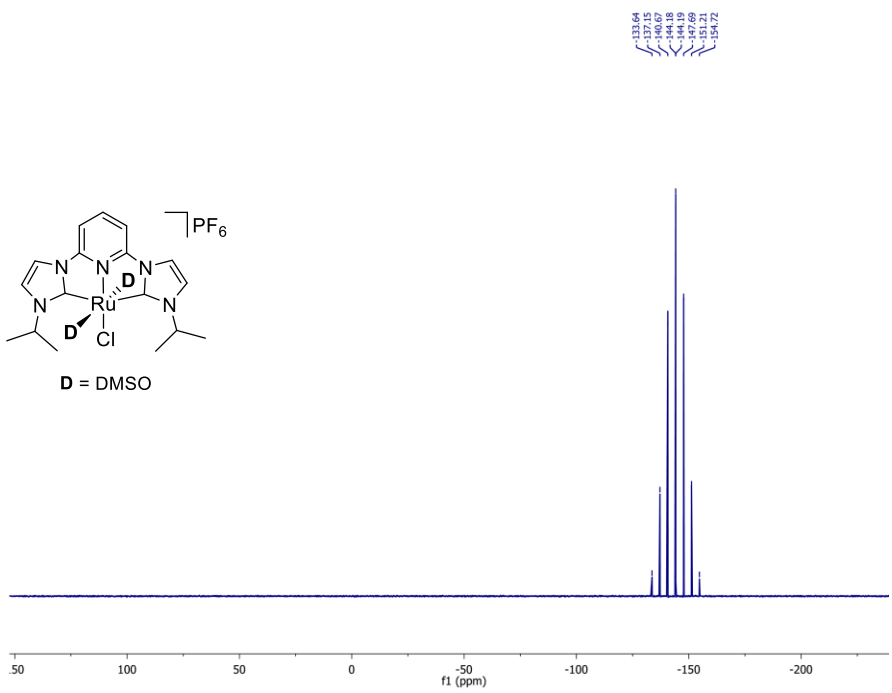

Figure 5.17 ^{31}P NMR spectrum of **10b**

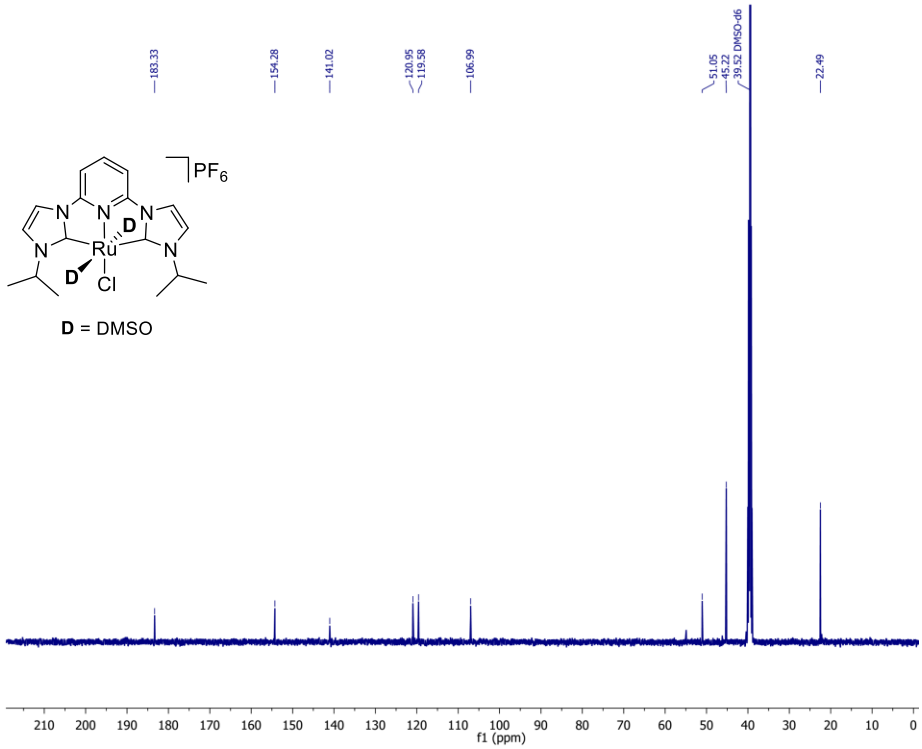

Figure 5.18 ^{13}C NMR spectrum of **10b**

Display Report

Analysis Info

Analysis Name	D:\Data\October 2021\h chem AKS-DY-DIPR-a_RA3_01_10202.d	Acquisition Date	10/21/2021 4:07:56 PM
Method	2. LCMS tune wide ACN.m	Operator	IIT Indore
Sample Name	h chem AKS-DY-DIPR-a	Instrument	micrOTOF-Q 228888.10348
Comment			

Acquisition Parameter

Source Type	ESI	Ion Polarity	Positive	Set Nebulizer	2.0 Bar
Focus	Not active	Set Capillary	4500 V	Set Dry Heater	250 °C
Scan Begin	50 m/z	Set End Plate Offset	-500 V	Set Dry Gas	7.0 l/min
Scan End	3000 m/z	Set Collision Cell RF	650.0 Vpp	Set Divert Valve	Waste

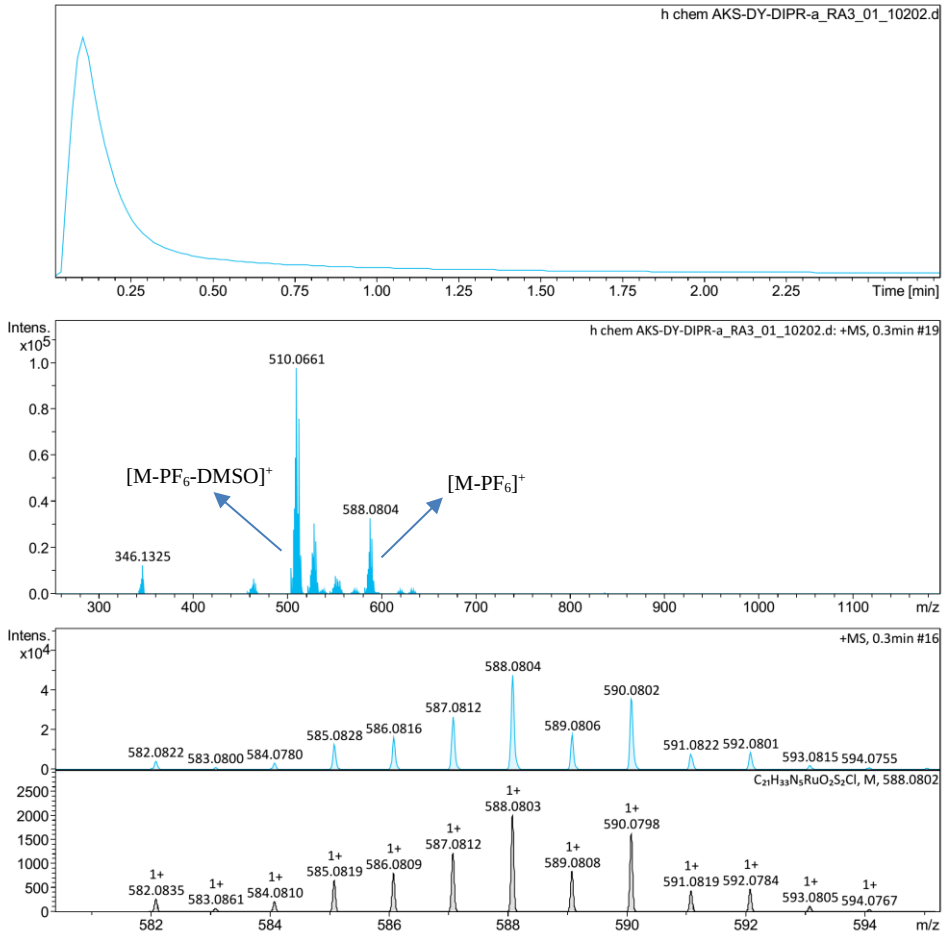

Figure 5.19 HRMS spectrum of **10b**

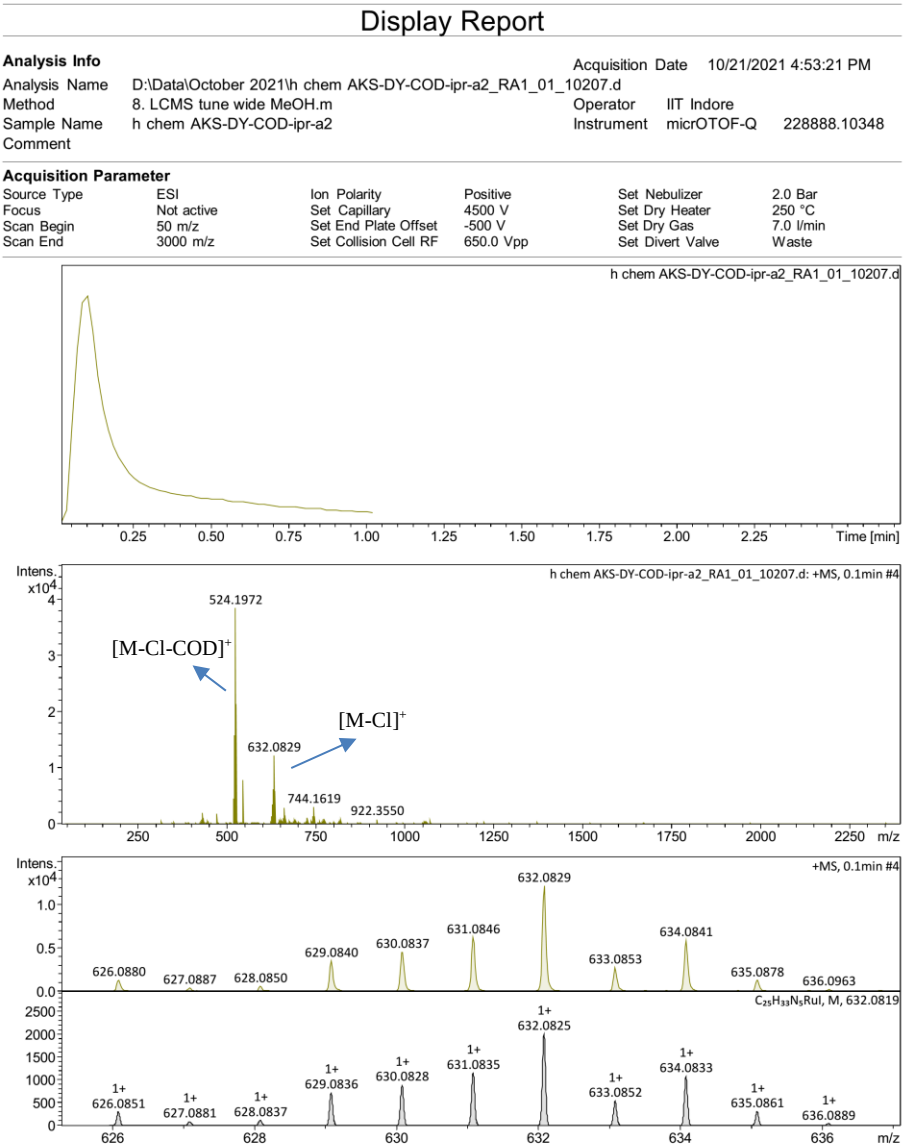

Figure 5.20 HRMS spectrum of **11b**

Characterization data for Transfer hydrogenation, acceptorless dehydrogenation and dehydrogenative coupling products

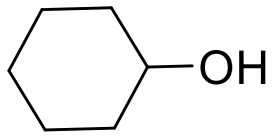

Cyclohexanol; ^{1}H NMR (500 MHz, $CDCl_3$, δ in ppm): δ 3.72 – 3.47 (m, 1H), 2.62 (d, *J* = 8.7 Hz, 1H), 1.99 – 1.84 (m, 2H), 1.81 – 1.66 (m, 2H), 1.39 – 1.20 (m, 5H), 1.20 – 1.06 (m, 2H).

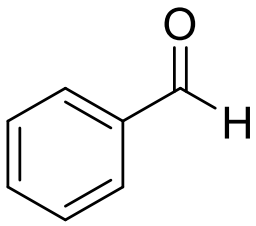

Benzaldehyde; ^{1}H NMR (500 MHz, $CDCl_3$, δ in ppm): 10.04 (s, 1H), 7.91 (d, *J*=7.91 Hz, 2H), 7.65 (t, *J*=7.65 Hz, 1H), 7.56 (d, *J*=7.56 Hz, 2H).

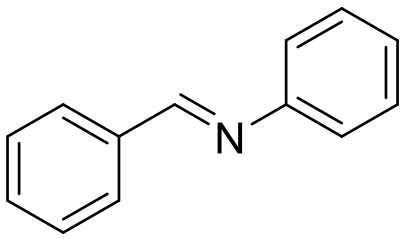

***N*-1-diphenylmethanimine;** ^{1}H NMR ($CDCl_3$, δ in ppm): 8.50 (s, 1H), 7.72-7.69 (m, 2H), 7.63-7.58 (m, 1H), 7.55-7.50 (m, 1H), 7.47-7.33 (m, 4H), 7.20-7.17 (m, 2H).

5.6 References

[1] Gunanathan C., Milstein D. (2014), Bond Activation and Catalysis by Ruthenium Pincer Complexes, *Chem. Rev.*, 114, 12024–12087 (https://doi.org/10.1021/cr5002782).

[2] Piccirilli L., Lobo Justo Pinheiro D., Nielsen M. (2020), Recent Progress with Pincer Transition Metal Catalysts for Sustainability, *Catalysts*, 10, 773 (https://doi.org/10.3390/catal10070773).

[3] Lawrence M. A. W., Green K.-A., Nelson P. N., Lorraine S. C. (2018), Review: Pincer ligands—Tunable, versatile and applicable, *Polyhedron*, 143, 11–27 (https://doi.org/10.1016/j.poly.2017.08.017).

[4] Peris E., Crabtree R. H. (2004), Recent homogeneous catalytic applications of chelate and pincer *N*-heterocyclic carbenes, *Coord. Chem. Rev.*, 248, 2239–2246 (https://doi.org/10.1016/j.ccr.2004.04.014).

[5] Chang W., Gong X., Wang S., *et. al.* (2017), Acceptorless dehydrogenation and dehydrogenative coupling of alcohols catalysed by protic NHC ruthenium complexes, *Org. Biomol. Chem.*, 15, 3466–3471 (https://doi.org/10.1039/C7OB00542C).

[6] Dutta I., Sarbajna A., Pandey P., *et. al*. (2016), Acceptorless Dehydrogenation of Alcohols on a Diruthenium(II,II) Platform, *Organometallics*, 35, 1505–1513 (https://doi.org/10.1021/acs.organomet.6b00085).

[7] Wei Z., Aguirre A. de, Junge K., *et. al.* (2018), Benyzl Alcohol Dehydrogenative Coupling Catalyzed by Defined Mn and Re PNP Pincer Complexes – A Computational Mechanistic Study, *Eur. J. Inorg. Chem.*, 2018, 4643–4657 (https://doi.org/10.1002/ejic.201800674).

[8] Borah D., Saha B., Sarma B., Das P. (2020), A cyclometalated Ir(III)–NHC complex as a recyclable catalyst for acceptorless dehydrogenation of alcohols to carboxylic acids, *Dalton Trans.*, 49, 16866–16876 (https://doi.org/10.1039/D0DT02341H).

[9] Olivares M., Knörr P., Albrecht M. (2020), Aerobic dehydrogenation of amines to nitriles catalyzed by triazolylidene ruthenium complexes with O_2 as terminal oxidant. *Dalton Trans.*, 49, 1981–1991 (https://doi.org/10.1039/C9DT04873A).

[10] Chai H., Yu K., Liu B., et. al. (2020), A Highly Selective Manganese-Catalyzed Synthesis of Imines under Phosphine-Free Conditions, *Organometallics*, 39, 217–226 (https://doi.org/10.1021/acs.organomet.9b00769).

[11] Maggi A., Madsen R. (2012), Dehydrogenative Synthesis of Imines from Alcohols and Amines Catalyzed by a Ruthenium N-Heterocyclic Carbene Complex, *Organometallics*, 31, 451–455 (https://doi.org/10.1021/om201095m).

[12] Albrecht M., Miecznikowski J. R., Samuel A., et. al. (2002), Chelated Iridium(III) Bis-carbene Complexes as Air-Stable Catalysts for Transfer Hydrogenation, *Organometallics*, 21, 3596–3604 (https://doi.org/10.1021/om020338x).

[13] Garg N., Paira S., Sundararaju B. (2020), Efficient Transfer Hydrogenation of Ketones using Methanol as Liquid Organic Hydrogen Carrier, *ChemCatChem* 12, 3472–3476 (https://doi.org/10.1002/cctc.202000228).

[14] Castellanos-Blanco N., Arévalo A., García J. J. (2016), Nickel-catalyzed transfer hydrogenation of ketones using ethanol as a solvent and a hydrogen donor, *Dalton Trans.*, 45, 13604–13614 (https://doi.org/10.1039/C6DT02725C).

[15] Zhao Q., Meng G., Nolan S. P., Szostak M. (2020), *N*-Heterocyclic Carbene Complexes in C–H Activation Reactions, *Chem. Rev.*, 120, 1981–2048 (https://doi.org/10.1021/acs.chemrev.9b00634).

[16] Díez-González S., Marion N., Nolan S. P. (2009), *N*-Heterocyclic Carbenes in Late Transition Metal Catalysis, *Chem. Rev.*, 109, 3612–3676 (https://doi.org/10.1021/cr900074m).

[17] Flanigan D. M., Romanov-Michailidis F., White N. A., Rovis T. (2015), Organocatalytic Reactions Enabled by N-Heterocyclic Carbenes, *Chem. Rev.*, 115, 9307–9387 (https://doi.org/10.1021/acs.chemrev.5b00060).

[18] Dorta R., Stevens E. D., Scott N. M., *et. al.* (2005), Steric and Electronic Properties of *N*-Heterocyclic Carbenes (NHC): A Detailed Study on Their Interaction with $Ni(CO)_4$, *J. Am. Chem. Soc.*, 127, 2485–2495 (https://doi.org/10.1021/ja0438821).

[19] Poyatos M., Mata J. A., Falomir E., *et. al.* (2003), New Ruthenium(II) CNC-Pincer Bis(carbene) Complexes: Synthesis and Catalytic Activity, *Organometallics*, 22, 1110–1114 (https://doi.org/10.1021/om020817w).

[20] Danopoulos A. A., Winston S., Motherwell W. B. (2002), Stable *N*-functionalised 'pincer' bis carbene ligands and their ruthenium complexes; synthesis and catalytic studies, *Chem. Commun.*, 1376–1377 (https://doi.org/10.1039/B202814J).

[21] Peris E., Loch J. A., Mata J., Crabtree R. H. (2001), A Pd complex of a tridentate pincer CNC bis-carbene ligand as a robust homogenous Heck catalyst, *Chem. Commun.*, 201–202 (https://doi.org/10.1039/B008038L).

[22] Danopoulos A. A., Braunstein P., Saßmannshausen J., *et. al.* (2020), "Pincer" Pyridine–Dicarbene–Iridium and -Ruthenium

Complexes and Derivatives Thereof., *Eur. J. Inorg. Chem.*, 2020, 3359–3369 (https://doi.org/10.1002/ejic.202000429).

[23] Andrew R. E., González-Sebastián L., Chaplin A. B. (2016), NHC-based pincer ligands: carbenes with a bite, *Dalton Trans.*, 45, 1299–1305 (https://doi.org/10.1039/C5DT04429D).

[24] Murayama H., Heike Y., Higashida K., *et. al.* (2020), Iridium-Catalyzed Enantioselective Transfer Hydrogenation of Ketones Controlled by Alcohol Hydrogen-Bonding and sp^3-C−H Noncovalent Interactions, *Adv. Synth. Catal.*, 362, 4655–4661 (https://doi.org/10.1002/adsc.202000615).

[25] Wang D., Astruc D. (2015), The Golden Age of Transfer Hydrogenation, *Chem. Rev.*, 115, 6621–6686 (https://doi.org/10.1021/acs.chemrev.5b00203).

[26] Wang R., Han X., Xu J., *et. al.* (2020), Transfer Hydrogenation of Ketones and Imines with Methanol under Base-Free Conditions Catalyzed by an Anionic Metal–Ligand Bifunctional Iridium Catalyst, *J. Org. Chem.*, 85, 2242–2249 (https://doi.org/10.1021/acs.joc.9b02957).

[27] Abubakar S., Bala M. D. (2020), Transfer Hydrogenation of Ketones Catalyzed by Symmetric Imino-*N*-heterocyclic Carbene Co(III) Complexes, *ACS Omega*, 5, 2670–2679 (https://doi.org/10.1021/acsomega.9b03181).

[28] Shahane S., Fischmeister C., Bruneau C. (2012), Acceptorless ruthenium catalyzed dehydrogenation of alcohols to ketones and esters, *Catal. Sci. Technol.*, 2, 1425–1428 (https://doi.org/10.1039/C2CY20066J).

[29] Fuse H., Mitsunuma H., Kanai M. (2020), Catalytic Acceptorless Dehydrogenation of Aliphatic Alcohols, *J. Am. Chem. Soc.*, 142, 4493–4499 (https://doi.org/10.1021/jacs.0c00123).

[30] Wang Z., Pan B., Liu Q., *et. al.* (2017), Efficient acceptorless dehydrogenation of secondary alcohols to ketones mediated by a PNN-Ru(II) catalyst, *Catal. Sci. Technol.*, 7, 1654–1661 (https://doi.org/10.1039/C7CY00342K).

[31] Crabtree R. H. (2017), Homogeneous Transition Metal Catalysis of Acceptorless Dehydrogenative Alcohol Oxidation: Applications in Hydrogen Storage and to Heterocycle Synthesis, *Chem. Rev.*, 117, 9228–9246 (https://doi.org/10.1021/acs.chemrev.6b00556).

[32] Miao Y., Samuelsen S. V., Madsen R. (2021), Vanadium- and Chromium-Catalyzed Dehydrogenative Synthesis of Imines from Alcohols and Amines, *Organometallics*, 40, 1328–1335 (https://doi.org/10.1021/acs.organomet.1c00123).

[33] Zhang G., Hanson S. K. (2013), Cobalt-Catalyzed Acceptorless Alcohol Dehydrogenation: Synthesis of Imines from Alcohols and Amines, *Org. Lett.*, 15, 650–653 (https://doi.org/10.1021/ol303479f).

[34] Sindhuja E., Ramesh R. (2014), Direct synthesis of imines from primary alcohols and amines using an active ruthenium(II) NNN–pincer complex, *Tetrahedron Lett.*, 55, 5504–5507 (https://doi.org/10.1016/j.tetlet.2014.08.035).

[35] Wu S., Zhang H., Cao Q., *et. al.* (2021), Efficient imine synthesis via oxidative coupling of alcohols with amines in an air atmosphere using a mesoporous manganese–zirconium solid solution catalyst, *Catal. Sci. Technol.*, 11, 810–822 (https://doi.org/10.1039/D0CY02288H).

[36] Belowich M. E., Stoddart J. F. (2012), Dynamic imine chemistry, *Chem. Soc. Rev.*, 41, 2003–2024 (https://doi.org/10.1039/C2CS15305J).

[37] Eizawa A., Nishimura S., Arashiba K., *et. al.* (2018), Synthesis of Ruthenium Complexes Bearing PCP-Type Pincer Ligands and Their Application to Direct Synthesis of Imines from Amines and Benzyl Alcohol, *Organometallics*, 37, 3086–3092 (https://doi.org/10.1021/acs.organomet.8b00465).

[38] Vinoth G., Indira S., Bharathi M., *et. al.* (2019), Synthesis of Imines via Reactions of Benzyl Alcohol with Amines Using Half-Sandwich (η^6-p-cymene) Ruthenium(II) Complexes Stabilised by 2-aminofluorene Derivatives, *Appl. Organomet. Chem.*, 33, e5200 (https://doi.org/10.1002/aoc.5200).

[39] Nielsen D. J., Cavell K. J., Skelton B. W., White A. H. (2006), Methyl-palladium(II) complexes of pyridine-bridged bis(nucleophilic heterocyclic carbene) ligands: Substituent effects on structure, stability, and catalytic performance, *Inorganica Chimica Acta*, 359, 1855–1869 (https://doi.org/10.1016/j.ica.2005.07.049).

[40] Yadav D., Misra S., Kumar D., Singh S., Singh A. K. (2021), Cationic ruthenium(II)–NHC pincer complexes: Synthesis, characterisation and catalytic activity for transfer hydrogenation of ketones, *Appl. Organomet. Chem.*, 35, e6287 (https://doi.org/10.1002/aoc.6287).

[41] Yadav D., Singh R.K., Singh S., Shirage P., Singh A. K. (2021) Cationic ruthenium(II)-NHC pincer complexes with hemilabile COD: Solid-state structural characterization and theoretical study of an η^2-(E,Z)-COD ligand, *J. Organomet. Chem.*, 953, 122061 (https://doi.org/10.1016/j.jorganchem.2021.122061).

[42] Ahmad N., Lavison J.J., Robinson S.D., Uttley M.F., *Inorganic Syntheses*, 15, 48.

[43] Hallman P. S., Stephenson T. A., Wilkinson G., (1970), Tetrakis(triphenylphosphine)dichlororuthenium(II) and

Tris(triphenylphosphine)dichlororuthenium(II), *Inorganic Syntheses*, 12, 238-239 (DOI: 10.1002/9780470132432.ch40).

[44] Albers M. O., Singleton E., Yates J. E., *Inorganic Syntheses*, 26, 253.

[45] Evans I. P., Spencer A., Wilkinson G., (1973), Dichlorotetrakis(dimethyl sulphoxide)ruthenium(II) and its use as a source material for some new ruthenium(II) complexes, *J. Chem. Soc., Dalton Trans.*, 204-209 (DOI: 10.1039/DT9730000204).

[46] Farrugia L. J. (2012), WinGX and ORTEP for Windows: an update, *J. Appl. Cryst.*, 45, 849–854 (https://doi.org/10.1107/S0021889812029111).

Chapter 6

Conclusions and future scope

6.1 Conclusions

In summary, my thesis work primarily focuses on the synthesis, characterization, and applications of Ru(II)-NHC pincer complexes with different co-ligands.

In ***chapter 1***, we briefly described the different types of pincer ligands and their transition metal catalysts. In particular, the synthesis, and application of ruthenium catalysts in various organic transformations is explained.

In ***chapter 2***, we synthesized and characterized several Ru(II)- NHC pincer complexes with different co-ligands.

In ***Chapter 3,*** we have investigated the application of the Ru(II)-NHC pincer complexes for Transfer hydrogenation of ketones and acceptorless dehydrogenation of alcohols. We observed that catalyst **1b** performs better compared to other analogous complexes for both transformations. The substrate scope for transfer hydrogenation reactions and acceptorless dehydrogenation of alcohols with several ketones and alcohols has been explored by using **1b** as a catalyst. In addition, detailed NMR and mass investigations were also carried out under catalytic and controlled reaction conditions, to explain the mechanistic pathway by identifying catalytic intermediates, like hydride and alkoxide-coordinated Ru species.

In ***Chapter 4***, the application of the Ru(II)-NHC pincer complexes for catalytic acceptorless dehydrogenative coupling of alcohols and amines has been studied. It was noticed that complex (**2b)** is better for catalytic transformation than the other analogous complexes, whereas complex (**1b)** is less reactive. The trend of catalytic

performance of Ru(II)-NHC pincer complexes in acceptorless dehydrogenative coupling is reversed in comparison to the transfer hydrogenation and acceptorless dehydrogenation reactions, because of the more trans effect of CO as a co-ligand than PPh_3. The present catalytic systems may provide new selectivity for various catalytic transformations. Substrate scope with **2b** has been performed with different substituted amines and alcohols under conventional and microwave heating (with reduced time and temperature), respectively. Biologically active imine precursors have been also synthesized by using **2b** as a catalyst.

In ***chapter 5***, we have synthesized and characterized Ru(II) NHC-pincer complexes with *N*-isopropyl and different co-ligands. We observed similar performance trends of *N*-isopropyl complexes with analogous *N*-methyl complexes for transfer hydrogenation, acceptorless dehydrogenation, and dehydrogenative coupling reactions, except for the DMSO complex. Likewise, complex **1b** is better compared to all the methyl and *N*-isopropyl complexes for transfer hydrogenation and acceptorless dehydrogenation reactions. In the case of dehydrogenative coupling reactions, *N*-isopropyl complexes proved to be better than methyl complexes, due to the electronic effects as well as steric crowdedness of *N*-isopropyl which facilitates the dissociation of catalytic substrates from the ruthenium metal centre.

6.2 Future scope

The development of more selective catalysts with different co-ligands can provide the opportunity for selective organic transformation reactions and reduce the formation of side products. Therefore, the synthesis of new and selective catalysts for a variety of organic transformations is highly desirable.

In the recent past, several researchers have extensively developed various catalysts, however, there is a lack of information on co-ligands influence on catalyst selectivity until now. Systematic studies in more selective catalysts towards different reactions can revolutionize the field in numerous aspects.

Even though rapid advancement in the field, the development of a robust catalytic system with pincer NHCs for various catalytic processes is still the top-most necessity of the scientific community. Development of the air-stable and low-cost metal homogeneous catalyst for the selective transformations using suitable reaction conditions is also under-explored.